EXPERIMENTAL STUDY ON STRESS CONCENTRATION FACTORS IN SINGLE AND GROUPS OF END BEARING AND FLOATING STONE COLUMNS

A THESIS SUBMITTED TO
THE GRADUATE SCHOOL OF NATURAL AND APPLIED SCIENCES
OF
MIDDLE EAST TECHNICAL UNIVERSITY

BY

ZEYNEP ÇEKİNMEZ

IN PARTIAL FULFILLMENT OF THE REQUIREMENTS
FOR
THE DEGREE OF DOCTOR OF PHILOSOPHY
IN
CIVIL ENGINEERING

JUNE 2014

Approval of the thesis:

EXPERIMENTAL STUDY ON STRESS CONCENTRATION FACTORS IN SINGLE AND GROUPS OF END BEARING AND FLOATING STONE COLUMNS

submitted by **ZEYNEP ÇEKİNMEZ** in partial fulfillment of the requirements for the degree of **Doctor of Philosophy in Civil Engineering Department, Middle East Technical University** by,

Prof. Dr. Canan Özgen   _____
Dean, Graduate School of **Natural and Applied Sciences**

Prof. Dr. Ahmet Cevdet Yalçıner   _____
Head of Department, **Civil Engineering**

Prof. Dr. Ahmet Orhan Erol   _____
Supervisor, **Civil Engineering Dept., METU**

Inst. Dr. Nabi Kartal Toker   _____
Co-Supervisor, **Civil Engineering Dept., METU**

Examining Committee Members:

Prof. Dr. Mehmet Ufuk Ergun   _____
Civil Engineering Dept., METU

Prof. Dr. Ahmet Orhan Erol   _____
Civil Engineering Dept., METU

Prof. Dr. Kemal Önder Çetin   _____
Civil Engineering Dept., METU

Prof. Dr. Bora Rojay   _____
Geological Engineering Dept., METU

Assoc. Prof. Dr. Sami Oğuzhan Akbaş   _____
Civil Engineering Dept., Gazi University

                              Date:

I hereby declare that all information in this document has been obtained and presented in accordance with academic rules and ethical conduct. I also declare that, as required by these rules and conduct, I have fully cited and referenced all material and results that are not original to this work.

Name, Last Name : Zeynep Çekinmez

Signature   :

ABSTRACT

EXPERIMENTAL STUDY ON STRESS CONCENTRATION FACTORS IN SINGLE AND GROUPS OF END BEARING AND FLOATING STONE COLUMNS

Çekinmez, Zeynep

Ph.D., Department of Civil Engineering

Supervisor   : Prof. Dr. Ahmet Orhan Erol

Co-Supervisor : Inst. Dr. Nabi Kartal Toker

June 2014, 220 pages

In this study, small scale model tests were performed in order to observe effects of column length and undrained shear strength on settlement reduction ratios at different zones, as well as the stress concentration factor. In these tests different loading conditions, i.e. single stone column loading, unit cell loading and group loading, were studied. Stress carried by stone columns under various foundation pressures were directly measured by soil pressure transducers. Surface and subsurface settlements were measured by dial gauge and potentiometric rulers. Variation of stress concentration factor with time is assessed. Unit cell and group behavior with floating and end-bearing columns are compared. An empirical equation to obtain the group settlements from the unit cell settlements, as a function of normalized column length and normalized foundation pressure is proposed. For infinite pattern of column groups, emipirical relationships between

total settlement reduction ratio and undrained shear strength and; stress concentration factor and undrained shear strength are proposed.

Keywords: Stone Columns, Group Effects, Floating Columns, Stress Concentration Factor, Settlement Reduction Ratio.

ÖZ

UÇ VE YÜZER TİP TEKİL VE GRUP TAŞ KOLONLARDAKİ GERİLME DAĞILIM KATSAYISI ÜZERİNE DENEYSEL ÇALIŞMA

Çekinmez, Zeynep

Doktora, İnşaat Mühendisliği Bölümü

Tez Yöneticisi   : Prof. Dr. Ahmet Orhan Erol

Yardımcı Tez Yöneticisi: Öğr.Gör. Dr. Nabi Kartal Toker

Haziran 2014, 220 sayfa

Bu çalışmada, tekil ve grup taş kolonlarda kolon boyunun ve drenajsız kayma dayanımının farklı bölgelerdeki oturma azaltım oranı ve gerilme dağılım katsayısı üzerindeki etkilerini incelemek amacıyla laboratuvar deneyleri yapılmıştır. Deneylerde üç farklı yükleme durumu çalışılmıştır: tekil kolon yüklemesi, hücresel yükleme ve grup yüklemesi. Değişik basınçlar altında taş kolonlar tarafından taşınan gerilmeler özel minyatür basınç hücreleri ile ölçülmüştür. Yüzey ve yüzeyaltı oturmalar kadranlı mikrometre ve potensiyometrik cetveller ile ölçülmüştür. Gerilme dağılım katsayısının zamana bağlı olarak değişimi incelenmiştir. Uç ve yüzer tipi kolonların hücresel ve grup yüklemeleri altındaki davranışları karşılaştırılmıştır. Normalize kolon boyu ve normalize temel gerilmesine bağlı olarak, hücresel yükleme altında gerçekleşen oturmalardan grup oturmasını tahmin etmeye yönelik ampirik denklem önerilmiştir. Tekrarlayan

düzende yerleştirilmiş taş kolon gruplarında, toplam oturma azaltım oranı ile drenajsız kayma dayanımı ve, gerilme dağılım katsayısı ile drenajsız kayma dayanımı arasında ampirik bağıntılar önerilmiştir.

Anahtar Kelimeler: Taş Kolonlar, Grup Etkileri, Yüzer Kolonlar, Gerilme Dağılım Katsayısı, Oturma Azaltım Oranı.

To My Family

ACKNOWLEDGMENTS

TABLE OF CONTENTS

LIST OF TABLES

LIST OF FIGURES

xxii

CHAPTER 1

INTRODUCTION

1.1. General

Stone columns are one of the most effective ground improvement techniques to increase shear strength of soil and rate of consolidation. In general, stone columns are constructed as a large group (infinite group) whereas the on-site acceptance tests are performed either on single column (single column loading) or on small group of few number of columns (finite group). On the contrary with the application, design is based on unit cell assumption. In other words, design, on-site acceptance tests and real case are all generated under different loading and boundary conditions.

The key design parameter in stone columns is the stress concentration factor. There are few studies on the stress distribution between soil and columns. Stress concentration factors were reported whether as a range or a relationship based on only for specific site conditions. There is a lack of information on the realistic selection of stress concentration factor for different cases.

In recent years, floating stone columns have also been used in some applications. There are also many unknowns in stress – settlement behavior related to settlement reduction ratio and stress concentration factor developed in floating column groups.

1.2. Scope and Experimental Program

In this study, small scale model tests were performed in order to observe effects of column length and undrained shear strength on settlement reduction ratios (SRR) at different zones and stress concentration factor (n). In these tests different loading conditions, i.e. single stone column loading, single columns loaded over a footing having same diameter with the unit cell and group loading, were studied. Stress carried by stone columns under various foundation pressures were directly measured by soil pressure transducers. Surface and subsurface settlements were measured by dial gauge and potentiometric rulers.

Chapter 2 presents literature review on stress – settlement behavior of stone columns under unit cell and group loading.

Chapter 3 presents the experiment setups and test procedures for different loading conditions. Consistency, strength and deformation parameters of soil materials are also reported in this chapter.

Chapter 4 includes the stresses and settlements measured in the experiments.

Chapter 5 presents the discussion of test results. Stress – settlement behavior of single column, single columns loaded over a footing having same diameter with the unit cell and group loading tests are presented. Effects of various parameters on the behavior are assessed. Comparison of single columns loaded over a footing having same diameter with the unit cell and group loading and; comparison of group tests in different initial undrained shear strengths of soil are also given.

The conclusions and future studies are presented in Chapter 6.

CHAPTER 2

LITERATURE REVIEW

2.1. Introduction

One of the principal issues in feasibility analyses is finding the construction on an appropriate soil by satisfying the design criteria requirements. Unfortunately, this is not possible in most of the cases. By conventional geotechnical design for the cases where shallow foundation with some foundation depth is not sufficient, pile foundations are used. However in soft clays, where long-term settlements (consolidation settlements) are high with relatively slower consolidation rate exceeding the construction duration, down drag forces (negative skin friction) would be generated on piles adversely affecting the pile capacity. Hence, tendency to ground improvement methods significantly increases for the structures planned to be constructed over sites with poor subsurface conditions.

Widely used ground improvement techniques in soft soils are as followings (Hughes and Withers, 1974):

- Preloading
- Vertical drains (sand or band types)
- Dynamic compaction
- Replacement of soft soil with stronger material
- Lime columns (deep mixing)
- Stone columns (also named as granular piles or granular columns)

First application of stone columns was done in 1830 by French Military engineers in order to support the heavy foundations of the ironworks artillery arsenal in Bayonne. Columns having diameter of 0.2 m and length of 2 m are made up of crushed limestone. Use of stone columns to improve soft soils began in late 1950's in Germany (Craig and Al-Khafaji, 1997). In time it becomes one of the most common techniques to improve soft soils and preferred rather than sand compaction piles which are less stiff. Since sand is more economic than stone, sand piles are used in projects where the large percentage of the soil will be improved. The stone column technique was firstly used in European countries and it extends throughout the world. Today columns up to 15 m length with 0.5 – 1.5 m diameter are able to carry loads up to 300 kN in soft clayey soils (Hughes and Withers, 1974).

Mitchell and Huber (1982) studied a case of wastewater treatment plant project in Santa Barbara in California completed in 1976, which is the first major use of stone columns in USA. They mainly emphasized three different ways to improve the bearing capacity, decrease the settlement and liquefaction potential of highly compressible estuarine deposits. Firstly, driven piles were planned to be used. But due to high noise and vibration levels during installation, loss of lateral support in the event of liquefaction and high cost, this choice was given up. Secondly, removing and replacing by an engineered fill method was proposed. However, due to dewatering and positive groundwater cut-off and groundwater monitoring would be required, this alternative was also eliminated. Finally, stone columns were found to be most effective way to overcome the problems previously defined (Mitchell and Huber, 1982).

Most important difference of stone columns than the other improvement methods is usage of granular material. There are two main advantages of using granular material: Firstly, the granular material is stiffer than other soil materials and has higher frictional strength than the soft clay. Secondly, granular material has

higher hydraulic conductivity. Thus, it fastens the consolidation sequence so the stiffening process (Wood et al., 2000).

Wood et al. (2000) mentioned that in general in order to improve the drainage conditions and accelerate the consolidation; closely spaced vertical drains or drain systems are used. Nevertheless, previous studies show that soil treated by stone columns have significantly larger consolidation rate benefitting from the advantages provided by radial draining path and relieving excess pore pressures by the transfer of load from soil to stone columns. Similarly, Han and Ye (2001) mentioned that stone columns are more effective way to decrease the time of consolidation than the vertical drain method. They stated that on the contrary with the vertical drains, the stress redistribution between the soft soil and the stone column is processed during the time of consolidation which is measured by stress concentration. Moreover, smaller diameter ratio about 1.5 – 5 for stone columns whereas, larger diameter ratio about 5 -100 for vertical drains are used. Due to these two major reasons stone columns are much more effective in increasing the consolidation rate than the vertical drains (Han and Ye, 2001; Van Impe et al., 1997). Also Datye (1982) indicated that the stone columns are more economic than the sand drains and up to 40% settlements can be reduced.

Datye (1982) mentioned that stone columns score over both piles and lime-columns. Stone columns have a main advantage of ability to redistribute the applied load between stone column and soil. That's why stone columns are better than piles by means of preventing the failure of superstructure although large settlements may occur. Moreover, lengths of stone columns are shorter than the required length of piles since stone columns not necessarily extend to bearing stratum. Furthermore, in the areas where drag forces expected to apply, piles are subjected to negative skin friction which significantly decreases the load capacity of them, stone columns score over the piles. In addition to those, stone columns have ability to satisfy extra drainage paths whereas this condition cannot be satisfied in lime columns. Thus, stone columns provide rapid consolidation.

Moreover, stone columns can be constructed by conventional equipment which can be used also for bored piles and vibro compactions. On the other hand, special equipment is used for lime columns.

Van Impe et al. (1997) stated that stone columns can carry larger loads and causes smaller settlements compared with untreated soft soils. In addition, in loose sands, they minimize the likelihood of liquefaction. Madhav (1982) and Murugesan and Rajagopal (2006) summarized the reasons for being the most ideal choice among many opportunities of ground improvement techniques as follows:

(i) moderately increase the bearing capacity

(ii) accelerate the consolidation settlement

(iii) simply be installed

(iv) economic

(v) increase resistance to liquefaction

(vi) increase slope stability of embankments on soft soils

Stone columns may either bear on stiff soil strata (end-bearing) or extend to some depth of highly compressible soft soil (floating). There are only limited studies on group of floating stone columns (Shahu and Reddy, 2011). Moroever, there are only few studies on small group of stone columns (Kirsch and Kirsch, 2010). Ambily and Gandhi (2004) stated that the design of stone columns is still empirical and still no well-defined comprehensive design code is available.

2.2. Theory of Stone Columns

2.2.1. Unit Cell Approach

Unit cell approach is the basic theory for stone columns proposed by Priebe, which is also known as Priebe Method. According to Priebe Method, stone

columns in a large group can be analyzed through unit cell approach (Kirsch and Kirsch, 2010). Unit cell approach assumes unique diameter of stone columns over an infinitely wide area distributed with unique spacing between them. Stone columns except the ones located at the edge of the group are assumed to show same behavior under loaded area.

In unit cell analyses, a stone column located at center of the tributary area and surrounded by soft soil is considered (Figure 2.1). Moreover, since all the columns in a wide area are simultaneously loaded through rigid raft no lateral deformations and shear forces at the boundary surface of the unit cell is assumed (Kirsch and Kirsch, 2010).

In Figure 2.1; D_e is equivalent diameter of unit cell, D is diameter of stone column, A is area of unit cell, A_c is area of stone column, Q is total applied load on unit cell, σ is total applied stress on unit cell, σ_c is stress carried by stone column and σ_s is stress carried by soil.

$$Q = A * \sigma$$

$$A_c = \pi D^2/4$$

$$A = \pi D_e{}^2/4$$
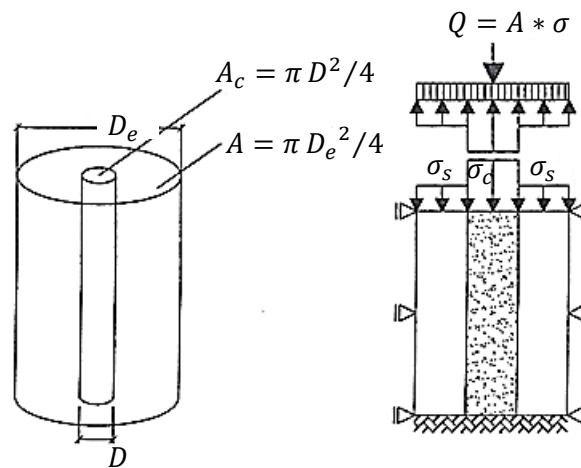
Figure 2.1. Unit cell concept (Kirsch and Kirsch, 2010)

Various group arrangements are illustrated in Figure 2.2 (Madhav, 1982). The equivalent diameter of circular unit cell, D_e, is a function of unique center to center spacing between stone columns, s, i.e.

7

$$D_e = C * s \tag{2.1}$$

Where the coefficient (C) is,

$$C = \begin{cases} 1.05 & for\ triangular\ pattern \\ 1.13 & for\ square\ pattern \\ 1.29 & for\ hexagonal\ pattern \end{cases}$$

Thus, area replacement ratio (a_r), which is defined as the ratio of area of soft soil replaced by stone column (A_c) to the area of unit cell (A), can be calculated by the following equation:

$$a_r = \frac{A_c}{A} = \frac{1}{C^2}\left(\frac{D}{s}\right)^2 \tag{2.2}$$

$$D_e = s\left(\frac{12}{\pi^2}\right)^{0.25}$$

$$D_e = 1.05s$$

(a)

$$D_e = s\left(\frac{16}{\pi^2}\right)^{0.25}$$

$$D_e = 1.13s$$

(b)

$$D_e = s\left(\frac{27}{\pi^2}\right)^{0.25}$$

$$D_e = 1.29s$$

(c)
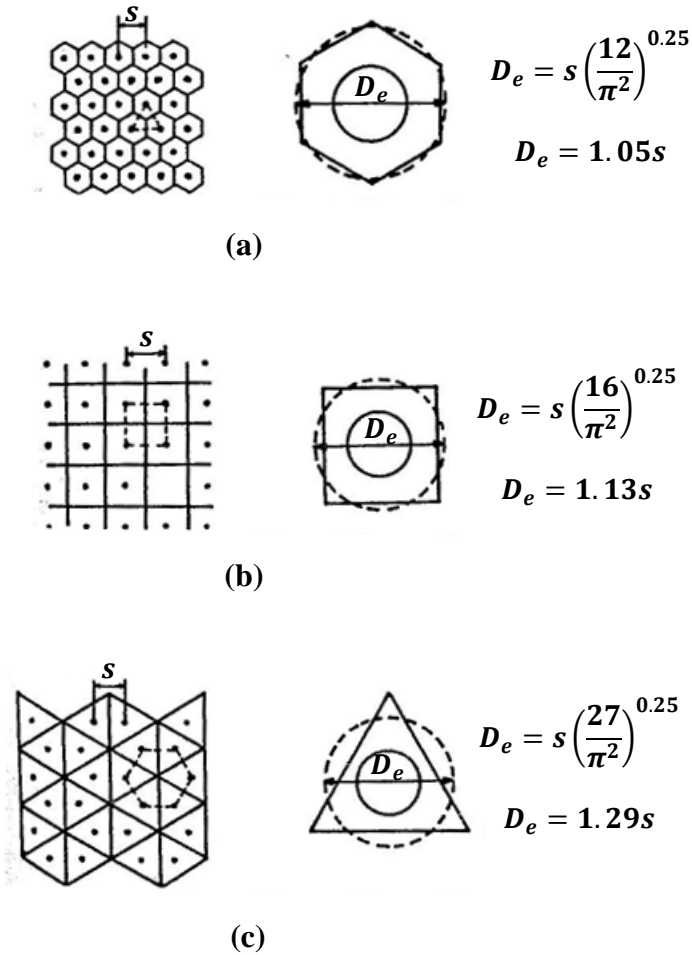
Figure 2.2. Different arrangements of stone column groups (a) triangular, (b) square and (c) hexagonal (Madhav, 1982)

8

Unit cell concept has been used by many researchers. Balaam and Booker (1981) stated that except edge columns in group, unit cell approach is valid through all stone columns.

Thus, analysis of a single unit cell is sufficient in many cases (Ambily and Gandhi, 2006). Kirsch and Kirsch (2010) stated that groups consisting of number of stone columns larger than about 50 can be realistically analyzed through unit cell approach. Furthermore, they also mentioned that if the width of testing area is larger than 3 times of length of stone column, unit cell approach is applicable.

2.2.2. Stress Concentration Factor (n)

Bachus and Barksdale (1989) stated that when a load is applied over soil improved by stone columns, shear strength of stone column increases while settlement in soil decreases. Since the settlement of soil and stone column are approximately same, due to compatibility requirements stress carried by stone columns are larger than the stress acting on soil where the columns are relatively stiffer than soil.

Kirsch and Kirsch (2010) pointed out that the most important parameter controlling the design of stone columns is the stress concentration factor. Stress concentration factor mainly depends on the stiffness of stone column and soil. Since stone column is relatively rigid than the surrounding soft soil, large proportion of applied stress is carried by stone columns. The stress concentration factor (n) is the ratio of stress carried by stone column (σ_c) to stress carried by soft soil (σ_s):

$$n = \frac{\sigma_c}{\sigma_s} \tag{2.3}$$

By the force equilibrium in vertical direction:

$$\sigma = \sigma_c \frac{A_c}{A} + \sigma_s \left(1 - \frac{A_c}{A}\right) = a_r \sigma_c + (1 - a_r)\sigma_s \tag{2.4}$$

and,

$$\sigma_c = \sigma \frac{n}{[1 + (n-1)a_r]} = \sigma\mu_c \ \ and \ \mu_c = \frac{n}{[1 + (n-1)a_r]} \tag{2.5 \ and \ 2.6}$$

$$\sigma_s = \sigma \frac{1}{[1 + (n-1)a_r]} = \sigma\mu_s \ \ and \ \mu_s = \frac{1}{[1 + (n-1)a_r]} \tag{2.7 \ and \ 2.8}$$

Where; μ_c is the ratio of stress carried by stone column to total applied stress and μ_s is the ratio of stress carried by soil to total applied stress. Stress ratios μ_c and μ_s are related to each other by the following equation:

$$\mu_c = n * \mu_s \tag{2.9}$$

Bachus and Barksdale (1989) showed the variation of the ratio of stress carried by soil to total applied stress (μ_s) with stress concentration factor (n) and area replacement ratio (a_r) as illustrated in Figure 2.3.
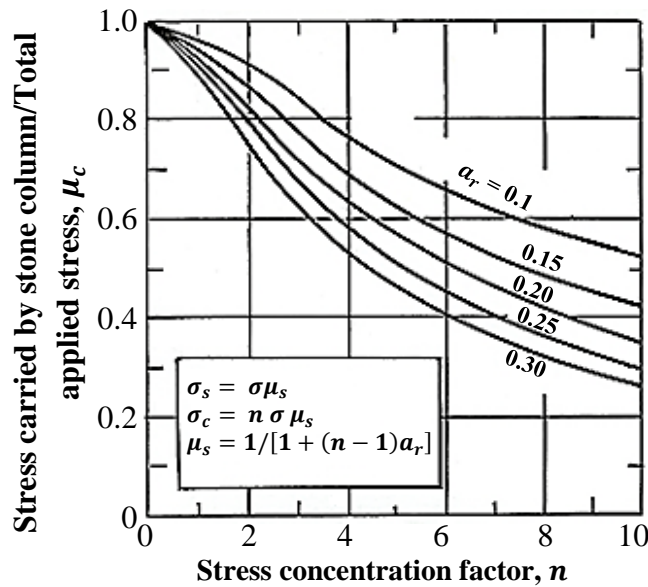
Figure. 2.3. Relation between μ_c, n and a_r (Bachus and Barksdale, 1989)

Han and Ye (2001) stated that the stress concentration factor, n, can be calculated by the following equation;

$$n = \frac{\sigma_c}{\sigma_s} = \frac{m_{vs}}{m_{vc}} = \frac{(1 + v_s)(1 - 2v_s)(1 - v_c)}{(1 + v_c)(1 - 2v_c)(1 - v_s)} \frac{E_c}{E_s} = \xi \frac{E_c}{E_s} \qquad (2.10)$$

Where; v_s: Poisson's ratio of soil, v_c: Poisson's ratio of stone column, E_c: deformation modulus of stone column, E_s: drained deformation modulus of soil, ξ: Poisson ratio factor, m_{vs} and m_{vc}: coefficient of volume compressibility of soil and stone column, respectively. Compressibility parameters should be obtained from the slope of vertical strain versus effective stress plots in the range of applied loads since they are stress-dependent parameters. Note that, in general the range of load is about 100 – 200 kPa for most of the shallow foundations.

From Equation (2.10) it is obvious that stress concentration factor is a function of Poisson ratio factor (ξ) and modular ratio (E_c/E_s) which highly depends on stress level. Han and Ye (2001) mentioned that this is the reason for variable stress concentration factor for different loading levels over a stone column treated soil.

Mitchell and Huber (1985) stated that stress concentration factor is approximately same with the modular ratio between soil and gravel. Moreover, researchers proposed that the stress concentration factor did not vary significantly with depth for a given soil type.

Barksdale and Bachus (1983) stated that the stress concentration factor depends on the relative stiffness between column and soil; in addition length of stone column, area replacement ratio and the characteristics of the granular blanket placed over the composite body. Values of stress concentration factor measured in several field and laboratory tests are given in Table 2.1. In this table, from five of the researchers four of them observed either constant or increasing stress

11

concentration factor depending on the consolidation process. Moreover, the range of average value of stress concentration factor is in between 2.5 to 5.0.

Kirsch and Kirsch (2010) mentioned that, field applications show that n is the range of 1.5 – 6.0. Similarly, Mitchell and Huber (1985) and Han and Ye (2001) stated that stress concentration factor is mainly in between 2 – 6, where mostly 3 – 4 is experienced.

On the other hand, Gniel and Bouazza (2009) stated that stress concentration on the stone columns is measured by means of miniature stress gauge in range of 2 – 3. Murugesan and Rajagopal (2010) mentioned the stress concentration factor is about maximum 9 at small settlements and minimum 3 at large settlements (settlement $> 0.01D$). They also noted that the reason for high values of stress concentration factor at small settlements is the quick loading through strain controlled of loading plate.

Aboshi et al. (1979) performed field tests on sand compaction piles in Japan. They mentioned that stress concentration factor slightly decreases with depth and larger than 3 at each case they studied.

 Han and Ye (2001) stated that due to the stress redistribution in between the stone columns and soil, stress concentration factor varies during constant loading as consolidation proceeds. In other words, initially generated excess pore pressure in soft soil due to the constant instantaneous loading starts to dissipate in time. Due to drainage of some of the excess pore water from the soil to the stone columns with load transfer in the same direction, excess pore pressure gradually decreases. On the other hand, due to lateral stress applied by stone columns as a reaction, excess pore pressure somehow increases. But the net excess pore pressure is decreasing.

Balaam (1978) stated that stress concentration factor will increase in time. Similarly, Barksdale and Bachus (1983) stated that n increases as time of consolidation proceeds since during consolidation process stress on stone column increases while stress on the improved soil decreases. Moreover, the stress concentration factor at the end of the consolidation is steady. Also, Murugesan and Rajagopal (2010) measured stress concentration factor and found out that it increases as lateral confinement increases. On the contrary, Al-Khafaji and Craig (2000) stated that the stress ratio is constant with load level and time.

Datye (1982) noted that, since there is stress redistribution between the soil and the stone columns, also total pressure on the soil decreases during consolidation process.

Table 2.1. Observed stress concentration factors (Barksdale and Bachus, 1983)

Test Type	Design	Location	Stress Concentration Factor (n)	Time variation of n	Stone column length (m)	Subsurface Conditions
Embankment	Square Grid, s=1.7m, D=0.9m, a_r=0.25	Rouen,France Vautrain (1977)	2.8 (average)	Approximately Constant	6.6-7.8	Soft clay c_u=19-29 kN/m^2
Load Test; 45 stone columns (91cmx127cm)	Triangular Grid, s =1.74m, D=1.2m, a_r=0.43	Hampton,Virginia Goughnour and Bayuk (1979)	3.0 (initial) 2.6 (final)	Decreasing	6.15	Very soft and soft silt and clay with sand c_u=9.6-38 kN/m^2
Test Fill 14 stone columns	Triangular grid s =2.1m, D=1.125m, a_r=0.26	Jourdan Road Terminal, New Orleans.	2.6-2.4 (initial) 4.0-4.5 (final)	Increasing	19.5	Very soft clay with organics, silt and sand lenses; loose clayey sand; soft sandy clay
Embankments	a_r = 0.1-0.3	Japanese Studies-Sand compaction piles Aboshi et.al.(1979)	2.5-8.5 4.9 (average)	Increases	Variable	Very soft and soft sediments
Model Test	a_r = 0.07-0.4 D =2.9cm	GaTech Model Tests; Unit cell; Sand column	1.5-5.0	Constant to slightly increasing	Variable	Soft clay; n appears to increase with a_r

*Vertical stress measured just below load except where indicated otherwise

This extra contribution is the reason for the relatively high effectiveness of the stone columns to decrease the time of consolidation (increase the consolidation rate) with respect to vertical drains where the stress concentration is zero.

Barksdale and Bachus (1983) carried out a parametric finite element study on a unit cell composed of single stone column in low compressible soils such as sands, silty sands and silts with linear elastic behavior. The model they used in this study is illustrated in Figure 2.4. For different area replacement ratios and modular ratios (E_c/E_s) where the ratio of length to diameter of stone columns (L/D) varies from 4.5 to 19.5 they obtained stress concentration factors. The relation between stress concentration factor and modular ratio is approximately linear as demonstrated in Figure 2.5. This figure implies that the stress concentration factor takes a value between 2 to 10. Moreover, area replacement ratio has a minor effect on stress concentration factor besides the modular ratio.

Barksdale and Bachus (1983) carried out another parametric finite element analysis on unit cell with nonlinear assumption for stress-strain behavior of both soil and column. Model including geometric and soil properties is illustrated in Figure 2.6. For different values of deformation modulus of clay (E_s) and the ratio of length to diameter of stone columns they obtained stress concentration factors. The relation between stress concentration factor and deformation modulus of clay is depends on L/D ratio as demonstrated in Figure 2.7. This figure implies that the stress concentration factor increases with L/D ratio and takes a value between 3 and 12 for L/D ratios of 5 to 20.

Han and Ye (2001) compared their study and the one carried out by Barksdale and Bachus shown in Figure 2.5 for Poisson's ratios of stone column and soil having 0.15 and 0.45, respectively. This comparison is illustrated in Figure 2.8. A general agreement was observed between two studies.
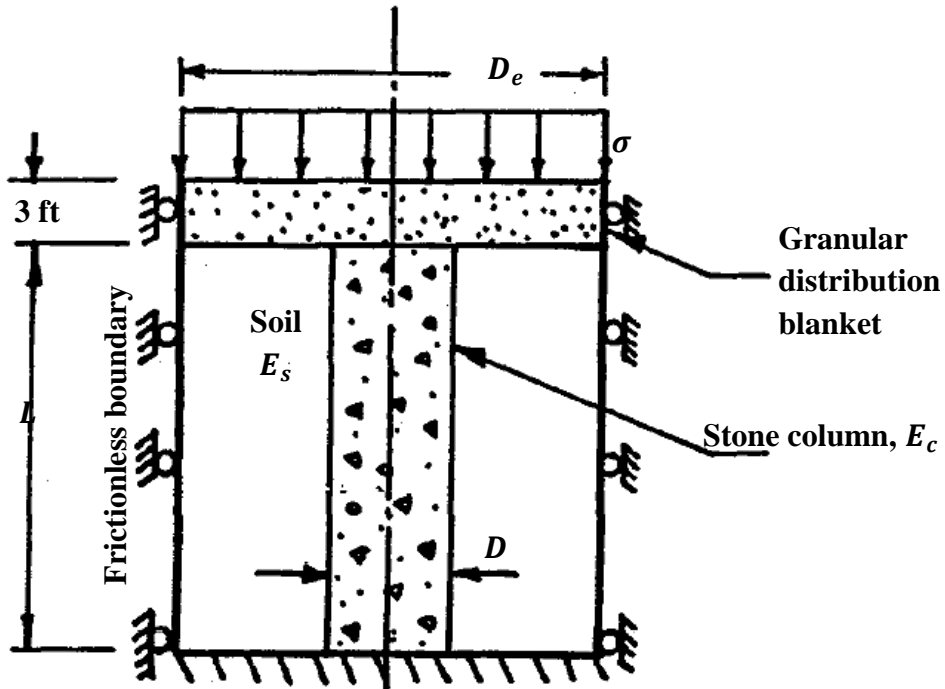
Figure 2.4. Finite element model for linear elastic unit cell analyses

(Barksdale and Bachus, 1983)
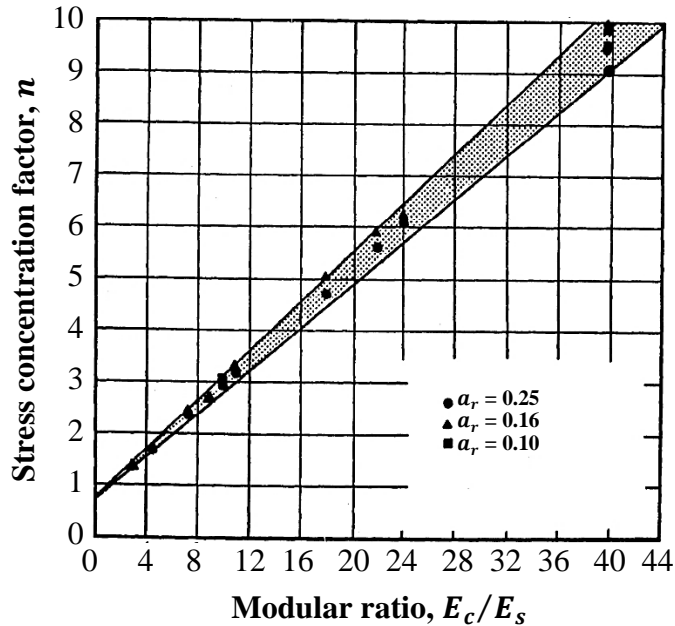
Figure 2.5. Relation between n, E_c/E_s and a_r – linear elastic analysis

(Barksdale and Bachus, 1983)

16
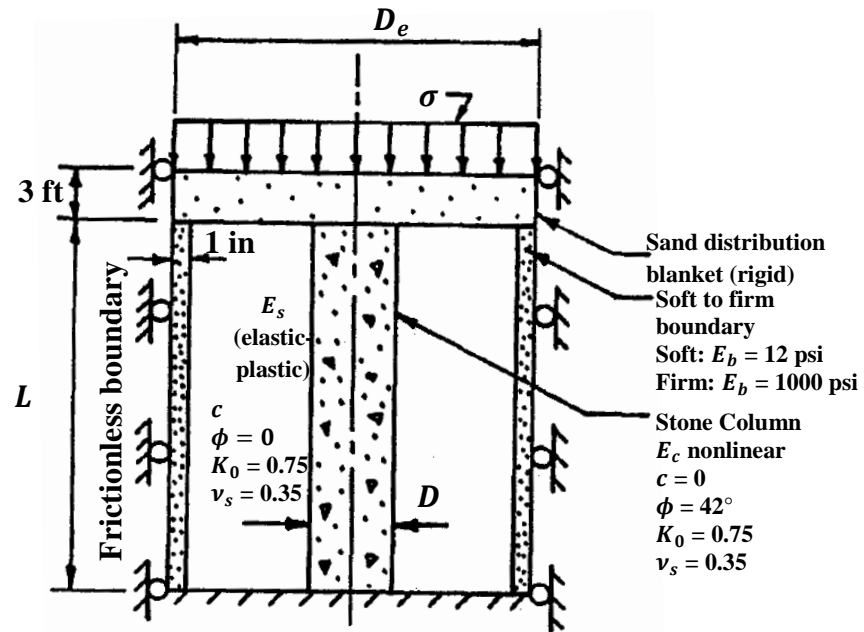
Figure 2.6. Finite element model for nonlinear unit cell analyses

(Barksdale and Bachus, 1983)

Özkeskin (2004) suggested an experimental relationship between modular ratio and stress concentration factor as follows:

$$n = (0.35 - 0.93)\frac{E_c}{E_s} \qquad (2.11)$$

McKelvey et al. (2004) obtained stress concentration factor calculated from the directly measured pressures both at the top of the clay and stone column by means of miniature stress gauges. They proposed that stress concentration factor depends on the length/diameter ratio of stone column (L/D) that in common working load levels, n is smaller than 2 and larger than 4 for short and long columns, respectively (Figure 2.9). This is because; since the short columns punch into the clay bed they are less resistant to loading than the longer columns. Stress concentration factor, n, approaches to value 3 at higher loadings irrespective from L/D ratios as shown in Figure 2.9. The authors stated that those

results are in good agreement with the previous studies based on field measurements.
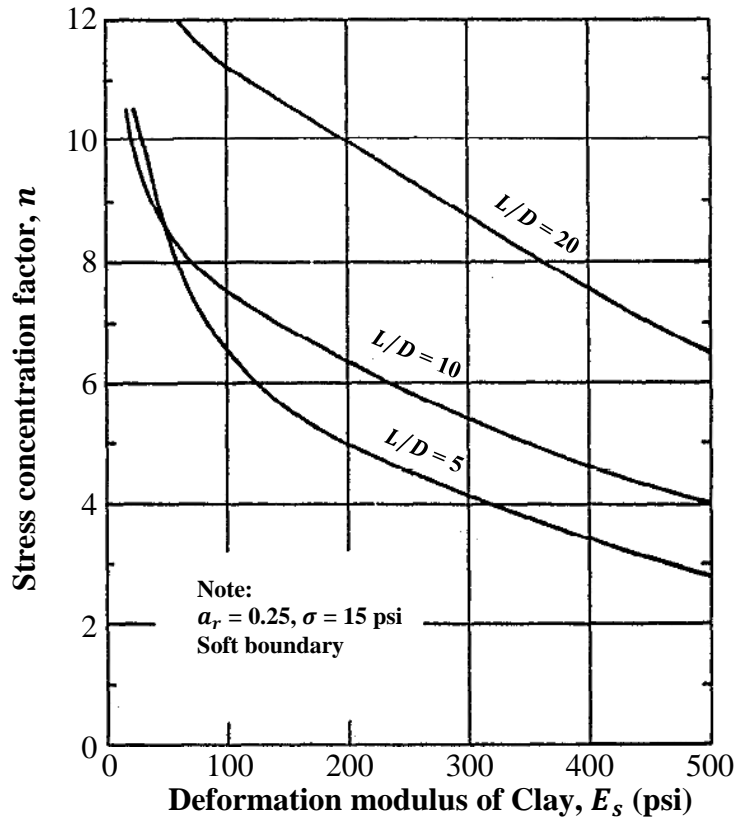
Figure 2.7. Relation between n, E_s and L/D – nonlinear analysis (Barksdale and Bachus, 1983)

Özkeskin (2004) carried out three full-scale load tests on stone columns having length of 3, 5 and 8 meters treating 8 m thick silty clay layer resting on very dense clayey sand layer. The author found that stress concentration factor varies in between 2.1 to 5.6 depending on the applied stress level. Moreover, the author stated that similar stress concentration factors develop for 5 m and 8 m columns since no further stress transformation takes place under 5 m depth. Variation of stress concentration factor with applied stress and length of stone column obtained from this study is given in Figure 2.10.
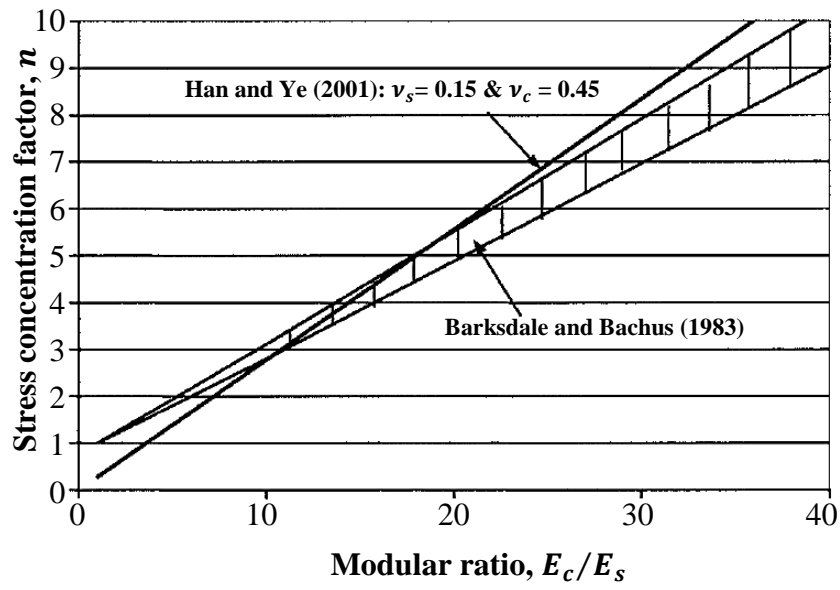
Figure 2.8. Relation between n and E_c/E_s (Han and Ye, 2001)
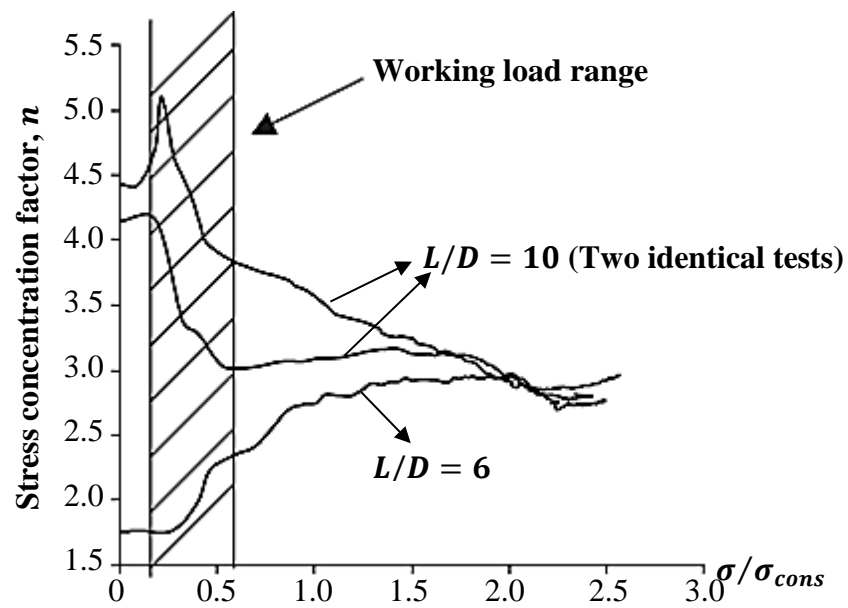
Figure 2.9. Relation between n, σ/σ_{cons} and L/D (McKelvey et al., 2004)

Greenwood (1991) carried out field tests on a single floating stone column constructed by vibrofloatation method. The water table exists at low depths and both column and soil showed drained behavior. Average pressures on stone columns were measured by stress gauges. The relation between stress concentration factor (n) and average ground pressure (σ) applied on footing is obtained as shown in Figure 2.11. It is obvious that, n decreases from 4 to 2 by the increase of ground pressure.
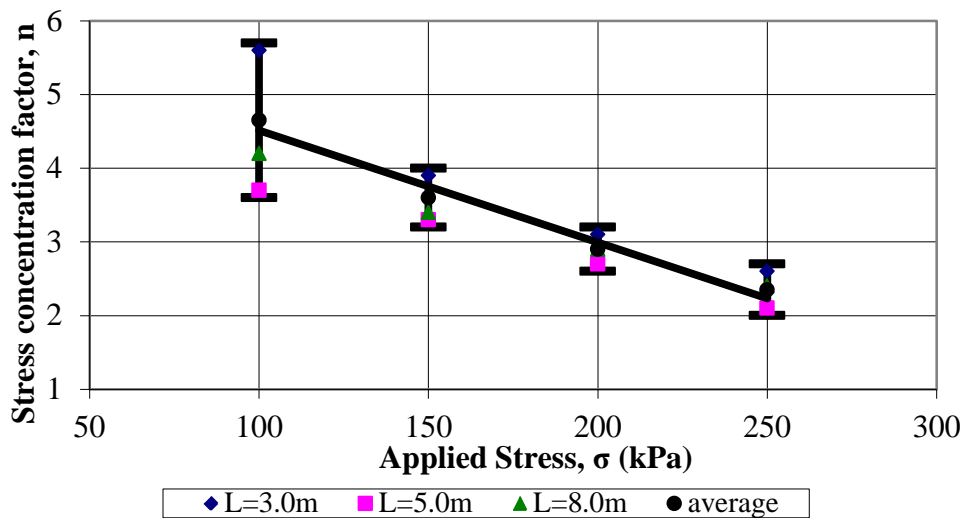
Figure 2.10. Relation between n, σ and L (Özkeskin, 2004)

Field test was performed by Greenwood (1991) at Humber Bridge South Approach site where the end-bearing stone columns are used to decrease the settlement under a fill. End-bearing stone columns are treating soft organic silty clay and resting on stiff boulder clay. Stresses measured on stone columns and soft soil with respect to time for two cycles of loading is illustrated in Figure 2.12 (a). Furthermore, stress concentration factor versus applied stress relation is given in Figure 2.12 (b). From these figures it is observed that stress on stone columns increases where stress on soil remains constant as consolidation proceeds. Moreover, for constant actual overburden stress, stress on columns gradually decreases. Furthermore, stress concentration factor increases as applied stress

increases and reaches 5 at the end of the second cycle where the bulging failure was observed.
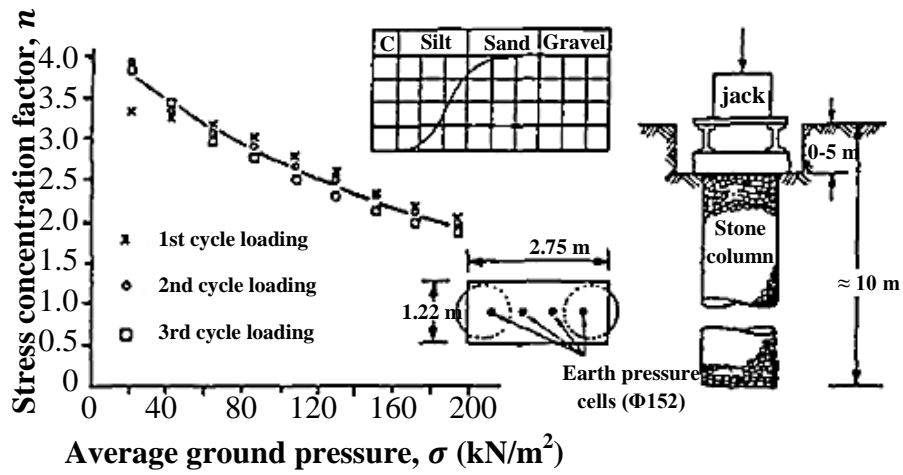
Figure 2.11. Relation between n and σ (Greenwood, 1991)
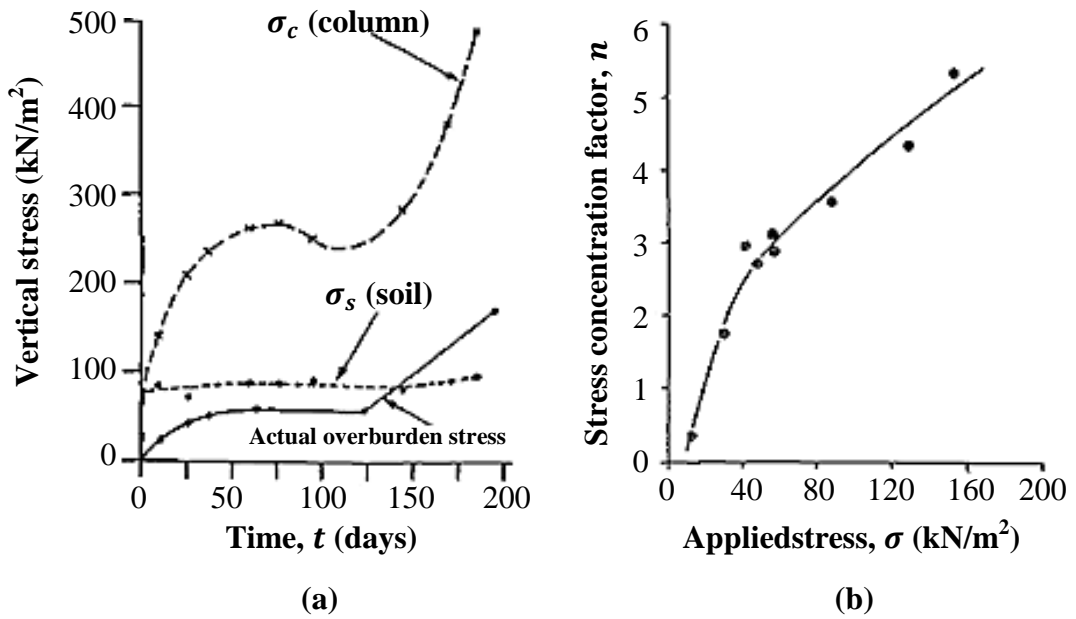
Figure 2.12. (a) Measured stresses and (b) stress concentration factors (Greenwood, 1991)

2.2.3. Settlement Improvement Factor (β)

As previously described, unit cell approach assumes equal settlements for stone column and surrounding soft soil, i.e.

$$S_c = S_s \qquad (2.12)$$

Where; S_c: settlement of stone column and S_s: settlement of surrounding soil.

Priebe (1976) is the first researcher who defines settlement improvement factor, β, which is the settlement ratio of untreated soil (S_u) to soil treated by stone columns (S_t). By using the equal settlement assumption, β can be calculated as in the following equation:

$$\beta = \frac{S_u}{S_t} = \frac{\sigma}{\sigma_s} = 1 + (n-1)a_r \qquad (2.13)$$

Some of the researchers in literature also use the reciprocal of β factor defined as 'settlement reduction ratio'. Settlement reduction ratio is notated by $1/\beta$ or SRR and can be calculated from the following equation:

$$SRR = \frac{1}{\beta} = \frac{S_t}{S_u} = \frac{\sigma_s}{\sigma} = \frac{1}{1 + (n-1)a_r} = \mu_s \qquad (2.14)$$

Although Kirsch and Kirsch (2010) ensured the accuracy of the above equations, they also claimed that settlement improvement ratio does not depend on stress concentration factor and area replacement ratio only but also depends on length of column and modular ratio. Moreover, as number of columns in a group decreases the accuracy of the equation decreases. Shahu and Reddy (2011) emphasized on this issue by stating that most of the designers prefer to analyze the stone columns based on unit cell assumption, in most cases number of stone

columns is limited in a group. Thus, group of stone columns must be studied instead of using unit cell approach.

Datye (1982) mentioned that settlement improvement factor depends on the following factors:

- applied stress level
- spacing between stone columns
- yield capacity of stone column
- thickness of soft layer
- preconsolidation pressure
- method of construction

Greenwood (1970) was the first researcher proposing a design chart for the infinite column grid providing a relationship between the settlement reduction ratio (SRR) and spacing of stone columns for clayey soil having undrained shear strength of 20 and 40 kPa as shown in Figure 2.13. This figure shows that improvement depends on the initial undrained shear strength of soil and increases as undrained shear strength of soil increases.
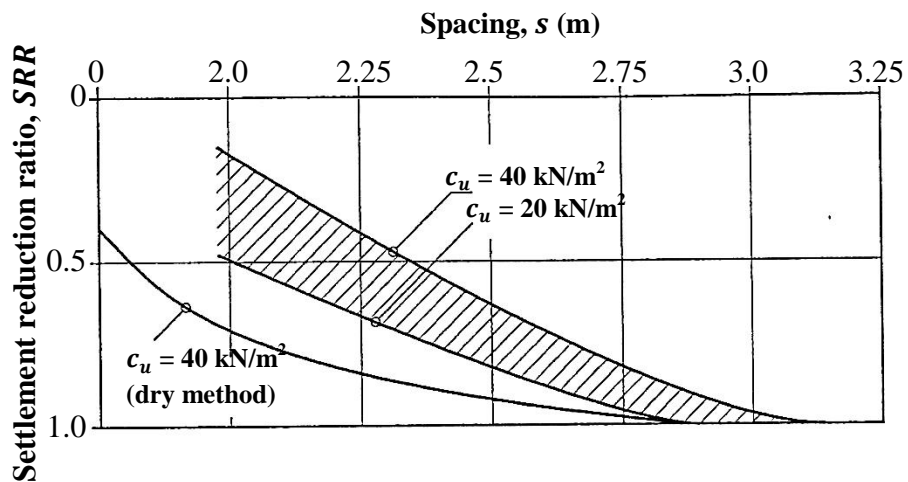
Figure 2.13. Relation between SRR, s and c_u (Greenwood, 1970)

23

Based on the compatibility equation given above, Priebe (1995) proposed the following expressions for settlement improvement factor, β :

$$\beta = \frac{S_u}{S_t} = 1 + \frac{A_c}{A}\left[\frac{1/2 + f(v_s, A_c/A)}{K_{ac}f(v_s, A_c/A)} - 1\right] \tag{2.15}$$

and,

$$f(v_s, A_c/A) = \frac{1 - v_s^2}{1 - v_s - 2v_s^2}\frac{(1 - 2v_s)(1 - A_c/A)}{1 - 2v_s + A_c/A} \tag{2.16}$$

and,

$$K_{ac} = \tan^2\left(45° - \frac{\phi_c}{2}\right) \tag{2.17}$$

Where; ϕ_c: angle of shearing resistance of stone column material and K_{ac}: Rankine's lateral active pressure coefficient for stone column material. Based on the above equations for $v_s=0.3$, Figure 2.14 is given by Priebe (1995).

Priebe (1995) also proposed charts for additional area replacement ratio $(\Delta(A/A_c))$ according to granular pile compressibility for columns in soils having $v_s= 0.3$ (Figure 2.15).

Parameter $\Delta(A/A_c)$ in Figure 2.15, is added to area replacement ratio stated in design and new reduced settlement improvement factor (β_1) is obtained from the following equation:

$$\beta_1 = 1 + \frac{\overline{A_c}}{A}\left[\frac{1/2 + f\left(v_s, \overline{A_c/A}\right)}{K_c f\left(v_s, \overline{A_c/A}\right)} - 1\right] \tag{2.18}$$

and,

$$\frac{\overline{A_c}}{A} = \frac{1}{A/A_c + \Delta(A/A_c)} \tag{2.19}$$

and,

$$f\left(v_s, \overline{A_c/A}\right) = \frac{1 - v_s^2}{1 - v_s - 2v_s^2} \frac{(1 - 2v_s)\left(1 - \overline{A_c/A}\right)}{1 - 2v_s + \overline{A_c/A}} \qquad (2.20)$$

Where; $\overline{A_c}$ is the corrected area of stone column.
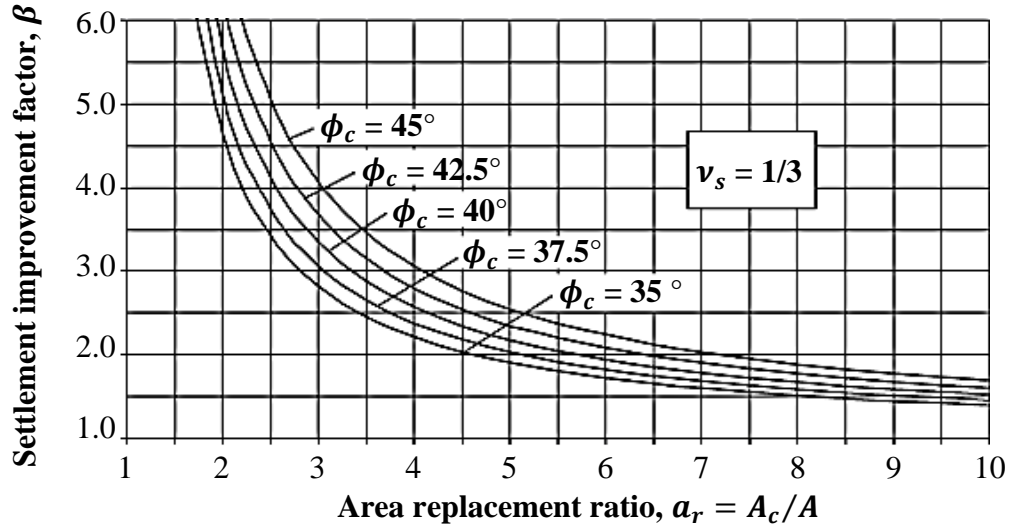
Figure 2.14. Design chart for vibro-replacement (Priebe, 1995)
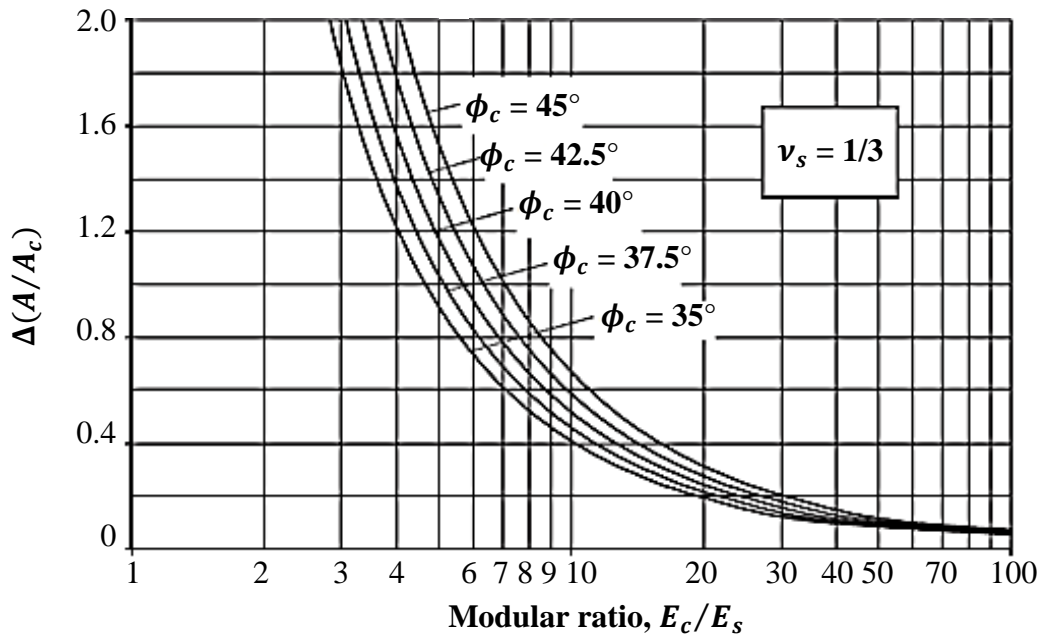
Figure 2.15. Effect of column compressibility (Priebe, 1995)

For the application of Equilibrium Method, for low applied stresses and long stone columns Barksdale and Bachus (1983) proposed a relation between area replacement ratio and settlement improvement factor for stress concentration factors equal to 3, 5 and 10.

This study was compared with the one obtained from Priebe Method, as shown in Figure 2.16. Equilibrium Method gives slightly higher values of improvement as shown in Figure 2.16.
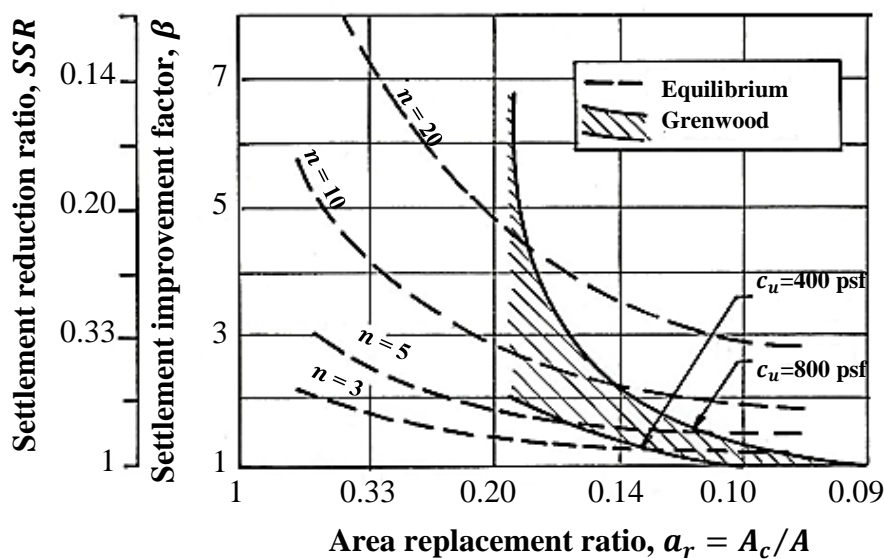
Figure 2.16. Comparison of SRR values (after Barksdale and Bachus, 1983)

Craig and Al-Khafaji (1997) stated that the major factor affecting the settlement improvement factor is the stiffness of granular column. They obtained a similar relation between settlement improvement factor and area replacement ratio with the one proposed by Priebe (1995), as shown in Figure 2.17.

Özkeskin (2004) reported that the settlement reduction ratio decreases by the increase of applied stress as shown in Figure 2.18. Settlement reduction ratio takes a value of 0.6 and 0.2 for lower and higher stress levels, respectively. In

26

addition, it is mentioned that length of stone column has minor effect on settlement reduction and for longer stone columns slightly larger the improvement in settlement was obtained.

Datye (1982) mentioned that as load intensity increases settlement reduction ratio increases. Larger values of SRR are encountered in groups of stone columns having small spacing (Figure 2.19).
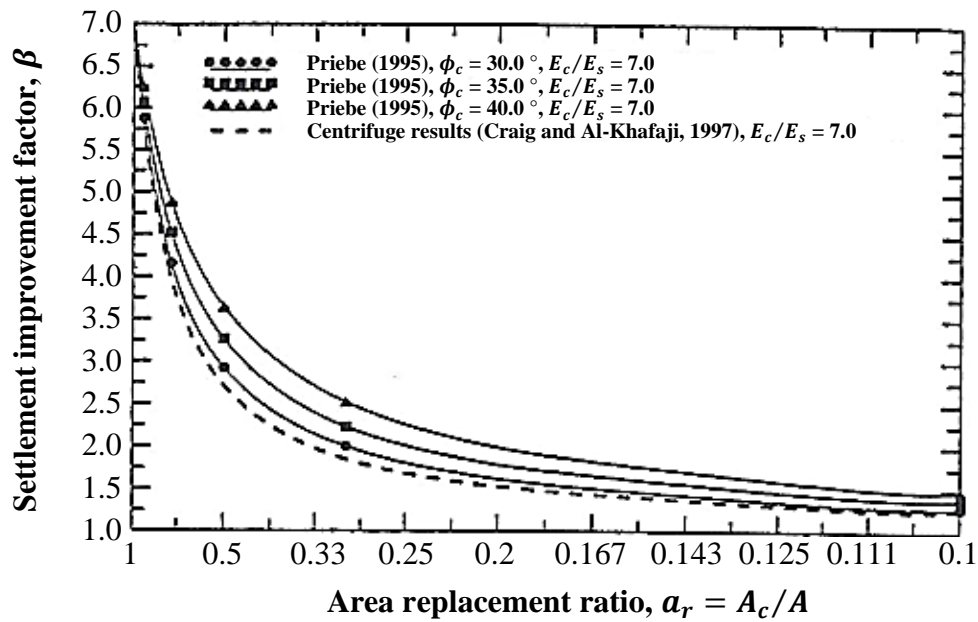
Figure 2.17. Comparison of SRR values (Craig and Al-Khafaji, 1997)

Wood et al. (2000) indicated that the settlement under same load decreases by increasing the diameter of stone column.
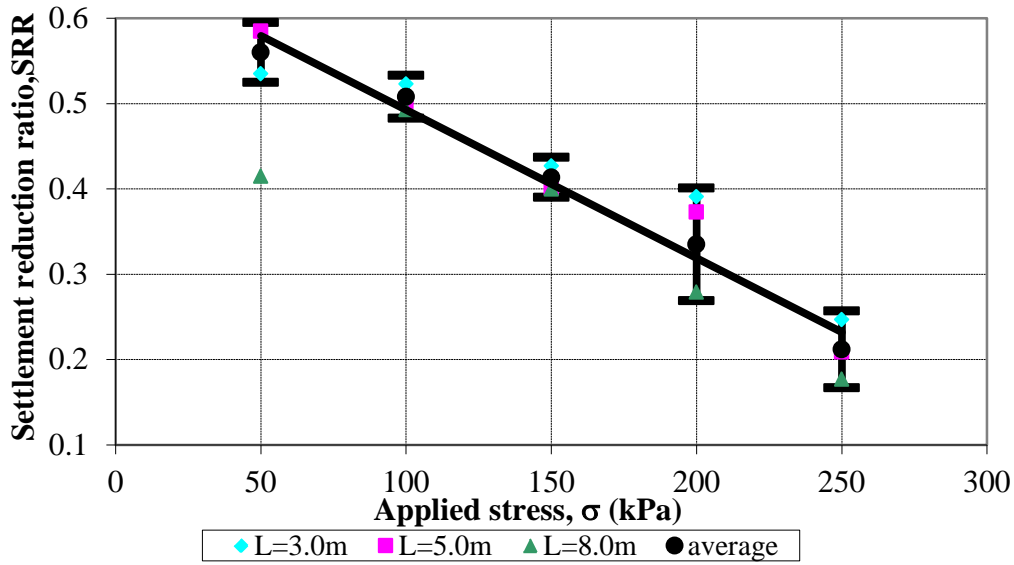
Figure 2.18. Relation between _SRR_ and _σ_ (Özkeskin, 2004)
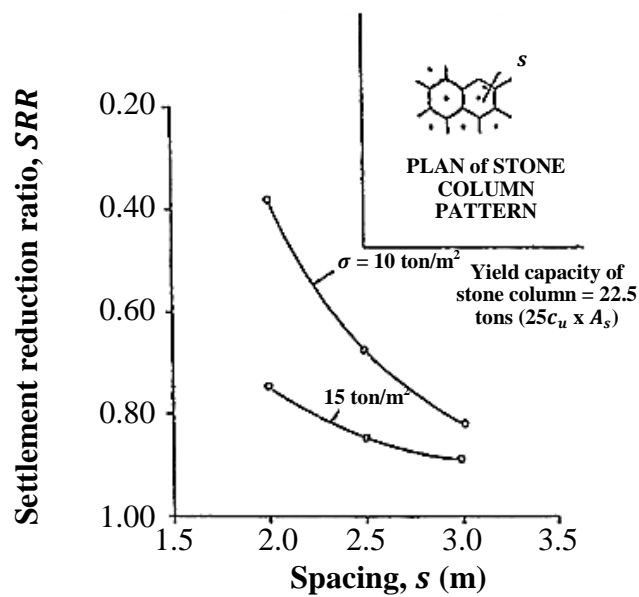
Figure 2.19. Relation between _SRR_, _s_ and _σ_ (Datye, 1982)

Mitchell and Huber (1985) analyzed the group of stone columns under the wastewater treatment plant project in Santa Barbara in California completed in

1976, which is the first major use of stone columns in USA, through axisymmetric non-linear finite element program. They compared the results of FEM analysis with the results of load-settlement behavior obtained from the field load tests. The authors stated that foundations should be placed on a gravel blanket over soft soil improved by stone columns, in order to provide uniform stress distribution to columns and to provide drainage. Thickness of this blanket varies between 0.3 – 1 m and should be determined according to spacing between stone columns. They indicated the settlement of the treated ground with stone columns is about 1/3 of the one of untreated ground according to Priebe's method. Whereas, Aboshi et al. (1979) reported this ratio is about 0.4 – 0.5. Finite element analyzes performed by Mitchell and Huber (1985) show that this ratio is about 0.3, similar to Priebe's method.

Zahmetkesh and Choobbasti (2010) stated that for floating stone columns ($L/H<$ 1 where H is thickness of compressible layer), larger area replacement ratios cause smaller settlement reduction factors.

On the other hand, as L/H decreases settlement reduction factor increases. They stated that settlement reduction ratio (SRR) can be obtained by the following equation:

$$SRR = \frac{E_s}{E_{eq}}$$

(2.17)

Where; E_s is deformation modulus of untreated soil at a stress level and E_{eq} is equivalent secant modulus of the composite body.

$$E_{eq} = \frac{\sigma}{\varepsilon}$$

(2.18)

and;

$$\varepsilon = \frac{S_t}{H} \qquad (2.19)$$

Where; σ is stress applied over the composite body, ε is strain developed through the composite body and S_t is average settlement of treated soil.

2.2.4. Failure Mechanisms of Stone Columns

Stone columns under compressive loads may fail through several failure mechanisms. Diameter, length and the spacing are the parameters defining the failure type of the stone columns (Wood et al., 2000).

Hughes and Withers (1974) stated that stone columns may be subjected to three different loading patterns:

(i) **Small Footing Loading:** Single columns to support loads applied by small footings where the lateral restraint is equal through periphery of the stone column.

(ii) **Widespread Loading:** Stone columns to support loads applied by large footings where the lateral restraint is equal in each direction and increases as soil settles.

(iii) **Strip Footing Loading:** Stone columns constructed through a line to support loads applied by strip footing where the lateral restraint is provided only in the direction of strip footing.

Kirsch and Kirsch (2010) proposed that principal loading situations of stone columns can be summarized as shown in Figure 2.20. Foundation stresses acting on granular mat or foundation, is distributed between stone column and soil

depending on the stiffness of them. Over material having higher stiffness, i.e. stone columns, higher contact stresses develop.

Moreover, Kirsch and Kirsch (2010) mentioned that failure mechanism would develop at one of the interfaces shown in Figure 2.21.

Single column   **Single column below footing**   **Column group below footing**   **Column grid below embankment**
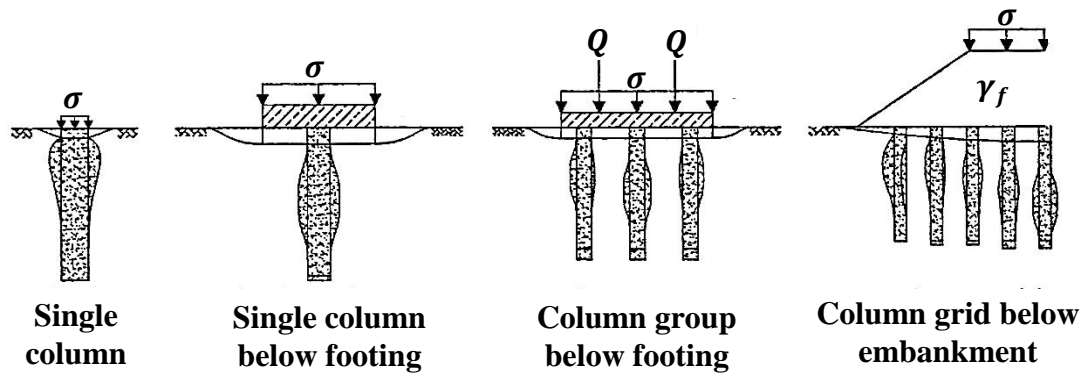
Figure 2.20. Different loading scenarios for stone columns

(Kirsch and Kirsch, 2010)

Interaction
① footing – column
② footing – soil
③ column – soil
④ column – column
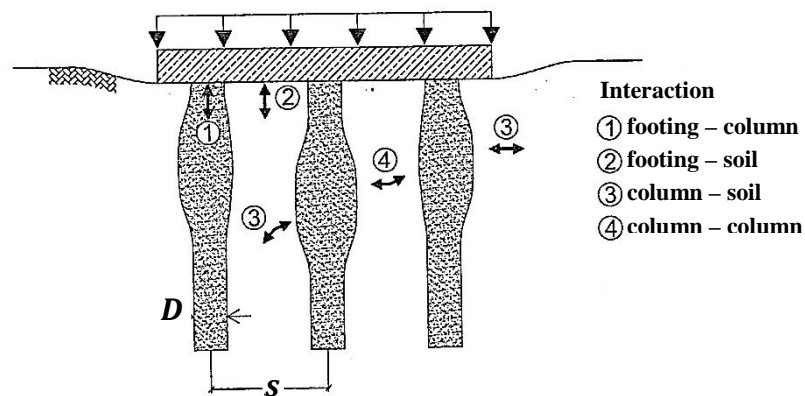
Figure 2.21. Interaction of load application with stone columns and soil

(Kirsch and Kirsch, 2010)

2.2.4.1. Single Stone Columns

In contrast to pile foundations where the load carrying mechanism develop depending on the tip and skin resistances, stone columns get strength by the lateral confinement depending on the load transfer by stimulating the lateral earth pressure by soil to column (Kirsch and Kirsch, 2010). By the excessive lateral stress, column bulges triggering the soil deformation due to the further increase in lateral stress.

Kirsch and Kirsch (2010) stated that isolated footings with single stone columns may fail due to following reasons:

- bulging of long, end-bearing columns
- shearing of short, end-bearing columns
- punching failure by sinking of short, floating columns
- bulging in deeper layers

Bulging of stone column is the main reason for the failure, when the surrounding soil cannot support any more lateral stress (Figure 2.22(a)). In homogenous soils bulging occurs at depth up to about $4D$. For short stone columns having length smaller than $4D$, punching of stone column would occur (Figure 2.22(c)).

On the other hand if such a short column is bearing on a hard stratum then shear surfaces will develop through the column head and the adjacent soil close to grade (Figure 2.22(b)). Failure also may occur due to bulging at deep say larger than $4D$ if there is sufficient thick soft soil layer under the stone column (larger than $2D$) as shown in Figure 2.22(d).
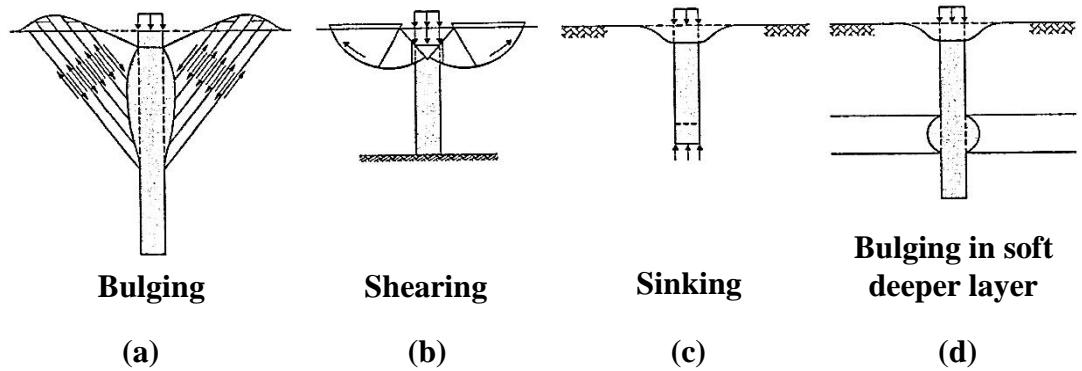
Figure 2.22. Failure mechanisms of isolated stone columns
(Kirsch and Kirsch, 2010)

Van Impe et al. (1997) mentioned that bulging and pile failure mechanisms occur in longer and shorter columns than the critical length, respectively. Thus both mechanisms are 'mutually exclusive' where the actual capacity is the limiting stress of this mutual mechanism.

Madhav (1982) mentioned that there is a critical length that for lengths larger than it, no significant further increase in bearing capacity is encountered and bulging failure occurs. On the other hand, columns shorter than this critical length show pile type failure since loads are transmitted to entire depth of stone columns, whereas in longer ones not. The critical length of granular pile (L_{cr}) can be obtained depending on internal friction angle of column material (ϕ_c), undrained shear strength of soil (c_u), unit weight of soil (γ_s), diameter of granular pile (D), diameter of footing (D_f) from Figure 2.23.
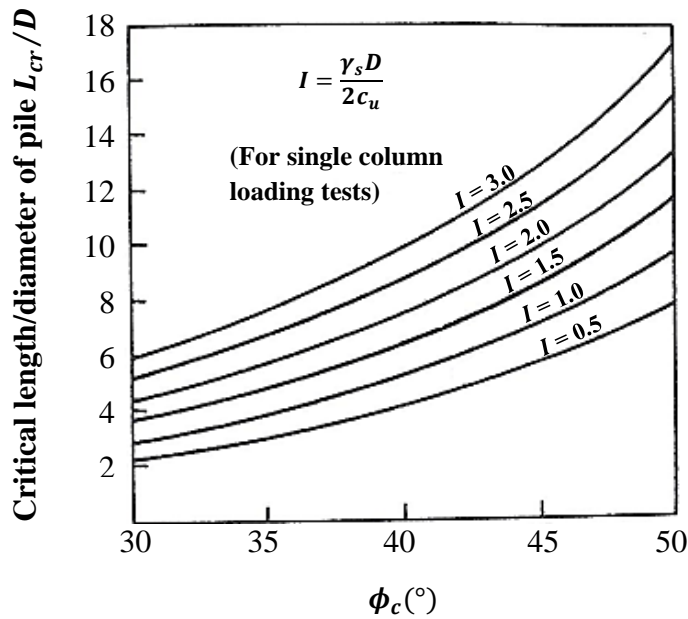
Figure 2.23. Relation between L_{cr}/D and ϕ_c (Madhav, 1982)

Bae et al. (2002) studied both single and group of end-bearing stone columns in a laboratory tank consolidation tests. Study was also supported by FEM analysis. From the results of model tests and FEM analysis, they concluded that single stone column bulges at a depth of 1.6 – 2.8 times of diameter of stone column. Similar to Wood et al. (2000), also Bae et al. (2002) stated that the depth of bulging is affected by diameter of column rather than length of stone column and undrained shear strength of soil. In addition, they indicated that the settlement under same load is smaller for larger the diameter of stone column.

Ambily and Gandhi (2006) carried out laboratory model tests and two dimensional axisymmetric FEM analyses on single stone column in a unit cell. They observed that single stone column fails due to bulging and they bulged at depth approximately equal to $0.5D$. This is confirmed also by FEM analyses.

Murugesan and Rajagopal (2006) studied single end bearing stone column through various FEM analyses. They found that the lateral stress mobilized around the stone column is similar for columns with different diameters under same loading. Moreover they mentioned that bulging of stone column upon loading will be occurring at a depth of 1.5D - 2.0D from the ground surface.

Various researches on failure mechanisms of single stone column show that depending on strength parameters of column and soil, length and diameter of column failure shape of it differs.

2.2.4.2. Group of Stone Columns

Kirsch and Kirsch (2010) stated that stone column groups show similar but more complicated failure mechanisms due to various interactions between soil-column, soil-mat and column-mat as demonstrated in Figure 2.21. Possible failure mechanisms observed under rigid foundations supported by group of stone columns are illustrated in Figure 2.24.

(a)	**(b)**	**(c)**
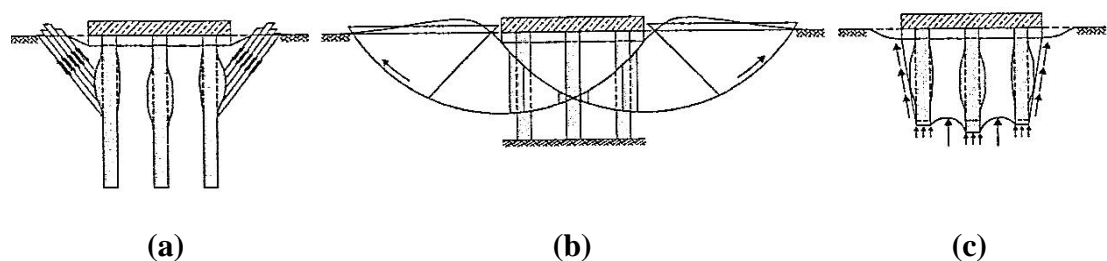
Figure 2.24. Failure mechanisms for column groups
(Kirsch and Kirsch, 2010)

Hughes and Withers (1974) mentioned that the bearing capacity problem is only valid for the columns at the edge of the group for large group of stone columns.

McKelvey et al. (2004) studied group of stone columns in two different materials: (a) Trinity College Dublin (TDC) transparent clay (b) commercially available kaolin clay.

TDC is relatively common in soil modeling having properties similar to Kaolin clay (similar compression and strength properties with the ones for Kaolin clay) and used to visualize deformation mode of the stone columns at each stage of the loading. From the shapes of failure, the failure types are estimated. On the other hand, Kaolin clay is used in tests to observe the load-deformation characteristics of the treated soil. Influence of the effects such as length/diameter ratio of stone column, spacing between stone columns so the area replacement ratio and shape of the loading plate (circular or strip) are also investigated through large scaled laboratory tests. Photos taken from group of stone column tests in TDC from different stages of loading for two different column length/diameter ratio (L/D) are illustrated in the Figure 2.25.

McKelvey et al. (2004) found that under circular footings both short ($L/D = 6$) and long ($L/D = 10$) floating columns tend to bulge in unrestrained directions as applied stress is increased. Entirely bulging of short column and punching about 10 mm into the soil are observed whereas the bulging in long column is observed only at a few diameters depth from the top of the stone column. This implies that only a small portion of the load is transmitted to larger depths in the case of long column. Those findings lead up authors to decide $L/D = 6$ is too short that the columns totally deform and somewhat punch into the clay where $L/D = 10$ is too long since bottom parts of the column is not deformed. Thus, they stated that the optimum L/D ratio of stone columns is in between 6 – 10. Moreover, for L/D ratio larger than 10 there is no significant increase in bearing capacity but significant increase in settlement improvement ratio is still valid.

Experiments carried out by McKelvey et al. (2004) show that stone columns may fail due to 3 different modes:

- Bulging
- Bending
- Shearing

They observed that short columns fail generally due to punching of the columns into the soft soil and bulging entirely. On the other hand, there is no punching and in general top portion of the long stone column bulges. Shear planes are encountered generally in long stone columns. All columns bend towards the unrestrained direction regardless of the L/D ratio.

McKelvey et al. (2004) also pointed out that experimental studies are rare in the area of group of small numbers of stone columns loaded under footings. The deformed shape of a single stone column is very different from the one in a large group.

Another study on the failure mechanisms of group of stone columns was performed by Wood et al. (2000). Similar to McKelvey et al. (2004) they also estimated the mode of failures and additionally the stress distributions from the shapes of the stone columns at the end of the test (Figure 2.26). Wood et al. (2000) added punching to failure mechanisms given by McKelvey et al. (2004). As a result, they described 4 different mode of failures (Figure 2.27) observed through laboratory tests as the followings:

Mode 1: Bulging: occurs if a column is loaded and able to radially expand freely by closely adjacent columns. Because of increase in the mean stress, column bulges. (Mode A in Figure 2.26). This type of failure generally occurs in columns at the center or near to the center of the footing. Note that depth of bulging increases as the area replacement ratio increases. This type of failure mostly

occurs columns under rigid footings in which a cone of somewhat undeforming soil is pushed down with the footing.

(a)   (b)
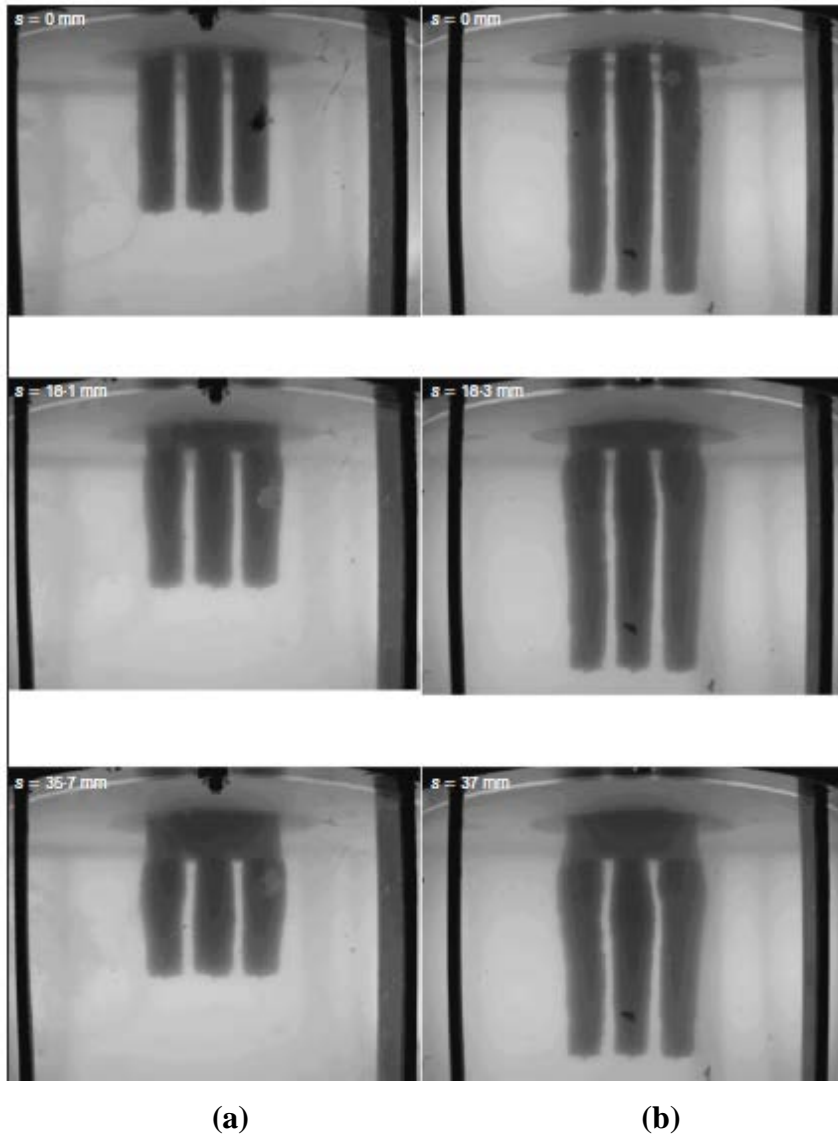
Figure 2.25. Photographs of group of sand columns (a) *L/D*= 6 and (b) *L/D*= 10 (McKelvey et al., 2004)

Mode 2: Shear Plane: occurs when high stress ratios are applied on stone column with little lateral restraint, thus little possibility of increase in mean stress.

Due to global concentration of deformation caused by overall failure mechanism, column fails by shearing though a diagonal plane (Mode B in Figure 2.26). Generally occur at columns near to edge of the footing.

Note: A combination of mode 1 and 2, a combination of locations of bulging and shear planes, can be used to estimate the zone of influence under the group of stone columns. This zone is approximately conical with an angle of θ near from the edges (Figure 2.28 (a)). Angle θ increases with increase of area replacement ratio (Figure 2.28 (b)). Moreover, they noticed that the influence depth strongly depends on the diameter of footing rather than the diameter of stone column.

Mode 3(a): Short Column Penetration in Soft Clay: occurs when columns are sufficiently short to transmit significant portion of the load to soft clay layer beneath the tip of the column. Thus, column penetrates into the soft clay (Figure 2.27 (b)). This effect is more pronounced in short columns with higher replacement ratios.

Model 3(b): Long column absorbs deformation along its length: As length of the column increases load transmitted to base soil decreases. If a column is sufficiently long then penetration of footing has been absorbed along the length of columns (Figure 2.27 (c)). This effect is more pronounced in long columns with smaller replacement ratios.

Model 4: Bending (buckling): occurs when column with no significant lateral strength is subjected to high axial loads. Columns behave like a laterally loaded piles and lateral movements occurring in the clay beneath the footing. Columns are like model inclinometers (Figure 2.27 (d)). Generally occurs in columns outside of the loading plate.
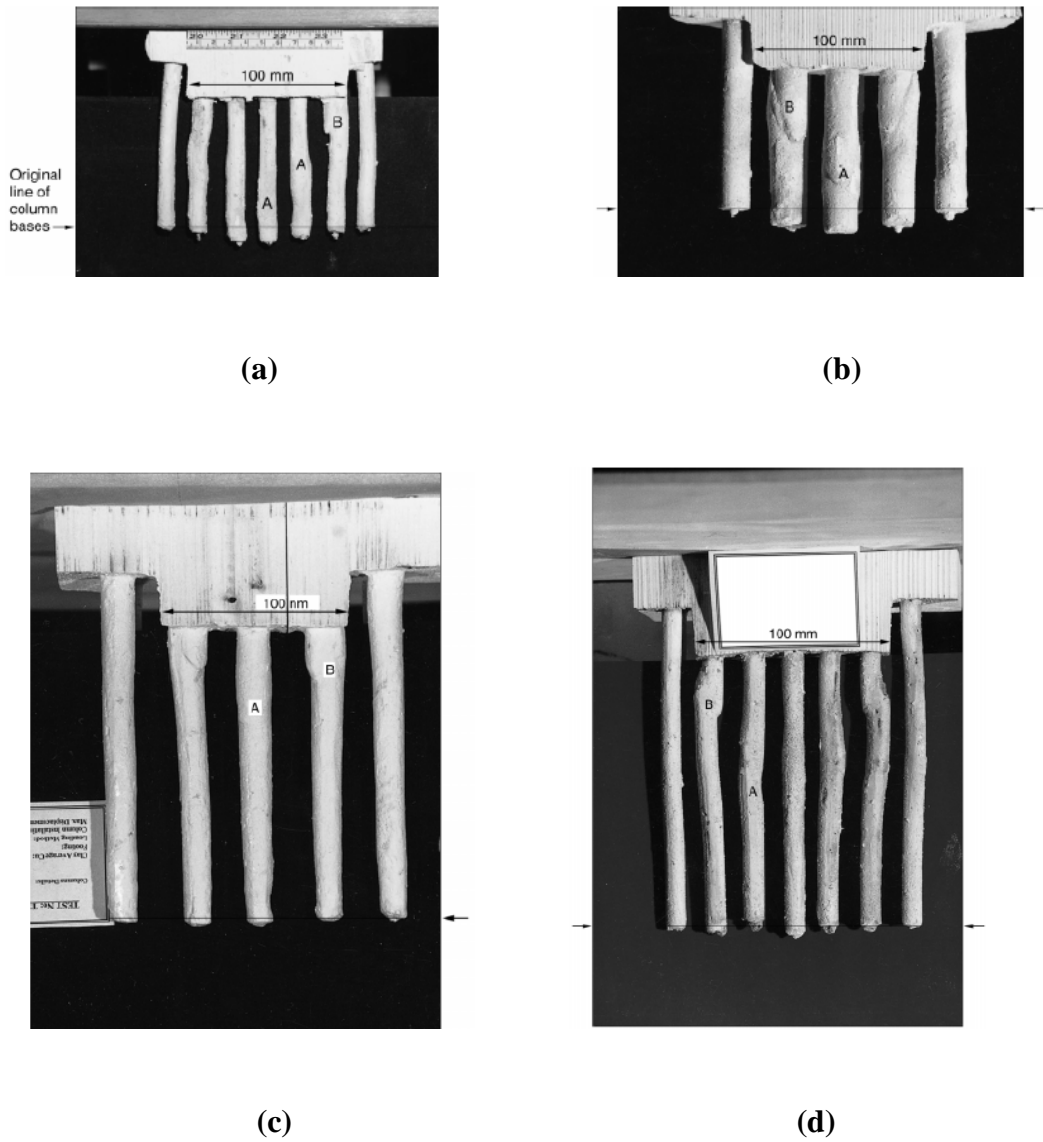
Figure 2.26. Photographs of deformed sand columns where the arrows indicate the original level (a) $L/D = 9$ and $a_r = 24\%$ (b) $L/D = 5.7$ and $a_r = 30\%$ (c) $L/D = 9.7$ and $a_r = 24\%$ and (d) $L/D = 14.5$ and $a_r = 24\%$ (Wood et al., 2000)
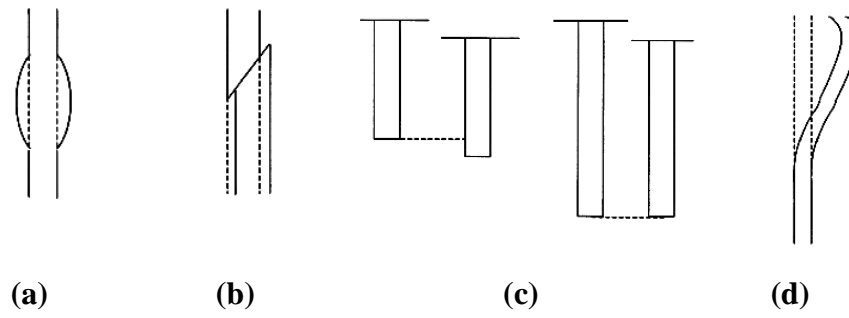
Figure 2.27. Modes of failure mechanisms develop in group of stone columns (a) bulging (b) shear failure (c) punching (d) bending (buckling) (Wood et al., 2000)
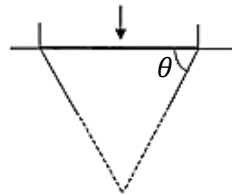
(a)
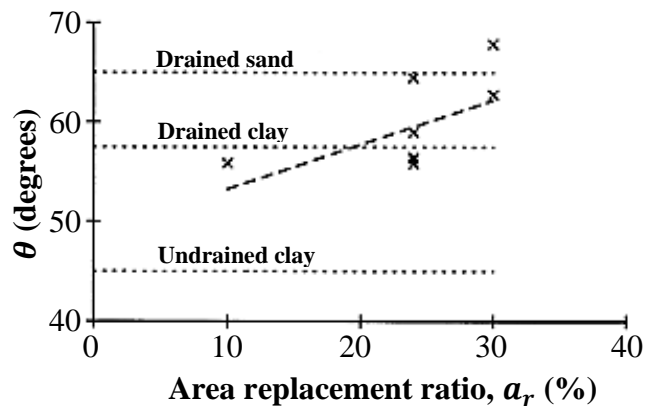
(b)

Figure 2.28. (a) 'Rigid' cone beneath footing and (b) relation between θ and a_r (Wood et al., 2000)

Bae et al. (2002) studied group of end-bearing stone columns in a laboratory tank consolidation tests. Tests were also supported by FEM analyses. Bae et al. (2002) stated that bearing capacity of stone column is highly depend on undrained shear strength of soil and area replacement ratio. FEM solutions showed that inner columns in a group of end bearing stone columns bulging failure mode is occurred conically due to confining effect around the columns. Moreover, they mentioned that failure angle (θ) is smaller in short columns (θ in shorter columns: 14 - 21°; θ in longer columns: 25 - 41°). FEM analyses show that bulging failure (in center columns) occurs earlier than the shear plane failure (in columns far away from the center of group).

Ambily and Gandhi (2006) observed there is no bulging failure in group of stone columns opposite to single stone columns. This result is also approved by FEM analyses.

2.3. Results of Previous Studies on Stone Columns

In this section, findings of previous studies are summarized. The details of the experimental setup are given in Appendix A.

2.3.1. Studies on Single Stone Column in a Unit Cell

As previously discussed, single stone column behavior is generally observed together with its tributary area in a unit cell. Van Impe et al. (1997) studied the ultimate load capacity of stone columns and effect of nonhomogeneity of stone columns on stiffness and settlement. They stated lateral reinforcement (for instance by geosynthetics) provides improvements in lateral confinement, so the strength and stiffness of soils around the stone columns. Previous observations indicate that original SPT-N values increase by more than 100%. Also, it is noted that compactibility of stone column material increases with depth by the increase of undrained shear strength of soil.

Van Impe et al. (1997) mentioned that settlement of single granular pile is affected from homogeneity of soil. Following two assumptions would lead to different settlement values:

Assumption 1: Constant deformation modulus with depth (homogeneous stiffness)

For simplicity deformation characteristic of materials are assumed to be constant and settlement of floating and end-bearing stone columns can be estimated by using one of the following methods:

(i) Continuum approach proposed by Poulos and Davis (1970)

(ii) Simple shear layer concept proposed by Randolph and Worth (1978)

Assumption 2: Increasing deformation modulus with depth (nonhomogeneous stiffness)

Increasing confining stress with depth would seriously affect the stiffness and strength of granular soils.

Settlement of floating and end-bearing stone columns can be estimated by a simple method proposed by Madhav and Rao (1996). Considered parameters are shown in Figure 2.29. Settlement decreases as rate of increase in deformation modulus of stone column material with depth increases (α) as shown in Figure 2.30. In Figure 2.29, E_{c0} is deformation modulus of stone column at the top, z is depth, δz is thickness of infinitely small element, E_b is deformation modulus of bearing stratum and ν_b is Poisson's ratio of bearing stratum.
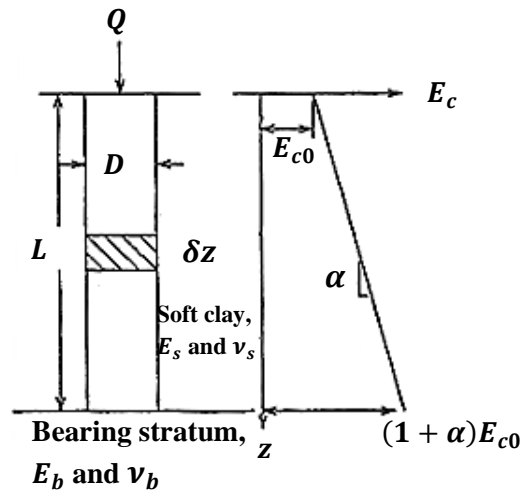
Figure 2.29. Nonhomogeneity of stone column (Van Impe et al., 1997)

Shahu et al. (2000) mentioned that the most of the stone columns fail due to bulging at a depth of few diameters near to the surface due to the high stress concentration at top of the stone columns. They also stated that those surface stresses are highly affected from the presence of the granular mat that if a suitable thickness of granular mat (t_f) is provided the stress concentration at top of the stone column significantly reduces. Moreover, the settlement reduction ratio decreases. Authors stated the sufficiently thick (rigid) and smooth granular mat, significantly decreases the dependency of bearing capacity on the parameters such as stress ratio, depth ratio etc.

Consequently, smaller area replacement ratio will be sufficient for thick granular fill. Moreover, sufficiently thick granular mat allows more uniform stress and settlement distribution. Figure 2.31 proposed by Shahu et al. (2000) shows the stress concentration at different depths of soil. It is clear that the adequate thickness of granular mat reduces the stresses carried by granular pile entirely. Shahu et al. (2000) also stated that the shear stress at the column-soil interface decreases as depth increases due to the load transfer from granular column to soil.

Bae et al. (2002) studied both single and group of end-bearing stone columns in a laboratory tank consolidation tests. Study was also supported by FEM analyses. Bae et al. (2002) also studied effect of rigidity of mat on the load sharing behavior. They concluded that when there is a rigid mat, the load carried by stone column is decreasing.
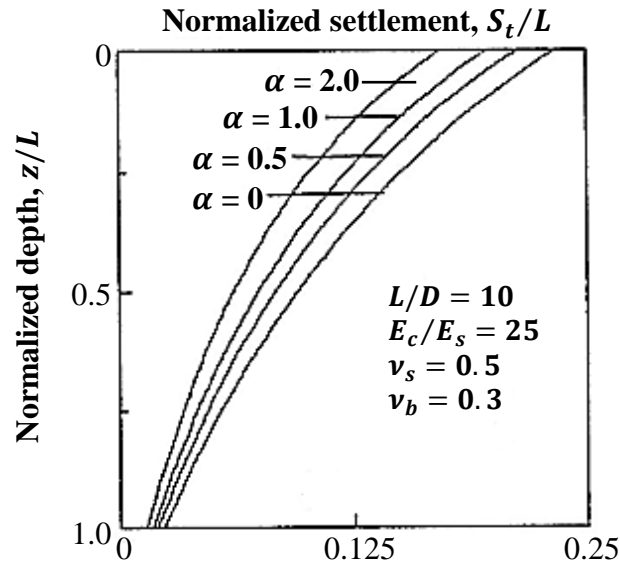
Figure 2.30. Relation between z/L, S_t/L and α (Van Impe et al., 1997)

According to Shahu et al. (2000) by assuming the uniform settlement at each depth of the composite system as illustrated in Figure 2.32; the settlement within stone column at any depth must be equal to settlement within the surrounding soil at same depth, i.e. $S_{ci} = S_{si}$ under totally applied load of $\sigma = \sigma_{ci} a_r + \sigma_{si}(1 - a_r)$ where, σ_{ci} and σ_{si} are the stresses in granular pile and soil within element i, respectively. In Figure 2.32, γ_f is unit weight of granular mat, H is thickness of compressible soil layer, τ_i is shear stress develop at interface for i^{th} element.

Settlement of the granular pile at any element i (S_{ci}) can be calculated from;

45

$$S_{ci} = \frac{\sigma_{ci}}{E_c} \delta z_i \qquad (2.20)$$

Settlement of the normally consolidated fine-grained soil in unit cell at any element i (S_{si}) can be calculated from;

$$S_{si} = 0.434 \frac{C_c}{(1 + e_0)} \delta z_i \ln\left(1 + \frac{\sigma_{si}}{\sigma'_{0i}}\right) \qquad (2.21)$$

Where; σ'_{0i} is effective overburden stress at the middle of the i [th] element.

$$\sigma'_{0i} = \gamma_f t_f + \gamma_s' z_i \qquad (2.22)$$

Where; γ_s' is submerged unit weight of soil and z_i is depth of element i.

Thus; from the compatibility equation of $S_{ci} = S_{si}$;

$$\frac{\sigma_{ci}}{E_c} \delta z_i = 0.434 \frac{C_c}{(1 + e_0)} \delta z_i \ln\left(1 + \frac{\sigma_{si}}{\sigma'_{0i}}\right) \qquad (2.23)$$

The stress concentration factor (n_i) for any element i is;

$$n_i = \frac{\sigma_{ci}}{\sigma_{si}} \qquad (2.24)$$

Malarvizhi and Ilamparuthi (2004) carried out studies on unit cell loading for floating and end-bearing stone columns. Test setups for this study are shown in the Figure 2.33.
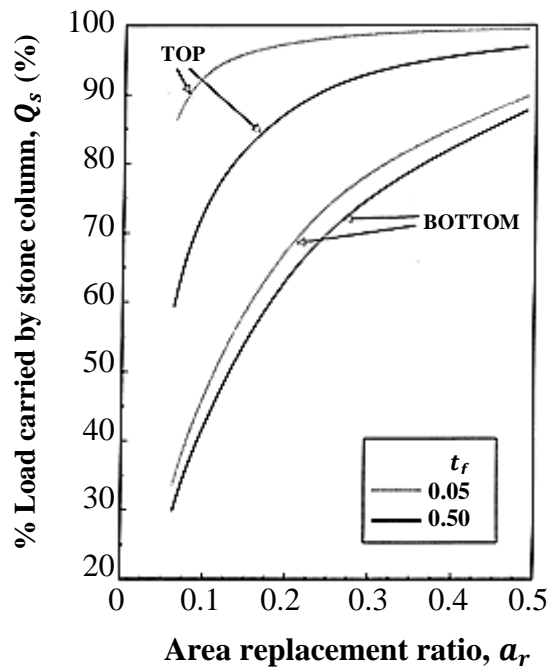
Figure 2.31. Relation between Q_s, a_r and t_f (Shahu et al., 2000)
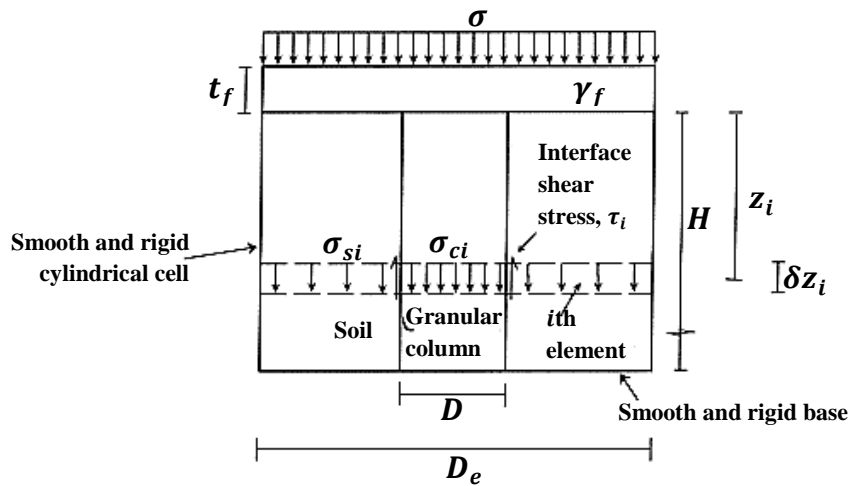
Figure 2.32. Unit cell and the definition of the terms used in the study

(Shahu et al., 2000)
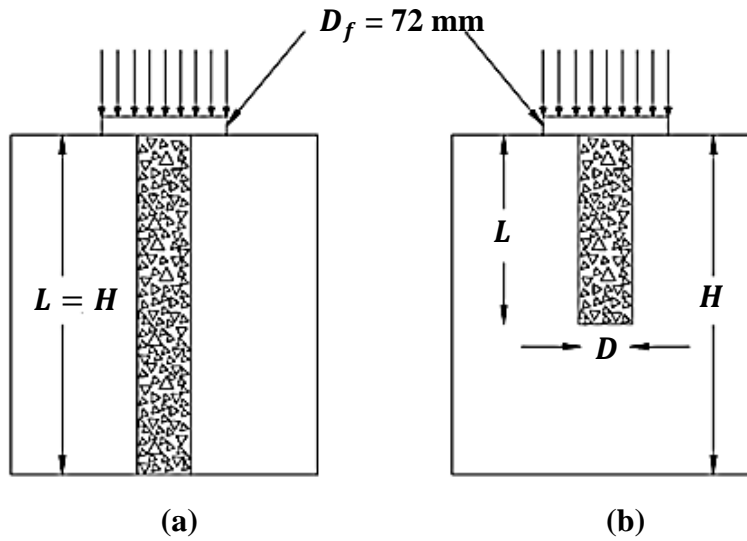
Figure 2.33. (a) end-bearing and (b) floating stone columns with different L/D ratios (Malarvizhi and Ilamparuthi, 2004)

Malarvizhi and Ilamparuthi (2004) found out that increase in L/D leads to increase in load carrying capacity of unit cell. They observed a significant difference between the load-settlement curves obtained from the end-bearing and floating stone columns as shown in Figure 2.34, that for same amount of load larger settlements occur in floating columns. Moreover they stated that all behaviors are strain hardening (the rate of increase in resistance decreases with settlement), whereas as L/D (slenderness) ratio increases behavior becomes more brittle. After bulging occurs settlement increases rapidly. Furthermore, the increase is higher for L/D ratio of 9.33 when compared to other L/D ratios; this may be attributed to the bearing resistance offered by the hard surface in which the column was founded. Moreover for larger L/D ratios, higher modulus of subgrade reaction coefficients (k) are encountered (for settlement larger than 10% of diameter of stone column).

Malarvizhi and Ilamparuthi (2004) also noted that as the thickness of the clay bed at the bottom of the column $(H - L)$ increases, bearing capacity of unit cell decreases (Figure 2.35). In this figure, sc is stone column and sc+net2 and sc+net3 are geosynthetics encased stone columns.
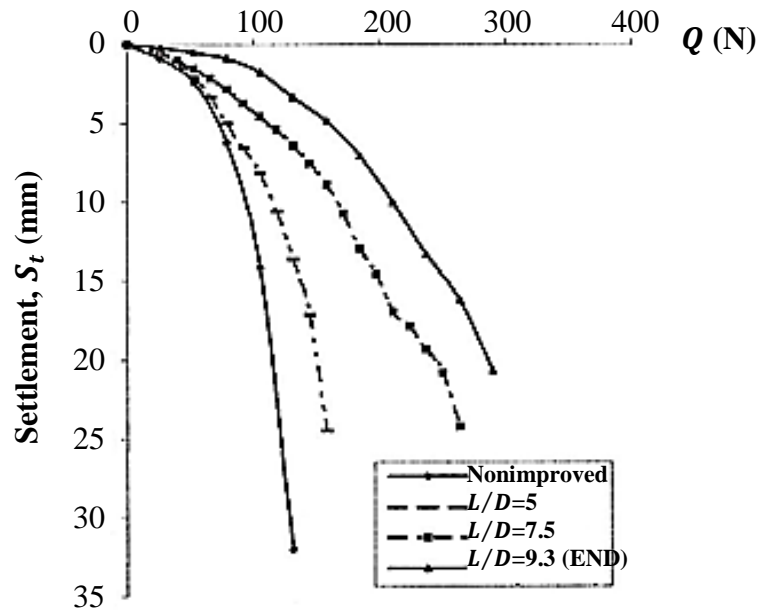
Figure 2.34. Load – settlement relation for various L/D ratios

(Malarvizhi and Ilamparuthi, 2004)
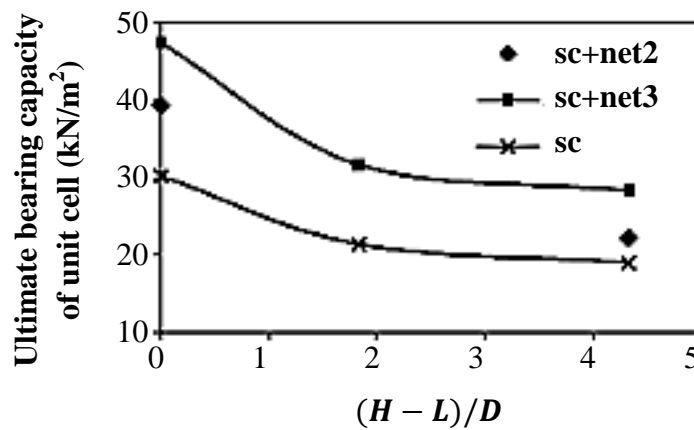
Figure 2.35. Relation between q_{ult} and $(H - L)/D$

(Malarvizhi and Ilamparuthi, 2004)

Ambily and Gandhi (2004) carried out ten tests for an end-bearing stone column in a unit cell for different moisture contents of clay and spacing values. The test setup is shown in Figure 2.36.

Results of the model tests are compared with FEM analysis performed through Plaxis 2D software. Loading was applied on entire area and a footing having diameter of $2D$. Ambily and Gandhi (2004) mentioned that tests on footing were resulted in bulging failure of the column at a depth of $(0.5 – 1.0)D$. On the other hand, the tests on entire area did not indicate any bulging failure due to the confining effect of tank wall. Difference between the load-settlement behaviors of loading entire area and only stone column are shown in Figures 2.37.

1	Loading plate	4	Stone column (D = 100 mm)
2	Sand pad	5	Cylindrical test tank
3	Soft clay		
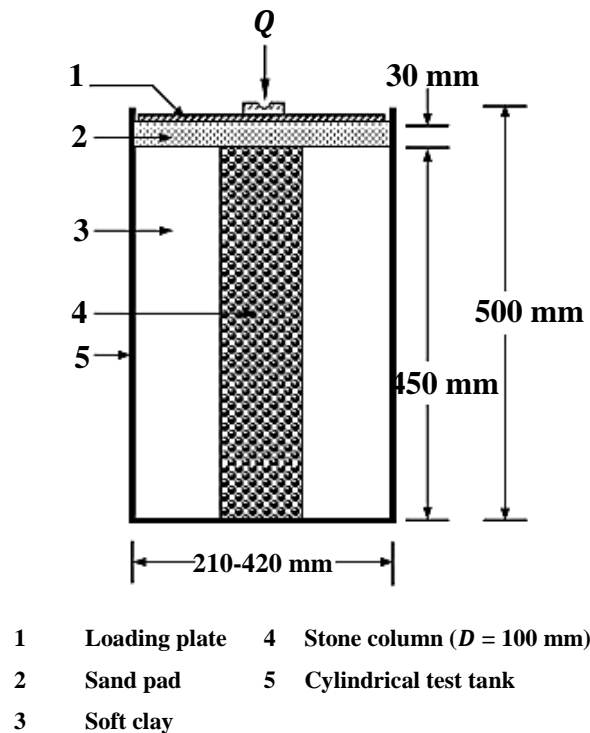
Figure 2.36. Test setup (Ambily and Gandhi, 2004)

Ambily and Gandhi (2006) carried out another study similar to one published in 2004. They performed laboratory tests on single end bearing stone column in a unit cell for different spacing/diameter (s/D) ratios and undrained shear strengths

of clay (c_u). Two different loading scenarios were studied: loading on (a) entire area of unit cell and (b) single stone column in order to obtain the axial load capacity of column. For both loading type test setups are shown in Figure 2.38.
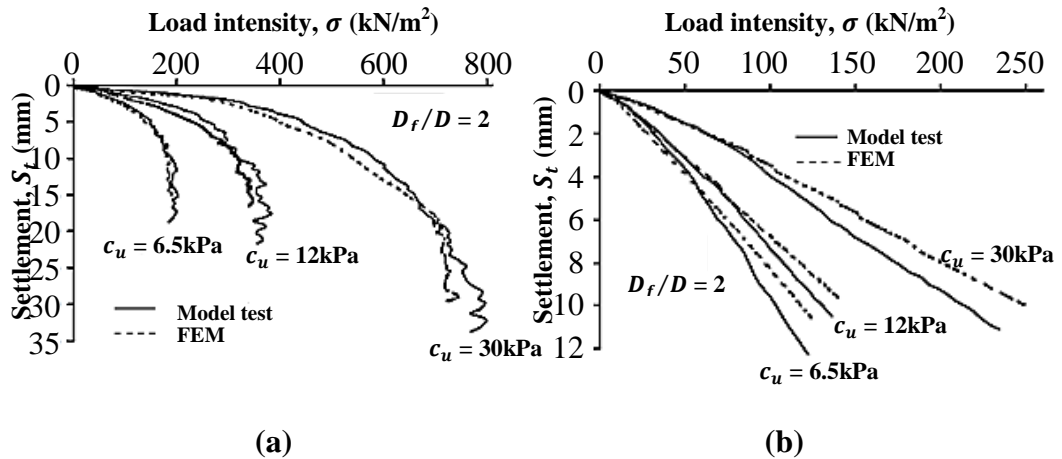
Figure 2.37. Stress-settlement curves for various c_u values (a) D_f = 210 mm and (b) D_f = 420 mm (Ambily and Gandhi, 2004)
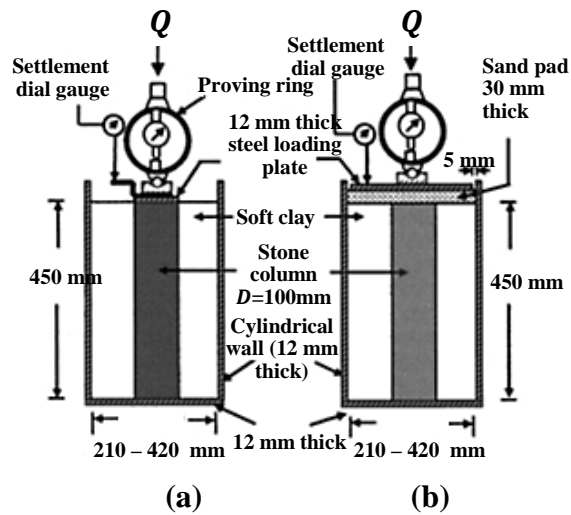
Figure 2.38. Single column test arrangement (a) column area loading and (b) entire area loading (Ambily and Gandhi, 2006)

Moreover, same tests were analyzed though an axisymmetric FEM axisymmetric model in Plaxis 2D. They found out that the results from Plaxis and lab model tests are in good agreement. The difference between the results obtained from FEM analysis and laboratory model tests are more pronounced in softer soils. Further parametric study was performed for different angle of internal friction of stones in Plaxis.

From the stress – settlement relations obtained from the experiments, Ambily and Gandhi (2006) stated that for greater values of undrained shear strength of clay higher ultimate bearing capacity of composite soil – stone column body (q_{ult}) is obtained. Furthermore they mentioned that although spacing has a minor effect on q_{ult} and smaller s/D ratios leads to increase in bearing capacity. Moreover, they observed that different c_u causes no response on q_{ult}/c_u. However, for larger s/d ratios smaller q_{ult}/c_u ratios are obtained. Through finite element analysis the relation between q_{ult}/c_u, s/d and ϕ_c is obtained. It is found that as ϕ_c increases, for the same s/d ratio, q_{ult}/c_u increases.

Settlement improvement factor (β), c_u and s/D relation is obtained from both laboratory model tests and FEM (Figure 2.39). It is found that c_u has no effect on β. Moreover as expected, as s/D increases, β decreases.

Similar to chart given by Priebe (1995), Ambily and Gandhi (2006) obtained a relation between β, s/D and ϕ_c (Figure 2.40). They found that as s/D increases and/or ϕ_c decreases, β decreases as shown by Priebe previously.

Furthermore, through finite element analyses Ambily and Gandhi (2006) obtained relation between stress concentration factor (n), s/D, c_u and modular ratio (E_c/E_s) as shown in Figure 2.41. They stated that larger s/D ratios and c_u values lead to smaller n values.

Gniel and Bouazza (2009) studied the behavior of both single and group of stone columns in enlarged oedometer test. They stated when stone columns are used in order to treat the soft soil time of consolidation decreases by a factor of 3 – 4 and load bearing capacity increases by a factor approximately 3 when compared to untreated soil.

Pham and White (2007) carried out full-scale load tests on rammed aggregate piers having different lengths. They proposed a solution to estimate the settlement of untreated zone which lies under stone columns. Figure 2.42 shows that the distribution of vertical stress underneath the stone columns can be estimated from the length of stone column using two linear functions with the following form:

$$\frac{\Delta\sigma}{\sigma} = a - b\frac{z - z_f}{L} \qquad (2.25)$$

Where; $\Delta\sigma$ is increase in vertical stress, z_f is depth of footing and coefficients a and b are for the upper and lower zone are shown in Figure 2.42.

Pham and White (2007) stated that as a conservative approach, settlements of rammed aggregate piers are calculated according to Westergaard's solution where both upper and lower zones are assumed to be not affected from the installation process. Other approaches such as Schmertmann's strain influence method, Boussinesq's solution, 1.67 – 2 V: 1H distributions can also be used. Pham and White (2007) found out from the FEM analyses that 95% of applied stress would be damped at a depth of 1.5 – 2 times of D_f from the depth of foundation. Whereas, Westergaard's solution gives this influence depth is about 2.5 times of D_f.
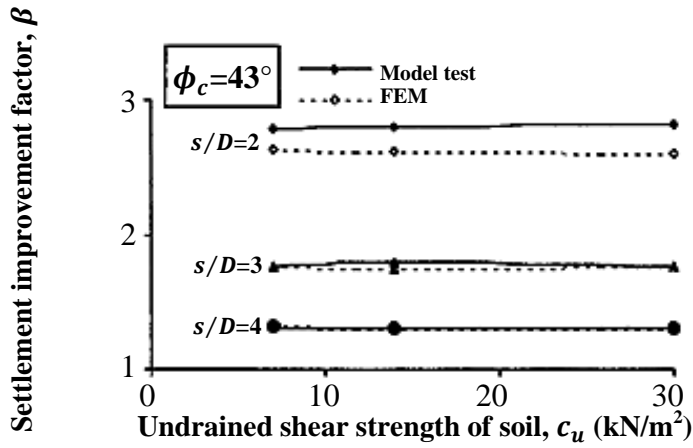
Figure 2.39. Relation between β, c_u and s/D (Ambily and Gandhi, 2006)
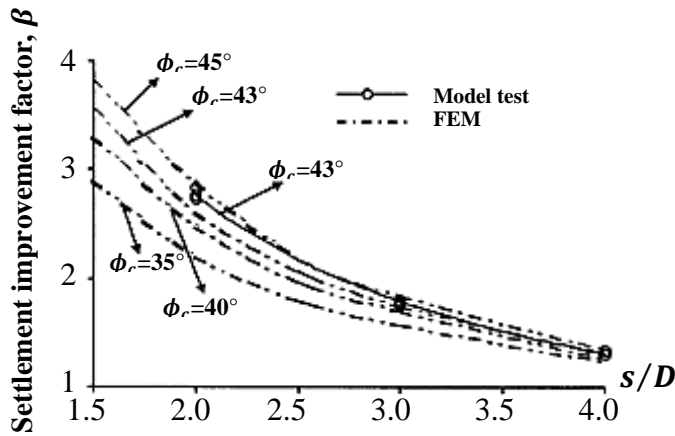
Figure 2.40. Relation between β, s/D and ϕ_c (Ambily and Gandhi, 2006)
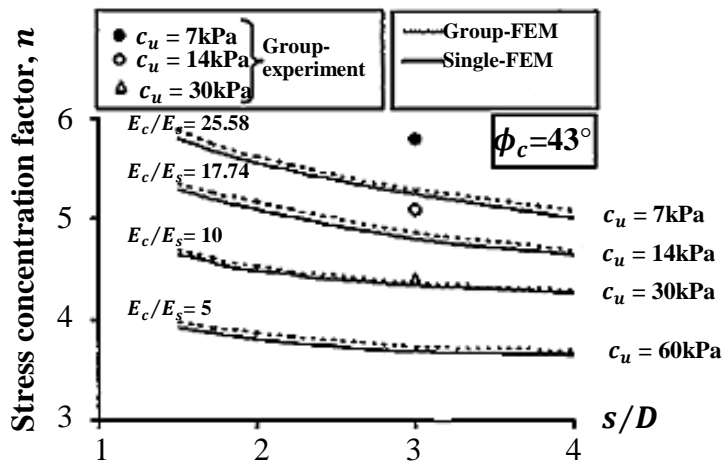
Figure 2.41. Relation between n, s/D and E_c/E_s (Ambily and Gandhi, 2006)
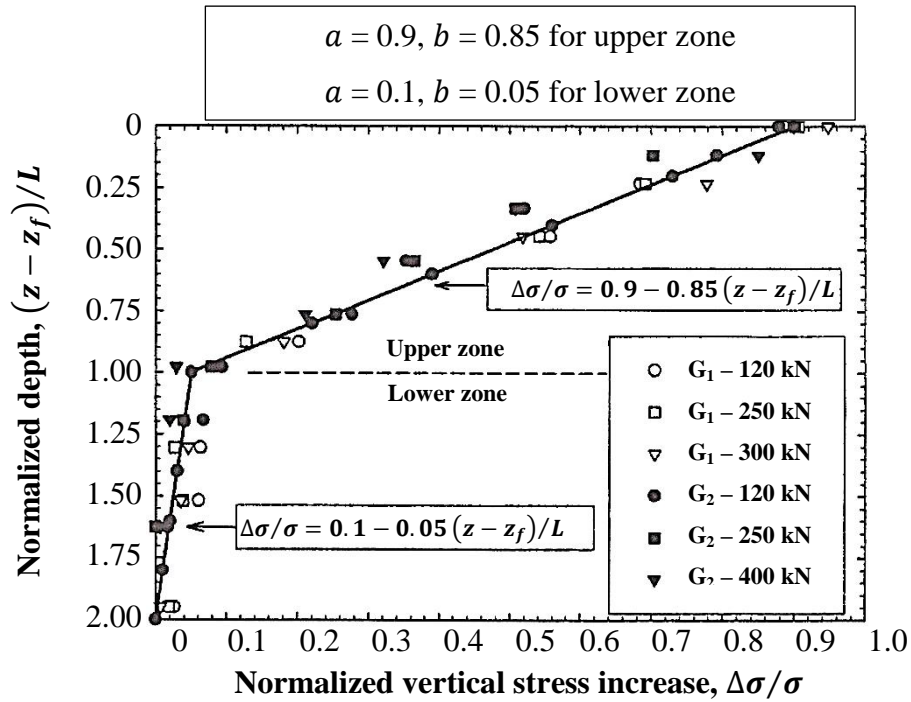
Figure 2.42. Distribution of $\Delta\sigma$ below the footings as a function of L

(Pham and White, 2007)

2.3.2. Studies on Group of Stone Columns

Datye (1982) stated that settlement of a single column in a unit cell and settlement of 3 columns loaded under same load intensity are in the same order. However, settlement of single stone column in a unit cell and large group of stone columns would be different due to the difference between sizes of footings based on the following plate load test equation:

$$\left[\frac{S_{uc}}{S_g} = \frac{B_g(B + 30)}{B(B_g + 30)}\right]^2 \tag{2.26}$$

Where; S_{uc}, S_g are settlement of single and group of stone columns, respectively and B, B_g are width of the test area of single and group of three stone columns, respectively.

Kirsch and Kirsch (2010) pointed the necessity of the full-scale loading tests on pile groups over actual footing dimensions because of the complex interaction between soil and stone columns. Moreover, for some cases performing tests on a footing over minimum three columns satisfy sufficient confidence. They mentioned that load tests on single stone columns with the load applied directly on the column itself do not reflect actual stress conditions and settlements.

Kirsch and Kirsch (2010) stated that for the cases where the thickness of soil to be improved is smaller than $5D_e$, tests on single columns loaded over a footing having same diameter with the unit cell (D_e) is indicative for the performance of group. From the load-settlement curve obtained from the unit cell loading test, an equivalent deformation modulus (E_{eq}) can be defined as given in the following equation:

$$E_{eq} = \frac{\sigma * L}{S_{uc}} \tag{2.27}$$

Where; S_{uc} is measured settlement through unit cell loading. Similarly, for the infinite grid with same equivalent deformation modulus:

$$E_{eq} = \frac{\sigma * L'}{S_g} \tag{2.28}$$

Where; S_g is settlement of infinite column grid and L' is equivalent column length. From parametric finite element analysis, Kirsch and Borchert (2006) found out that equivalent column length (L') is independent from the length of stone column and stiffness ratio of column material and surrounding soil but only depends on diameter of unit cell (D_e) as shown in Figure 2.43.

$$L' = (5.0\ldots6.5)D_e^{0.2}$$
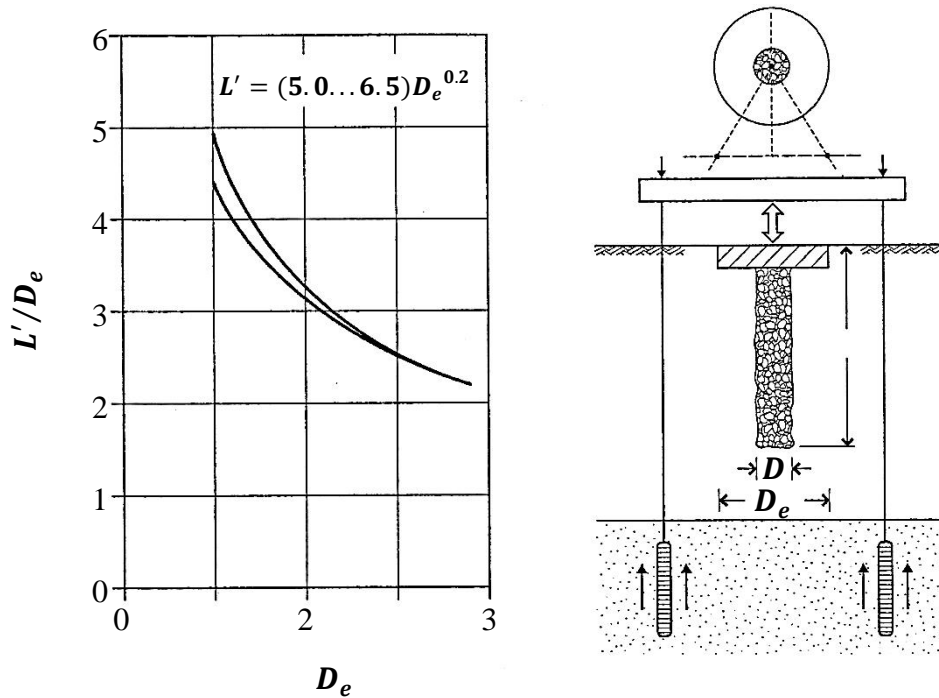
Figure 2.43. Relation between L' and D_e (Kirsch and Borchert, 2006)

Hence, for some cases unit cell testing is indicative for infinite column grid. By the determination of E_{eq} from the unit cell test and using design chart given in Figure 2.43, settlement of infinite column grid can be estimated. Kirsch and Kirsch (2010) stated the necessity of the further studies on this issue.

Al-Khafaji and Craig (2000) performed a series of centrifuge tests at acceleration level of 105g to simulate large area improved by as many as 572 stone columns under a tank having diameter of 34 m and total weight of 160 kPa. Model tests are composed of 380 mm diameter, reconsolidated clay having length of 200 mm and 10 mm diameter of stone columns. Al-Khafaji and Craig (2000) stated that ratio of total settlement of footing to thickness of clay layer (S_t/H) is a function of undrained shear strength (c_u), total applied stress (σ) and area replacement ratio (a_r) as shown in Figure 2.44.

57
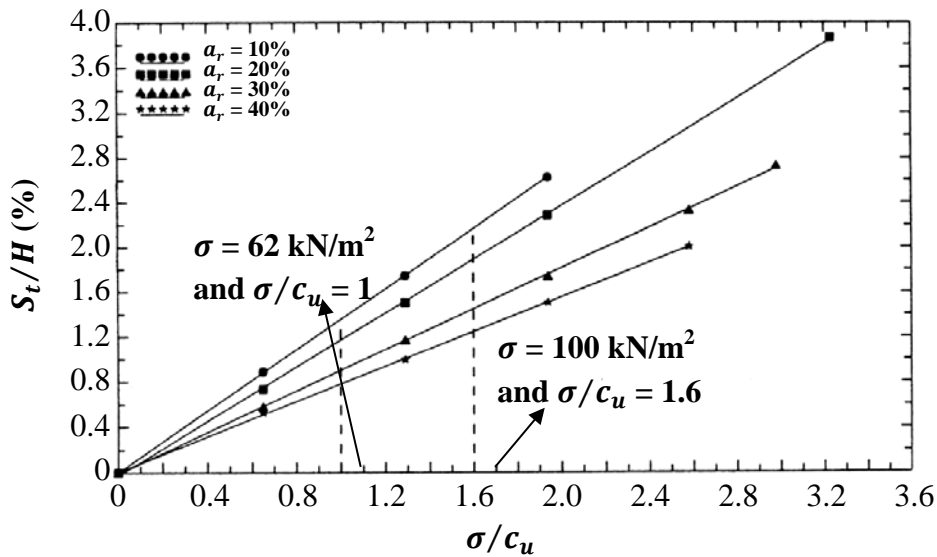
Figure 2.44. Relation between S_t/H, σ/c_u and a_r

(Al-Khafaji and Craig, 2000)

Al-Khafaji and Craig (2000) also reported the final undrained shear strength values (c_{uf}) obtained from the various samples taken from different distances from center and depth (Figure 2.45).

Wood et al (2000) conducted laboratory model tests and numerical analysis for group of stone columns and observe the influence of diameter, length and spacing between the stone columns which are the parameters defining the failure type (bulging, plane failure or bending). Miniature pressure transducers are used to measure the contact stresses at stone columns and clay bed during the loading. They compared their study with the one carried by Greenwood (1991). By using similar area replacement ratio ($a_r = 24\%$) but rigid footing instead of flexible one, they obtained the relation between ratio of applied stress to initial undrained shear strength and stress concentration factor as shown in Figure 2.46.

Moreover, Wood et al. (2000) stated that increasing column length after a point has no significant influence on the load carrying capacity. On the other hand, as

58

expected increasing area replacement ratio leads to increase in stiffness and strength.
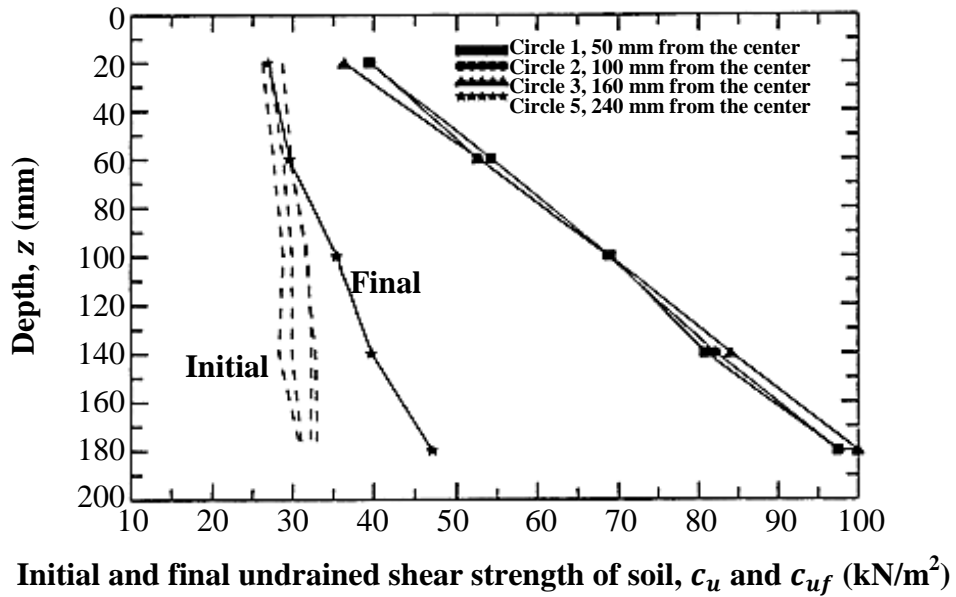
Figure 2.45. Initial and final undrained shear strength values versus depth (Al-Khafaji and Craig, 2000)
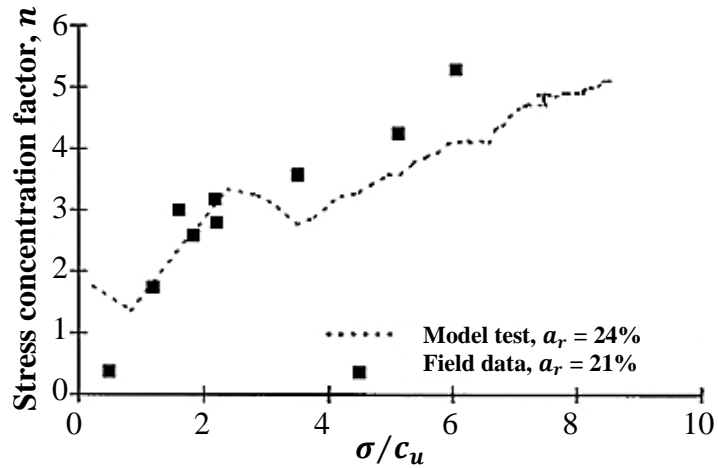
Figure 2.46. Relation between n and σ/c_u (Wood et al., 2000)

Ambily and Gandhi (2006) prepared a model test setup consisting of a group of stone columns (5 stone columns) (Figure 2.47).

Ambily and Gandhi (2006) compared the load settlement behavior of single stone column with the behavior of group of stone columns. They concluded that unit cell is a suitable and reliable way to analyze the behavior of internal stone columns in a group (Figure 2.48).
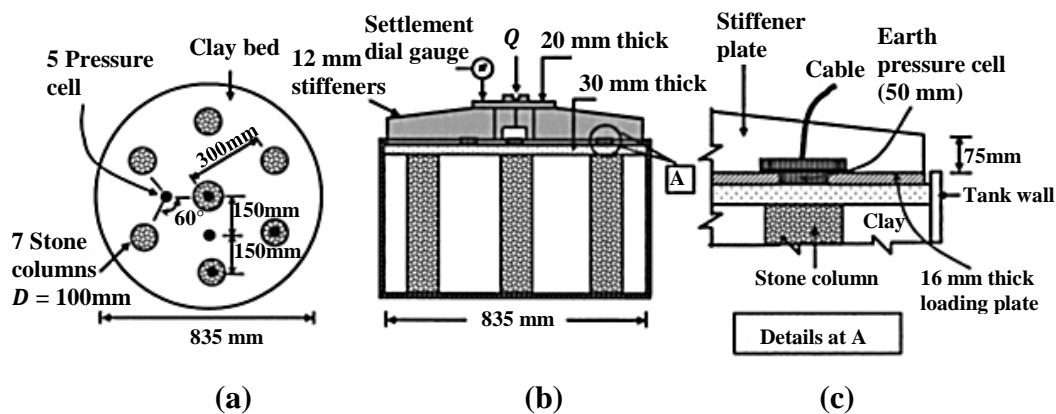
Figure 2.47. Group test arrangement: (a) plan view, (b) section of test tank and (c) details of pressure cell (Ambily and Gandhi, 2006)

Gniel and Bouazza (2009) studied on both single and group of stone columns in enlarged oedometer test. They also noticed different behavior between single (unit cell) and group of stone columns. For group columns, clay between the columns has drained boundary conditions. Those boundaries provide additional confinement so that columns may expand laterally without failing.

Murugesan and Rajagopal (2007) studied on both single and group of stone columns. They stated group of stone columns sign the failure with a strain-softening (plastic) behavior where failure is probably due to excessive bulging.

Zahmetkesh and Choobbasti (2010) stated that vibration during installation of stone columns causes improvement in shear strength of soil. This improvement is more pronounced at near distances from the stone column and decreases at far distances.

In other words the lateral earth pressure coefficient is equal to K_0-at rest condition at far distances whereas it is larger than 1 at near distances or larger than even K_p. Moreover, due to installation of stone column lateral strains may as large as 45% in soft clay next to the stone column and decreases towards edges of the unit cell.
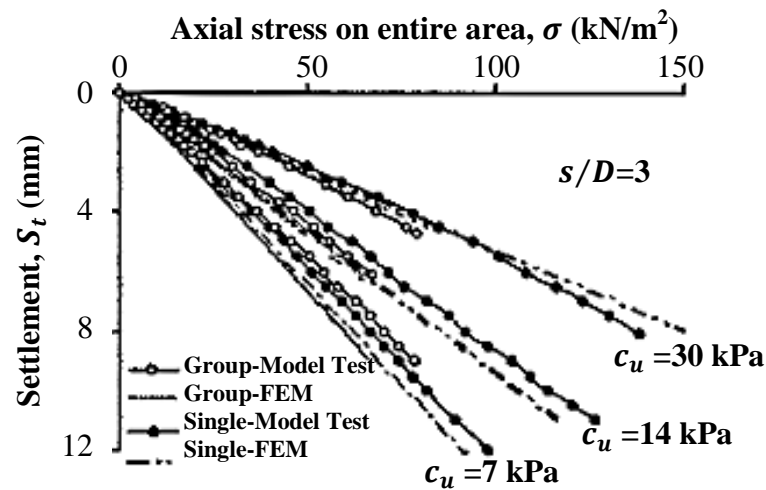
Figure 2.48. Stress – settlement behaviors of single stone column and group tests (Ambily and Gandhi, 2006)

Similarly, Kirsch (2004) measured the lateral earth pressure coefficient before and after the installation of stone columns by displacement method. They measured this effect in a field test on two groups composed of 25 stone columns in silty clay and sandy silt, respectively. Relationship between the ratio of lateral earth pressure coefficient at rest after installation to before installation (K_0/K_{0i}) and normalized distance from the center of the group (r/D_f) is demonstrated in Figure 2.53(a). In this figure, for silty clay and sandy silt soils maximum K_0/K_{0i}

ratio develop at a distance about 4-5D from the center of the group on the order of 1.7 and 1.3, respectively.

In addition the ratio of Menard's modulus of soil after installation to before installation obtained from PMT (E_M/E_{Mi}) and normalized distance from the center of the group (r/D_f) is demonstrated in Figure 2.49 (b).

It is obvious that the modular ratio is maximum at a distance about 4-6D from the center of the group on the order of 2.5.

Elshazly et al. (2008) summarized the values of ratio of post-installation horizontal to vertical stresses (K^*) published by different researchers in literature (Table 2.2)
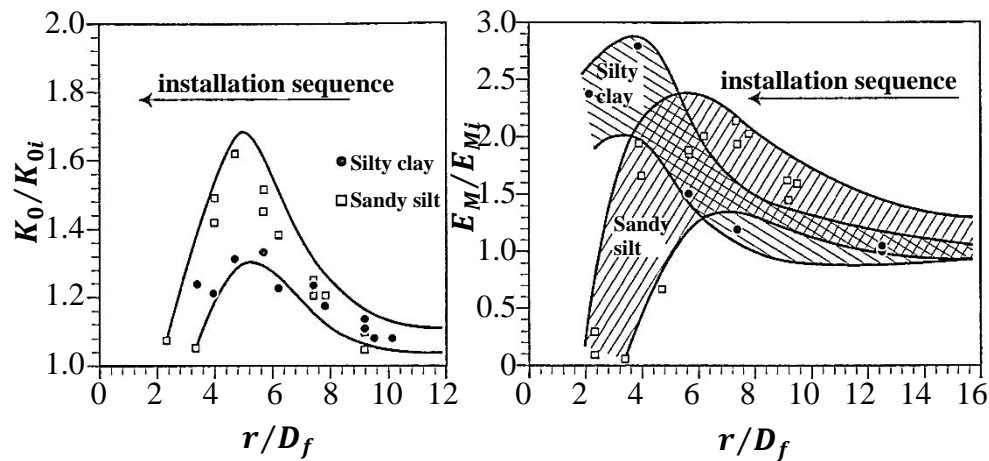
Figure 2.49. (a) Horizontal stress increase and (b) development of ground stiffness during installation of stone columns (Kirsch, 2004)

Shahu and Reddy (2011) studied on group of floating stone columns. Group of stone columns are tested in 'fully drained' and 'load controlled' laboratory tests and their numerical simulations have been done. They stated that although usually the short term behavior of soil is considered, long term behavior must be assessed since long term settlement is the main issue for soils improved by stone

columns. Thus, tests must be conducted in 'fully-drained' condition. Moreover, the actual fully-drained loading condition can be resembled more by the 'load-controlled' tests that are enabling the completion of the consolidation instead of 'deformation-controlled' tests. A parametric study was performed through model tests by observing the effects of nominal length of pile, area replacement ratio, water content of clay, relative density. The results of the parametric study were compared with the ones obtained from the FEM analysis. The setup illustrated in Figure 2.50.

Shahu and Reddy (2011) stated that major factors affecting the settlement of treated soil (S_t) are;

- applied vertical stress on footing, σ
- spacing between stone columns in group, s
- length of each stone column, L
- diameter of each stone column, D
- initial effective vertical stress, σ_0'
- preconsolidation pressure, P_c'
- coefficient of consolidation and reconsolidation indices, λ and κ
- critical stress ratio
- secant modulus
- number of columns, N

Where the minor factors are;
- thickness of mat, t_f
- dilation angle of sand, ψ
- angle of shearing resistance of column material, ϕ_c

Similar to Ambily and Gandhi (2006), also Shahu and Reddy (2011) obtained nonlinear stress – settlement relation. They found out increasing area replacement

ratio from 10% to 30%, load carrying capacity increase about 20%. They pointed out the significant effect of length of stone column on load carrying capacity. Shahu and Reddy (2011) mentioned that, as area replacement ratio increases settlement decreases regardless of the level of stress. This decrease is more pronounced between $10\% < a_r < 20\%$ (Figure 2.51).

Table 2.2. Published K^* values (Elshazly et al., 2008)

References	*K^* value*	*Method of determination*
Elshazy et al. (2006)	Between 1.1 and 2.5, with best estimate of 1.5	Back calculations form full-scale load test performed on a stone column within an extended array of column.
Elkasabgy (2005)	Between 0.7 and 2.0, with average of 1.2	Back calculations from 3 full-scale load tests performed on stone columns within three extended arrays of columns.
Pitt et al. (2003)	Between 0.4 and 2.2, with average of 1.2	Full-scale load tests on vibro-displacement stone columns in compressible clays and silts underlain by highly weathered shale.
Watts et al. (2000)	Between K_0 and K_p	Full-scale load tests on vibro-displacement stone columns in variable fill.
Priebe (1995)	1.0	Analytical solution of end-bearing incompressible columns, neglecting the geo-field stress effect.
Goughnour (1983)	Between K_0 and $1/K_0$	Analytical solution based on elastic and rigid-plastic behaviour using the unit cell concept.
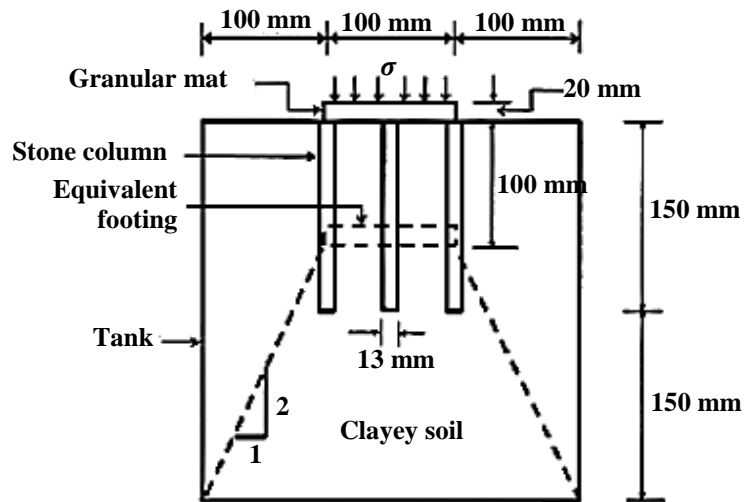
Figure 2.50. Schematic view of stone column foundation
(Shahu and Reddy, 2011)

Shahu and Reddy (2011) mentioned that there is a high consistency between the load carrying capacities and maximum settlement values obtained from laboratory model tests and FEM analyses (Table 2.3). They added small differences between FEM analysis and results of model tests may be come up due to mesh convergence, uncertainties obtaining the secant modulus, inappropriateness of the parameters and the used constitutive model for stone columns.
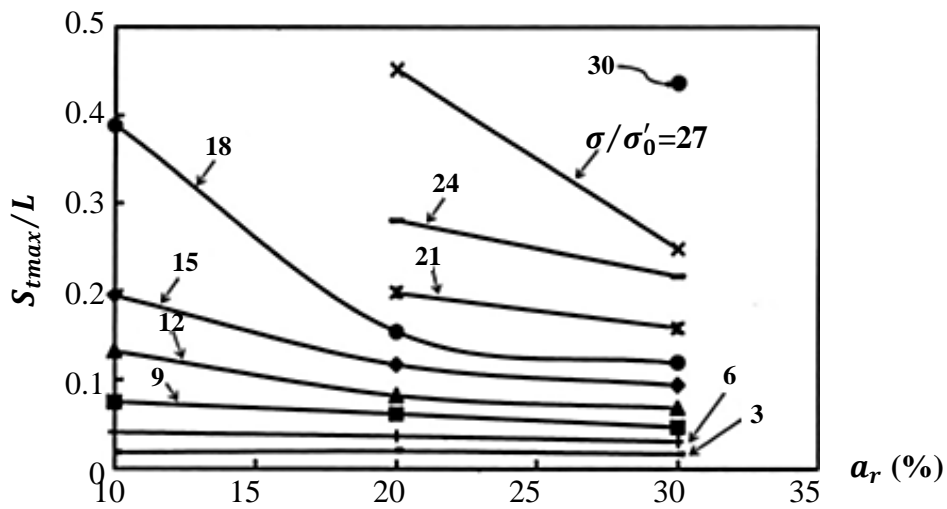
Figure 2.51. Relation between S_{tmax}/L, a_r and σ/σ'_0

(Shahu and Reddy, 2011)

Table 2.3. Comparison of Model Tests and FEM (Shahu and Reddy, 2011)

L (mm)	a_r (%)	σ'_0 (kPa)	Q_{ult}			S_{tmax}		
			FEM	Model Tests	% change	FEM	Model Tests	% change
100	10	3	79	75	-5	20	19	-5
	20		90	120	25	29	28	-4
	30		95	135	30	27	25	-8
150	10	3	106	120	12	31	26	-19
	20		108	150	28	35	29	-21
	30		105	165	36	26	32	19
100	10	5	77	75	-3	12	19	37
	20		105	120	13	24	28	14
	30		106	135	21	18	25	28
150	10	5	120	120	0	25	26	4
	20		120	150	20	26	29	10
	30		135	165	18	27	32	16

CHAPTER 3

EXPERIMENTAL WORKS

3.1. Introduction

In this study, model tests were performed in order to observe the effects of column length and undrained shear strength on stress concentration factor, surface and subsurface settlements. In model tests different loading conditions, i.e. single stone column loading, single columns loaded over a footing having same diameter with the unit cell and group loading, were studied. Stress carried by stone columns due to foundation loading was directly measured by soil pressure transducers having 3 cm diameter and capacity of 1 MN/m^2. Moreover, settlements were measured by means of dial gauge and potentiometric rulers. All the transducers and potentiometric rulers were connected to 8 channel data acquisition system. Both foundation pressure and confining stress were provided by pneumatic pistons.

In this chapter, properties of the materials, the details of the model test setup and the general procedure followed in model tests are briefly explained.

3.2. Materials and Properties

3.2.1. Properties of Kaoline

Kaoline bought from Kalemaden Company was used as bedding soil material. It was dried in oven for several days and then grounded in Transportation

Laboratory to obtain powder form. Kaoline, in powder form, was mixed with 45% of water content, which is approximately equal to liquid limit of kaoline, and paste form was obtained.

Paste kaoline was kept in curing room to provide homogeneous moisture content. Wet sieve-hydrometer, Atterberg limits, specific gravity, oedometer and consolidated-drained (CD) triaxial tests were performed in order to get characteristic, compressibility and strength properties of the paste. Vane shear test (at the end of the consolidation and foundation loading stages) and unconsolidated undrained (UU) triaxial test (at the end of the foundation loading stage) were also performed to get strength parameters of Kaoline for each test. Values of undrained shear strength are reported in Chapter 4.

In order to obtain the grain size distribution of the kaolinite, first the soil was wet sieved and then hydrometer test was performed. Grain size distribution curve of kaolinite is plotted as shown in Figure 3.1.
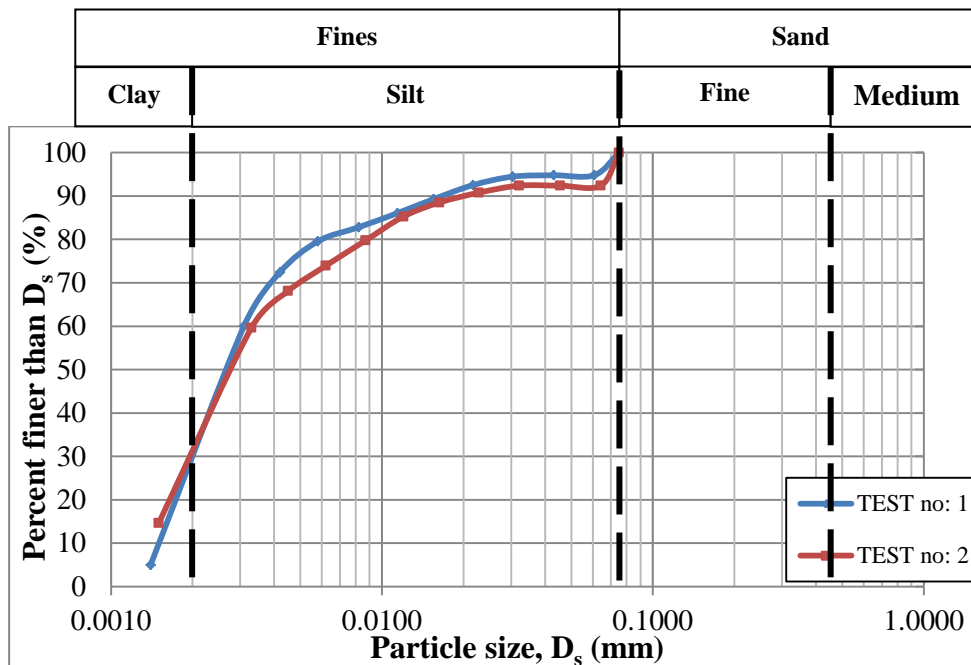
Figure 3.1. Grain size distribution (kaolinite)

It is found that kaolinite is clayey silt which consists of 32% clay and 68% silt size particles.

Atterberg limits of kaolinite were determined through several tests and consistency limits obtained are as follows: shrinkage limit (*SL*) is 33%, plastic limit (*PL*) is 34%, liquid limit (*LL*) is 46% and plasticity index (*PI*) is 12% as shown in Figure 3.2.

Atterberg limit tests show that kaolinite is clayey silt having intermediate plasticity, i.e. MI according to Unified Classification System.

The results of the specific gravity tests indicate that the average specific gravity of the kaolinite is $G_s = 2.611$.
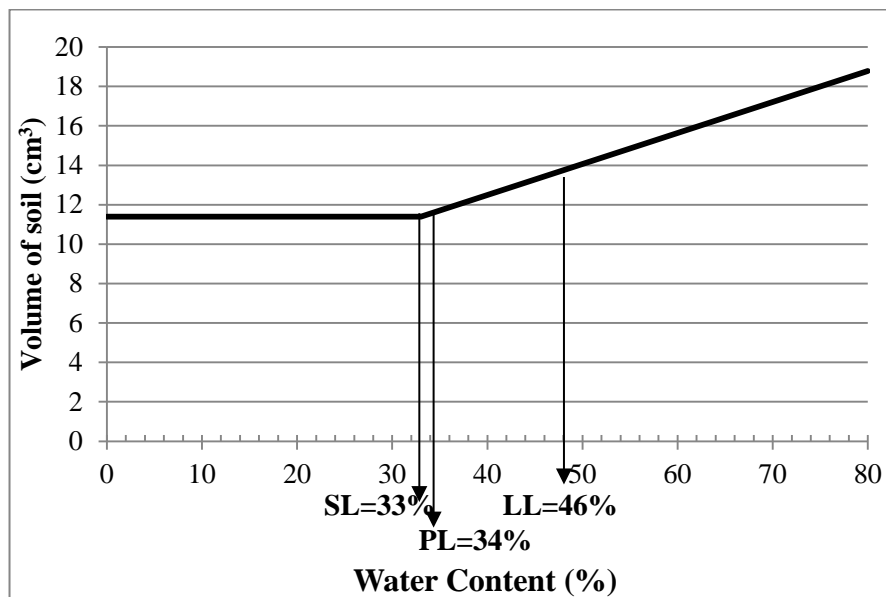
Figure 3.2. Atterberg limits (kaolinite)

Two one-dimensional consolidation tests were performed on kaolinite soil having 45% moisture content. Tests were done for loading and unloading sequence for

axial stresses in range from 0 to 200 kN/m^2. Void ratio versus effective stress on semi-log scale for both tests is given in Figure 3.3. Compressibility parameters obtained from the consolidation tests are given in Table 3.1. In this table, m_v is coefficient of volume compressibility, c_v is coefficient of vertical consolidation, C_c and C_r are compression and recompression indices, respectively.

Effective strength parameters of kaolinite paste were determined in consolidated drained (CD) triaxial tests. Initial water content of kaolinite paste is 36.5%. The results of CD tests are summarized in Figures 3.4-3.5 and Table 3.2. In Table 3.2, E'_{50} is secant deformation modulus at 50% strength.

(a)　　　　　　　　　　　　　(b)
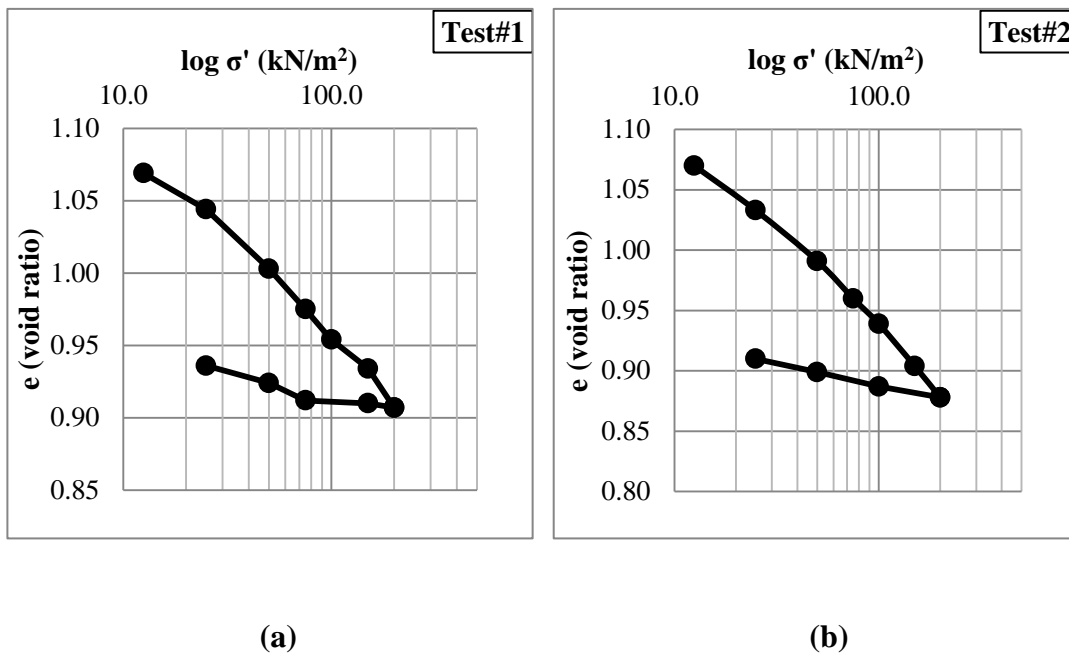
Figure 3.3. e - log σ' curves for loading-unloading sequences (kaolinite paste)

Table 3.1. Consolidation parameters (kaolinite paste)

Stress range (kN/m²)	m_v (m²/kN)		c_v (cm²/min)		C_c		C_r	
	Test#1	Test#2	Test#1	Test#2	Test#1	Test#2	Test#1	Test#2
12.5 – 25.0	0.0020	0.0030	0.038	0.070				
25.0 – 50.0	0.0016	0.0017	0.265	0.072				
50.0 – 75.0	0.0011	0.0012	0.191	0.151	0.152	0.159	0.032	0.035
75.0 – 100.0	0.0008	0.0008	0.265	0.151				
100.0 – 150.0	0.0004	0.0007	0.122	0.105				
150.0 – 200.0	0.0005	0.0007	0.016	0.025				
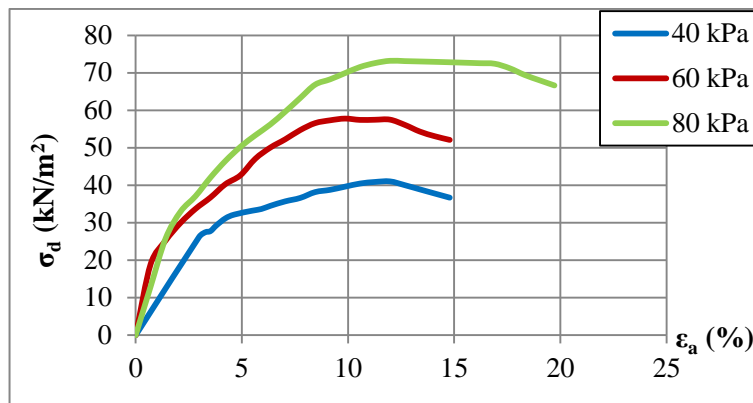
Figure 3.4. Stress-strain relation (kaolinite paste)
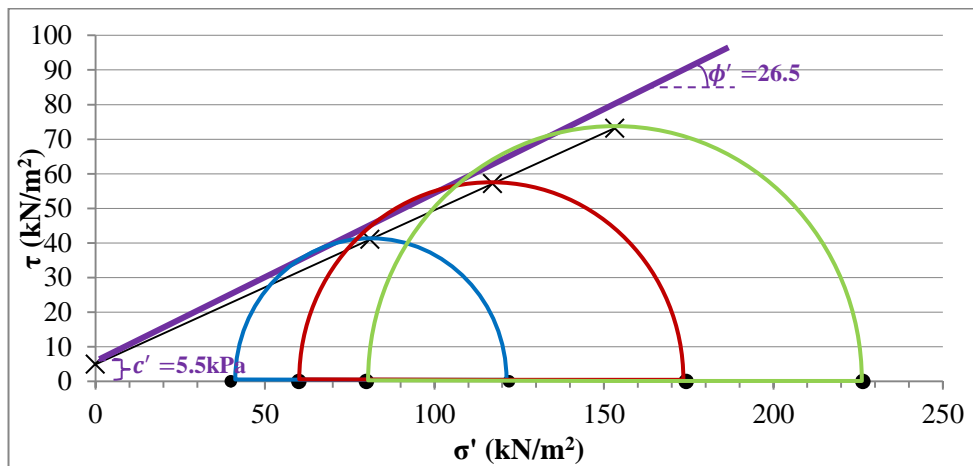
Figure 3.5. Mohr envelope (kaolinite paste)

71

Table 3.2. Effective strength and deformation properties (kaolinite)

Confining stress, σ_3' (kN/m^2)	$E_{50}'/\sqrt{\sigma_3'}$ ($\sqrt{kN}/m$)	Effective angle of shearing resistance, ϕ'	Apparent cohesion, c' (kN/m^2)
40	291		
60	310	26.5°	5.5
80	291		

3.2.2. Properties of Basalt Stone

Basalt stone was used as stone column material. In stone column application, ratio of diameter of stone column (D) to nominal diameter of stone grain (D/D_s) is important. Thus, grain size distribution of the stone is based on this ratio. Literature review points out that, in general the D/D_s ratio is in between 10 and 30 (i.e. $10 \leq D/D_s \leq 30$). Since the diameter of the stone column in this study is 30 mm; grain size of the stone is in between 1.0 mm (No. 18 sieve according to ASTM) and 3.36 mm (No. 6 sieve according to ASTM) revealing the ratio in between $9 < D/D_s \leq 30$. Basalt stones were crushed in Transportation Laboratory and wet sieved to obtain the grain size range. Specific gravity, minimum-maximum void ratio, and drained triaxial tests were performed in order to get index and strength properties of basalt stone.

Average value specific gravity of basalt stone is found as $G_s = 2.616$ which is obtained from two tests.

Through minimum-maximum void ratio tests, minimum void ratio, $e_{min} = 0.751$ and maximum void ratio, $e_{max} = 1.177$ were found. Those values corresponds to maximum dry density of $\rho_{dmax} = 1.49$ gr/cm^3 and minimum dry density of ρ_{dmin} = 1.20 gr/cm^3.

For basalt stone at relative density of $D_r = 80\%$, drained triaxial test was performed in order to obtain strength and deformation properties of it. The results of triaxial tests are summarized in Figures 3.6-3.7 and Table 3.3.
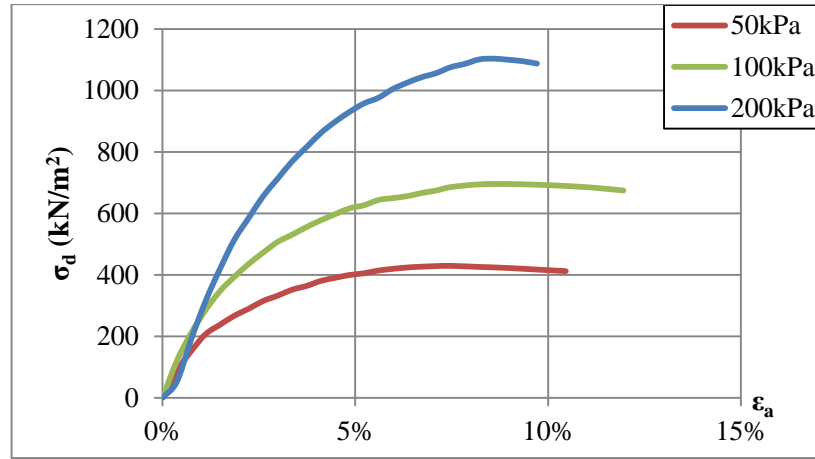
Figure 3.6. Stress-strain relation (basalt stone)
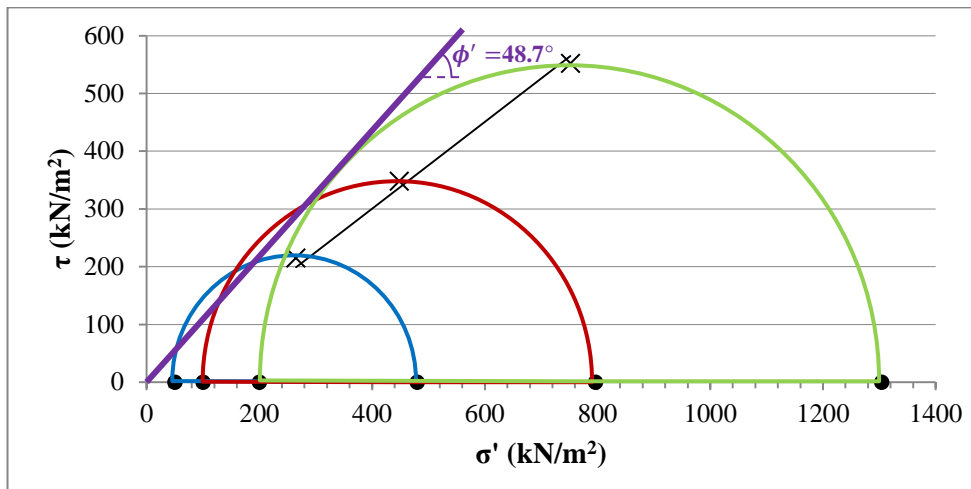
Figure 3.7. Mohr envelope (basalt stone)

Table 3.3. Strength and deformation properties (basalt stone)

Confining stress, σ_3' (kN/m²)	$E_{50}'/\sqrt{\sigma_3'}$ ($\sqrt{kN}$/m)	Effective angle of shearing resistance, ϕ'	Effective cohesion, c' (kN/m²)
50	2673		
100	2320	48.7°	0
200	1846		

3.3. Model Test Setup

3.3.1. Tanks

Six tanks were used as throughout the testing program. Height and diameter of each tank is 38 cm and 41 cm, respectively. A 55 cm diameter base plate, with mini drainage holes, was placed at the bottom of the tanks. Four steel rods having 1.8 m length are bolted to this base plate to constitute the loading frame.

3.3.2. Loading Pistons

Nine pneumatic pistons having range of diameter from 5 cm to 20 cm were used in this study. All pistons were calibrated by proving rings before usage. Pistons were connected to main air compressor having ultimate capacity of 1 MN/m². For each loading piston maximum safe pressures were calculated to prevent any leakage of gas during loading. Each loading piston is bolted to steel rigid plate (upper cross plate) in order to hold the steel rods bolted, on the perimeter of the base plate as previously stated.

3.3.3. Elements of Loading Frame

Loading frame is different for consolidation and foundation loading stages. Also different frames for single stone column, single columns loaded over a footing

having same diameter with the unit cell and group tests were used in loading phases. Consolidation and loading phases for all tests are illustrated in Figure 3.8. In Figure 3.8, D_f is diameter of circular foundation, D_e is equivalent diameter of unit cell, σ_{cons} is consolidation stress, σ_f is foundation pressure and σ_o is overburden stress to provide confinement around the stone column.

(a)

(b)
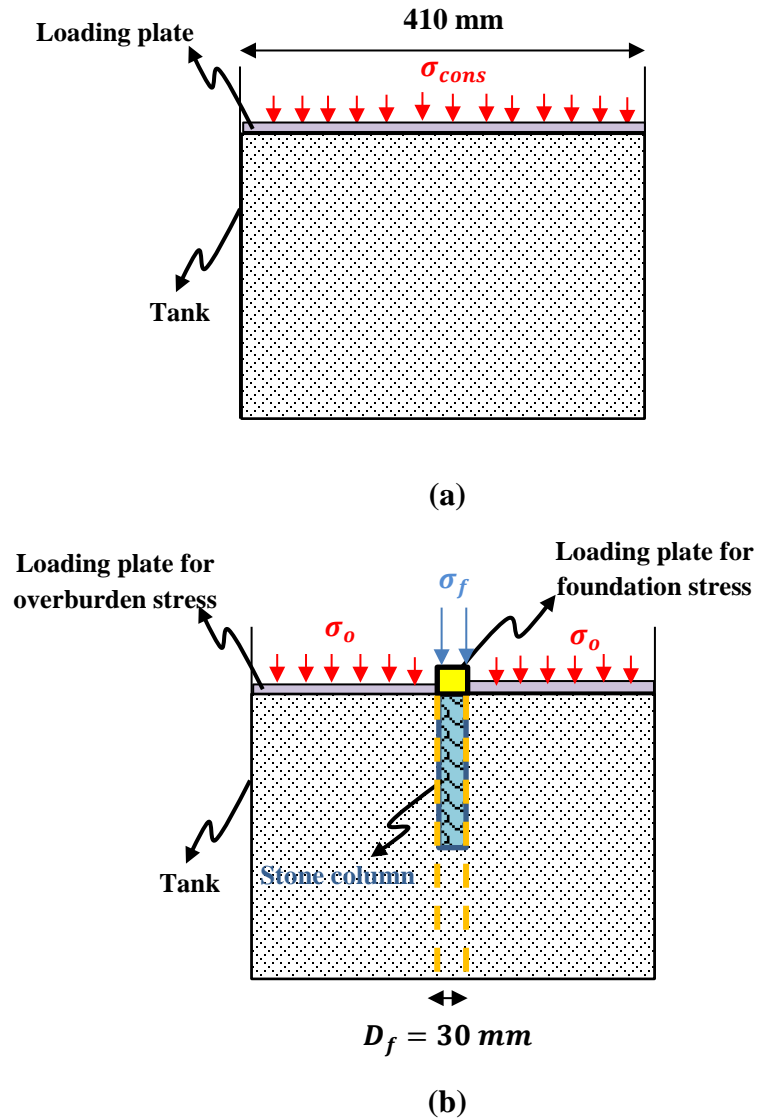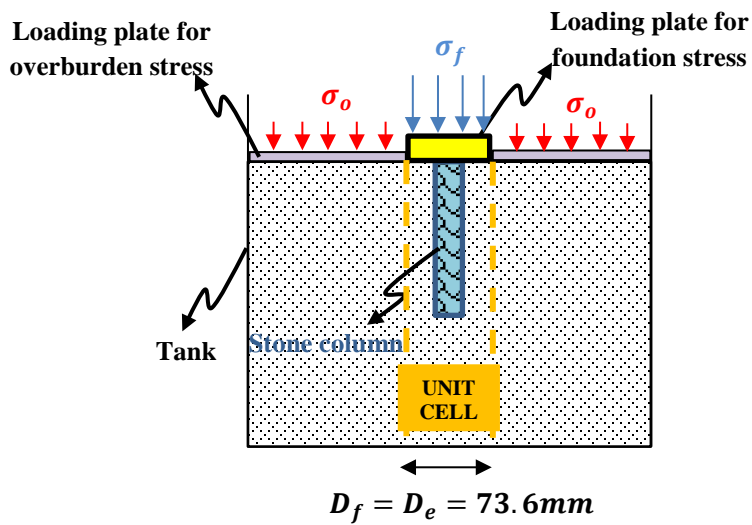
(c)
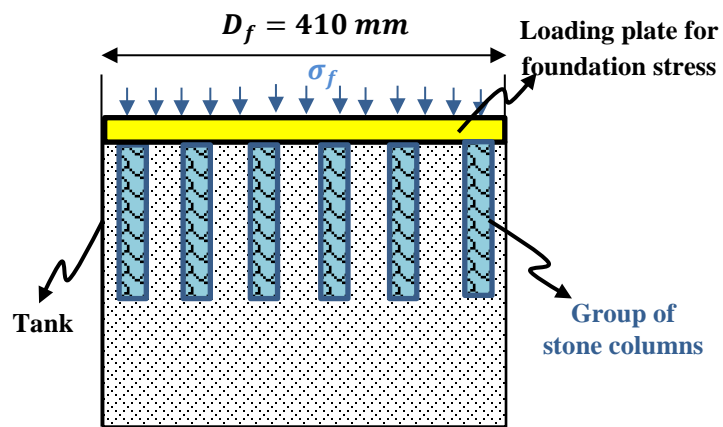
(d)

Figure 3.8. Sketches of loading patterns (a) consolidation phase (b) single column loading (c) single columns loaded over a footing having same diameter with the unit cell and (d) group loading

3.3.3.1. Loading Frame Used in Consolidation Phase

For the consolidation phase of the tests, loading plate having same diameter with tank, i.e. D_f = 410 mm, is used. Loading frame used in the consolidation phases is illustrated in Figure 3.9.
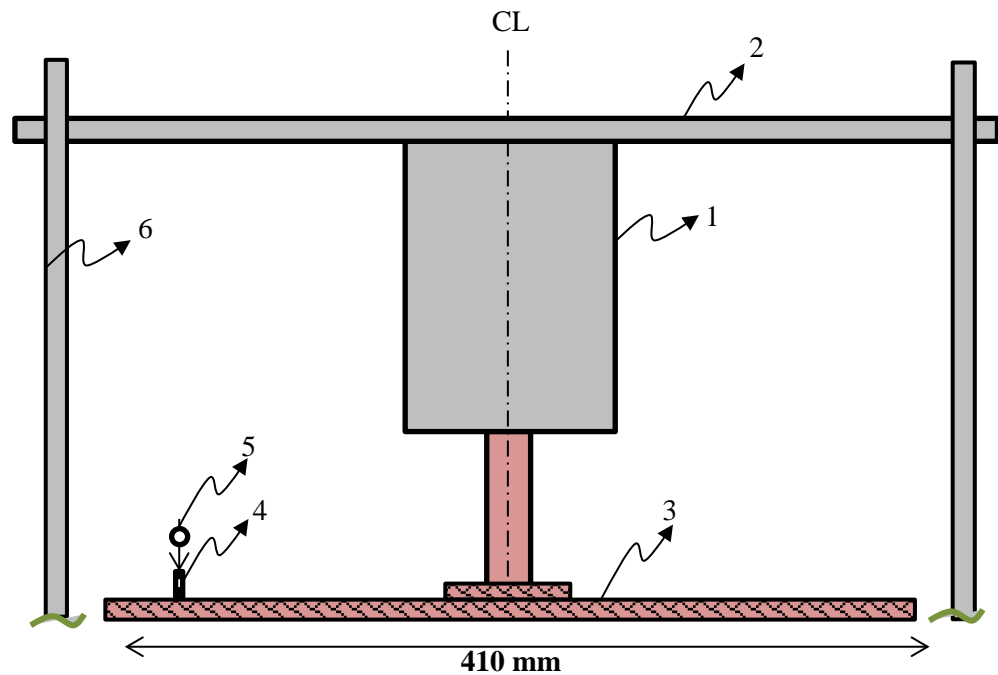
Figure 3.9. Loading frame used in consolidation phases

Where;

1: Loading piston

2: Upper cross plate

3: Loading plate

4: Bearing rod for settlement gage

5: Dial gage for settlement measurement

6: Vertical rods of loading frame

Note: In Figure 3.9, the parts colored **grey** are fixed members of loading frame.

Both the loading frame and the loading procedure for consolidation phase are same for all tests.

3.3.3.2. Loading Frames Used in Loading Phases

After the completion of consolidation, loading phase was performed.

For *single column loading*, there is one stone column at the center of the tank and it is concentrically loaded through a plate having same diameter with the stone column, i.e. 30 mm.

For *single columns loaded over a footing having same diameter with the unit cell*, there is one stone column at the center of the tank and it is loaded through a plate having same area with the equivalent area of the unit cell for a specific area replacement ratio of $a_r = 16.6\%$.

For *group loading*, there are 31 stone columns having diameter of 30 mm satisfying two conditions:

(i)   spacing between stone columns are same and calculated for equilateral triangular pattern for an area replacement ratio of $a_r = 16.6\%$ and,

(ii)   ratio of total area of stone columns to entire area is equal to area replacement ratio of $a_r = 16.6\%$.

Diameter of foundation used in single stone column, single columns loaded over a footing having same diameter with the unit cell and group tests are summarized in Table 3.4.

Table 3.4. Diameter of foundation used in loading phases

Number of stone columns (N)	Diameter of foundation, D_f (mm)
Single Column ($N = 1$)	30.0
Single columns loaded over a footing having same diameter with the unit cell ($N = 1$)	73.6
Group ($N = 31$)	410.0

Tests for Single Column Loading

Loading frame consists of two main elements: (i) to provide overburden stress over the clay body surrounding stone column and (ii) to apply foundation stress over loading plate placed at top of stone column. Two different stresses, overburden and foundation stresses, are applied through two different pneumatic pistons. Loading frame used in loading phase of single column tests is illustrated in Figure 3.10.

Total settlement of column is measured by potentiometric rulers.
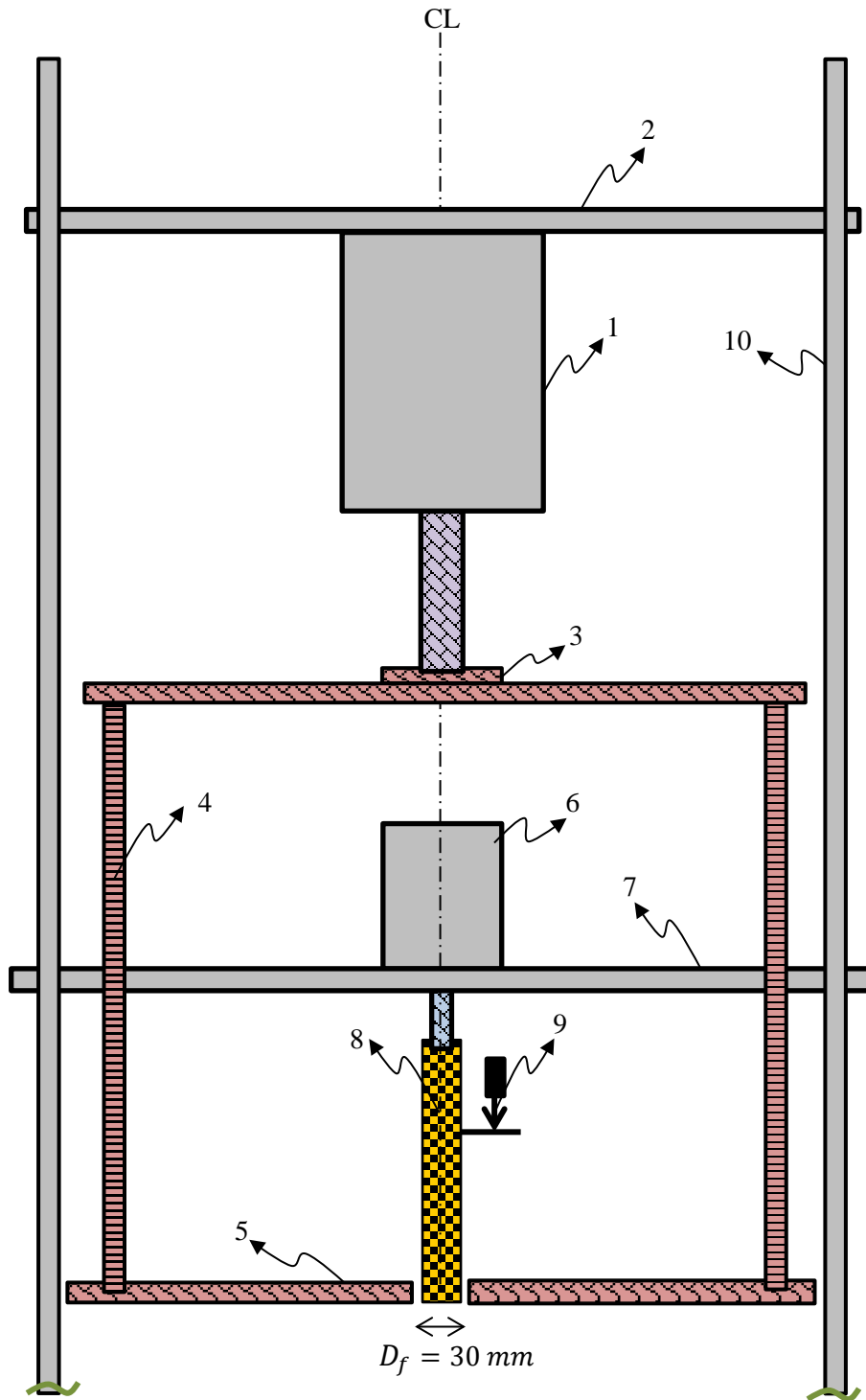
Figure 3.10. Loading frame used in loading phase of single column tests

Where;

1: Loading Piston 1 (applies overburden stress)

2: Upper cross plate

3: Bearing plate of Piston 1

4: Vertical rods of frame for overburden stress

5: Loading plate for overburden stress

FRAME for OVERBURDEN STRESS

6: Loading Piston 2 (applies foundation pressure)

7: Lower cross plate

8: Column transmitting the foundation pressure

9: Potentiometric ruler measuring the total settlement of column

10: Vertical rods of loading frame

Tests for Single Columns Loaded over a Footing Having Same Diameter with the Unit Cell

Loading frame is composed of two main elements: (i) to provide overburden stress over the clay body surrounding stone column and (ii) to apply foundation stress over loading plate placed at top of unit cell having same diameter with it. Two different stresses, overburden and foundation stresses, are applied through two different pneumatic pistons. Loading frame used in loading phase of single columns under a footing having same diameter with the unit cell tests is illustrated in Figure 3.11.

As seen in Figure 3.11 (a), there is a hole at the center of the loading plate, where a miniature soil pressure transducer was placed into this hole letting the face of diaphragm is in contact with the column in order to measure the stress carried by the column.

Also there is another hole at the midpoint of center and edge of the foundation to pass the settlement rod (Figure 3.11 (a), item #13) through it in order to measure the subsurface settlement at the level of the tip of stone column.

Total and the subsurface settlement were measured by potentiometric rulers.

Figure 3.11. (a) Sketch and (b) photograph of loading frame used in loading phase of single columns under a footing having same diameter with the unit cell

(b)

Figure 3.11. (a) Sketch and (b) photograph of loading frame used in loading phase of single columns under a footing having same diameter with the unit cell (continued)

Where;

1: Loading Piston 1 (applies overburden stress)

2: Upper cross plate

3: Bearing plate of Piston 1 　　　　　　　 ⎤ **FRAME for**

4: Vertical rods of frame for overburden stress ⎬ **OVERBURDEN**

5: Loading plate for overburden stress 　　　 ⎦ **STRESS**

6: Loading Piston 2 (applies foundation pressure)

7: Lower cross plate

8: Column transmitting the foundation pressure

9: Double stage loading plate for foundation stress

10: Miniature soil pressure transducer

11: Potentiometric rulers

12: Vertical rods of loading frame

13: Settlement rod to measure the subsurface settlement

Tests for Group Loading

Loading frame is composed of system applying foundation pressure over loading plate, having same diameter with tank, placed at top of the bedding soil which is treated by group of stone columns. Foundation stress is applied by a pneumatic piston. Loading frame used in loading phase of group tests is illustrated in Figure 3.12.

As seen in Figure 3.12 (a), there are two holes for transducers: one is at the center and other is near to the center of the loading plate. Miniature soil pressure transducers were placed into these holes letting the face of diaphragm of them in contact with columns in order to measure the stresses carried by the center column and near-to-center column. Also there is another hole at the midpoint of center and edge of the loading plate to pass the settlement rod (Figure 3.12 (a), item #9) through it in order to measure the subsurface settlement at the level of the tip of stone column.

Total settlement of group and the subsurface settlement were measured by potentiometric rulers.

(a)
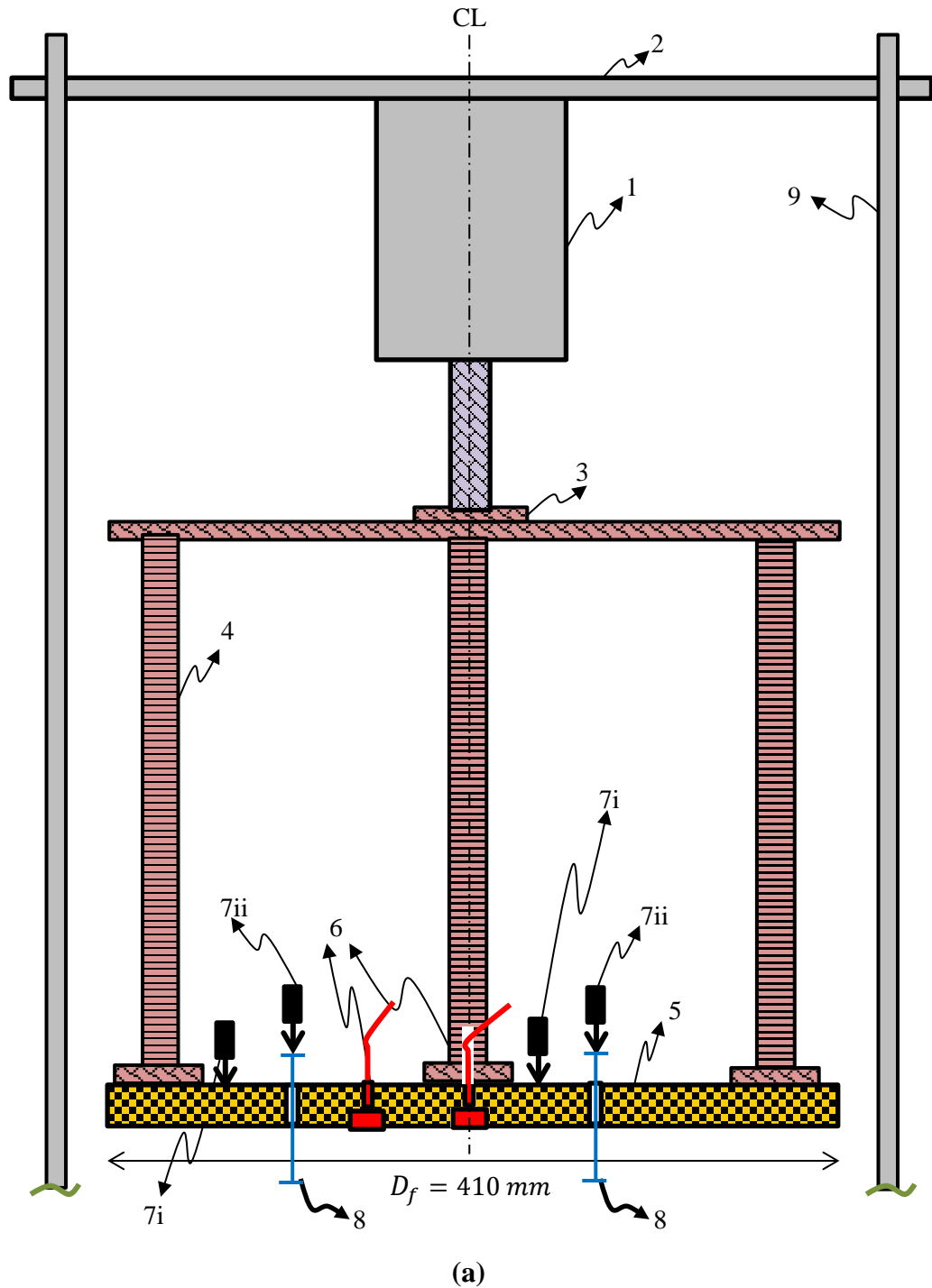
Figure 3.12. (a) Sketch and (b) photograph of loading frame used in loading phase of group tests

(b)

Figure 3.12. (a) Sketch and (b) photograph of loading frame used in loading phase of group tests (continued)

Where;

1: Loading piston (applies foundation pressure)

2: Upper cross plate

3: Bearing plate of piston

4: Vertical rods of load application frame

LOAD APPLICATION FRAME

5: Loading plate

6: Miniature soil pressure transducers

7: Potentiometric rulers for **i)** surface settlement **ii)** subsurface settlement

8: Settlement rods to measure the subsurface settlement

9: Vertical rods of entire loading frame

3.3.4. Miniature Soil Pressure Transducers

To measure stresses on the stone columns due to applied loading, soil pressure transducers which are a product of Kyowa Company – Model: BED-A-1MP were used. Transducer is shown in Figure 3.13. The details of the geometry are given in Figure 3.14. Other specifications are given in Appendix B.

Figure 3.13. Miniature soil pressure transducer
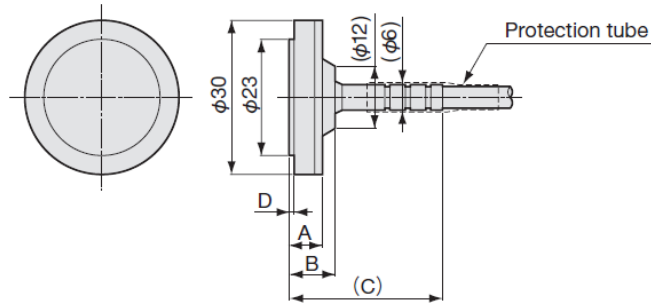
Model	A	B	C	D
BED-A-200KP	6.2	8.7	29.7	0.5
BED-A-500KP	6.5	9	30	0.8
BED-A-1MP				

Figure 3.14. Geometry of the miniature soil pressure transducer

Both transducers were periodically calibrated by using hydro pressure-oil stress equipment connected to the calibration device which was specially designed for this study. Calibration charts for both transducers are given in Appendix C.

3.3.5. Potentiometric Rulers

Potentiometric rulers which are product of ELE Company having range of 50 mm and sensitivity up to 6 digits of milivoltage shown in Figure 3.15 were used in order to monitor the settlements during loading phase. All potentiometric rulers were calibrated in triaxial apparatus by connecting them to data acquisition system.

Figure 3.15. Potentiometric ruler

88

3.3.6. Data Acquisition System

Data acquisition system having 8 channels provided 5V or 10V excitation voltage, which is a product of Teknik Destek Grup (TDG) Company. The data acquisition box is shown in Figure 3.16. TestLAB software was used to interpret the data obtained by the acquisition system.

Figure 3.16. Data acquisition system

3.3.7. Settlement Rods

Settlement rods are used for measurement of subsurface settlement at the level of tip of stone columns. Bottom and top plates having 10 mm and 20 mm in diameter, respectively, are bolted at both ends of the settlement rod having 3 mm diameter. Settlement rod is shown in Figure 3.17.

Figure 3.17. Settlement rod to measure subsurface settlements

3.4. Test Procedure

Model tests were performed mainly in the following three stages:

Stage 1: Preparation of paste

Stage 2: Consolidation of bedding soil

Stage 3: Loading of treated/untreated soil

In the following sections detailed procedure of each stage is described. Unless stated, each stage in procedure is same for all *single column*, *single columns under a footing having same diameter with the unit cell* and *group loading tests*.

3.4.1. Preparation of Paste

- The powder form of kaolin is mixed with water to attain 45% water content in a large mixer to obtain paste (Figure 3.18).

Figure 3.18. Preparation of paste in large mixer

- To get homogeneous soil with same water content, paste is bagged and kept in curing room for minimum 4 days.

3.4.2. Consolidation of Bedding Soil

- Geotextile pads are provided at the bottom and top of the specimen to provide drainage surfaces during the consolidation phase.
- Tank was filled with 75 – 80 kg of paste by slightly kneading and compacting to avoid air voids.
- Top of the soil is flattened and top geotextile pad is placed.
- Loading frame and the loading plate with settlement gages are assembled, and the consolidation pressure (σ_{cons}) is applied by the pneumatic piston.
- Consolidation pressure (σ_{cons}) was applied through piston gradually. Each stress was kept up to minimum 90% degree of consolidation. The experimental setup for consolidation stage is shown in Figure 3.19.

Figure 3.19. Setup for consolidation phase

3.4.3. Loading of Treated Soil

- The loading frame is dismantled and the surface is leveled to obtain exactly 30 cm height of the specimen.
- Vane shear tests were performed at different locations in order to get the undrained shear strength of the soil after the consolidation stage.
- A template is used to precisely locate the holes according to their predefined pattern in the plan view. Templates used in *single column/ single columns under a footing having same diameter with the unit cell* and *group loading tests* are shown in Figure 3.20 (a) and (b), respectively.
- The stone columns were installed by drilling a 30 mm diameter hole in the specimen using a helical auger to a predetermined depth.
- Samples were taken from the extracted specimen to get the water content at the end of the consolidation phase.

(a)   (b)

Figure 3.20. Templates used for stone columns in (a) single column/single columns under a footing having same diameter with the unit cell and (b) group loading tests

- For *single columns under a footing having same diameter with the unit cell* and *group loading tests*, deep settlement rods (item 13 in Figure 3.11 (a); item 8 in Figure 3.12 (a)) are fixed by a special tool through the drilled hole for stone column (Figure 3.21).

Figure 3.21. Placement of settlement rod

- Required mass of stone corresponding to 80% relative density after compaction was filled for the column into the hole in 3 cm increments and compacted by a tamper (Figure 3.22).
- Stretch film was placed over the tank in order to avoid drying of the test specimen.
- For *single column* and *single columns under a footing having same diameter with the unit cell tests*, frame for overburden stress (items 3, 4 and 5 in Figures 3.10 and 3.11 (a)) was placed on the top of the bedding soil as shown in Figure 3.23.
- For *single column loading tests*, column to transmit the load (item 8 in Figure 3.10) is placed on the stone column.

For *single columns under a footing having same diameter with the unit cell tests*, column + double stage loading plate including the transducer at the center of the plate (items 8, 9 and 10 in Figure 3.11(a)) were placed over the treated soil as shown in Figure 3.24.

(a)

(b)   **(c)**

Figure 3.22. (a) Mass of stones corresponding to 3 cm height of stone column (b) filling and (c) compacting stones to predefined depth

For *group loading tests*, load application frame and the transducers (items 3, 4, 5 and 6 in Figure 3.12(a)) were placed as shown in Figure 3.25.

- For *single column* and *single columns under a footing having same diameter with the unit cell tests*, lower cross plate and piston#2 (items 6 and 7 in Figures 3.10 and 3.11 (a)) was placed.

Figure 3.23. Frame for overburden stress

Figure 3.24. Placing column + double stage foundation plate including the transducer

- For *single column* and *single columns under a footing having same diameter with the unit cell tests*, upper cross plate and piston#1 (items 1 and 2 in Figures 3.10 and 3.11 (a)) was placed.

  For *group loading tests*, upper cross plate and piston (items 1 and 2 in Figure 3.12 (a)) was placed.
- Potentiometric rulers and dial gauge were placed on the system.
- For *single column* and *single columns under a footing having same diameter with the unit cell tests* firstly, overburden stress (σ_o) was applied through piston#1.
- Consequently, foundation stress (σ_f) was applied through piston#2 for *single column* and *single columns under a footing having same diameter with the unit cell tests*. Initial foundation stress was same with the consolidation pressure. Settlements were monitored to observe the cease of consolidation settlements. After the completion on settlement, load is increased to next level.
- For *group loading tests*, foundation stress (σ_f) was applied through piston. Initial foundation stress was same with the consolidation pressure. Settlements were monitored to observe the cease of consolidation settlements. After the completion on settlement, load is increased to next level.

Figure 3.25. Placing load application frame

- Experiment setups for *single columns under a footing having same diameter with the unit cell and group loading tests* are shown in Figure 3.26 (a) and (b), respectively.

3.4.4. Data Interpretation

During loading phase following values were measured by data acquisition system shown in Figure 3.27.

- Settlement of foundation by potentiometric rulers
- Subsurface settlements at the level of tip of the stone column (*single columns under a footing having same diameter with the unit cell tests*) and two different levels (*group loading tests*) by potentiometric rulers
- Stress carried by stone columns by miniature soil pressure transducers

(a)

Figure 3.26. Experimental setups for (a) single columns under a footing having same diameter with the unit cell and (b) group loading tests

(b)

Figure 3.26. Experimental setups for (a) single columns under a footing having same diameter with the unit cell and (b) group loading tests (continued)

Figure 3.27. Data acquisition system

CHAPTER 4

PRESENTATION OF TEST RESULTS

4.1. Introduction

In this study, model tests of stone column for single column, single columns loaded over a footing having same diameter with the unit cell and group loading were investigated. Surface settlement, subsurface settlement and stress on the stone column were directly and continuously measured in all tests. In group tests, stress carried by center column and a column near to center were measured.

In all model tests, diameter of stone column (D), compressible layer thickness (H), and area replacement ratio (a_r) values are constant as 3 cm, 30 cm and 16.6%, respectively.

In tests of single column loading and single columns loaded over a footing having same diameter with the unit cell, overburden stress of 20 kN/m^2 is applied to provide confinement around the loaded area (σ_o). This pressure is applied to satisfy the lateral confinement at a shallow depth near to the top of the stone column where stress concentration factor is defined.

In the testing program the main variables are type of loading, length of stone column (L) and undrained shear strength of compressible soil (c_u). Values of these variables are summarized in Table 4.1.

Series of tests conducted in this study are summarized in Table 4.2. In this chapter, the results of these tests are presented.

Table 4.1. Values of variable parameters

Variable Parameters	Values
Type of loading	S: Single column loading ($N=1$) SCF: single columns loaded over a footing having same diameter with the unit cell ($N=1$) G: Group loading ($N=31$)
Undrained shear strength, c_u (kN/m^2)	20 30
Length of stone column/Height of soil (L/H)	0.4 (short-floating) 0.7 (long-floating) 1.0 (end-bearing)

*N: number of stone columns

Table 4.2. Series of tests

Test No.	Type of loading	Initial c_u (kN/m^2)	L/H
1	S	20	0.4
2	S	20	0.7
3	S	20	1.0
4	SCF	20	Untreated
5	SCF	20	0.4
6	SCF	20	0.7
7	SCF	20	1.0
8	G	20	Untreated
9	G	20	0.4
10	G	20	0.7
11	G	20	1.0
12	G	30	Untreated
13	G	30	0.4
14	G	30	0.7
15	G	30	1.0

4.2. Single Column Loading (Type-S)

Single column loading tests were performed for three different lengths of stone columns in soil having initial undrained shear strength (c_u) of 20 kN/m². Aim of single column loading tests is to obtain deformation modulus of stone column and soil under floating columns. Stone column was loaded through a foundation plate having same diameter with column, i.e. 30 mm. Overburden stress to provide confinement around the column (σ_o) with an amount of 20 kN/m² is applied.

Initial (at the end of consolidation phase) and final (at the end of loading phase) values of water content (w) and undrained shear strength (c_u) for each test are given in Table 4.3.

Table 4.3. Initial and final values of w and c_u (Type-S)

	Water content, w (%)		Undrained shear strength, c_u (kN/m²)	
L/H	Initial	Final	Initial	Final
0.4	39.3	38.9	18	22
0.7	39.4	38.9	19	23
1.0	38.9	37.4	20	23

Surface settlement was measured during each test. At each loading stage, load was kept constant until the rate of settlement was smaller than 0.004 mm/min in successive 60 minutes regarding to TS 5744 criteria. Tests were finalized whether punching of foundation into soil or continuous increase in settlement was observed.

Values of measured surface settlement at the end of each loading stage are summarized in Table 4.4. In Table 4.4, σ_f is applied foundation pressure and S_t is surface settlement of the column.

Table 4.4 Values of surface settlements (Type-S)

L/H = 0.4		L/H = 0.7		L/H = 1.0	
σ_f (kN/m²)	S_t (mm)	σ_f (kN/m²)	S_t (mm)	σ_f (kN/m²)	S_t (mm)
50	1.3	50	0.9	200	1.0
100	2.0	100	1.6	250	1.4
200	3.7	200	2.5	350	2.4
250	5.5	300	Failure	400	2.9
300	Failure			450	Failure

4.3. Single Columns Loaded over a Footing Having Same Diameter with the Unit Cell Tests (Type-SCF)

Type-SCF tests were performed for three different lengths of stone columns and untreated soil having undrained shear strength (c_u) of 20 kN/m². Unit cell is loaded through a foundation plate having diameter of 73.6 mm to simulate an area replacement ratio (a_r) of 16.6%. Overburden stress to provide confinement around the loaded area (σ_o) with an amount of 20 kN/m² is applied.

Initial (at the end of consolidation phase) and final (at the end of loading phase) values of water content (w) and undrained shear strength (c_u) for each test are given in Table 4.5.

Surface settlement and subsurface settlement at depth of column tip were directly measured during tests. At each loading stage, load was kept constant until the rate of settlement was smaller than 0.009 mm/min in successive 60 minutes regarding to TS 5744 criteria. Tests were finalized whether punching of foundation into soil or continuous increase in surface settlement was observed.

Table 4.5. Initial and final values of w and c_u (Type-SCF)

	Water content, w (%)		Undrained shear strength, c_u (kN/m^2)	
L/H	Initial	Final	Initial	Final
Untreated	39.0	36.7	19	-
0.4	40.0	36.8	22	29
0.7	39.2	37.1	19	30
1.0	39.6	37.2	21	32

Values of measured surface settlement and subsurface settlement at the end of each loading stage are summarized in Table 4.6 for all Type-SCF tests. In Table 4.6, σ_f is applied foundation pressure, S_u is surface settlement of untreated soil, $S_{u-0.4}$ is subsurface settlement of untreated soil at depth of $z/H = 0.4$ (where, z is depth from the surface), $S_{u-0.7}$ is subsurface settlement of untreated soil at depth of $z/H = 0.7$, S_t is surface settlement of treated soil, $S_{t-0.4}$ is subsurface settlement of treated soil at depth of $z/H = 0.4$ and $S_{t-0.7}$ is subsurface settlement of treated soil at depth of $z/H = 0.7$.

Table 4.6 Values of surface and subsurface settlements (Type-SCF)

σ_f (kN/m^2)	UNTREATED			L/H = 0.4		L/H = 0.7		L/H = 1.0
	S_u	$S_{u-0.4}$	$S_{u-0.7}$	S_t	$S_{t-0.4}$	S_t	$S_{t-0.7}$	S_t
35	3.5	1.4	0.7	1.5	0.7	1.2	0.4	0.7
50	6.1	2.4	1.4	3.0	1.1	2.5	0.7	1.8
75	8.3	3.0	1.7	4.5	2.0	3.6	1.1	3.0
100	Failure			Failure		Failure		5.1
125	-	-	-	-	-	-	-	Failure

All settlement values are in mm.

Settlement profiles at each loading stage for untreated and floating column tests are illustrated in Figure 4.1.

Stress carried by stone column (σ_c) is directly measured during tests. Stress carried by soil in unit cell (σ_s) is calculated from the difference between total applied load and the load carried by stone column is divided by the area of soil (Equation 2.4).

Measured stress carried by stone column (σ_c) and calculated stress carried by soil (σ_s) values at the end of each loading stage are summarized in Table 4.7 for all treated Type-SCF tests. Stress values written in *italic* are corresponding to values under the foundation pressure which the failure was observed. The variation of stresses carried by column and soil with time are shown in Figure 4.2.

Table 4.7. Stress carried by column and soil (Type-SCF)

σ_f (kN/m^2)	$L/H = 0.4$		$L/H = 0.7$		$L/H = 1.0$	
	σ_c (kN/m^2)	σ_s (kN/m^2)	σ_c (kN/m^2)	σ_s (kN/m^2)	σ_c (kN/m^2)	σ_s (kN/m^2)
35	76.4	26.8	120.4	18.0	147.9	12.5
50	172.0	25.7	195.5	21.0	212.9	17.6
75	258.0	38.5	285.2	33.1	267.1	36.7
100	282.0	63.7	317.9	56.6	313.2	57.5
125	NA	NA	NA	NA	412.6	67.7
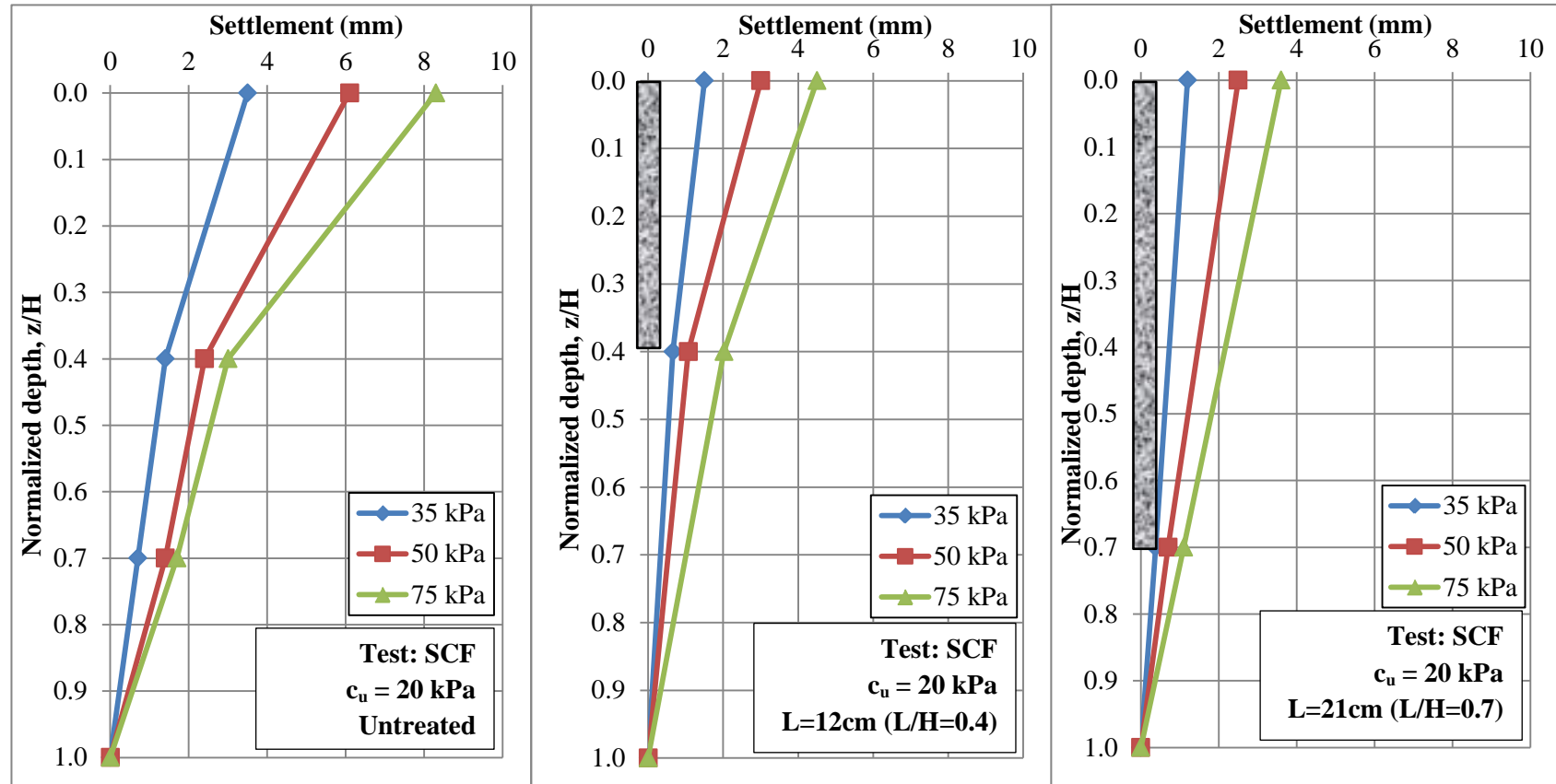
Figure 4.1. Settlement profiles (Type-SCF)
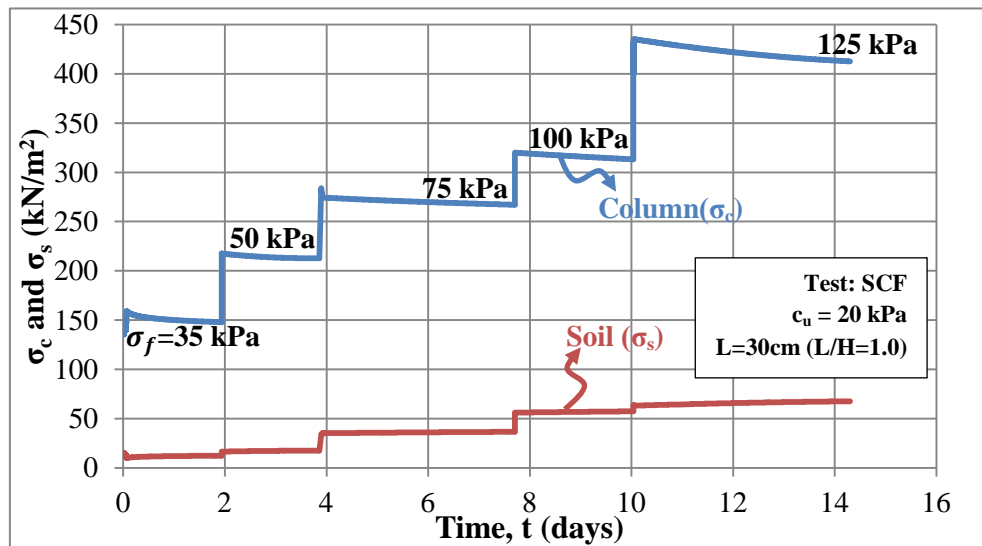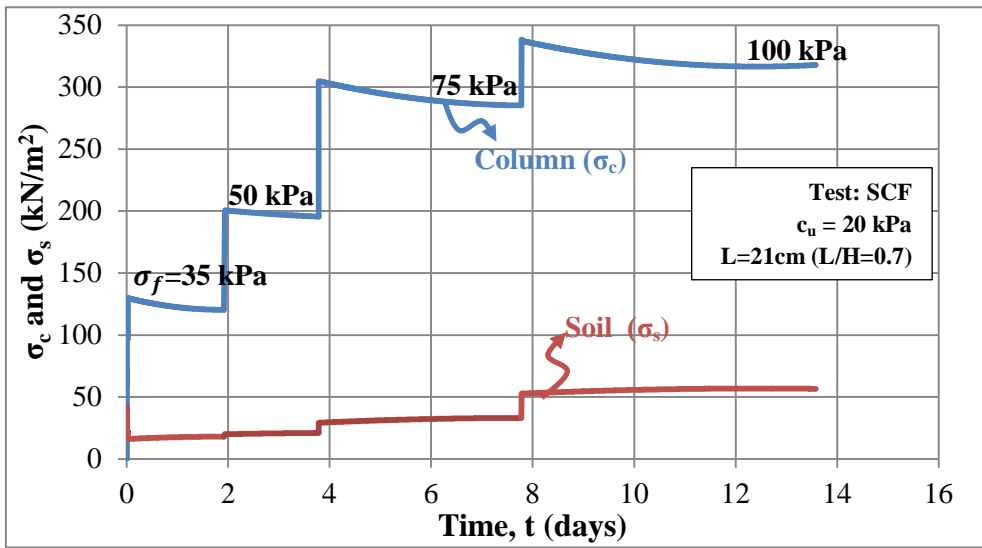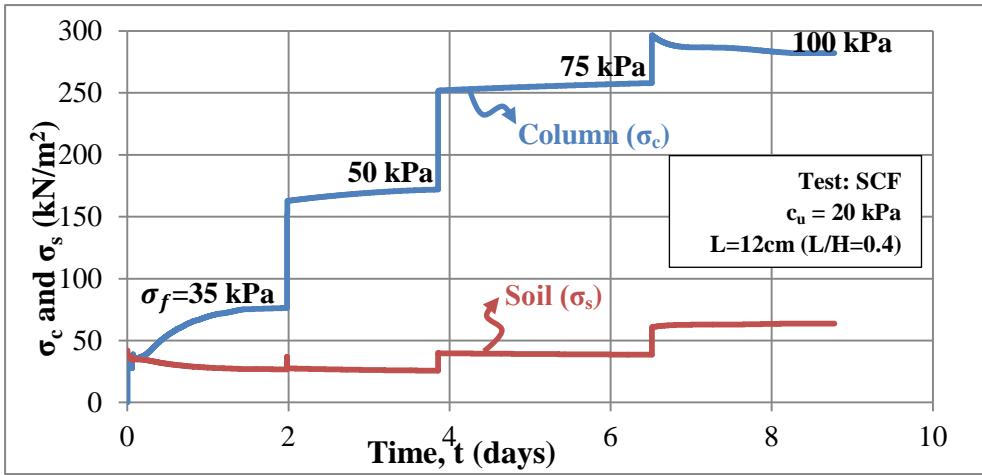
Figure 4.2. σ_c and σ_s – time relation (Type-SCF)

4.4. Group Loading (Type-G)

Two different sets of group loading tests, Group 1 and Group 2, were performed in soil having undrained shear strength (c_u) of 20 and 30 kN/m², respectively. Three different lengths of stone column group and untreated soil were tested in each set. Groups are composed of 31 stone columns having equal length and 7 cm center to center spacing revealing to area replacement ratio (a_r) of 16.6%. Entire area of the group was loaded through 41 cm diameter rigid loading plate.

Initial (at the end of consolidation phase) and final (at the end of loading phase) values of water content (w) and undrained shear strength (c_u) for each test in Group 1 and 2 are given in Table 4.8 and 4.9, respectively.

Table 4.8. Initial and final values of w and c_u (Type-G1)

	Water content, w (%)		Undrained shear strength, c_u (kN/m²)	
L/H	Initial	Final	Initial	Final
Untreated	39.4	25.5	20	-
0.4	38.6	36.8	20	35
0.7	38.2	36.5	19	36
1.0	38.9	36.3	18	42

Table 4.9. Initial and final values of w and c_u (Type-G2)

	Water content, w (%)		Undrained shear strength, c_u (kN/m²)	
L/H	Initial	Final	Initial	Final
Untreated	38.4	25.8	30	-
0.4	38.8	34.5	29	45
0.7	37.2	33.6	28	43
1.0	38.3	33.3	30	54

Surface settlement and subsurface settlement at two different depths were measured during tests. At each loading stage, load was kept constant until the rate of settlement was smaller than 0.05 mm/min in successive 60 minutes regarding to TS 5744 criteria. No failure was observed in group tests up to 150 kPa which is the maximum capacity of loading pistons.

Measured surface settlement and subsurface settlement values at the end of each loading stage are summarized in Tables 4.10 and 4.11 for Group 1 and 2 tests, respectively.

Settlement profiles at each loading stage for untreated and floating column tests in Group 1 and 2 are illustrated in Figures 4.3 and 4.4, respectively.

Stresses carried by center (σ_{c1}) and near to center stone columns (σ_{c2}) were directly measured during tests. It is assumed that the same vertical stress is mobilized in all columns and the average of two measured stress values on columns are taken as average stress carried by columns, σ_c. Stress carried by soil (σ_s) is calculated from the difference between total applied load and the total load carried by stone columns is divided by the area of soil (Equation 2.4).

Measured stresses carried by stone columns (σ_c) and calculated stress carried by soil (σ_s) values at the end of each loading stage are summarized in Tables 4.12 and 4.13 for Group 1 and 2 tests, respectively. In these tables, σ_{c1} and σ_{c2} are stresses measured at top of the columns 1 and 2 respectively; σ_c is the average stress carried by stone columns and σ_s is average stress carried by soil. The variation of average stresses carried by column and soil with time are shown in Figures 4.5 and 4.6 for Group 1 and 2, respectively.

Table 4.10 Values of surface and subsurface settlements (Type-G1)

σ_f (kN/m²)	UNTREATED			L/H = 0.4			L/H = 0.7			L/H = 1.0
	S_u (mm)	$S_{u-0.4}$ (mm)	$S_{u-0.7}$ (mm)	S_t (mm)	$S_{t-0.4}$ (mm)	$S_{t-0.7}$ (mm)	S_t (mm)	$S_{t-0.4}$ (mm)	$S_{t-0.7}$ (mm)	S_t (mm)
35	5.0	2.4	1.4	3.1	2.2	1.5	2.3	1.7	1.0	1.1
50	8.3	4.4	2.2	5.5	4.1	2.4	4.4	3.1	1.9	2.7
75	12.8	6.3	3.1	8.3	6.1	3.0	6.5	5.1	2.9	4.3
100	16.1	8.8	4.0	11.1	8.2	4.2	8.4	6.0	3.8	5.7
125	18.5	10.3	5.5	12.8	10.1	5.3	NA	NA	NA	NA
150	20.7	11.4	6.2	15.0	11.4	6.1	11.7	8.2	6.0	7.4

111

Table 4.11 Values of surface and subsurface settlements (Type-G2)

σ_f (kN/m²)	UNTREATED			L/H = 0.4			L/H = 0.7			L/H = 1.0
	S_u (mm)	$S_{u-0.4}$ (mm)	$S_{u-0.7}$ (mm)	S_t (mm)	$S_{t-0.4}$ (mm)	$S_{t-0.7}$ (mm)	S_t (mm)	$S_{t-0.4}$ (mm)	$S_{t-0.7}$ (mm)	S_t (mm)
65	6.1	3.2	1.2	4.3	3.1	1.1	3.1	2.0	1.1	2.4
75	6.7	3.5	1.7	4.8	3.5	1.5	3.8	2.5	1.5	2.8
100	8.8	4.5	2.2	6.2	4.3	2.3	4.8	3.6	2.0	3.9
125	11.0	6.5	2.8	8.2	6.2	2.8	6.2	4.7	2.7	4.6
150	14.3	8.0	4.2	10.1	7.7	4.0	7.6	5.9	3.8	5.9
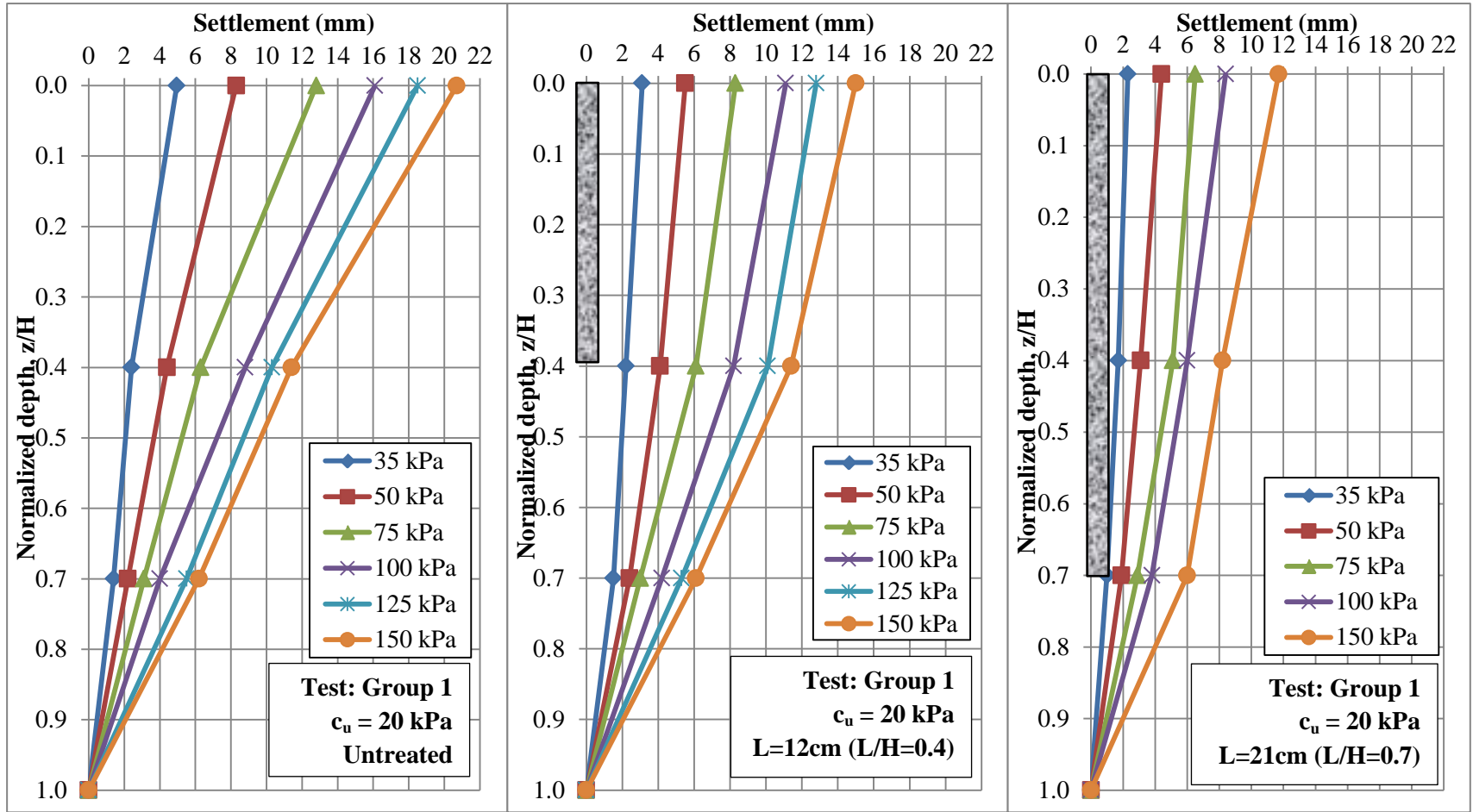
Figure 4.3. Settlement profiles (Type-G1)
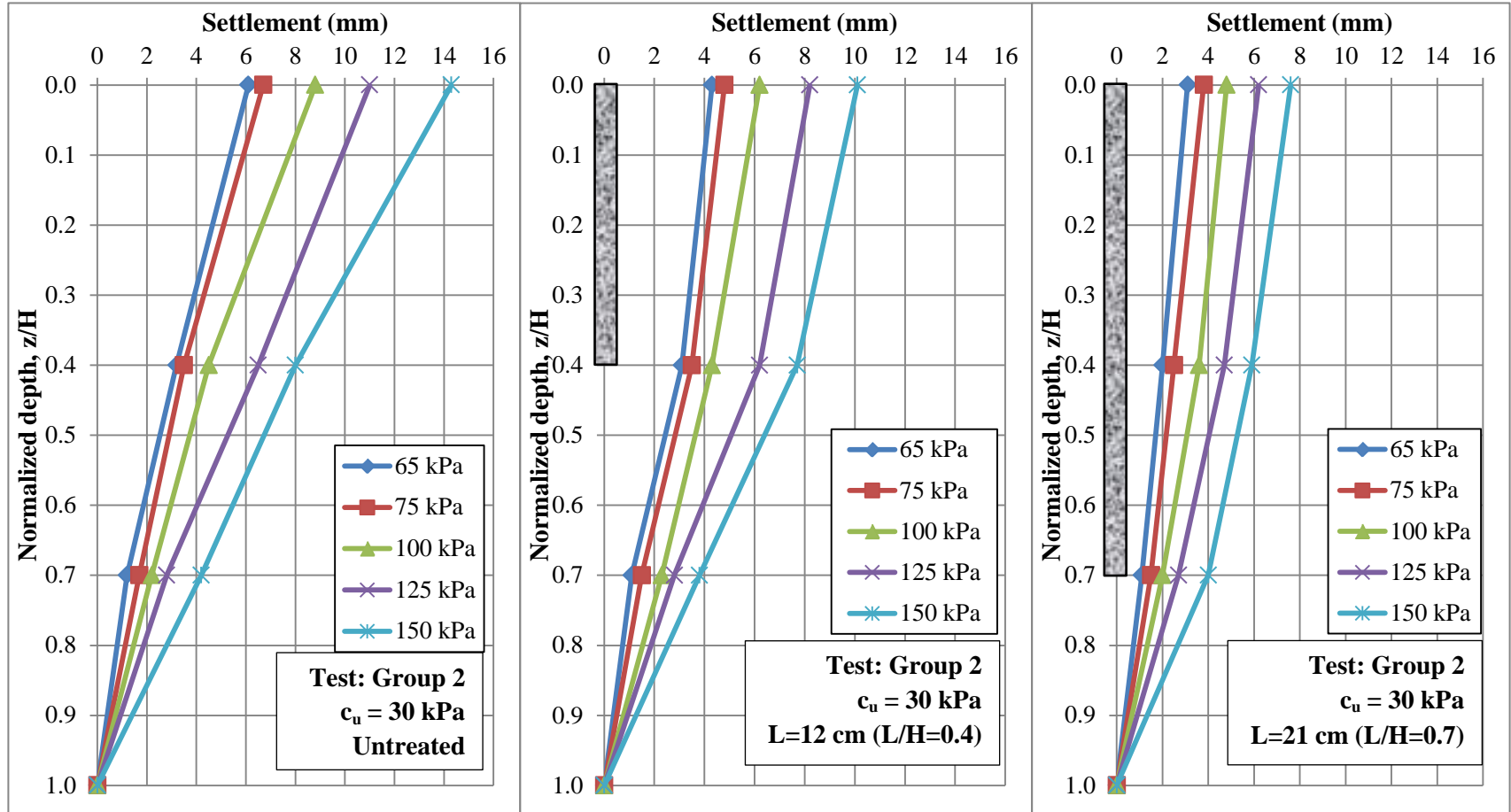
Figure 4.4. Settlement profiles (Type-G2)

Table 4.12. Stresses carried by columns and soil (Type-G1)

σ_f (kN/m²)	L/H = 0.4				L/H = 0.7				L/H = 1.0			
	σ_{c1} (kN/m²)	σ_{c2} (kN/m²)	σ_c (kN/m²)	σ_s (kN/m²)	σ_{c1} (kN/m²)	σ_{c2} (kN/m²)	σ_c (kN/m²)	σ_s (kN/m²)	σ_{c1} (kN/m²)	σ_{c2} (kN/m²)	σ_c (kN/m²)	σ_s (kN/m²)
35	96.5	103.3	99.9	22.0	136.6	128.2	132.4	16.2	157.2	144.9	151.0	12.8
50	191.5	175.1	183.3	23.3	200.3	193.1	196.7	21.3	216.1	181.9	199.0	22.8
75	273.5	258.7	266.1	36.8	292.1	272.7	282.4	35.1	318.4	274.5	296.5	34.0
100	325.7	314.1	319.9	56.0	360.7	336.2	348.4	52.3	396.1	354.2	375.2	48.2
125	362.5	359.0	360.7	77.8	-	-	-	-	-	-	-	-
150	441.5	411.0	426.3	94.7	444.1	430.7	437.4	93.8	521.3	491.3	506.3	81.2

Table 4.13. Stresses carried by columns and soil (Type-G2)

σ_f (kN/m²)	L/H = 0.4				L/H = 0.7				L/H = 1.0			
	σ_{c1} (kN/m²)	σ_{c2} (kN/m²)	σ_c (kN/m²)	σ_s (kN/m²)	σ_{c1} (kN/m²)	σ_{c2} (kN/m²)	σ_c (kN/m²)	σ_s (kN/m²)	σ_{c1} (kN/m²)	σ_{c2} (kN/m²)	σ_c (kN/m²)	σ_s (kN/m²)
65	124.1	92.2	108.2	56.4	194.3	140.1	167.2	44.6	219.1	184.5	201.8	37.6
75	177.7	134.4	156.0	58.8	240.3	202.7	221.5	45.7	267.4	234.6	251.0	39.8
100	253.9	191.3	222.6	75.5	317.7	304.1	310.9	57.8	337.2	333.7	327.6	54.5
125	321.3	265.3	293.3	91.3	420.8	375.2	398.0	70.4	438.4	410.9	411.6	67.6
150	406.0	343.9	375.0	105.0	463.9	444.9	454.4	89.1	515.8	469.4	492.6	81.4
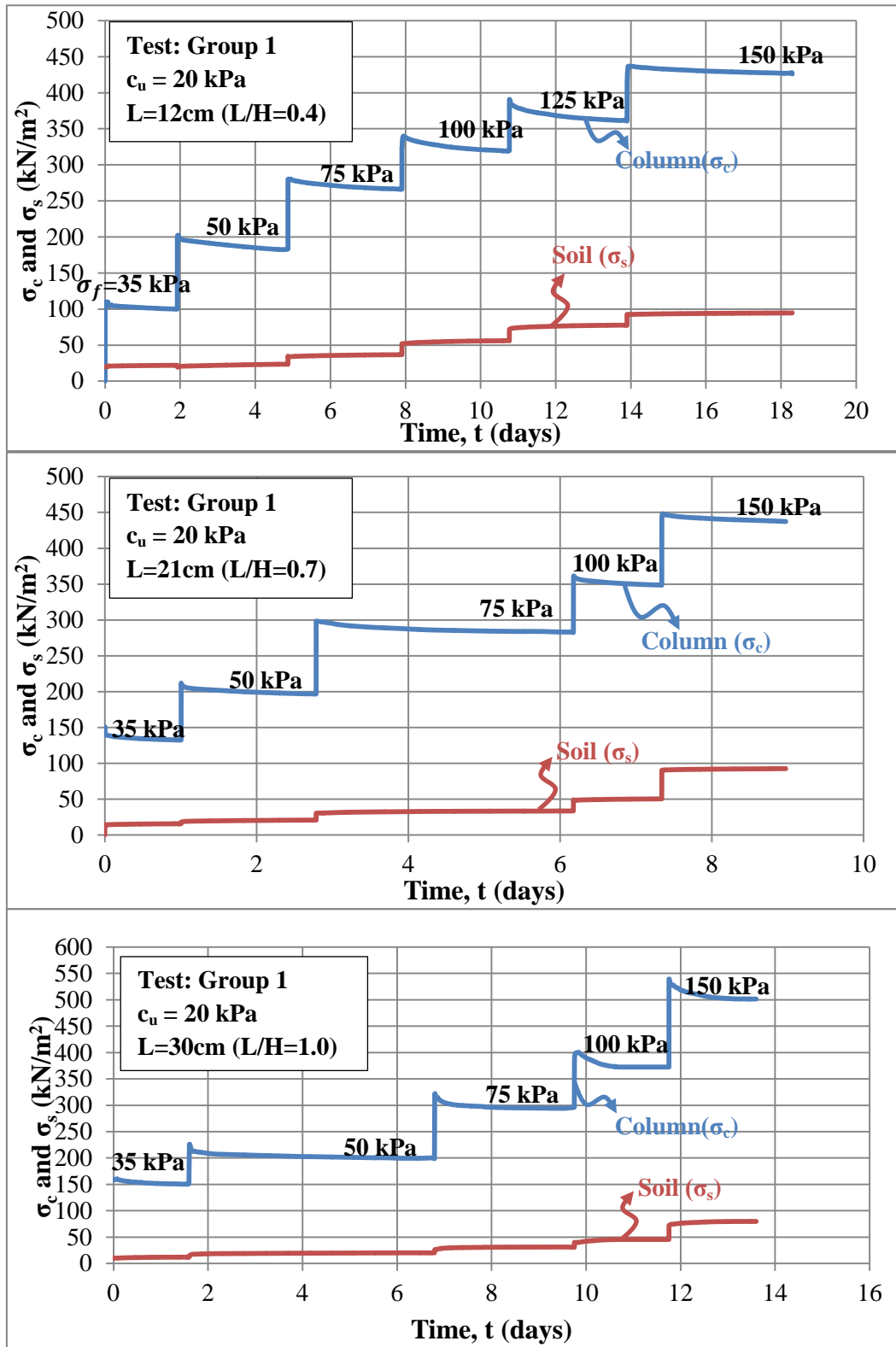
Figure 4.5. Average σ_c and σ_s – time relation (Type-G1)

115
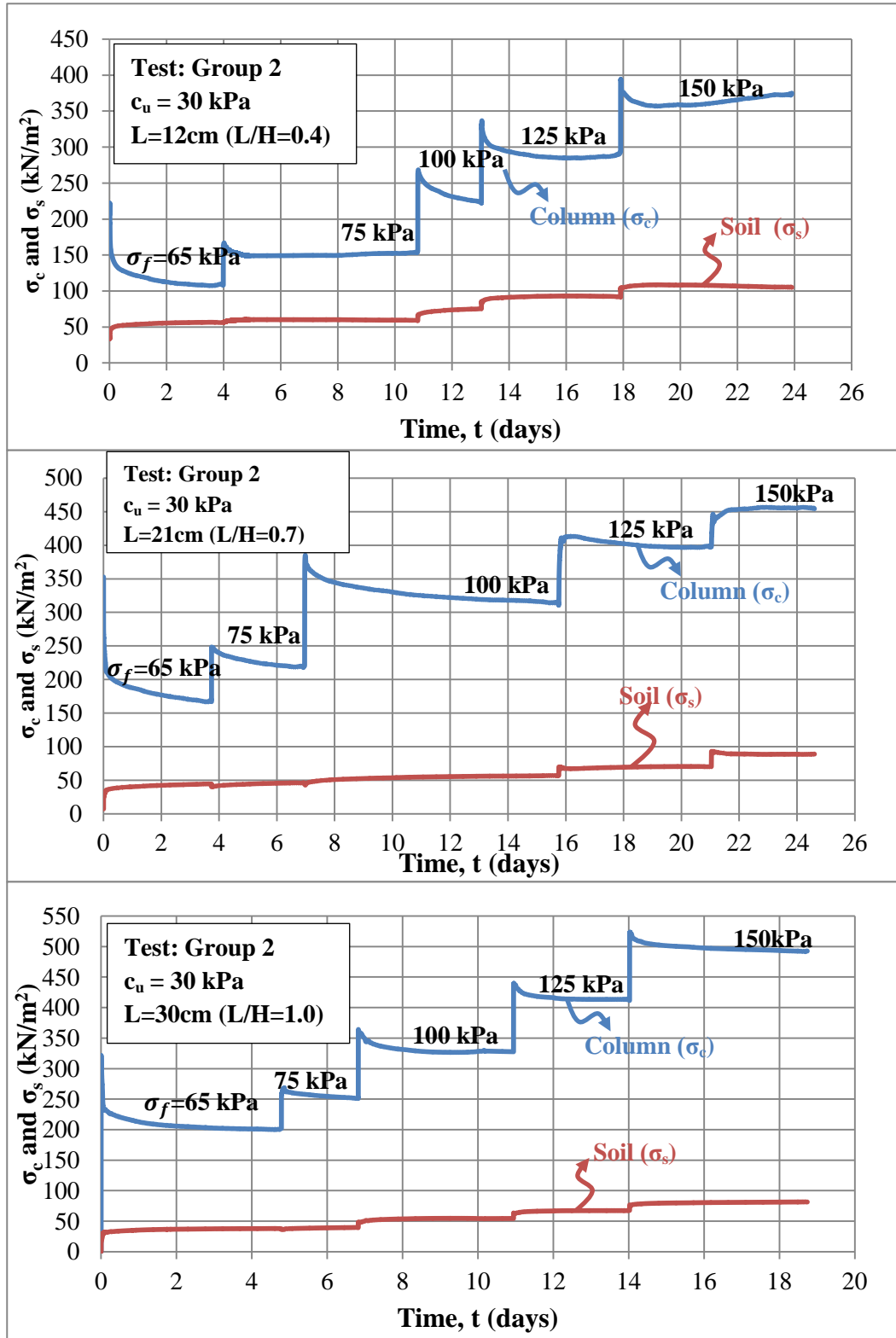
Figure 4.6. Average σ_c and σ_s – time relation (Type-G2)

116

CHAPTER 5

DISCUSSION OF TEST RESULTS

5.1. Introduction

Test results are presented in Chapter 4. In this chapter, discussion on stress – deformation behavior of single column, single columns loaded over a footing having same diameter with the unit cell and group loading tests are presented. Moreover, comparison between single columns loaded over a footing having same diameter with the unit cell and group behavior on stress – deformation behavior is given. Effects of column length and undrained shear strength on the stone column behavior are also discussed.

In single column loading tests failure modes, ultimate bearing capacities and critical length concepts are discussed. In addition, deformation moduli of stone column at different foundation pressures were obtained through back-calculations, using Plaxis 2D software.

In single columns loaded over a footing having same diameter with the unit cell and group loading tests, settlement reduction ratios (SRR) at different zones and stress concentration factors (n) for different foundation pressures and column lengths are compared. Both parameters, SRR and n, are compared with equilibrium method. Variation of stress concentration factor with time is assessed. Moreover, single columns loaded over a footing having same diameter with the unit cell and group behavior with floating and end-bearing columns are

compared. Whether or not the single columns loaded over a footing having same diameter with the unit cell behavior can represent the group behavior is discussed. A method to obtain the group settlement from the measured single columns loaded over a footing having same diameter with the unit cell settlement is proposed. Furthermore, relationships between total settlement reduction ratio (SRR_T) and undrained shear strength and; stress concentration factor (n) and undrained shear strength are proposed.

5.2. Interpretation of Test Results

Test results obtained from single column loading (Type-S), single columns loaded over a footing having same diameter with the unit cell (Type-SCF) and both group tests (Type-G1 and Type-G2) are presented in Sections 5.2.1, 5.2.2 and 5.2.3, respectively.

5.2.1. Single Column Loading Tests (Type-S)

5.2.1.1. Bearing Capacity and Failure Mechanisms

Aim of single column loading tests is to observe the load-settlement behavior of stone column, bearing capacity and failure mechanism for different column lengths. The normalized stress-settlement behaviors of stone columns having different lengths are shown in Figure 5.1. In this figure the data corresponding to maximum foundation pressure on each curve represents the last measured settlement under failure load. Failure of stone columns having L/H ratios of 0.4, 0.7 and 1.0 occurred at foundation pressures equal to 300 kPa, 300 kPa and 450 kPa, respectively. It is found that, bearing capacities of both floating stone columns are same (300 kPa) where the end bearing one has a higher bearing capacity. Ratio of ultimate bearing capacity (σ_{ult}) of end bearing stone column to initial undrained shear strength of soil (c_u), i.e. σ_{ult}/c_u, is compared with findings of previous studies (Figure 5.2). The methods used in this comparison

118

are summarized in Table 5.1. The σ_{ult}/c_u ratio obtained in this study is generally in agreement with the findings of previous studies.

At the end of each test, test specimen was extracted from tank and vertically cut through the center line in order to observe the failure mode of the stone column. Photographs taken from the deformed shape of stone columns are shown in Figure 5.3. In this figure, full red lines are representing the external boundary of failed shape where dashed red lines are illustrating the original shape of stone columns.
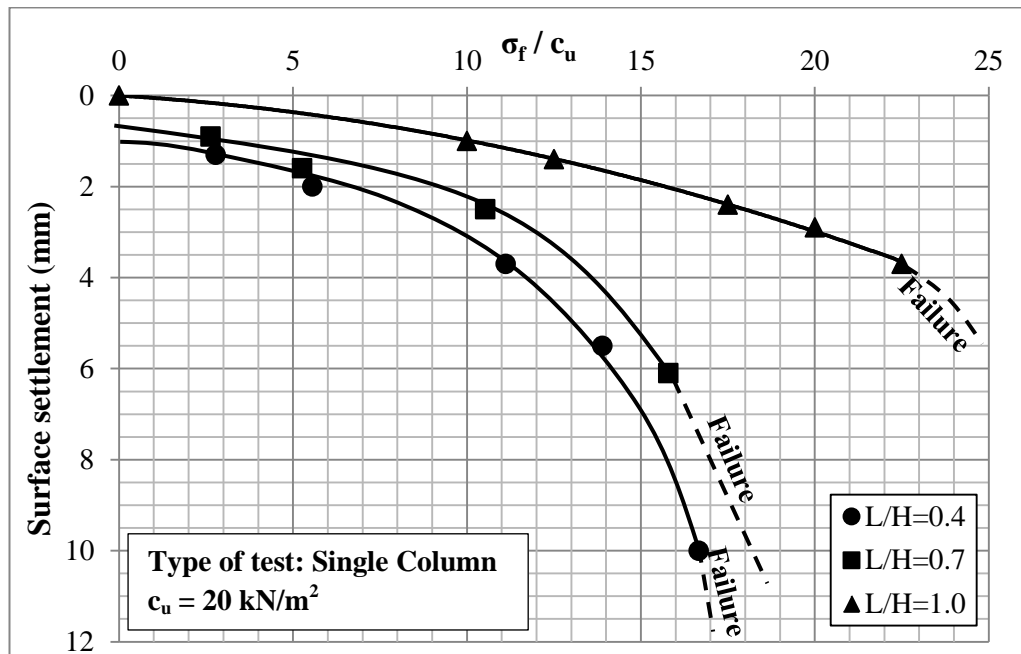
Figure 5.1. σ_f/c_u – surface settlement behavior (Type-S)

Deformed shape of the short floating column ($L/H = 0.4$) indicates that failure was due to punching and bulging through entire length of column (Figure 5.3a). Bulging mode of column implies that the length of stone column is inadequate to carry the applied pressure alone and transmitting the load to surrounding soil by causing passive failure through the entire length. On the other hand, deformed
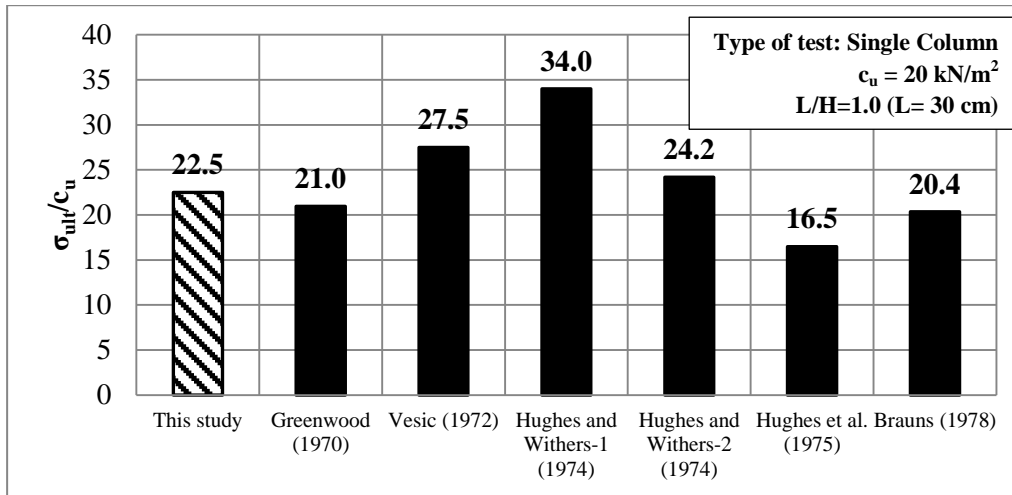
Figure 5.2. Comparison of σ_{ult}/c_u values with previous studies (Type-S)

Table 5.1. Details on methods used in Figure 5.2

Method	Theory based on	Proposed equation
Greenwood (1970)	Passive resistance failure	$\sigma_{ult} = \{\gamma z + 2c_u\} * \left(\frac{1+\sin\phi_c}{1-\sin\phi_c}\right)$ Where; ϕ_c: angle of shearing resistance of column material, γ: unit weight of soil and z: depth
Hughes and Withers-1 (1974)	Cylindrical expansion theory	$\sigma_{ult} = \frac{1+\sin\phi_c}{1-\sin\phi_c} * (\sigma_{Ro} + 4c_u)$ Where; σ_{Ro}: total in-situ lateral stress
Brauns (1978)	Triaxial confinement	$\sigma_{ult} = (q + 2c_u)\tan^2\left(\frac{\pi}{4} + \frac{\phi_c}{2}\right)$ Where; q: surcharge pressure
Vesic (1972) Hughes and Withers-2 (1974) Hughes et al. (1975)	Model tests and FEM	$\sigma_{ult} = 27.5c_u$ $\sigma_{ult} = 24.2c_u$ $\sigma_{ult} = 16.3c_u$

shape of long floating column ($L/H = 0.7$) indicates that column fails due to punching and local bulging occurred at depth, between $2.8D - 5.5D$ where, D is diameter of stone column (Figure 5.3b). Deformed shape of end bearing stone column ($L/H = 1.0$) indicates that local bulging is the only reason for failure (Figure 5.3c). Bulging occurred at depth between $1.3D$ and $3.9D$.

For single column loading tests with different length of stone column, initial undrained shear strength (c_u), ultimate bearing capacity of column (σ_{ult}) and failure mode are summarized in Table 5.2.

In literature, many researchers (Hughes and Withers 1974, Madhav 1982, Madhav and Miura 1994, Van Impe et al. 1997) stated that the failure mode of stone column can be determined by using critical length (L_{cr}) concept. According to critical length concept:

- If length of stone column (L) is less than the critical length (L_{cr}), i.e. $L < L_{cr}$, mode of failure is pile type failure (punching).
- If length of stone column (L) is greater than the critical length (L_{cr}), i.e. $L > L_{cr}$, mode of failure is bulging failure.

Results obtained in single column loading tests imply that the critical length (L_{cr}) is in between $4D–7D$. This finding is consistent with the one proposed by Madhav (1982) which states L_{cr} is equal to $6D$ for $c_u = 20$ kPa and $\phi_c = 48°$ (Figure 2.23).

Madhav and Miura (1994) noted that bulging and pile failure are not mutually exclusive. While the tendency for bulging is predominant, it occurs in conjunction with the pile action since the applied load is transmitted through resistances mobilized around the shaft and tip of column. This statement agrees

with the failure shape of long floating stone column (L/H=0.7) as shown in Figure 5.2(b).

For end bearing column, comparison between ratio of depth of bulging (z_b) to diameter of stone column, i.e. z_b/D, obtained in this study and reported by previous researchers is shown in Figure 5.4. Range of z_b/D obtained in this study is in agreement with previous findings.

(a)   (b)   (c)

Figure 5.3. Failure shapes of stone columns (a) $L/H = 0.4$, (b) $L/H = 0.7$ and (c) $L/H = 1.0$ (Type-S)

Table 5.2. Summary of ultimate bearing capacities and failure modes (Type-S)

L/H	c_u (kN/m^2)	σ_{ult} (kN/m^2)	Failure Mode
0.4	18	300	Punching and entire bulging
0.7	19	300	Punching and local bulging
1.0	20	450	Local bulging
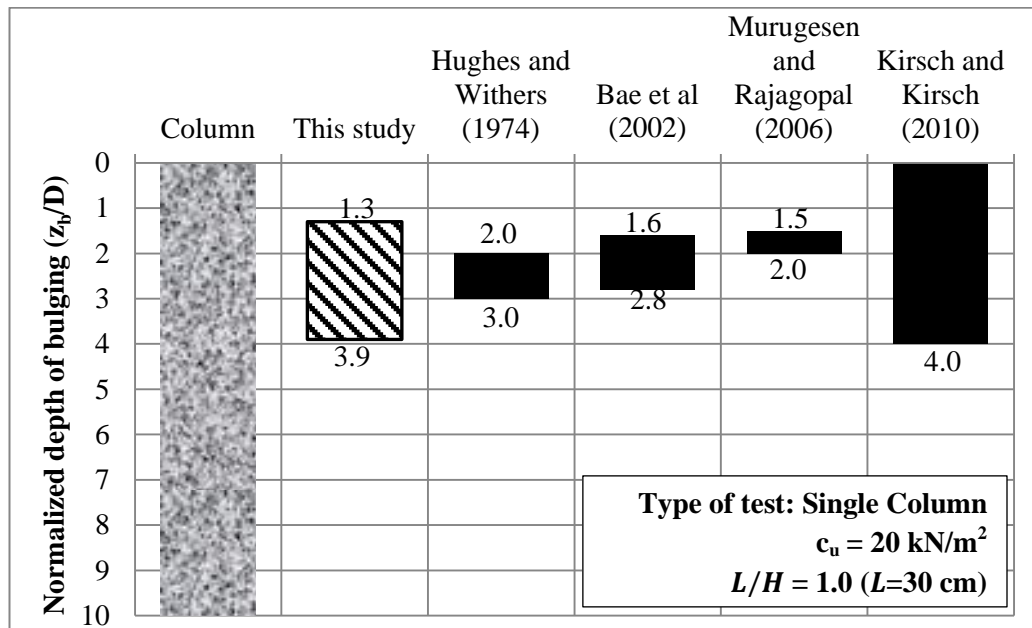
Figure 5.4. Comparison of z_b/D values (Type-S)

5.2.1.2. Deformation Modulus of Stone Column

Deformation modulus of stone column under different foundation pressures were back-calculated from the measured settlement of end bearing stone column under the known magnitude of foundation pressure by carrying out finite element analyses in Plaxis 2D. An axisymmetric model of single column loading test was used. The model and deformed mesh of the end bearing single column are

illustrated in Figure 5.5. Deformation modulus of column (E_c) under different pressures applied on column (σ_c) are listed in Table 5.3.

(a)

(b)
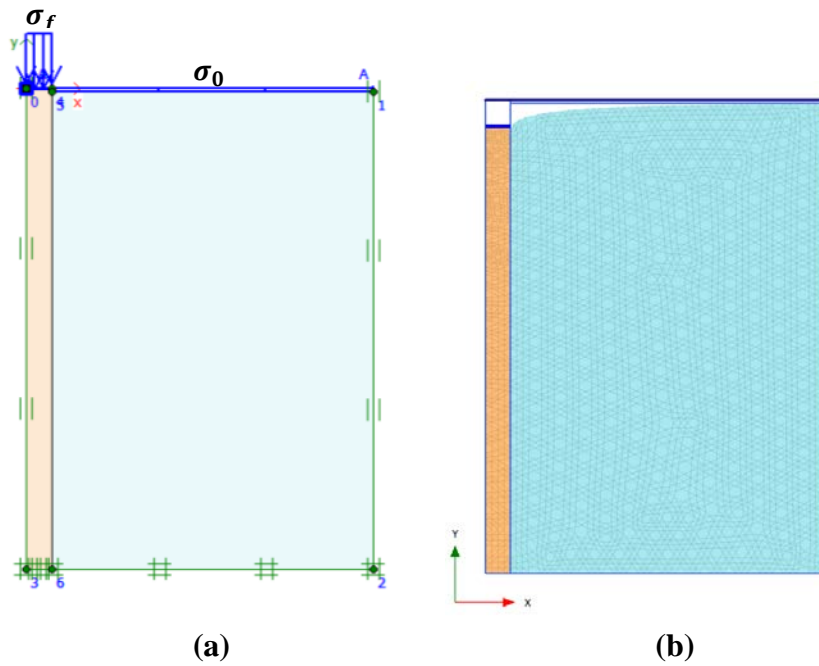
Figure 5.5. (a) Axisymmetric model and (b) deformed mesh

Table 5.3. Deformation modulus of column under different pressures

σ_c (kN/m²)	E_c (MN/m²)
200	24.0
250	19.0
350	12.4
400	11.0

5.2.2. Tests for Single Columns Loaded over a Footing Having Same Diameter with the Unit Cell (Type-SCF)

5.2.2.1. Settlements

5.2.2.1.1. End Bearing Column

Normalized foundation pressure (σ_f/c_u) versus surface settlement behavior for untreated soil and soil treated by end bearing column under Type-SCF loading are shown in Figure 5.6. Failure of untreated soil and end bearing stone column under Type-SCF loading occurred at foundation pressures equal to 100 kPa and 125 kPa, respectively.
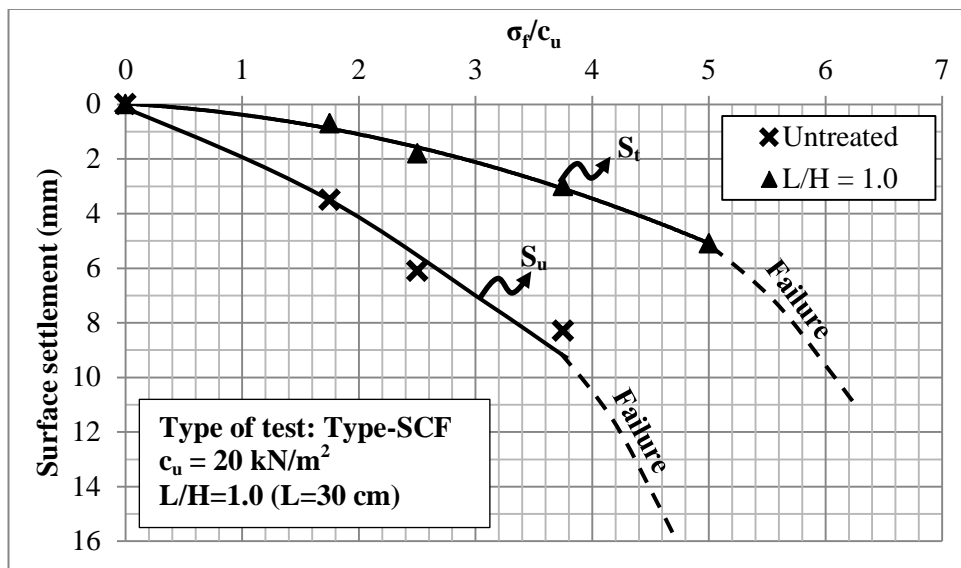
Figure 5.6. σ_f/c_u – surface settlement behavior (Type-SCF: end bearing)

Total settlement reduction ratio (SRR_T) versus normalized foundation pressure (σ_f/c_u) behavior for Type-SCF test with end bearing column is illustrated in Figure 5.7. As shown in this figure, for end bearing column under Type-SCF

loading as normalized foundation pressure increases from 1.75 to 3.75, SRR_T increases from 0.20 to 0.35, respectively, the relationship being almost linear.
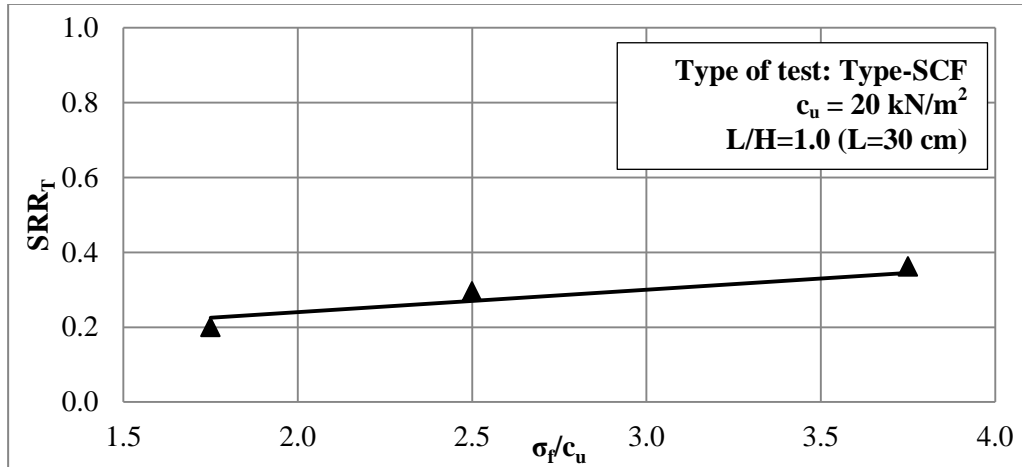
Figure 5.7. σ_f/c_u **-** SRR_T **behavior (Type-SCF: end bearing)**

Total settlement reduction ratios (SRR_T) obtained in end bearing test under Type-SCF loading are compared with the values calculated from equilibrium method by using stress concentration factors obtained in this study. In Figure 5.8, values of measured total settlement reduction ratios (SRR_T - measured) versus total settlement reduction ratios calculated from equilibrium method (SRR_T - predicted) are plotted. This figure implies that, equilibrium method underestimates the settlement improvement for Type-SCF loading with end bearing column, where the measured values are considerably smaller than the calculated ones.
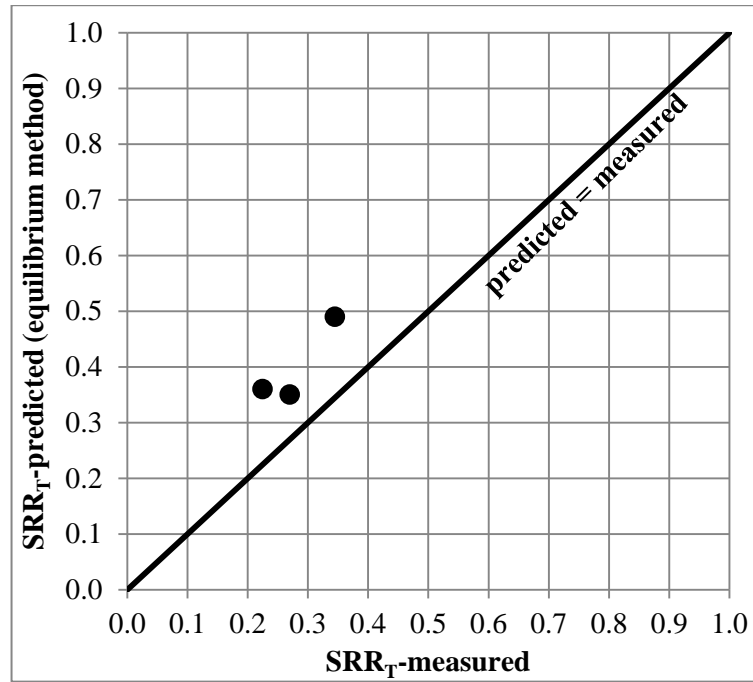
Figure 5.8. Comparison of SRR_T values with equilibrium method
(Type-SCF: end bearing)

5.2.2.1.2. Floating Columns

Normalized foundation pressure (σ_f/c_u) versus surface settlement behavior for untreated soil and soil treated by floating columns under Type-SCF loading are shown in Figure 5.9. Normalized foundation pressure (σ_f/c_u) versus subsurface settlements behavior for untreated soil and soil treated by floating columns under Type-SCF loading are shown in Figure 5.10. Failure of both short and long floating columns under Type-SCF loading occurred at foundation pressures equal to 100 kPa.

Settlement reduction ratios for total settlement (SRR_T), upper zone (SRR_{UZ}) and lower zone (SRR_{LZ}) versus normalized foundation pressure (σ_f/c_u) behavior for Type-SCF tests with floating column are shown in Figures 5.11, 5.12 and 5.13, respectively.

As shown in Figure 5.11, as normalized foundation pressure increases from 1.75 to 3.75, SRR_T increases from 0.43 to 0.54 and 0.34 to 0.43 for short ($L/H = 0.4$) and long ($L/H = 0.7$) floating column in Type-SCF tests, respectively.

Figure 5.12 shows that, as normalized foundation pressure increases from 1.75 to 3.75, settlement reduction ratio calculated for upper (treated) zone (SRR_{UZ}) increases from 0.40 to 0.47 and 0.29 to 0.38 for short ($L/H = 0.4$) and long ($L/H = 0.7$) floating column Type-SCF tests, respectively.

Figure 5.13 shows that, values of settlement reduction ratio calculated for lower (untreated) zone (SRR_{LZ}) are similar for both floating columns under Type-SCF loading. As normalized foundation pressure increases from 1.75 to 3.75, SRR_{LZ} increases from 0.51 to 0.66, respectively.

These results indicate that floating columns settlement reduction ratios at different zones slightly increase with increasing foundation pressure. Moreover, SRR_T and SRR_{UZ} are smaller as column length increases. Whereas, SRR_{LZ} values are similar for both floating columns.
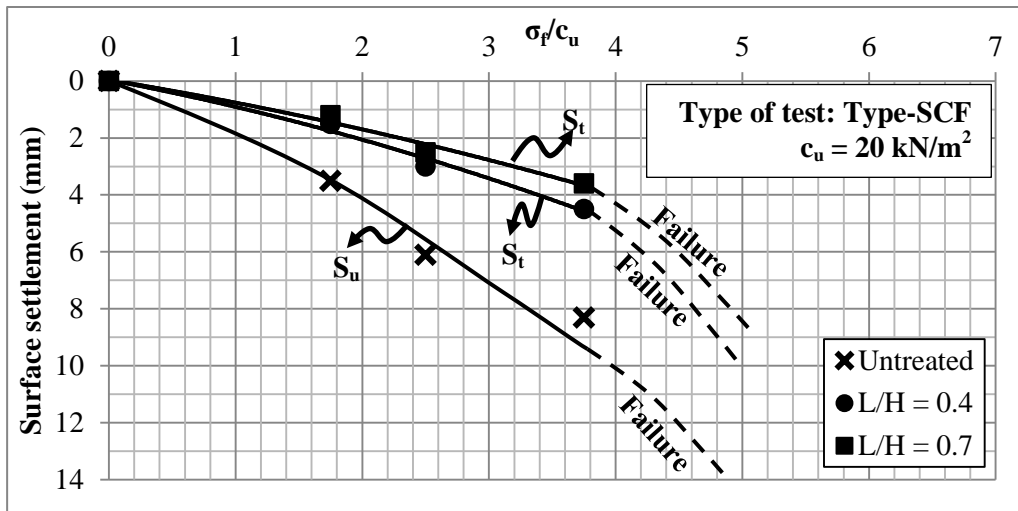
Figure 5.9. σ_f/c_u – surface settlement behavior (Type-SCF: floating)

(a)

(b)
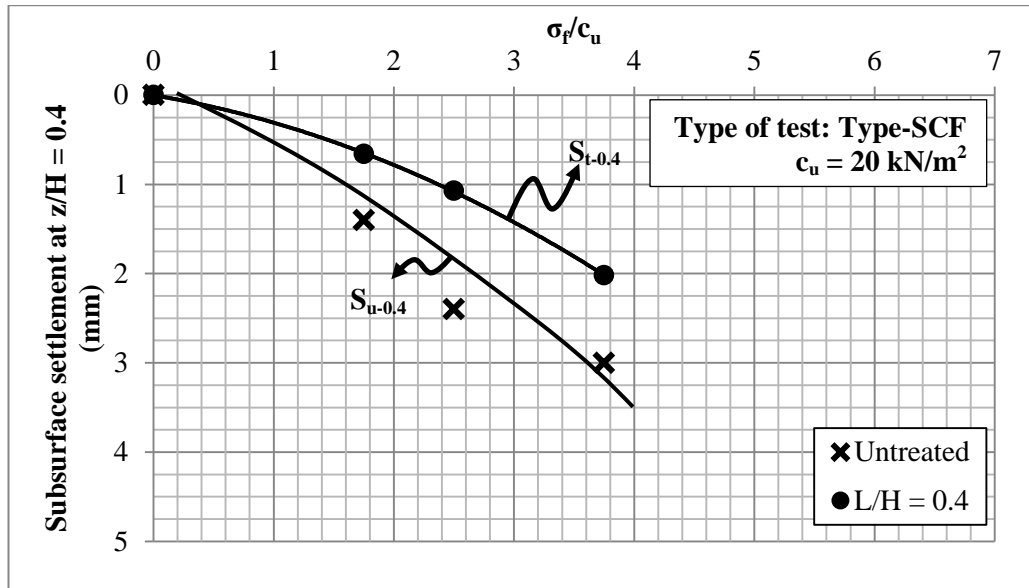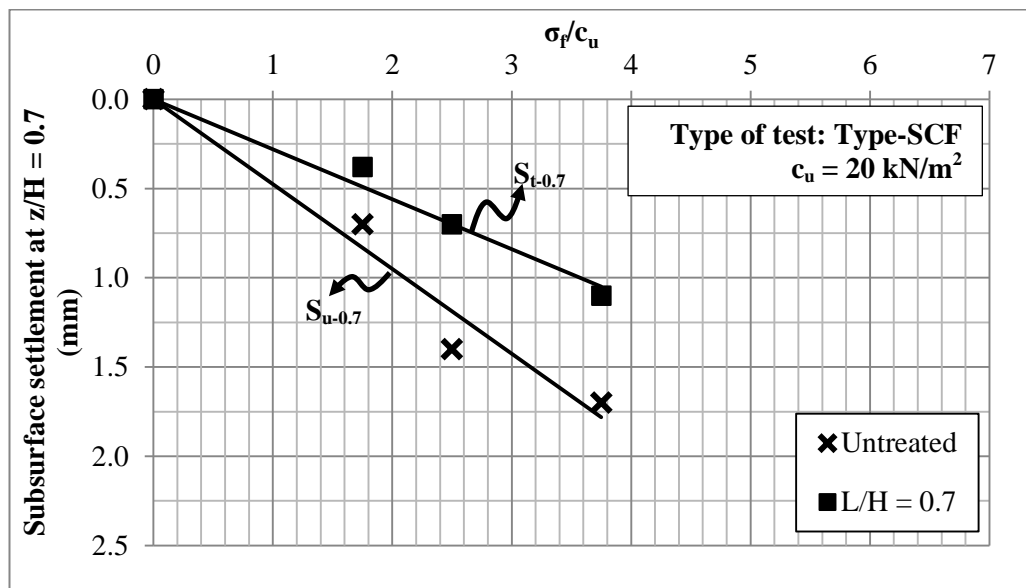
Figure 5.10. σ_f/c_u – subsurface settlement behavior (a) at depth $z/H = 0.4$ and (b) at depth $z/H = 0.7$ (Type-SCF: floating)
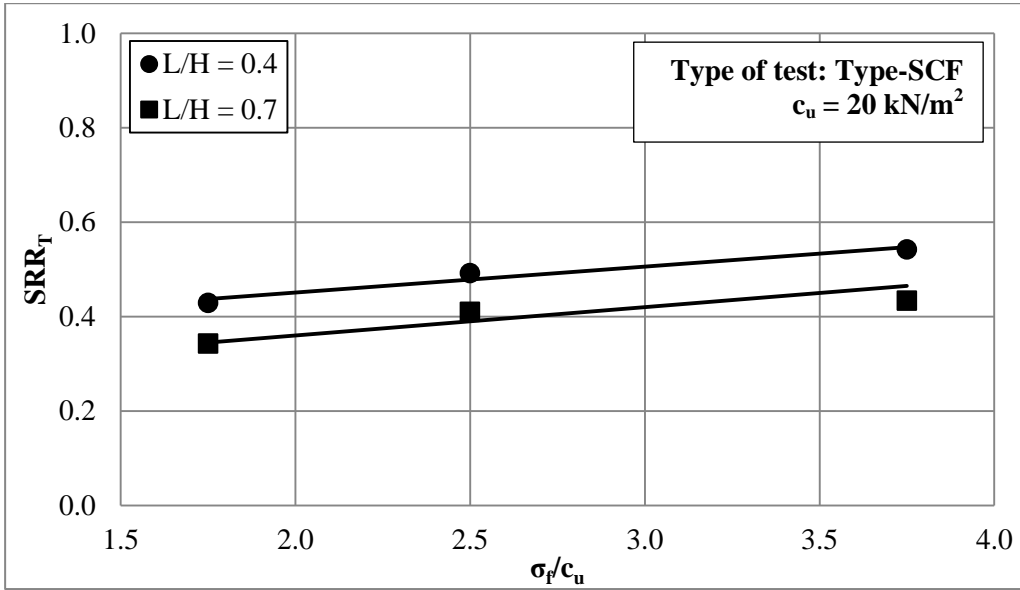
Figure 5.11. σ_f / c_u - SRR_T behavior (Type-SCF: floating)
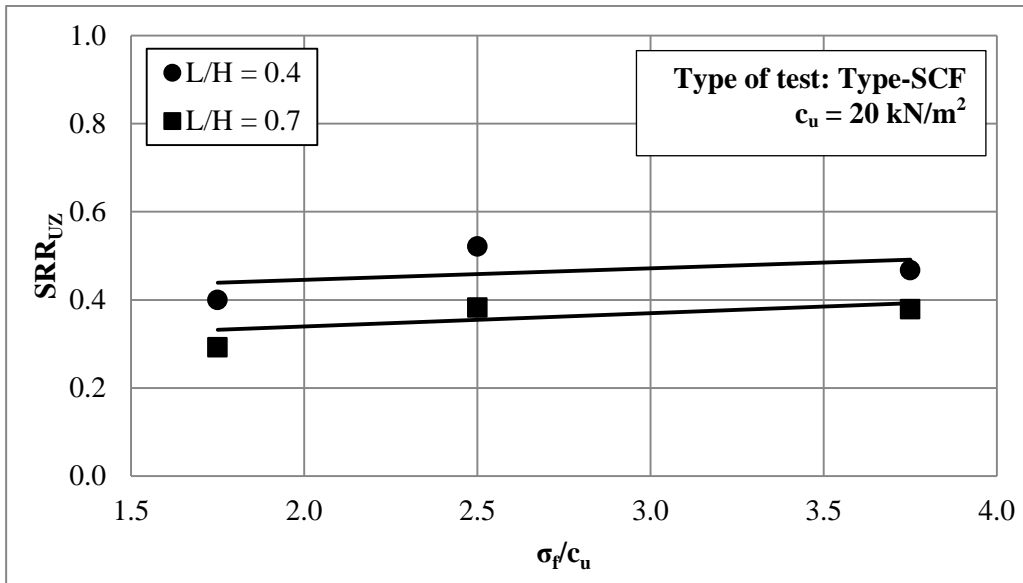
Figure 5.12. σ_f / c_u - SRR_{UZ} behavior (Type-SCF: floating)

130
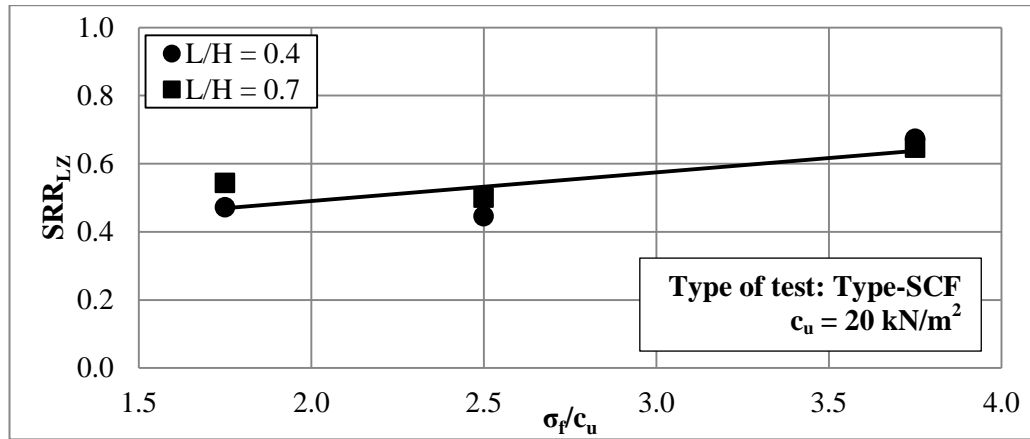
Figure 5.13. σ_f/c_u - SRR_{LZ} behavior (Type-SCF: floating)

5.2.2.1.3. Comparison of End Bearing and Floating Column Behavior

Total settlement reduction ratio (SRR_T) versus normalized foundation pressure (σ_f/c_u) behavior for single columns loaded over a footing having same diameter with the unit cell tests with different lengths of column are illustrated in Figure 5.14. For Type-SCF loading tests with $c_u = 20$ kN/m^2, SRR_T increases as the column length shortens and foundation pressure increases. This indicates that improvement on settlement increases as column lengthens for Type-SCF loading tests. In other words, amount of settlement improvement is significantly depend on the length of column, for Type-SCF tests with $c_u = 20$ kN/m^2.

Figure 5.14. σ_f/c_u - SRR_T behavior (Type-SCF)

131
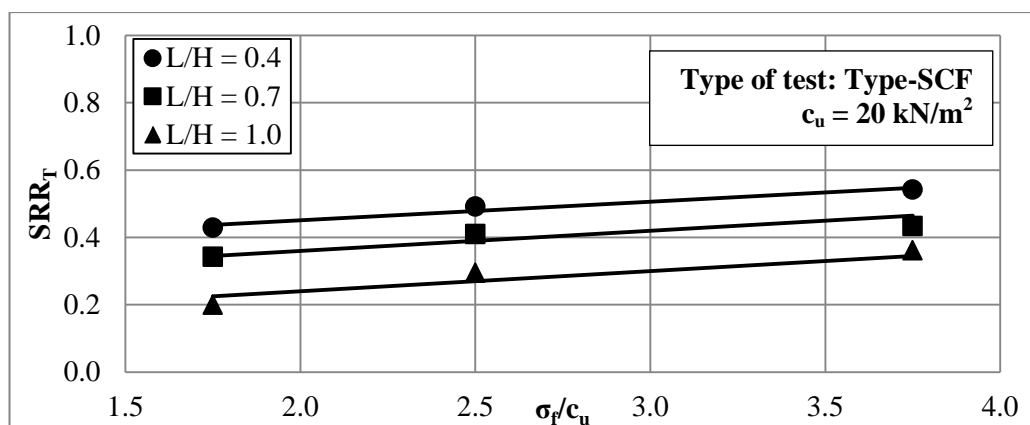
5.2.2.2. Column and Soil Stresses

5.2.2.2.1. End Bearing Column

Relationship between stresses carried by the column and the surrounding soil (σ_c and σ_s) and normalized foundation pressures (σ_f/c_u) for Type-SCF test with end bearing column is shown in Figure 5.15. Stresses both carried by column and surrounding soil increase as foundation pressure increases. Moreover, stress carried by column increases with decreasing rate, whereas soil stress increases with increasing rate indicating decrease in stress concentration factor with increasing foundation pressure.

For Type-SCF test with end bearing column, stress concentration factors (n) at the beginning (initial) and at the end (final) of each loading step at various normalized foundation pressures (σ_f/c_u) are shown in Figure 5.16. In figure the terms 'initial' and 'final' correspond to the values of stress concentration factor at the beginning and at the end of each loading step, respectively. The initial and final values of stress concentration factors are almost same for end bearing column under Type-SCF loading. In other words, there is no significant variation in stress concentration factor during time of consolidation. Moreover, stress concentration factor gets smaller as foundation pressure increases for Type-SCF test in end bearing column. Under Type-SCF loading, for end bearing column and $c_u = 20$ kN/m^2 final stress concentration factor decreases from 12.1 to 6.1 as normalized foundation pressure increases from 2.50 to 6.25, respectively.
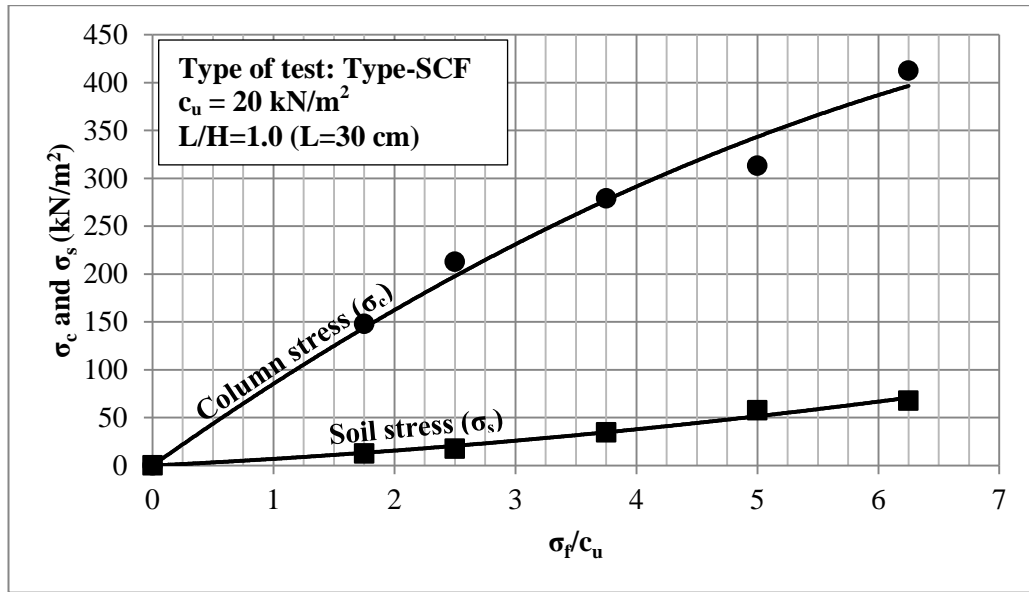
Figure 5.15. Relationships between $\sigma_f/c_u - \sigma_c$ and σ_s

(Type-SCF: end-bearing)
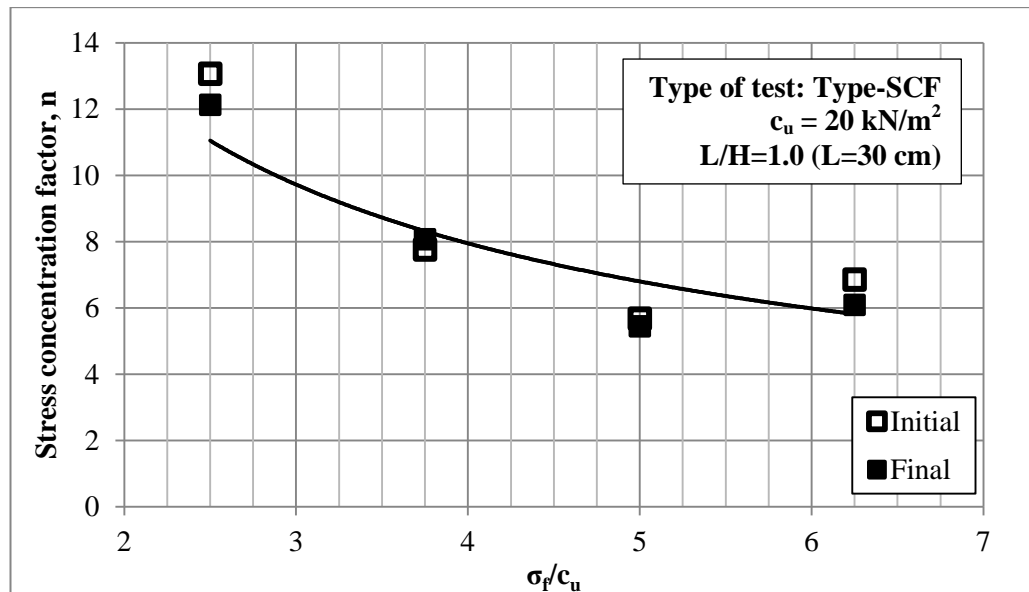
Figure 5.16. Relationships between σ_f/c_u – initial and final n

(Type-SCF: end bearing)

5.2.2.2.2. Floating Columns

Relationships between stresses carried by column and surrounding soil (σ_c and σ_s) and normalized foundation pressures (σ_f/c_u) for floating columns under Type-SCF loading are shown in Figure 5.17. For both floating column tests, stresses both carried by column and soil increase as foundation pressure increases. Moreover, stresses carried by column increase with decreasing rate whereas stresses carried by surrounding soil increase with increasing rate indicating decrease in stress concentration factor.

Stress concentration factors (n) at the beginning (initial) and at the end (final) of each loading step for various normalized foundation pressures (σ_f/c_u) are shown in Figures 5.18 and 5.19 for short (*L/H* =0.4) and long (*L/H*=0.7) floating column tests, respectively. The initial and final values of stress concentration factors are almost same for both floating columns under Type-SCF loading. In other words, there is no significant variation in stress concentration factor in time.

Moreover, stress concentration factor gets smaller as foundation pressure increases for Type-SCF test in floating columns. For short and long floating columns under Type-SCF loading and $c_u = 20$ kN/m^2, final stress concentration factors decrease from 6.7 to 4.5 and from 9.3 to 5.6 as normalized foundation pressure increases from 2.50 to 6.25, respectively.
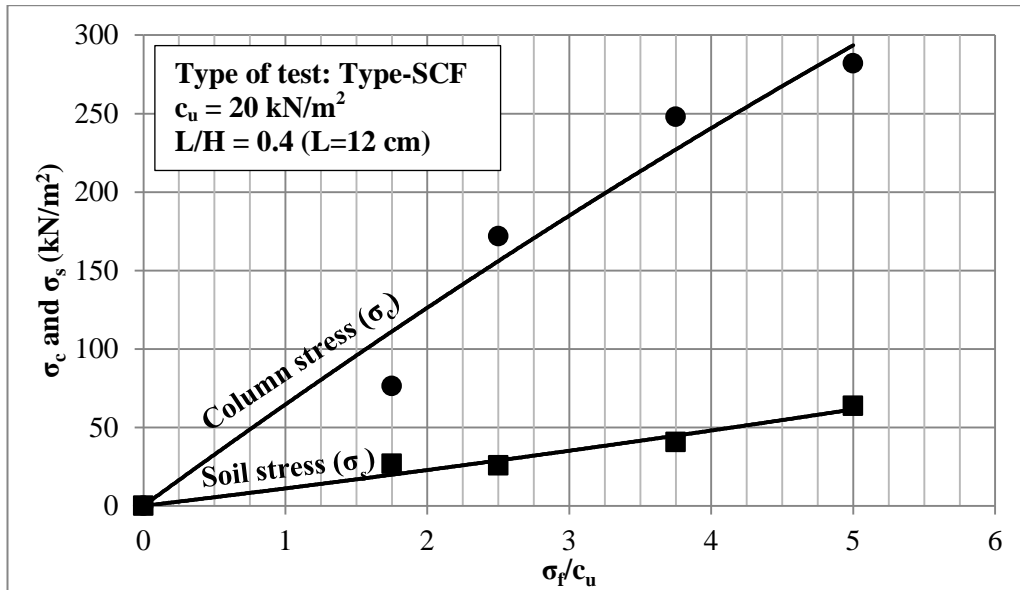
(a)
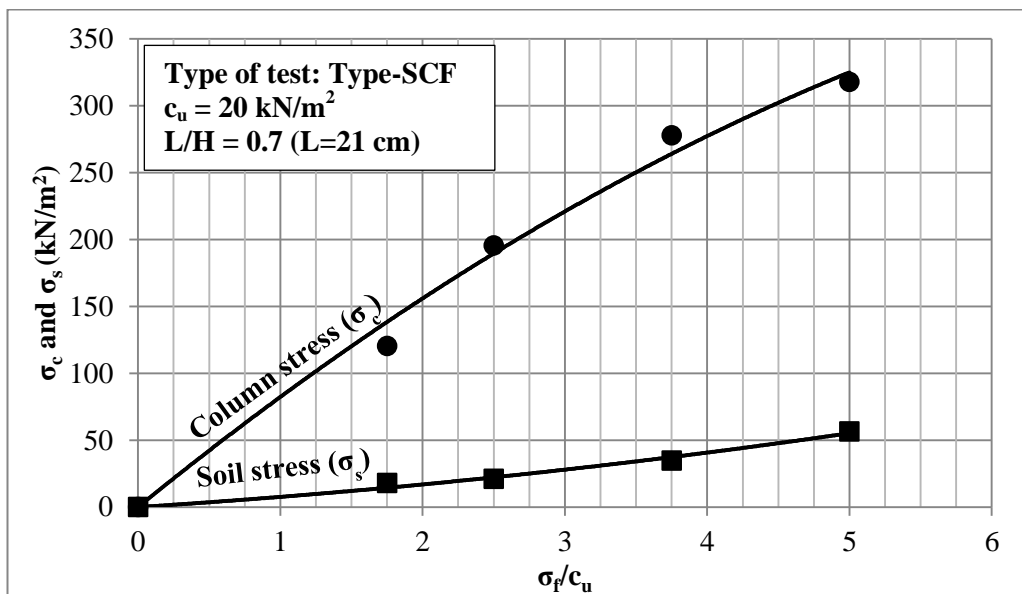
(b)

Figure 5.17. Relationships between $\sigma_f/c_u - \sigma_c$ and σ_s (a) $L/H = 0.4$ and (b) $L/H = 0.7$ (Type-SCF: floating)

135
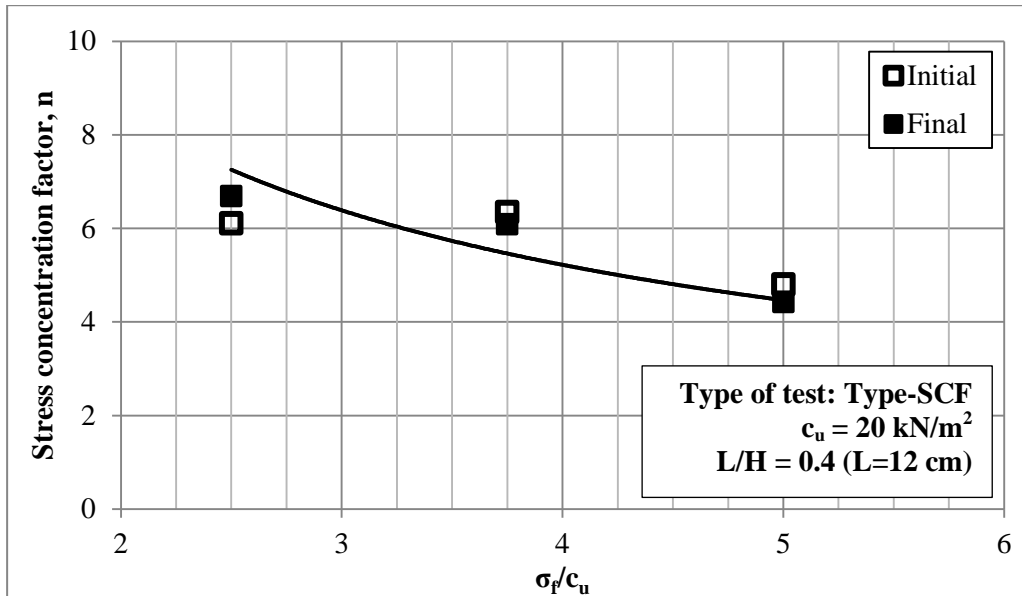
Figure 5.18. Relationships between σ_f/c_u – initial and final n

(Type-SCF: L/H=0.4)
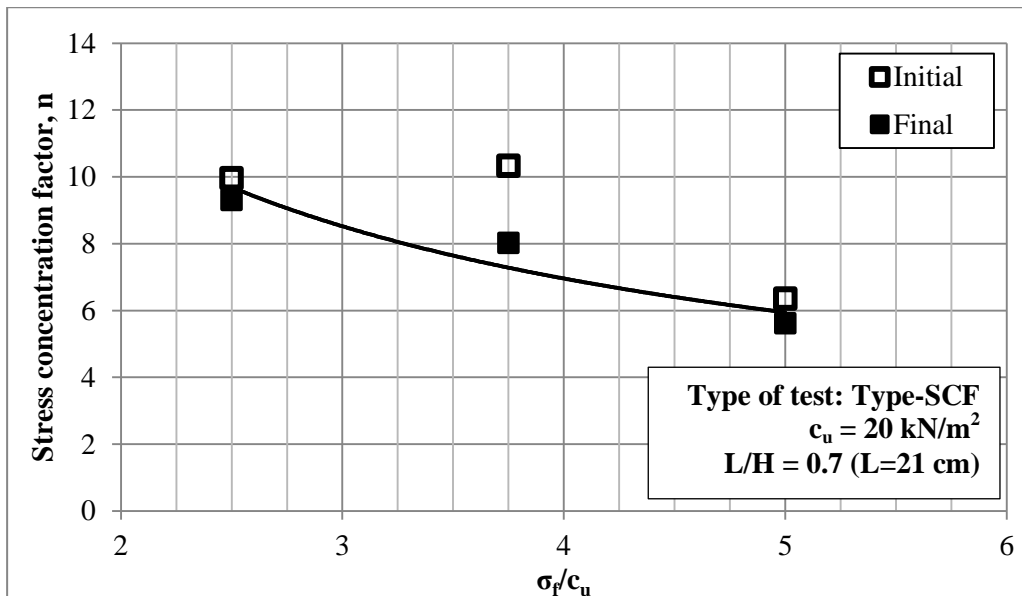
Figure 5.19. Relationships between σ_f/c_u – initial and final n

(Type-SCF: L/H=0.7)

5.2.2.2.3. Comparison of End Bearing and Floating Column Behavior

Figures 5.16, 5.18 and 5.19 show that variation of stress concentration factor with time is negligible for different lengths of column under Type-SCF loading. Relationships between stress concentration factor (n) and normalized foundation pressure (σ_f/c_u) for different lengths of column under Type-SCF loading are shown in Figure 5.20. For Type-SCF loading tests with $c_u = 20$ kN/m^2, stress concentration factor (n) decreases by the increase of foundation pressure regardless of the column length. Moreover, for longer column larger stress concentration factor develops.
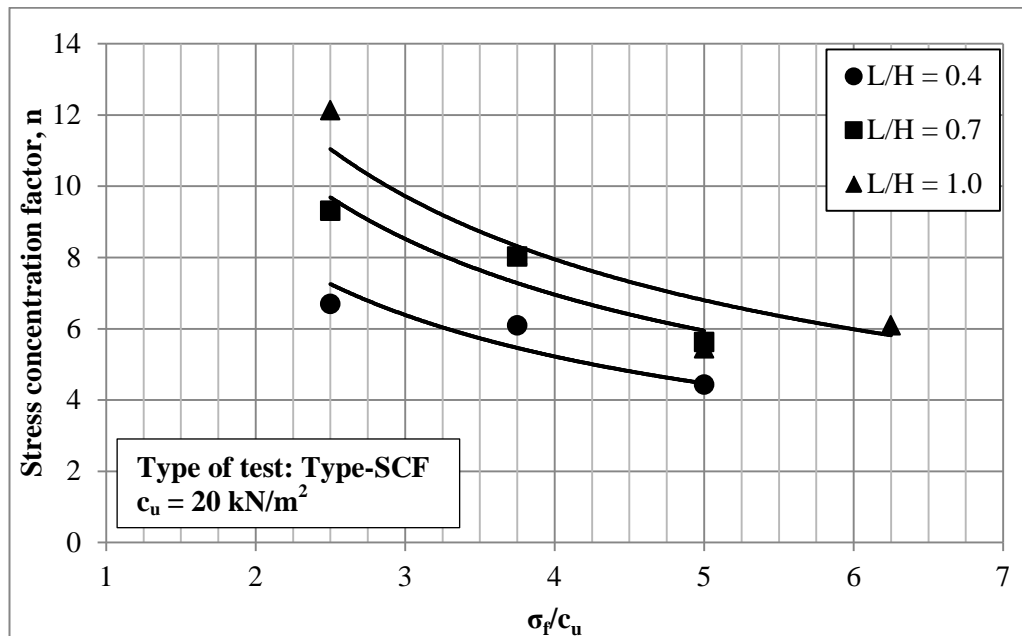
Figure 5.20. Relationships between $\sigma_f/c_u - n$ (Type-SCF)

5.2.3. Group Loading Tests (Type-G)

5.2.3.1. Settlements

5.2.3.1.1. End Bearing Columns

Normalized foundation pressure versus surface settlement behavior for Group 1 (c_u = 20 kN/m^2) and Group 2 (c_u = 30 kN/m^2) tests with end bearing columns are shown in Figures 5.21 and 5.22, respectively. In all of these tests, failure is not observed up to maximum applied pressure at an amount of 150 kN/m^2.
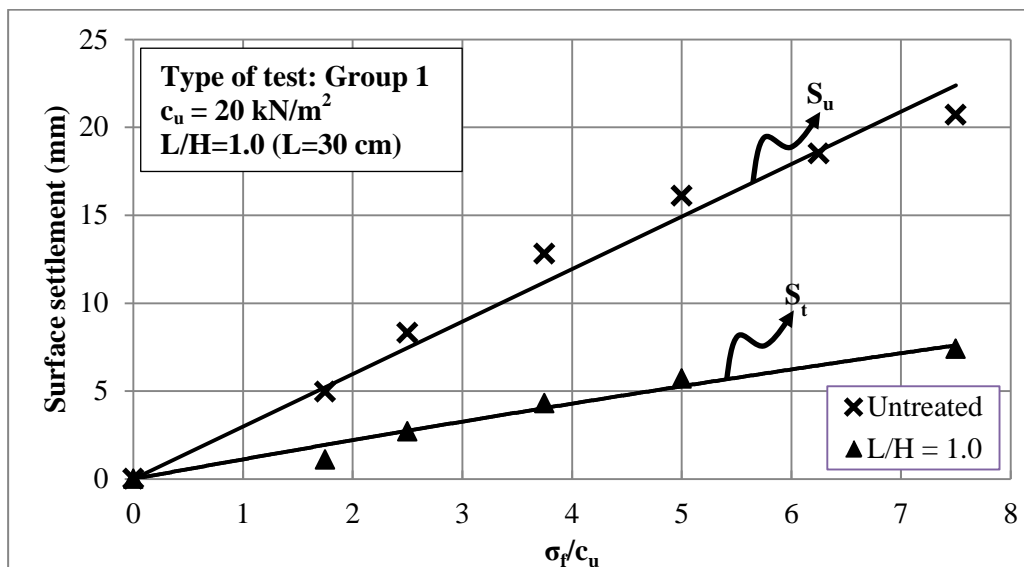
Figure 5.21. σ_f/c_u – surface settlement behavior (Type-G1: end bearing)

Total settlement reduction ratio (SRR_T) versus normalized foundation pressure (σ_f/c_u) behavior for Groups 1 and 2 with end bearing columns are shown in Figures 5.23 and 5.24, respectively. For Group 1 (c_u = 20 kN/m^2) with end bearing columns as normalized foundation pressure increases from 1.75 to 7.50, SRR_T increases from 0.22 to 0.36, respectively. Whereas for Group 2 (c_u = 30

kN/m^2) with end bearing columns, SRR_T is equal to 0.42 being independent of
the magnitude of applied pressure.
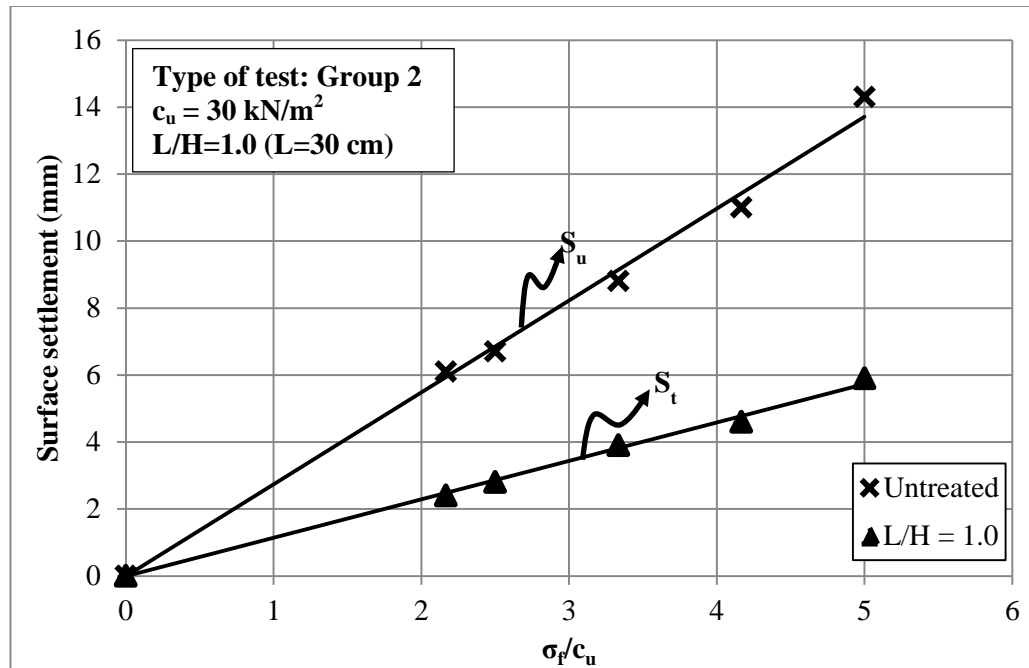
Figure 5.22. σ_f/c_u – surface settlement behavior (Type-G2: end bearing)
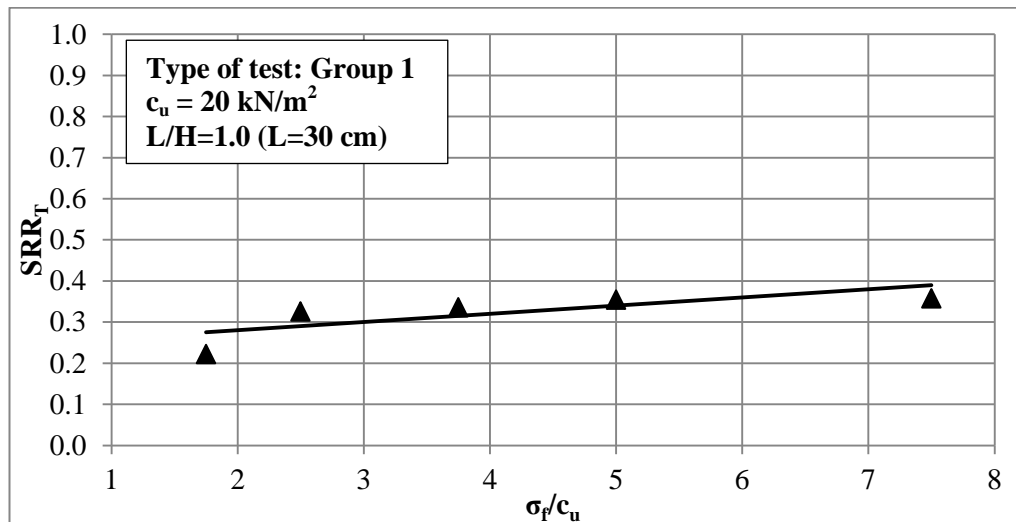
Figure 5.23. σ_f/c_u - SRR_T behavior (Type-G1: end-bearing)
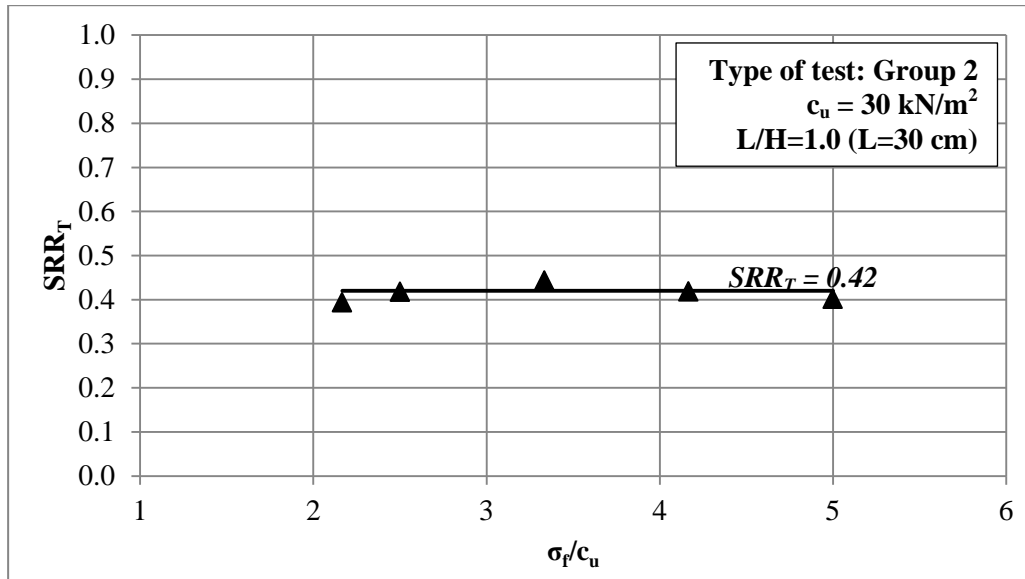
Figure 5.24. σ_f/c_u - SRR_T behavior (Type-G2: end-bearing)

Total settlement reduction ratios (SRR_T) obtained in Groups 1 and 2 with end bearing columns are compared with the values calculated from equilibrium method by using stress concentration factors obtained in this study. In Figures 5.25 and 5.26, values of measured total settlement reduction ratios (SRR_T - measured) versus total settlement reduction ratios calculated from equilibrium method (SRR_T - predicted) are plotted for Group 1 and 2, respectively. These figures imply that, equilibrium method underestimates the settlement improvement for group loading on end bearing columns, where the measured values are considerably smaller than the calculated ones.

For both Group 1 and 2, equilibrium method underestimates the improvement in surface settlement. Total settlement reduction ratios (SRR_T) obtained in group tests are 74% of the values calculated from unit cell concept irrespective from the initial undrained shear strength of soil. This finding indicates that equilibrium method based on the unit cell approach cannot realistically represent the settlement reduction in column groups.

140
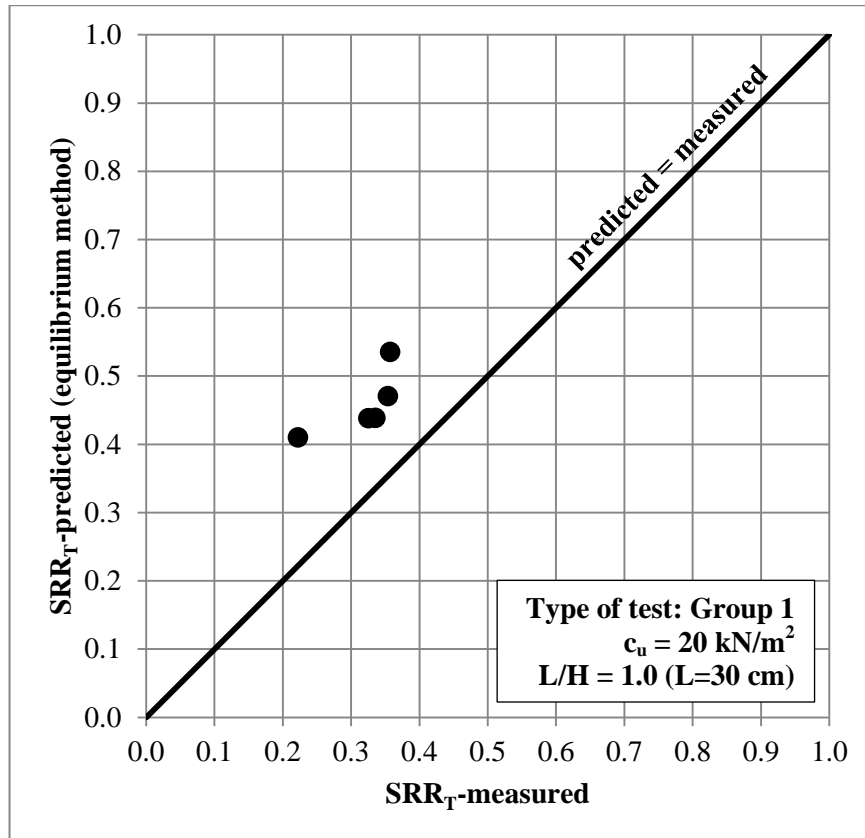
Figure 5.25. Comparison of SRR_T values with equilibrium method

(Type-G1: end bearing)
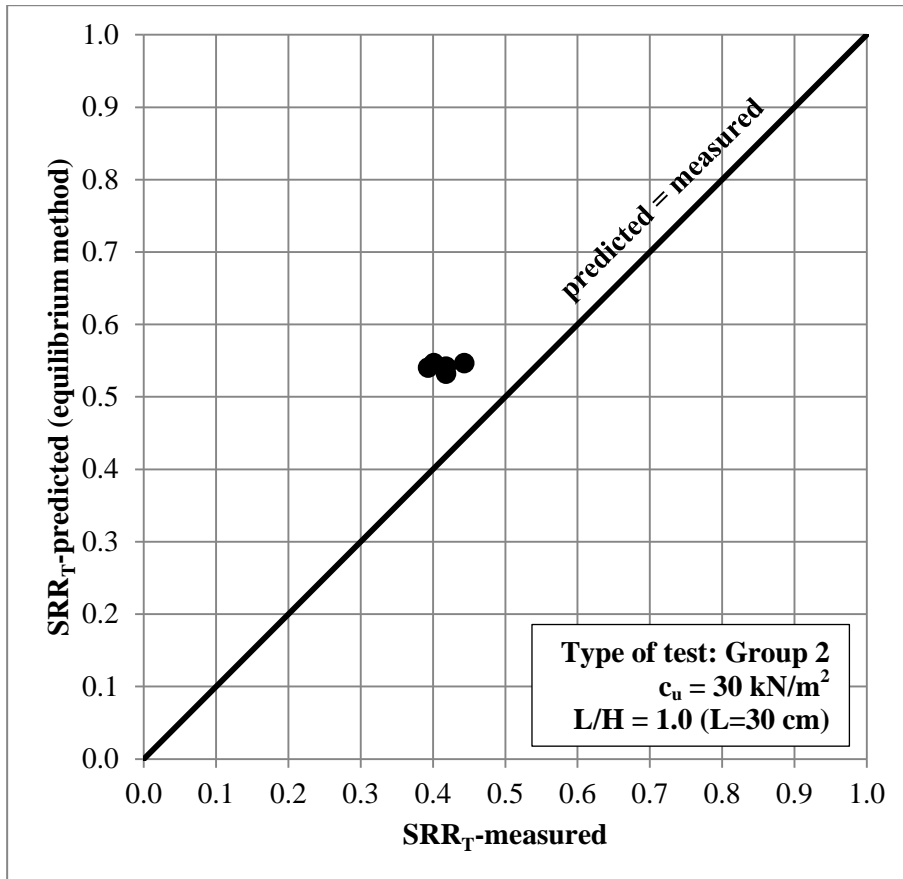
Figure 5.26. Comparison of SRR_T values with equilibrium method (Type-G2: end bearing)

5.2.3.1.2. Floating Columns

Normalized foundation pressure (σ_f / c_u) versus surface and subsurface settlement behavior for Group 1 tests ($c_u = 20$ kN/m²) with floating columns are shown in Figures 5.27 and 5.28, respectively. In all of these tests, failure is not observed up to maximum applied pressure at an amount of 150 kN/m².

Normalized foundation pressure (σ_f / c_u) versus surface and subsurface settlement behavior for Group 2 tests ($c_u = 30$ kN/m²) with floating columns are shown in

Figures 5.29 and 5.30, respectively. In all of these tests, failure is not observed up to maximum applied pressure at an amount of 150 kN/m^2.
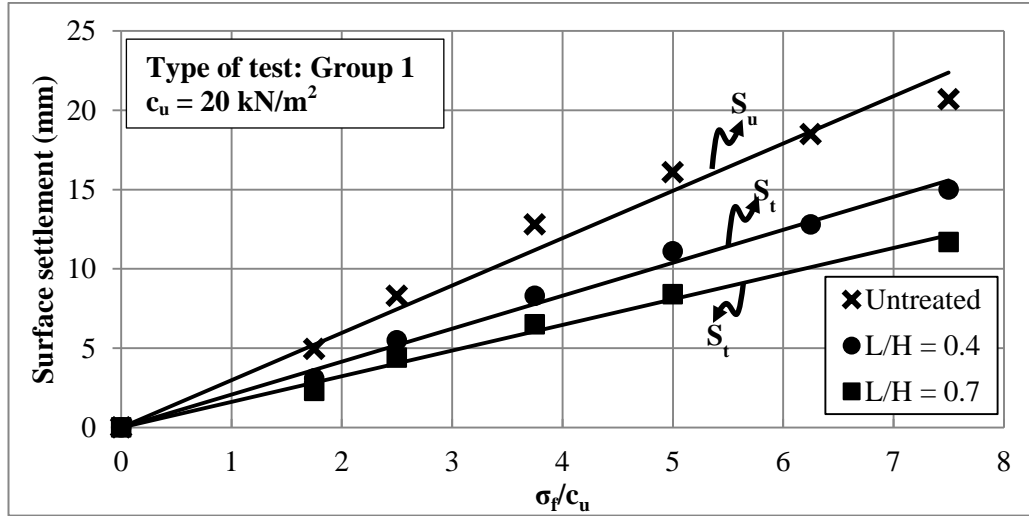
Figure 5.27. σ_f/c_u – surface settlement behavior (Type-G1: floating)
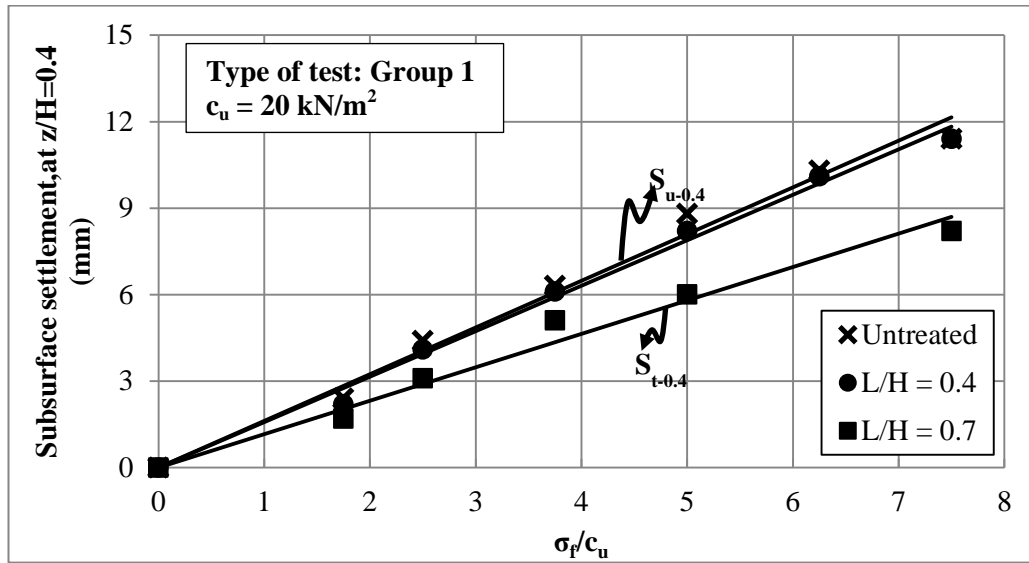
(a)

Figure 5.28. σ_f/c_u – subsurface settlement behavior (a) at depth $z/H = 0.4$ and (b) at depth $z/H = 0.7$ (Type-G1: floating)

(b)
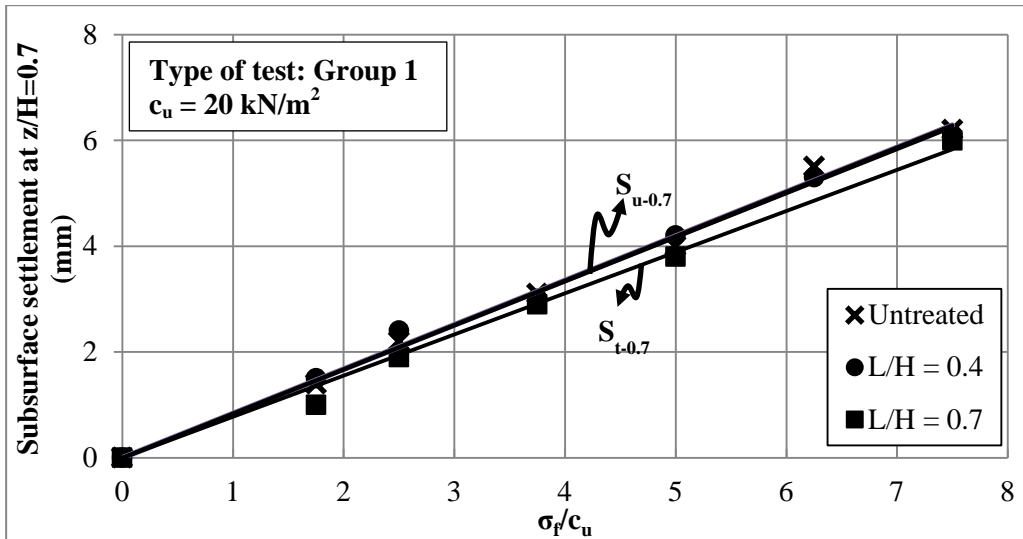
Figure 5.28. σ_f/c_u – subsurface settlement behavior (a) at depth $z/H = 0.4$ and (b) at depth $z/H = 0.7$ (Type-G1: floating) (continue)
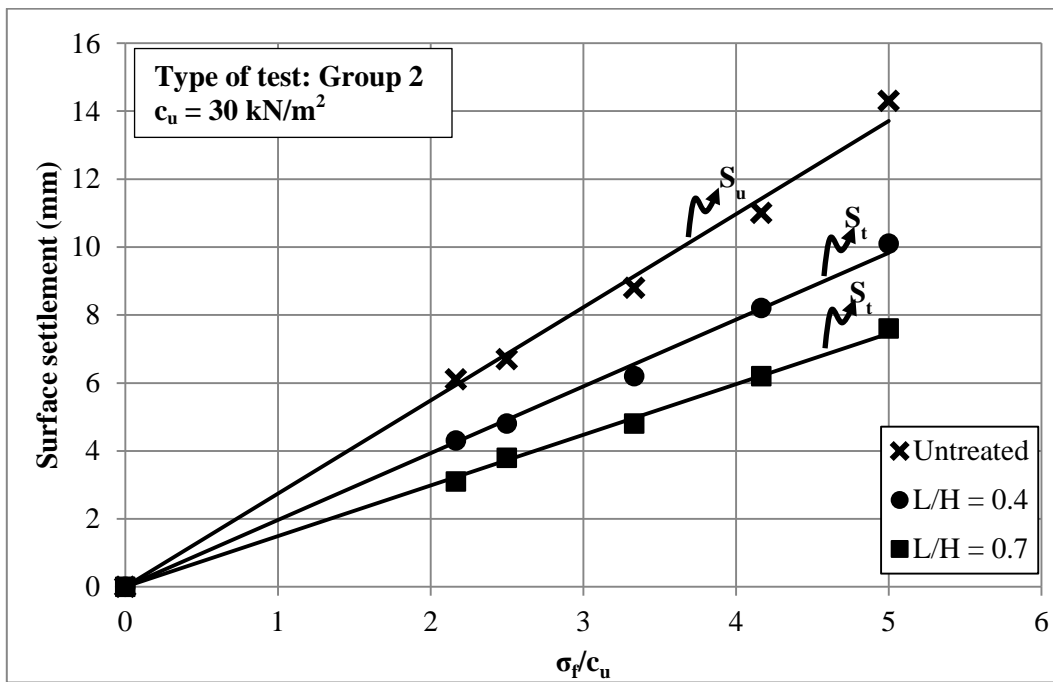
Figure 5.29. σ_f/c_u – surface settlement behavior (Type-G2: floating)

(a)

(b)
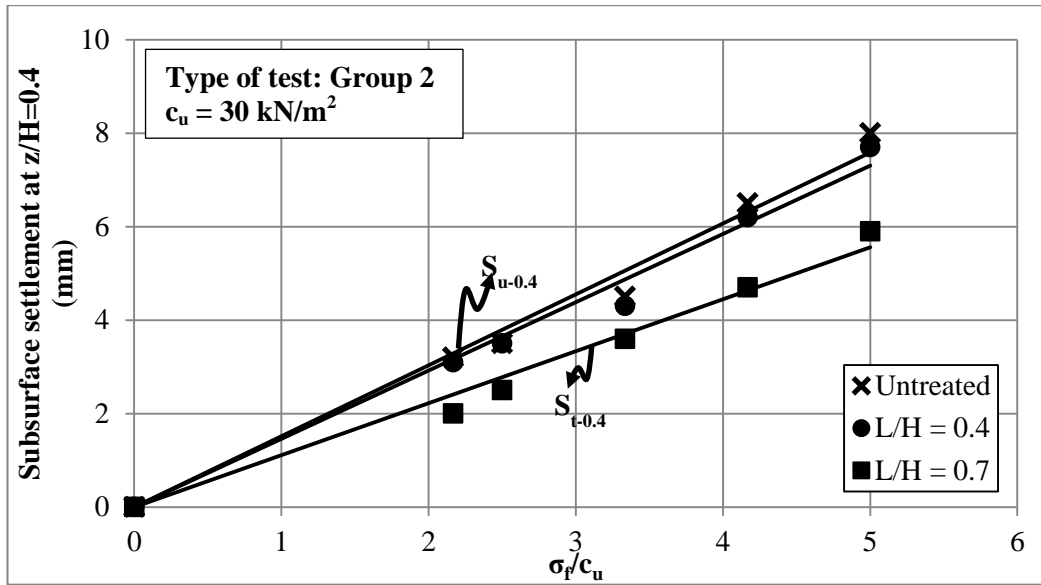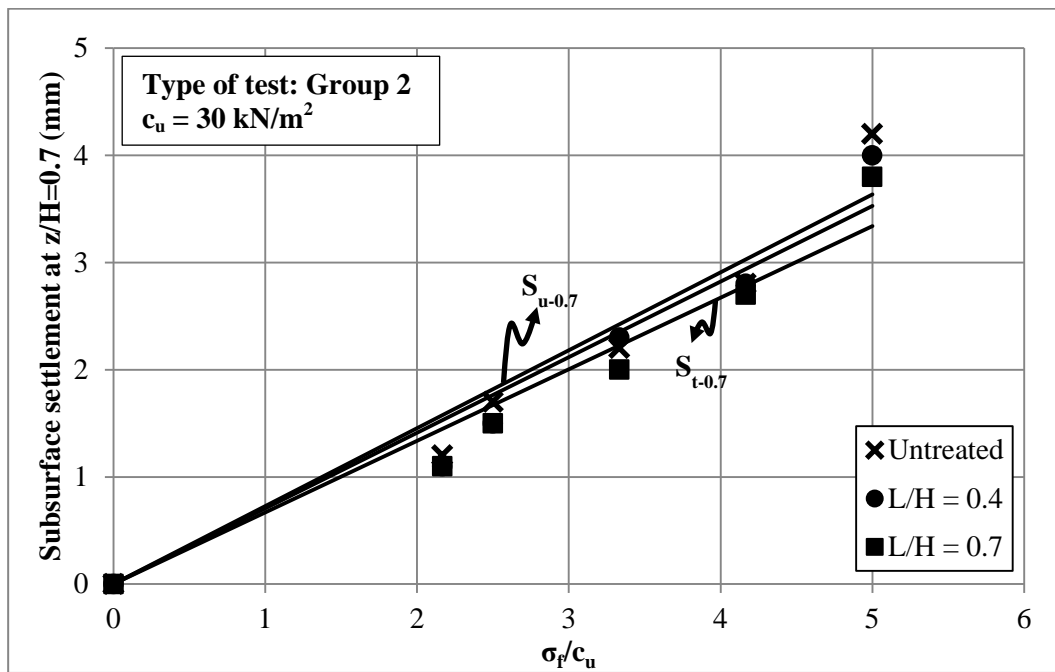
Figure 5.30. σ_f/c_u – **subsurface settlement behavior (a) at depth** $z/H = 0.4$

and (b) at depth $z/H = 0.7$ **(Type-G2: floating)**

Settlement reduction ratios for total (SRR_T), upper (SRR_{UZ}) and lower zones (SRR_{LZ}) versus normalized foundation pressure (σ_f/c_u) behavior for Group 1 tests with floating columns are illustrated in Figures 5.31, 5.32 and 5.33, respectively.

As normalized foundation pressure increases from 1.75 to 7.50, for short (L/H=0.4) and long (L/H=0.7) floating column tests, SRR_T increases from 0.63 to 0.74 and from 0.48 to 0.57, respectively.

For both floating column tests SRR_{UZ} is almost same and equal to 0.37 being independent of the magnitude of applied pressure. As normalized foundation pressure increases from 1.75 to 7.50, for both floating column tests SRR_{UZ} is almost same and SRR_{LZ} is close to unity, respectively.

These results indicate that Group 1 tests ($c_u = 20$ kN/m^2) with floating columns settlement reduction ratios calculated for total and lower zones increase by the increase of foundation pressure. Whereas, SRR_{UZ} is constant being independent of the magnitude of applied pressure. SRR_{UZ} and SRR_{LZ} values are nearly same for both floating columns. Moreover, SRR_{LZ} values are close to unity indicating that there is no significant improvement in lower zone due to provision of stone columns. This finding is in agreement with Som and Das (2003), Ishikura et al. (2009). Under the infinite group loading settlement of untreated zone (lower zone) is nearly same with untreated soil since the stress transmitted to lower zone (equal to foundation pressure) and undrained shear strength of soil is same with the untreated conditions. Hence, SRR_{LZ} is independent from the length of column.
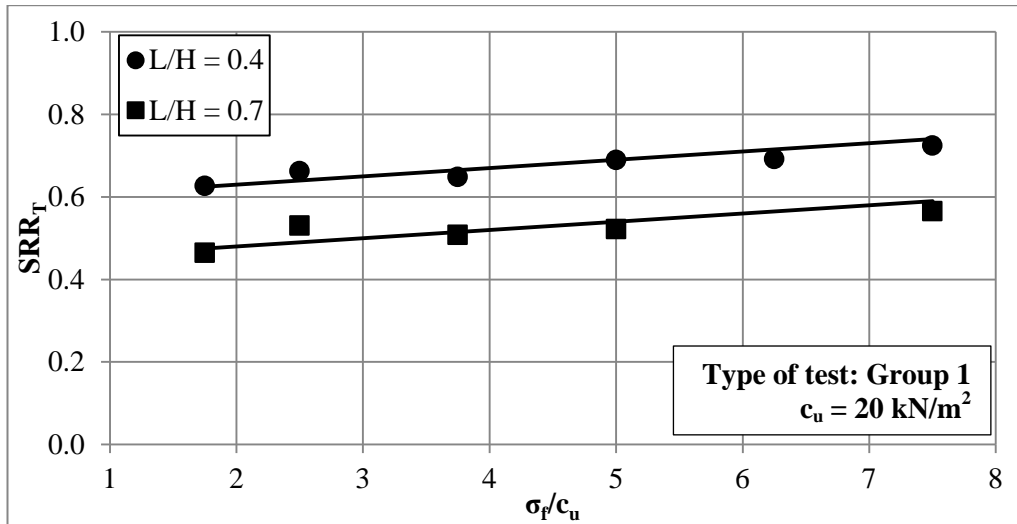
Figure 5.31. σ_f/c_u - SRR_T behavior (Type-G1: floating)
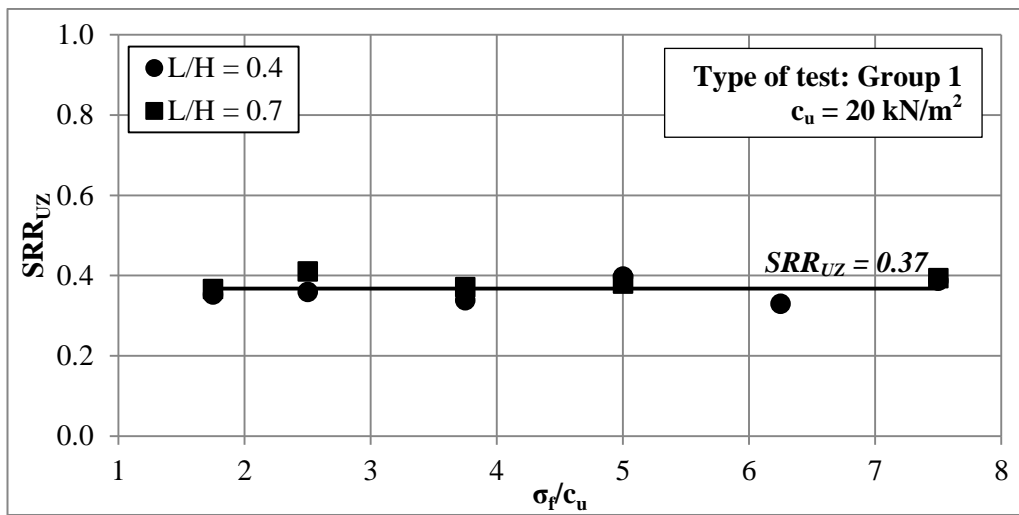
Figure 5.32. σ_f/c_u - SRR_{UZ} behavior (Type-G1: floating)

147
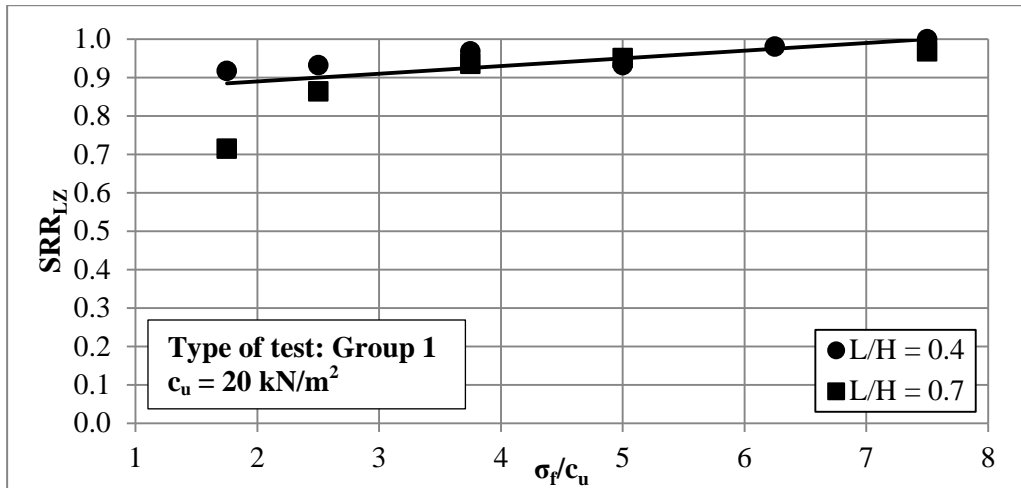
Figure 5.33. σ_f/c_u - SRR_{LZ} behavior (Type-G1: floating)

Settlement reduction ratios for total (SRR_T), upper (SRR_{UZ}) and lower zones (SRR_{LZ}) versus normalized foundation pressure (σ_f/c_u) behavior for Group 2 tests with floating columns are shown in Figures 5.34, 5.35 and 5.36, respectively. As shown in these figures, for Group 2 tests ($c_u = 30$ kN/m^2) with floating columns having $L/H = 0.4$ and 0.7, SRR_T, SRR_{UZ} and SRR_{LZ} are equal to 0.72 and 0.55, 0.42, 0.95, respectively, being independent of the magnitude of applied pressure.

These results indicate that in Group 2 tests ($c_u = 30$ kN/m^2) with floating columns settlement reduction ratios calculated for zones are independent of the magnitude of applied pressure. Furthermore, total settlement reduction ratio decreases for groups with longer columns, whereas settlement reduction ratios in upper and lower zones are independent from the length of column similar to Group 1.

Similar to Group 1, also for Group 2 SRR_{LZ} values are close to unity indicating that there is no significant improvement in lower zone due to one dimensional loading. Hence, SRR_{LZ} is independent from the length of column.

148

Settlement reduction ratio versus normalized foundation pressure behavior for Group 1 and 2 tests implies that, for settlement reduction ratio dependency on magnitude of foundation pressure is being negligible as undrained shear strength of soil increases. Moreover, for infinite group loading settlement reduction ratio in upper and lower zones are constant at various foundation pressures and different length of columns.
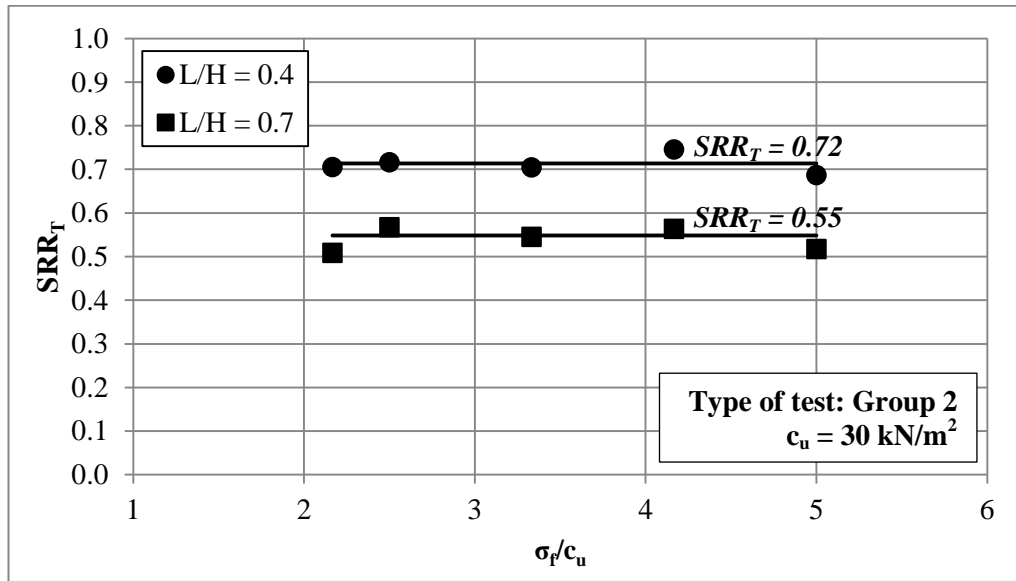
Figure 5.34. σ_f/c_u – SRR_T behavior (Type-G2: floating)
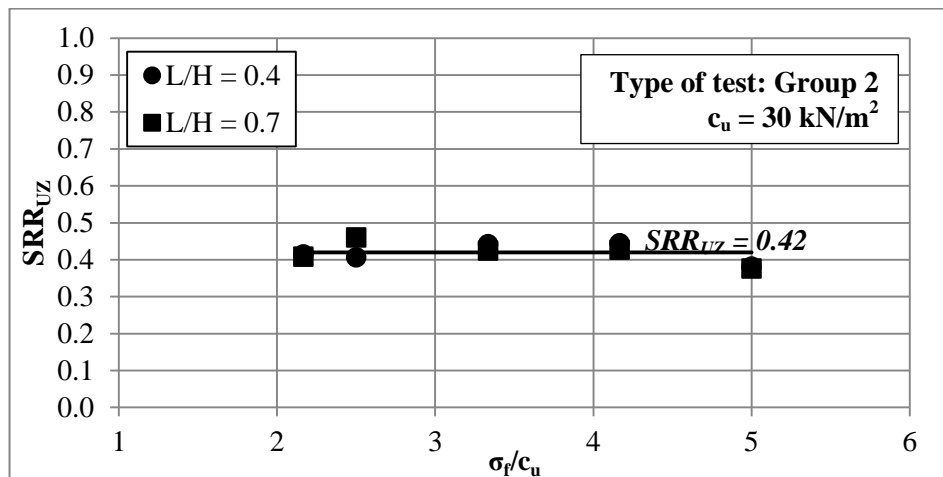
Figure 5.35. σ_f/c_u – SRR_{UZ} behavior (Type-G2: floating)
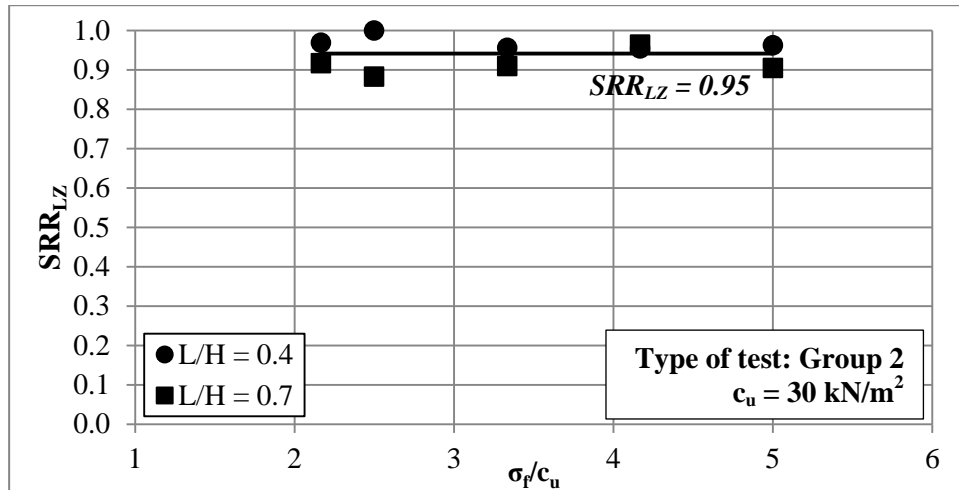
Figure 5.36. σ_f/c_u – SRR_{LZ} **behavior (Type-G2: floating)**

5.2.2.2.3. Comparison of End Bearing and Floating Column Behavior

Settlement reduction ratios (SRR_T) versus normalized foundation pressure (σ_f/c_u) behavior for Groups 1 and 2 with different column lengths are shown in Figures 5.37 and 5.38, respectively. For Group 1 tests with $c_u = 20$ kN/m^2, SRR_T increases slightly as foundation pressure increases. Whereas for Group 2 tests with $c_u = 30$ kN/m^2, SRR_T is constant being independent of the magnitude of applied pressure. Moreover, irrespective of the initial undrained shear strength of soil, SRR_T decreases as the length of column increases.

150
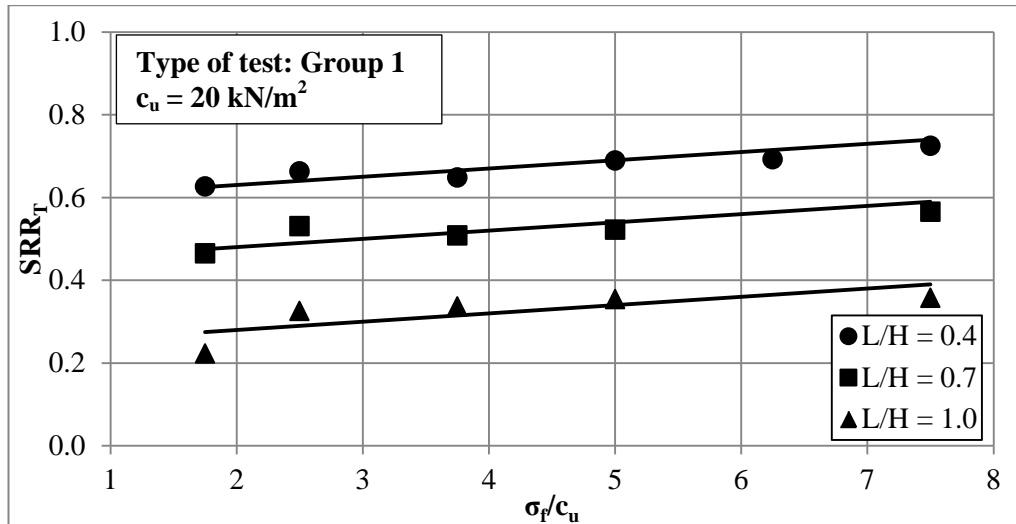
Figure 5.37. σ_f/c_u - SRR_T behavior (Type-G1)

Figure 5.38. σ_f/c_u - SRR_T behavior (Type-G2)

151
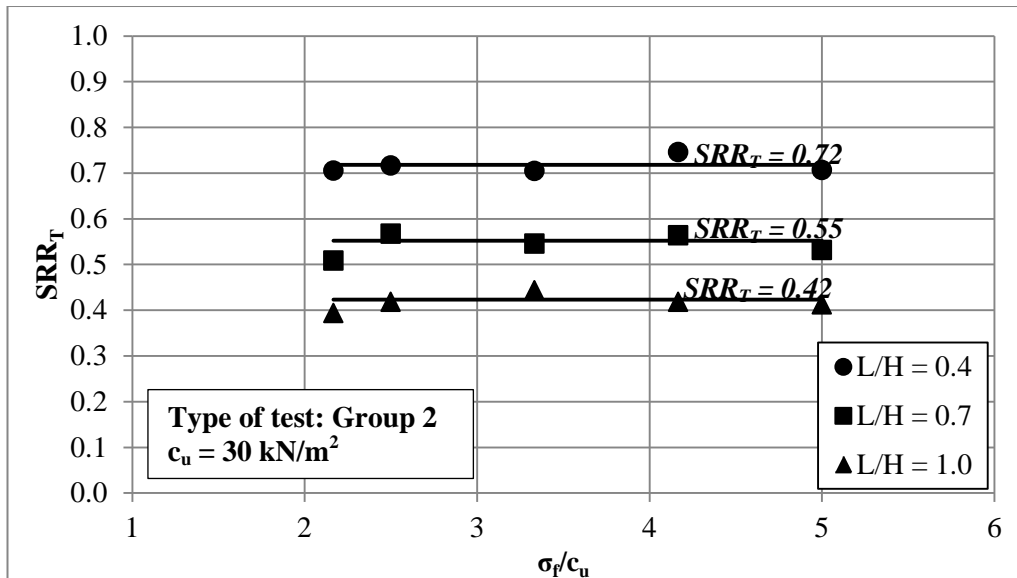
5.2.3.2. Column and Soil Stresses

5.2.3.2.1. End Bearing Columns

As previously stated, in group loading tests there are two stress transducer measuring stresses carried by center column (Column 1) and near to center column (Column 2). Stresses carried by Column 1 and 2 (σ_{c1} and σ_{c2}) at the end of each loading step are compared in Figures 5.39 and 5.40 for Group 1 and Group 2 with end bearing columns, respectively. Irrespective of the foundation pressure, σ_{c1} and σ_{c2} are similar where in general σ_{c2} is slightly lower than σ_{c1} for both groups. Thus in further calculations, average of σ_{c1} and σ_{c2} is used as stress carried by column (σ_c) in calculations of average stress carried by soil (σ_s) and stress concentration factor (n).
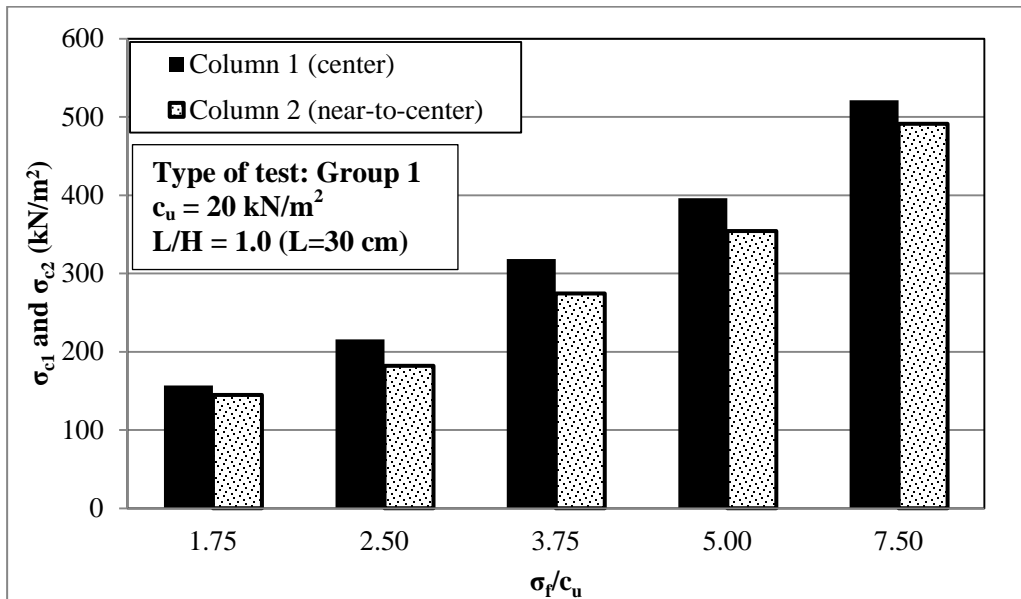
Figure 5.39. σ_{c1} and σ_{c2} **values at various** σ_f/c_u **(Type-G1: end bearing)**
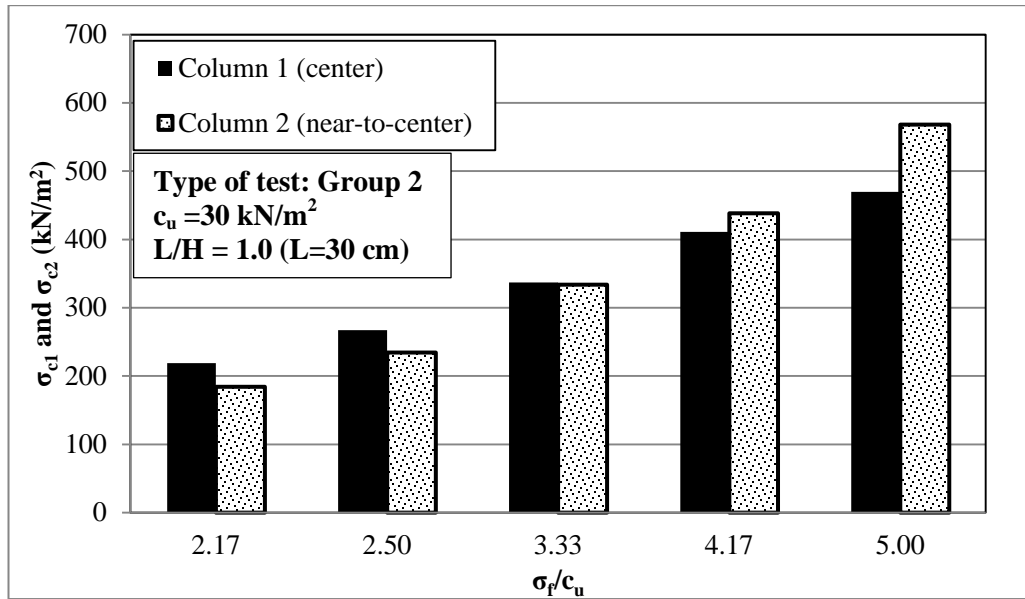
Figure 5.40. σ_{c1} and σ_{c2} values at various σ_f/c_u (Type-G2: end bearing)

Relationships between stresses carried by columns and surrounding soil (σ_c and σ_s) and normalized foundation pressures (σ_f/c_u) for Groups 1 and 2 with end-bearing columns are shown in Figures 5.41 and 5.42, respectively. Stresses both carried by column and soil increase as foundation pressure increases. For Group 1 test with end bearing columns, stresses carried by columns increases with decreasing rate whereas stress carried by surrounding soil increases with increasing rate indicating decrease in stress concentration factor with increase in foundation pressure. For Group 2 test with end bearing columns, stresses carried by columns and surrounding soil linearly increase indicating constant stress concentration factors at various foundation pressures.
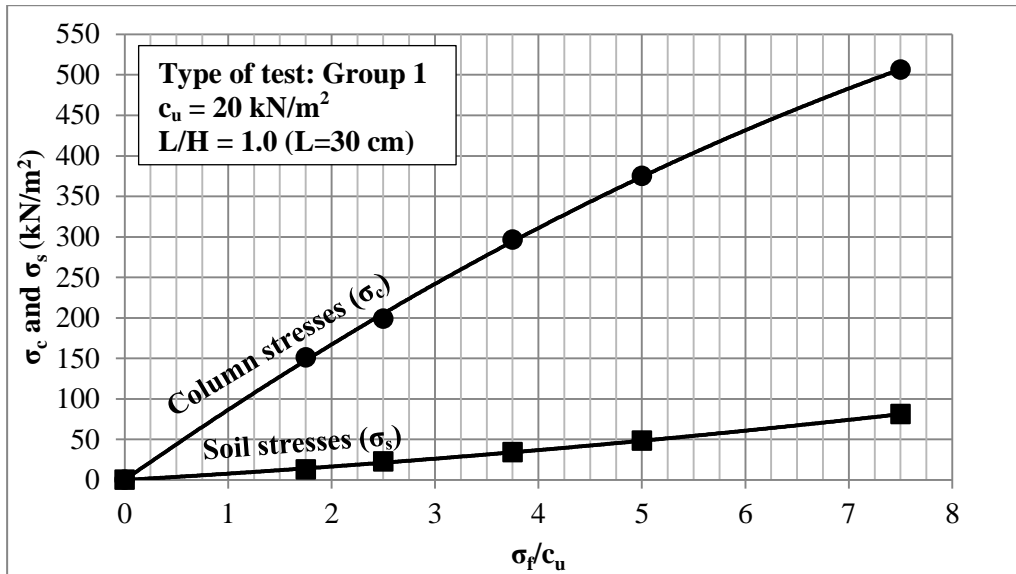
Figure 5.41. Relationships between $\sigma_f/c_u - \sigma_c$ and σ_s

(Type-G1: end-bearing)
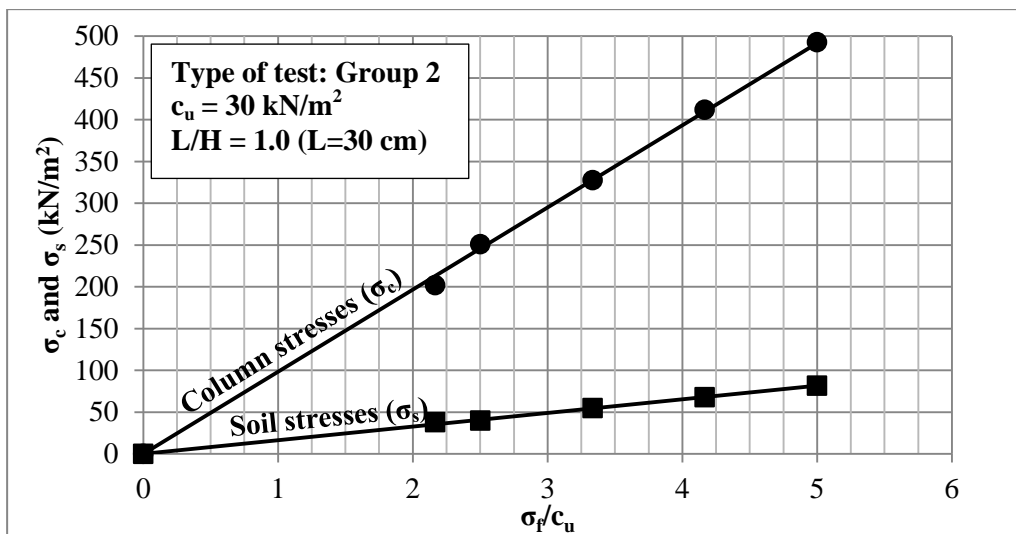
Figure 5.42. Relationships between $\sigma_f/c_u - \sigma_c$ and σ_s

(Type-G2: end-bearing)

Stress concentration factors (n) at the beginning (initial) and at the end (final) of each loading step for various normalized foundation pressures (σ_f/c_u) are shown

in Figures 5.43 and 5.44 for Groups 1 and 2 with end bearing columns, respectively. Irrespective of the foundation pressure and the initial undrained shear strength of soil, values of stress concentration factors decreases with time in end bearing columns. As consolidation proceeds, undrained shear strength of soil increases. Hence additional load can be carried by soil leading to stress transfer from column to soil. Consequently, stress concentration factor decreases as consolidation proceeds.

For Group 1 (c_u = 20 kN/m^2) test with end bearing columns, stress concentration factor decreases as foundation pressure increases. Under group loading, for end bearing column and c_u = 20 kN/m^2 final stress concentration factor decreases from 8.7 to 6.2 as normalized foundation pressure increases from 2.5 to 7.5, respectively.

For Group 2 (c_u = 30 kN/m^2) test with end bearing columns, final stress concentration factor is equal to 6.1 being independent of the magnitude of the applied pressure.
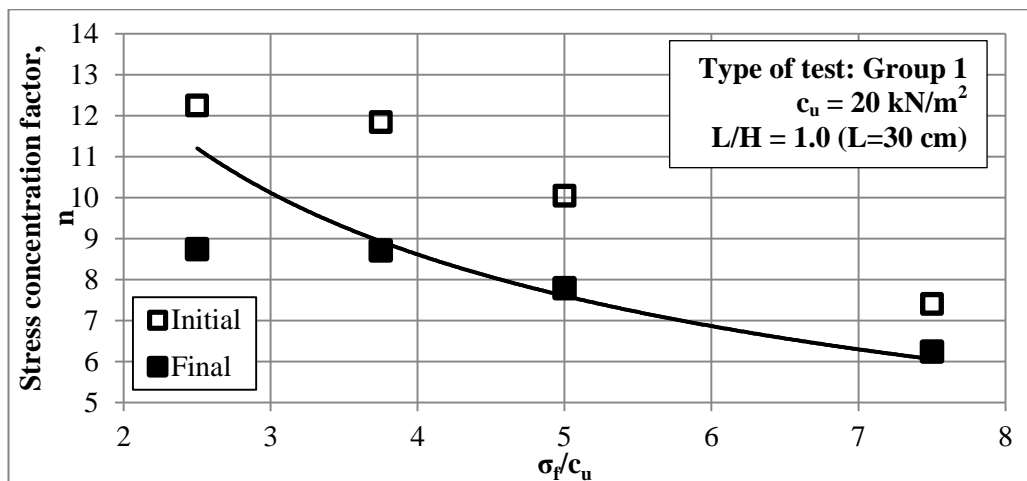
Figure 5.43. Relationship between σ_f/c_u – initial and final n

(Type-G1: end bearing)
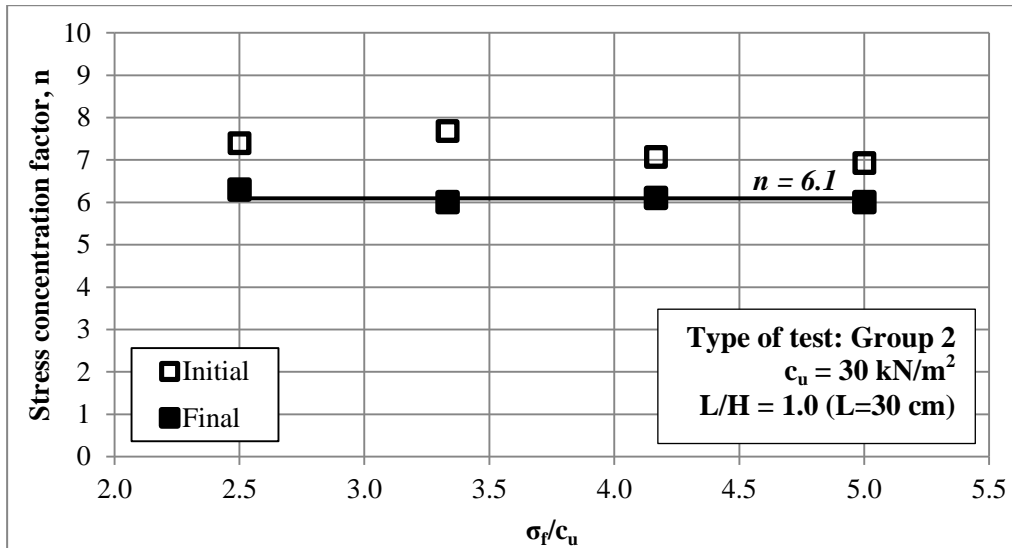
Figure 5.44. Relationship between σ_f/c_u – initial and final n
(Type-G2: end bearing)

5.2.3.2.2. Floating Column Tests

Stresses on Column 1 (center column) and Column 2 (a column near-to-center column) at the end of each loading step are shown in Figures 5.45 and 5.46 for Groups 1 and 2 with floating columns, respectively. Due to similar stresses on both columns, in further calculations average of σ_{c1} and σ_{c2} is used as stress carried by column (σ_c). In addition, average stress on soil (σ_s) and stress concentration factor (n) are also calculated by using the value of average stress carried by columns.

Relationships between stresses carried by column and surrounding soil (σ_c and σ_s) and normalized foundation pressures (σ_f/c_u) for Groups 1 and 2 with floating columns are shown in Figures 5.47 and 5.48, respectively. For both group tests, stresses both carried by column and soil increase as foundation pressure increases. For Group 1 test with floating columns, stresses carried by columns increases with decreasing rate whereas soil stress increases with increasing rate

156

indicating decrease in stress concentration factor with increase in foundation pressure. For Group 2 test with floating columns, stresses carried by columns and surrounding soil linearly increase indicating constant stress concentration factors at various foundation pressures.

(a)

(b)

Figure 5.45. σ_{c1} and σ_{c2} values at various σ_f/c_u (a) L/H=0.4 and (b) L/H=0.7 (Type-G1: floating)
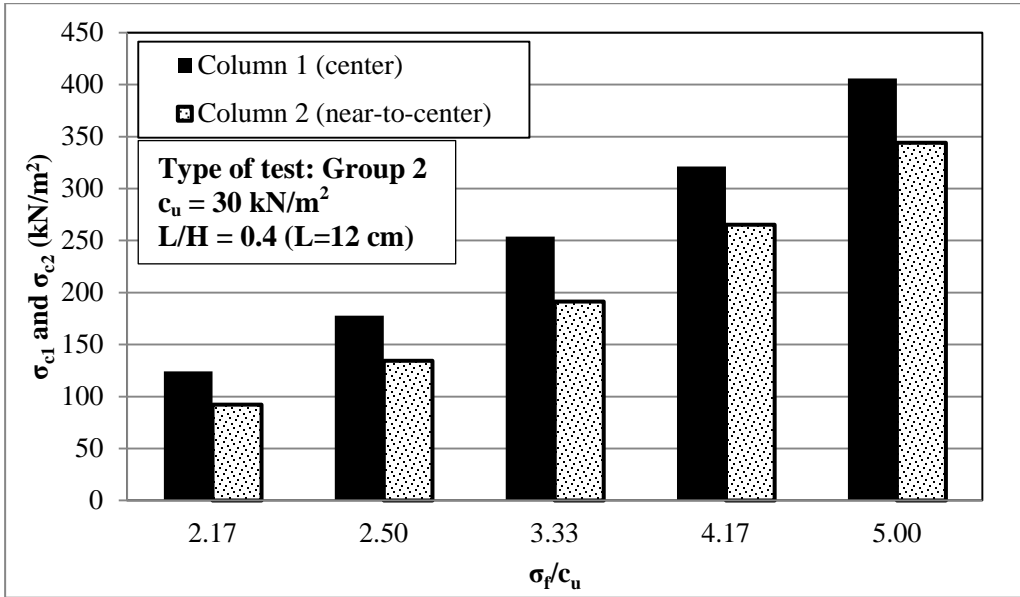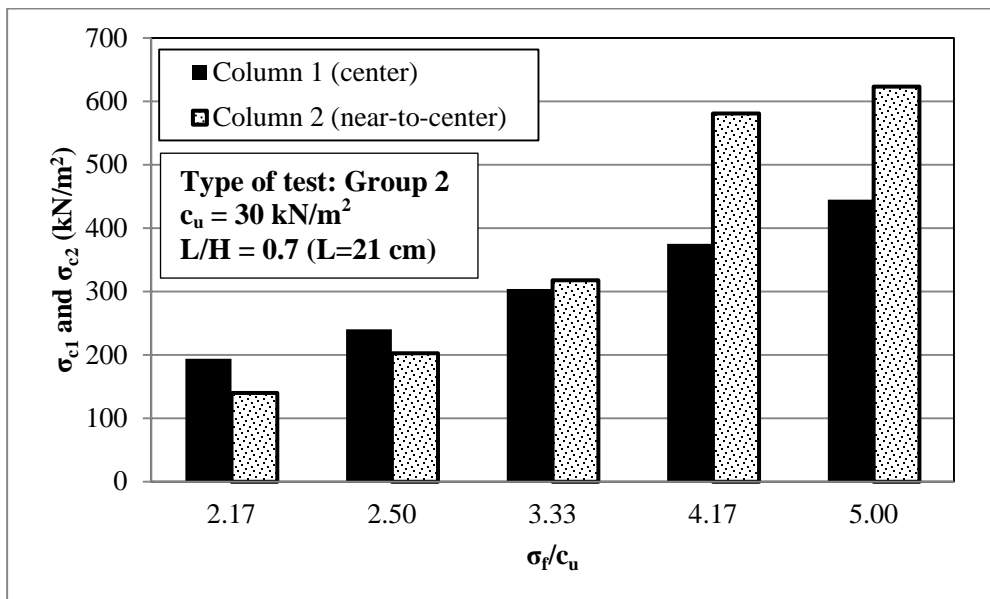
157

(a)

(b)

Figure 5.46. σ_{c1} and σ_{c2} values at various σ_f/c_u (a) L/H=0.4 and (b) L/H=0.7 (Type-G2: floating)

158
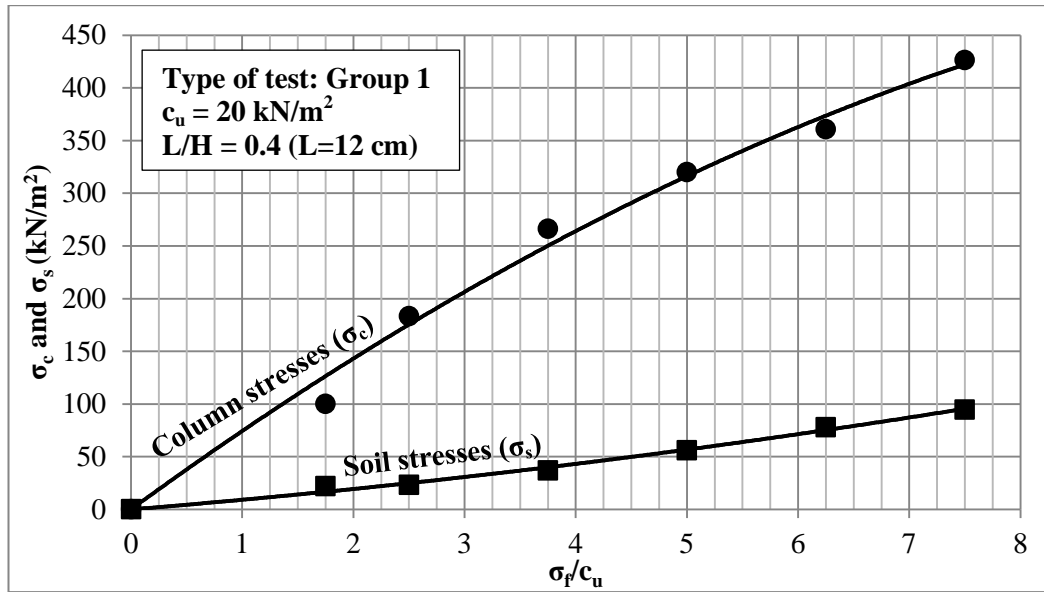
(a)
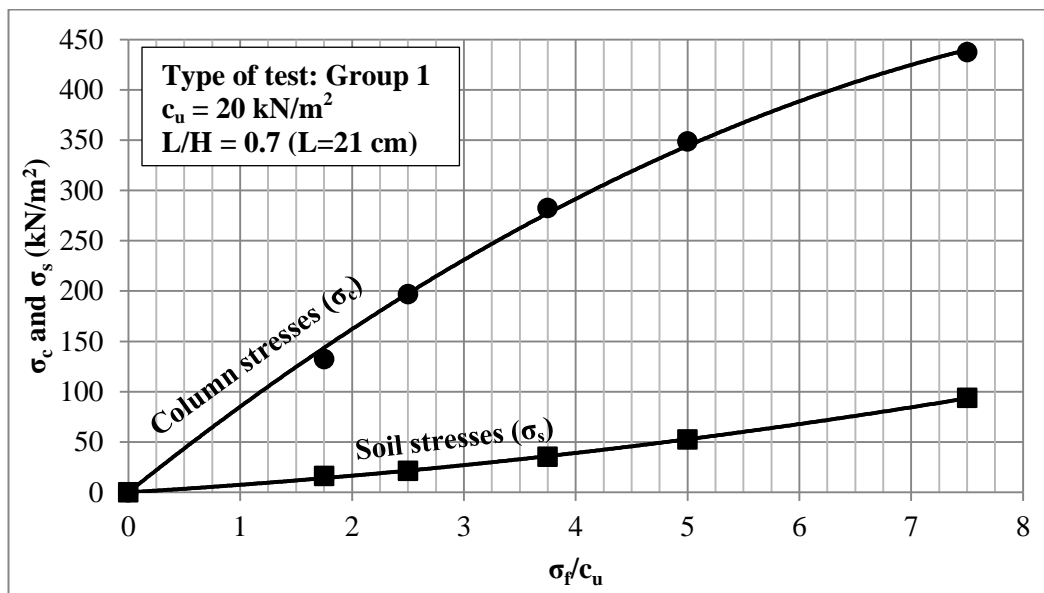
(b)

Figure 5.47. Relationships between σ_f/c_u – σ_c and σ_s (a) L/H=0.4 and (b) L/H=0.7 (Type-G1: floating)
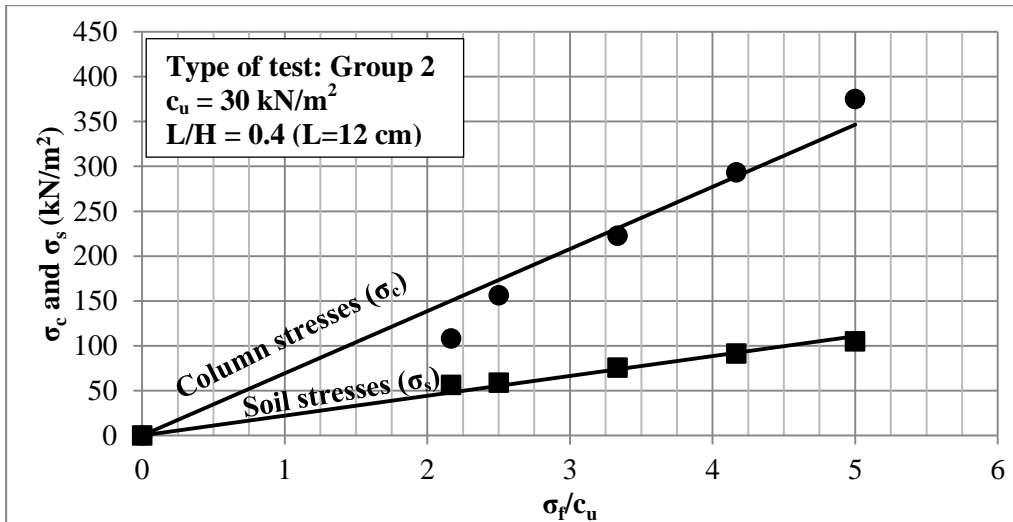
(a)
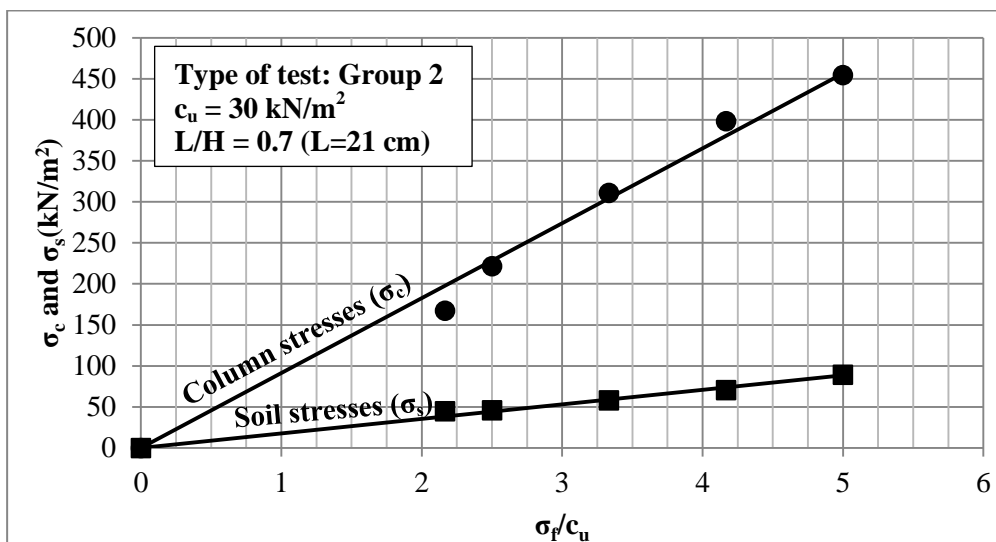
(b)

Figure 5.48. Relationships between $\sigma_f/c_u - \sigma_c$ and σ_s (a) L/H=0.4 and (b) L/H=0.7 (Type-G2: floating)

Stress concentration factors (n) at the beginning (initial) and at the end (final) of each loading step for various normalized foundation pressures (σ_f / c_u) are shown in Figures 5.49 and 5.50 for Groups 1 and 2 with floating columns, respectively. Irrespective of the foundation pressure and initial undrained shear strength of soil, values of stress concentration factors decreases with time in floating columns. As consolidation proceeds, undrained shear strength of soil increases. Hence additional load can be carried by soil leading to stress transfer from column to soil. Consequently, stress concentration factor decreases as consolidation proceeds.

In Group 1 ($c_u = 20$ kN/m^2) test with floating columns, stress concentration factor decreases as foundation pressure increases. Under group loading and for $c_u = 20$ kN/m^2, for columns having $L/H = 0.4$ and 0.7 final stress concentration factor decreases from 7.9 to 4.5 and from 9.2 to 4.7 as normalized foundation pressure increases from 2.5 to 7.5, respectively.

In Group 2 ($c_u = 30$ kN/m^2) test with floating columns having $L/H = 0.4$ and 0.7, final stress concentration factor is equal to 3.1 and 5.3, respectively, being independent of the magnitude of the applied pressure.
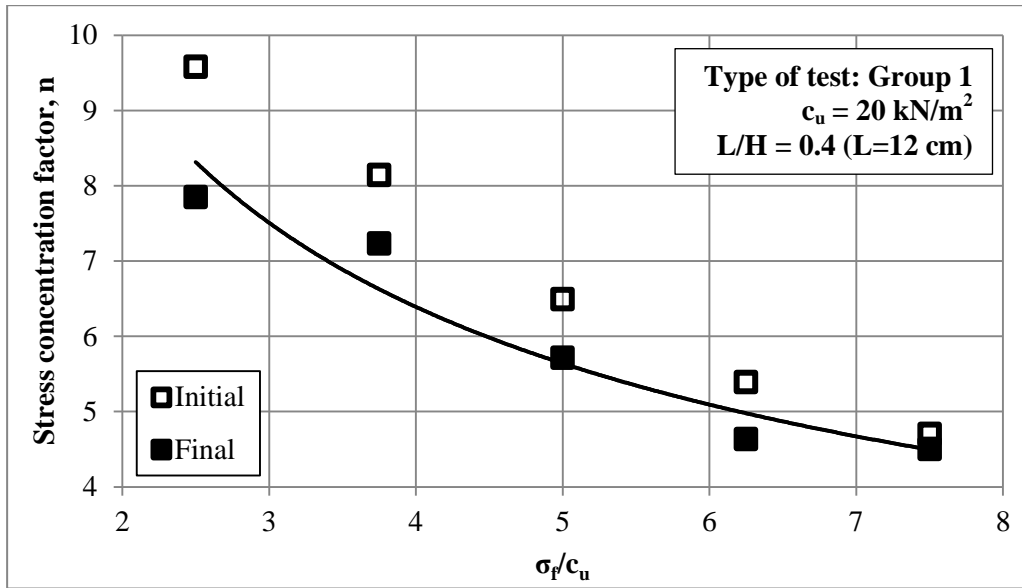
(a)
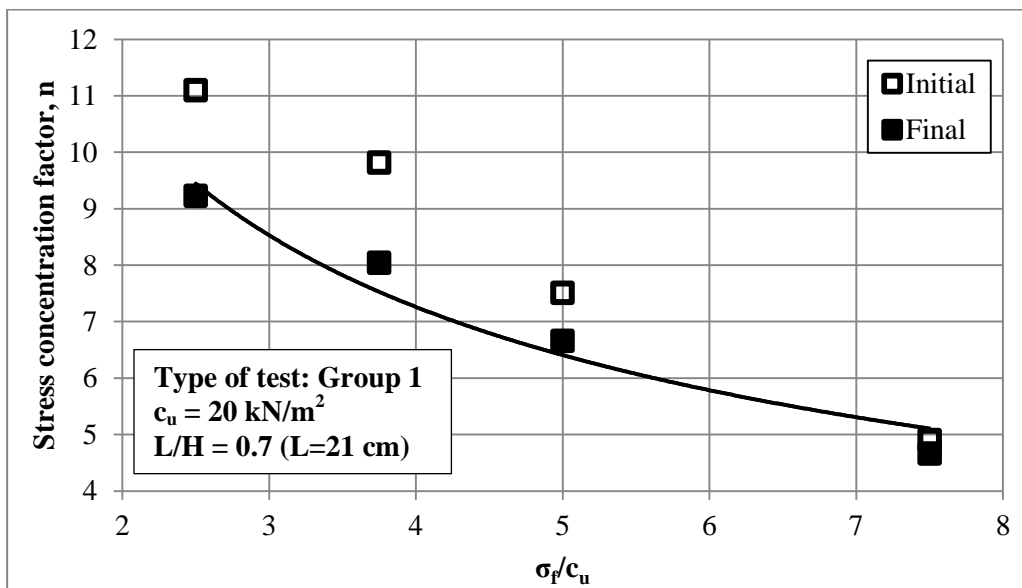
(b)

Figure 5.49. Relationships between σ_f/c_u – initial and final n (a) L/H=0.4 and (b) L/H=0.7 (Type-G1: floating)
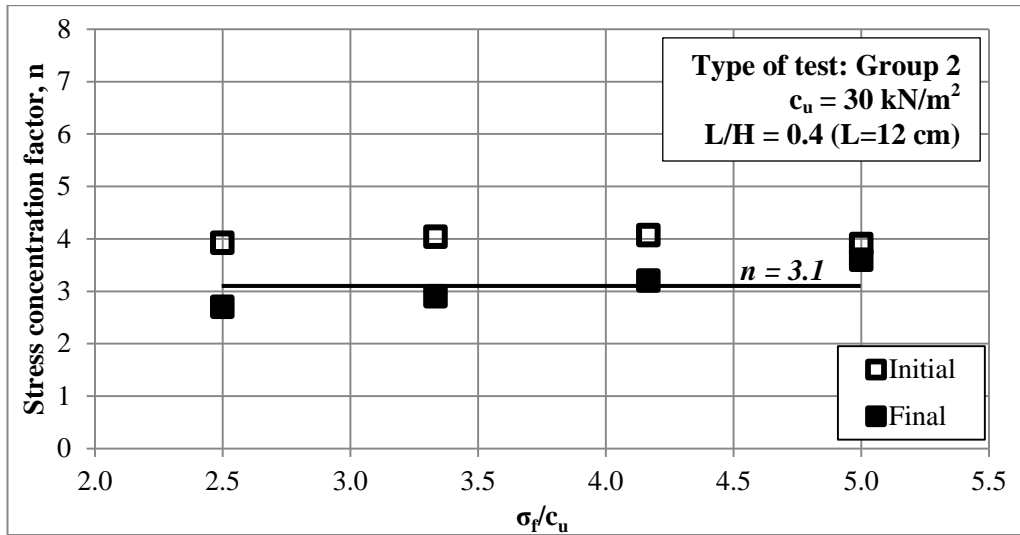
(a)
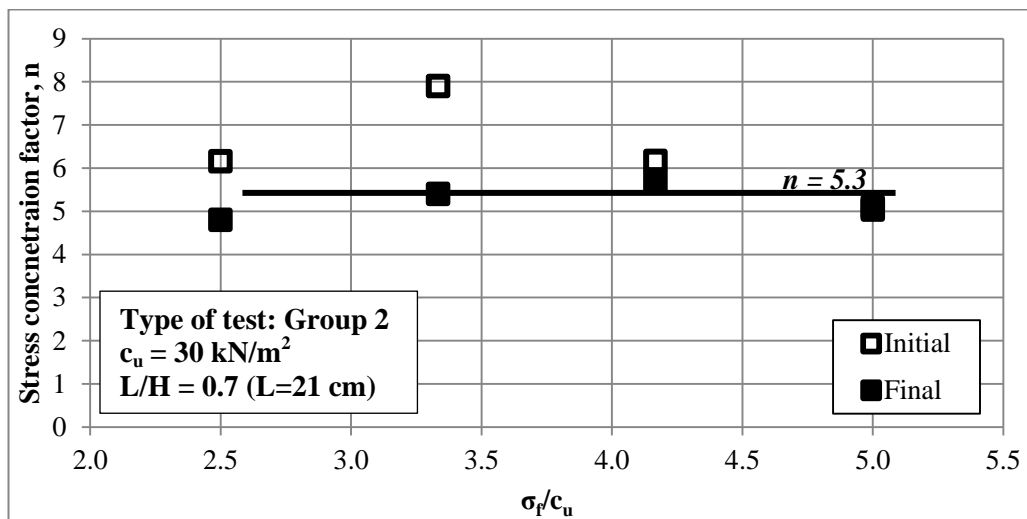
(b)

Figure 5.50. Relationships between σ_f/c_u – initial and final n (a) L/H=0.4 and (b) L/H=0.7 (Type-G2: floating)

5.2.3.2.3. Comparison of End Bearing and Floating Column Behavior

Figures 5.43, 5.44, 5.49 and 5.50 show that for group tests, irrespective of the length of column and the undrained shear strength of soil, stress concentration factor decreases as consolidation proceeds.

Relationships between stress concentration factor (n) and normalized foundation pressure (σ_f/c_u) for Groups 1 and 2 with different length of columns are shown in Figures 5.51 and 5.52. Irrespective of the column length, stress concentration factor (n) decreases by the increase of foundation pressure for Group 1 having c_u = 20 kN/m^2. Whereas, n is almost constant at various foundation pressures for Group 2 having c_u = 30 kN/m^2, irrespective of the column length. These results imply that dependency of stress concentration factor on normalized foundation pressure is less pronounced as soil stiffens. Moreover, regardless of the initial undrained shear strength of soil, for longer columns, larger stress concentration factor develops since thickness of soft soil beneath the columns decreases.
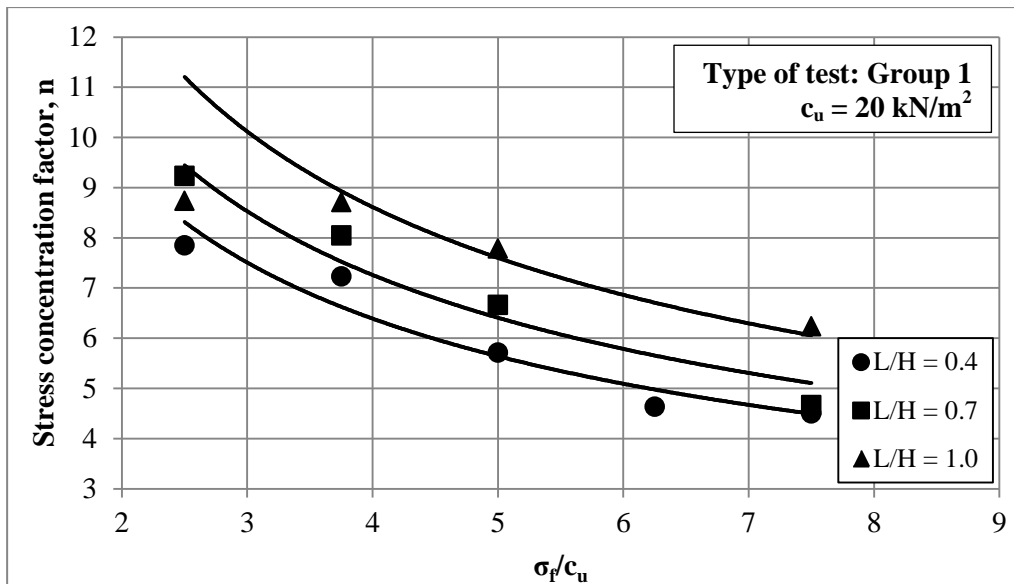
Figure 5.51. Relationships between $\sigma_f/c_u - n$ (Type-G1)
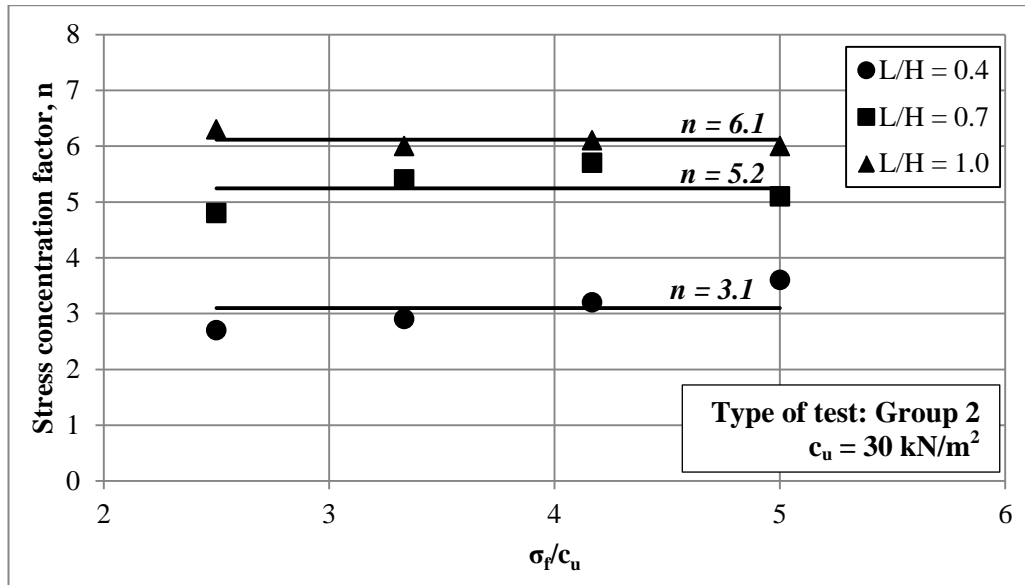
Figure 5.52. Relationships between $\sigma_f/c_u - n$ (Type-G2)

5.3. Comparison of Single Columns Loaded over a Footing Having Same Diameter with the Unit Cell (Type-SCF) and Group (Type-G1) Behavior

In this section, settlement reduction ratio and stress concentration factor versus normalized foundation pressure behavior of Type-SCF and Type-G1 tests having both c_u = 20 kN/m² of initial undrained shear strength of soil are compared. The aim of the comparison is to comprehend the suitability of single columns loaded over a footing having same diameter with the unit cell to represent the group behavior.

5.3.1. Settlement

Stress – settlement behavior of single columns loaded over a footing having same diameter with the unit cell and group loading tests show that regardless of the column length, settlements are different under same magnitude of foundation pressure. This was also mentioned by Kirsch and Borchert (2006). In group tests, load was applied through a plate having a larger diameter than the loading plate

165

used in Type-SCF tests. In addition, group tests were performed in one-dimensional loading, whereas Type-SCF tests were performed with different boundary conditions leading to three dimensional loading. These differences in boundary conditions and the loading geometry give rise to differences in settlement patterns.

Relationships between normalized foundation pressure and ratio of surface settlement of group to single columns loaded over a footing having same diameter with the unit cell tests (S_G/S_{SCF}) having same initial undrained shear strength for different length of columns are shown in Figure 5.53. The relationship between normalized length of column (L/H), normalized foundation pressure (σ_f/c_u) and surface settlement ratio (S_G/S_{SCF}) is represented by Equation 5.1.

$$S_G/S_{SCF} = 2.55 - 0.11\left(\sigma_f/c_u\right) - 0.76\left(L/H\right) \tag{5.1}$$

By using Equation 5.1, settlement under group loading can be estimated from measured settlement under Type-SCF loading with coefficient of determination (R^2) equal to 0.87. Plot of measured versus predicted surface settlement ratios (S_G/S_{SCF}) is illustrated in Figure 5.54.
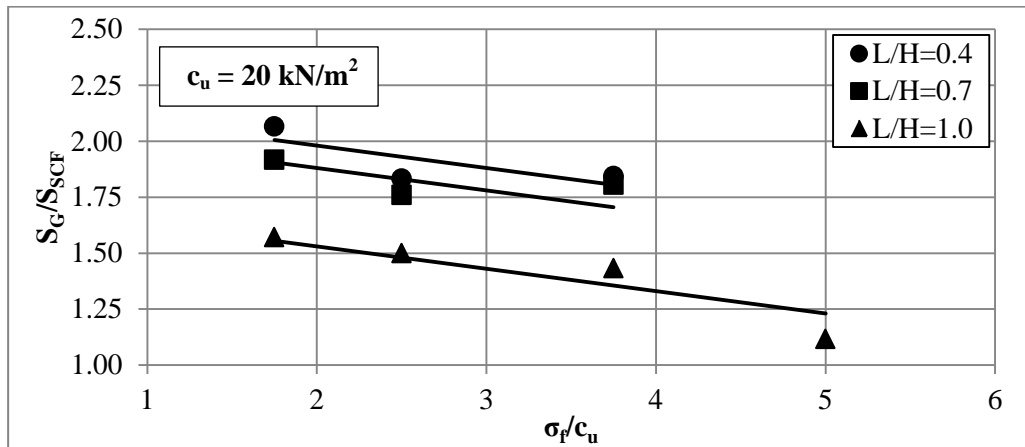
Figure 5.53. Relationships between (S_G/S_{SCF}) - (σ_f/c_u)

(Type-SCF and Type-G1 tests)

166
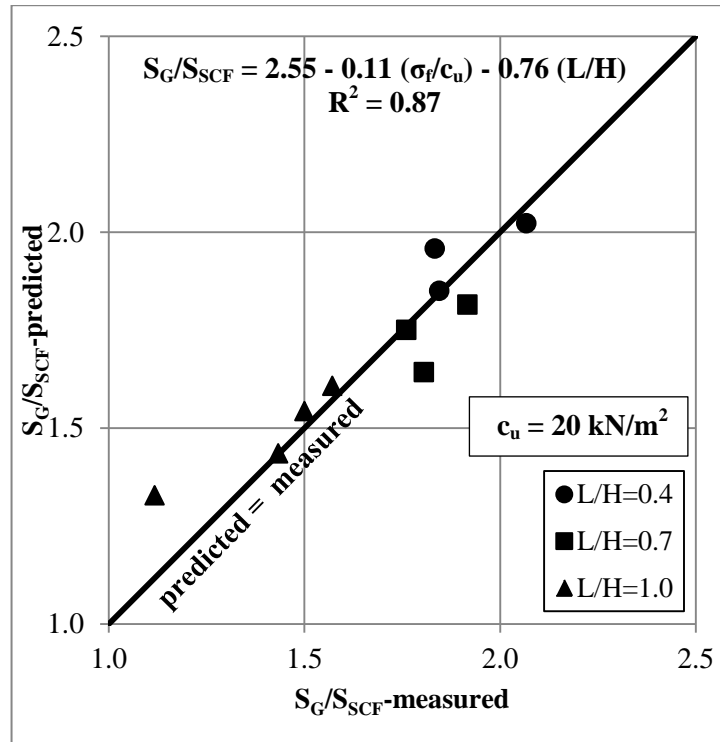
Figure 5.54. Comparison of measured and predicted values of S_G/S_{SCF}
(Type-SCF and Type-G1 tests)

For different length of stone columns, total settlement reduction ratios (SRR_T) obtained in single columns loaded over a footing having same diameter with the unit cell and group loading tests in soil with initial undrained shear strength of c_u = 20 kN/m^2, are compared as shown in Figure 5.55. SRR_T values obtained in single columns loaded over a footing having same diameter with the unit cell and group loading in end bearing columns are almost same. On the other hand, for floating columns SRR_T values obtained in group loading tests are higher than the values obtained in Type-SCF loading tests. In conclusion, settlement reduction ratios obtained in group loading tests in floating columns are higher than the values obtained in Type-SCF tests and this difference is more pronounced as length of column shortens. In other words, to represent the stress – settlement behavior of groups, unit cell approach loses validity as column length shortens.
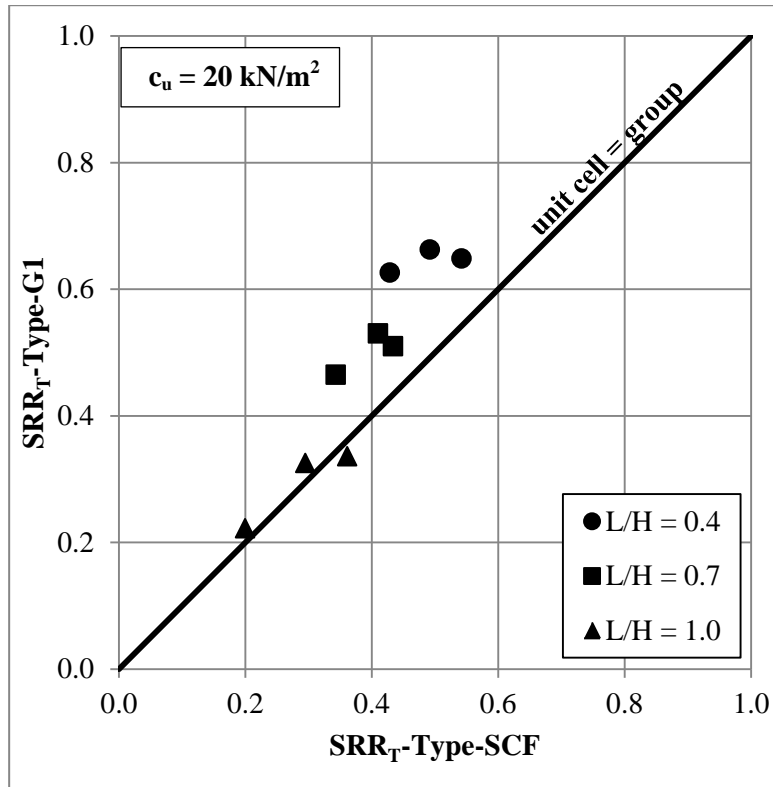
Figure 5.55. Comparison of SRR_T values for different L/H (Type-SCF and Type-G1 tests)

5.3.2. Stress Concentration Factor

Relationships between normalized foundation pressure and average stresses carried by column and surrounding soil are almost same for single columns loaded over a footing having same diameter with the unit cell and group loading tests.

For different length of columns, stress concentration factors obtained in single columns loaded over a footing having same diameter with the unit cell and group loading tests having same initial undrained shear strength of $c_u = 20$ kN/m^2, are compared as shown in Figure 5.56. Regardless of the length of column, n values obtained in single columns loaded over a footing having same diameter with the

unit cell and group loading are almost same. Hence, single columns loaded over a footing having same diameter with the unit cell behavior can realistically represent the stress distribution between column and soil in group loading for any length of column.
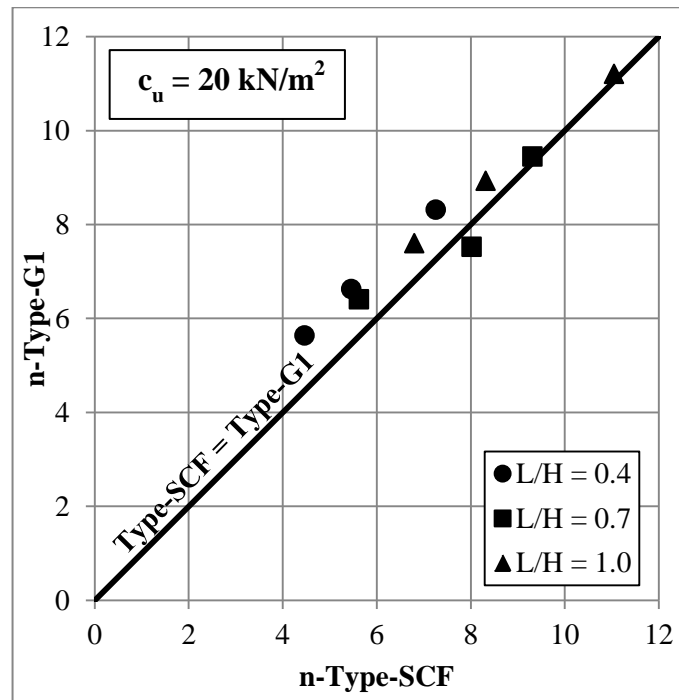
Figure 5.56. Comparison of n values for different L/H
(Type-SCF and Type-G1 tests)

5.4. Comparison of Groups with Different c_u of Soil (Type-G1 and Type-G2 Tests)

In this section, settlement reduction ratio and stress concentration factor versus normalized foundation pressure behavior of Type-G1 ($c_u = 20$ kN/m^2) and Type-G2 ($c_u = 30$ kN/m^2) tests having different initial undrained shear strength of soil are compared. The aim of the comparison is to comprehend the effect of undrained shear strength on stress-settlement behavior.

5.4.1. Settlement Reduction Ratio

In Chapter 4, values of initial (at the end of consolidation stage) and final (at the end of loading stage) undrained shear strengths were listed for all group tests (Tables 4.8 and 4.9). From these values the ratios of increase in undrained shear strength (Δc_u) to increase in foundation pressure ($\Delta \sigma_f$), i.e. $\Delta c_u / \Delta \sigma_f$, are calculated and listed in Table 5.4. By using the calculated $\Delta c_u / \Delta \sigma_f$ ratios, final undrained shear strength at the end of each loading step is estimated.

Table 5.4. Ratios of $\Delta c_u / \Delta \sigma_f$ (Types-G1 and G2)

	$\Delta c_u / \Delta \sigma_f$	
L/H	*Group 1*	*Group 2*
0.4	0.13	0.19
0.7	0.15	0.18
1.0	0.21	0.28

For different length of stone columns, total settlement reduction ratio (SRR_T) versus undrained shear strength behavior obtained in group loading tests having initial undrained shear strength of c_u = 20 and 30 kN/m^2 are shown in Figure 5.65.

As previously stated, SRR_T values decrease as length of column increases regardless of the undrained shear strength of soil. Moreover, SRR_T increases as undrained shear strength increases. Increase in SRR_T values depending on the undrained shear strength is less pronounced at higher undrained shear strength of soil as previously mentioned in Group 2 tests.

Relationship between total settlement reduction ratio, undrained shear strength and L/H shown in Figure 5.57 is represented by Equation 5.2.

$$SRR_T = [0.42 - 0.25(L/H)] * (c_u)^{0.23} \tag{5.2}$$

By using Equation 5.2, total settlement reduction ratio can be estimated depending on L/H and undrained shear strength with coefficient of determination (R^2) equal to 0.95. Plot of measured versus predicted total settlement reduction ratios (SRR_T) is illustrated in Figure 5.58.
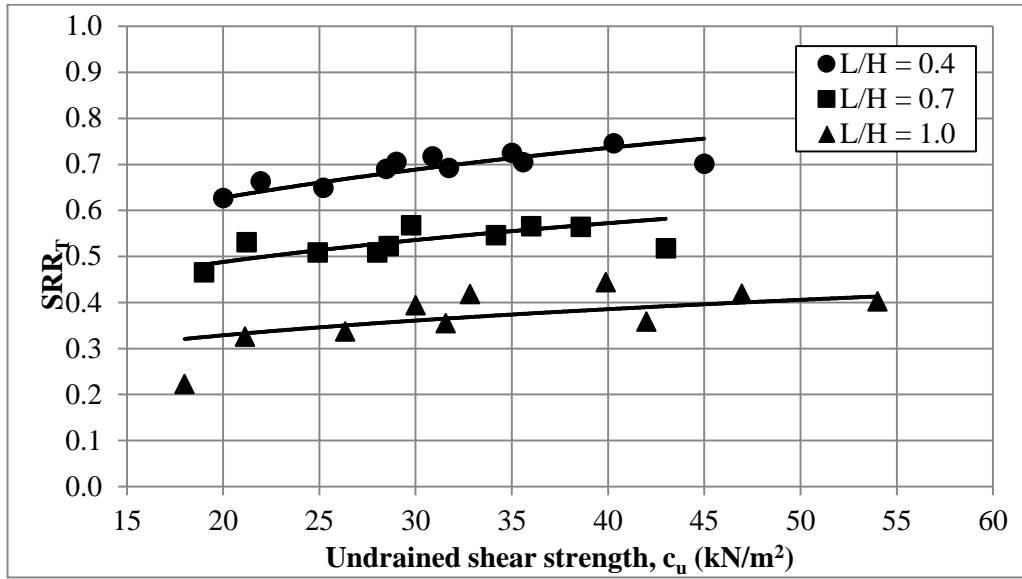
Figure 5.57. Relationship between SRR_T, c_u and L/H

(Type-G1 and Type-G2 tests)

The figure shows a scatter plot comparing SRR_T-measured (x-axis) versus SRR_T-predicted (y-axis), both ranging from 0.0 to 1.0. The equation shown is:

$$SRR_T = (0.42 - 0.25(L/H))\,(c_u)^{0.23}$$

$$R^2 = 0.95$$

A diagonal line labeled "predicted = measured" is shown. Legend: ● L/H = 0.4, ■ L/H = 0.7, ▲ L/H = 1.0
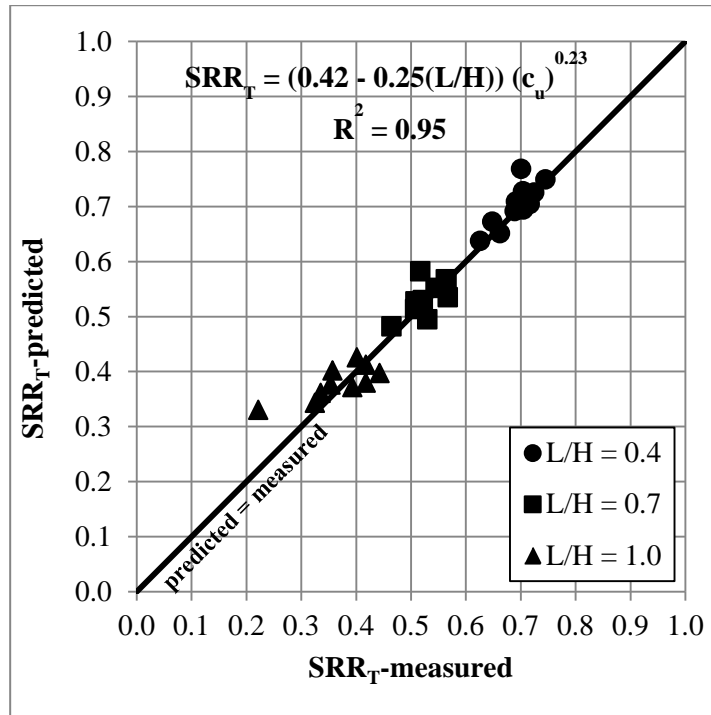
Figure 5.58. Comparison of measured and predicted values of SRR_T
(Type-G1 and Type-G2 tests)

5.4.2. Stress Concentration Factor

The variation between undrained shear strength and stress concentration factor at the end of each loading step for Groups 1 and 2 with different lengths of column are shown in Figure 5.59.
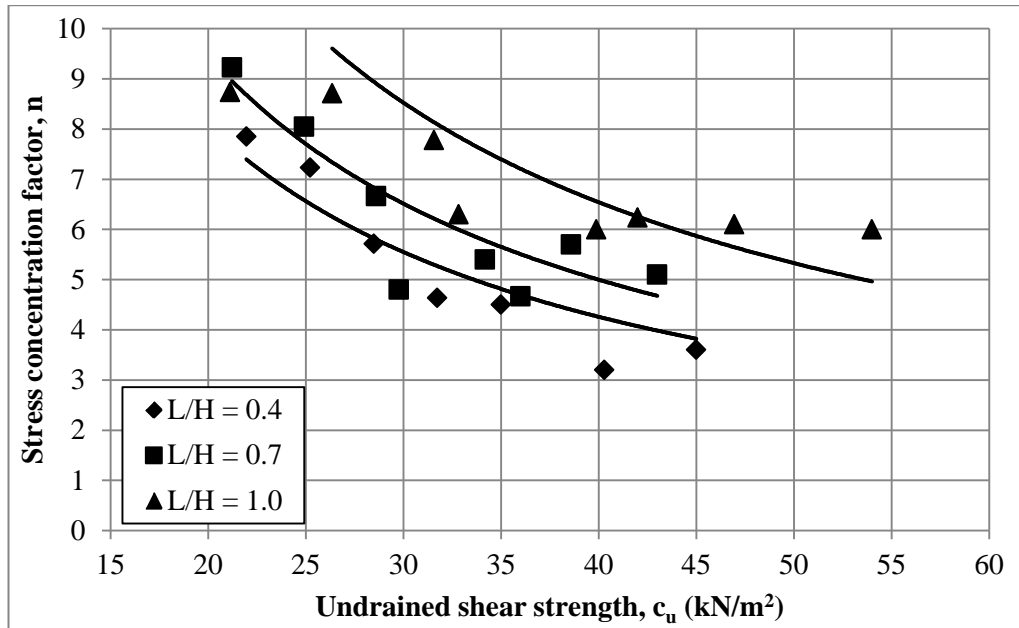
Figure 5.59. Relationship between n, c_u and L/H

(Type-G1 and Type-G2 tests)

Relationship between undrained shear strength, stress concentration factor and normalized column lengths is represented by Equation 5.3 with coefficient of determination (R^2) equal to 0.87.

$$n = [120.0(L/H) + 74.2] * (c_u)^{-0.92} \qquad (5.3)$$

Plot of measured versus predicted values of stress concentration factor (n) is illustrated in Figure 5.60.
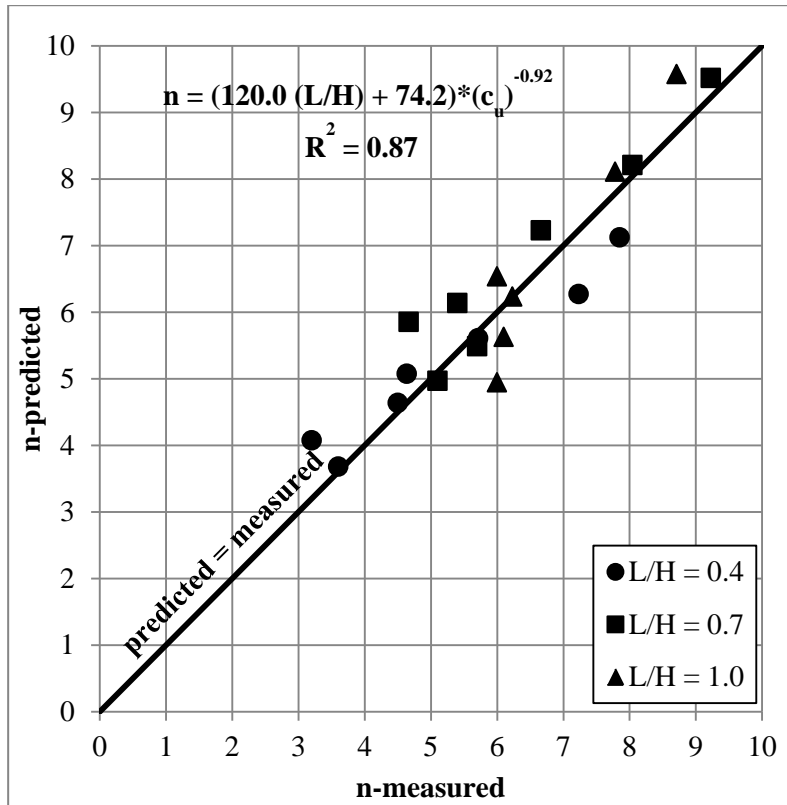
Figure 5.60. Comparison of measured and predicted values of n
(Type-G1 and Type-G2 tests)

It should be noted that, total settlement reduction ratio and stress concentration factor are inversely proportional to each other. As Figures 5.57 and 5.59 indicate, as undrained shear strength increases total settlement reduction ratio increases whereas stress concentration factor decreases.

CHAPTER 6

CONCLUSION

6.1. General

Small scale model tests were performed in order to observe effects of column length and undrained shear strength on settlement reduction ratios (SRR) at different zones and stress concentration factor (n). In these tests different loading conditions, i.e. single stone column loading, single columns loaded over a footing having same diameter with the unit cell and group loading, were studied. Stress carried by stone columns under various foundation pressures were directly measured by soil pressure transducers. Surface and subsurface settlements were measured by dial gauge and potentiometric rulers.

Tests were carried out for three different column lengths (L/H = 0.4, 0.7 and 1.0), two different initial undrained shear strengths (c_u = 20 and 30 kN/m^2) and various foundation pressures (σ_f = 35 – 150 kN/m^2). Diameter of stone column (D = 3 cm), compressible layer thickness (H = 30 cm) and area replacement ratio (a_r = 16.6%) were same for all tests. Overburden stress (σ_0) of 20 kN/m^2 was applied in single column loading and single columns loaded over a footing having same diameter with the unit cell tests. Group tests were conducted under one-dimensional loading in order to represent the applications in extensively wide areas.

In single column loading tests failure modes, ultimate bearing capacities and critical length concepts are discussed. In single columns loaded over a footing having same diameter with the unit cell and group loading tests, settlement reduction ratios (SRR) at total, upper and lower zones and stress concentration factors (n) for different foundation pressures and column lengths are compared. Variation of stress concentration factor with time is assessed. Single columns loaded over a footing having same diameter with the unit cell and group behavior with floating and end-bearing columns are compared. Whether or not the single columns loaded over a footing having same diameter with the unit cell behavior can represent the group behavior is discussed. An equation to obtain the group settlement from the single columns loaded over a footing having same diameter with the unit cell settlement depending on L/H and σ_f/c_u parameters is proposed. Empirical relationships between total settlement reduction ratio (SRR_T) and undrained shear strength and; stress concentration factor (n) and undrained shear strength are proposed. These correlations are valid for range of undrained shear strength between 20 and 50 kN/m^2.

6.2. Load – Settlement Behavior of Single Column

Single column tests were performed for three different lengths of column in soil having initial undrained shear strength of 20 kN/m^2. Failure of stone columns having L/H ratios of 0.4, 0.7 and 1.0 occurred at foundation pressures equal to 300 kPa, 300 kPa and 450 kPa, respectively. Failure modes of stone columns having L/H ratios of 0.4, 0.7 and 1.0 are punching-full length bulging, punching-local bulging and local bulging, respectively. For end bearing column, the ratio of ultimate load capacity to initial undrained shear strength (σ_{ult}/c_u) and range of normalized depth of bulging (z_b/D) are obtained as 22.5 and 1.3 – 3.9, respectively.

6.3. Load – Settlement Behavior of Single Columns Loaded over a Footing Having Same Diameter with the Unit Cell

Single column tests were performed for untreated soil and three different column lengths in soil having initial undrained shear strength of 20 kN/m^2. Failure of stone columns having L/H ratios of 0.4, 0.7 and 1.0 occurred at foundation pressures equal to 100 kPa, 100 kPa and 125 kPa, respectively.

For single columns loaded over a footing having same diameter with the unit cell tests total settlement reduction ratio (SRR_T) increases as the column length shortens and foundation pressure increases. For single columns loaded over a footing having same diameter with the unit cell tests with column having $L/H = 0.4, 0.7, 1.0$ obtained total settlement reduction ratios are in the range of 0.43 – 0.54, 0.29 – 0.38 and 0.20 – 0.35, respectively. Moreover, for floating columns settlement reduction ratios in upper zone (SRR_{UZ}) increases with decreasing length of column and increasing foundation pressure. Furthermore, settlement reduction ratio in lower zone (SRR_{LZ}) is same for both floating column tests and increases with increasing applied foundation pressure.

For single columns loaded over a footing having same diameter with the unit cell tests, there is no significant variation in stress concentration factor (n) during time of consolidation. On the contrary with the total settlement reduction ratio, stress concentration factor decreases with increasing foundation pressure. It is found that, for longer stone columns larger stress concentration factors develop. For single columns loaded over a footing having same diameter with the unit cell tests with column having $L/H = 0.4, 0.7, 1.0$ obtained stress concentration factors are in the range of 4.5 – 6.7, 5.6 – 9.3 and 6.1 – 12.5, respectively.

Equilibrium method (conventional unit cell concept) is found to be underestimating the settlement improvement for single end bearing column loaded over a footing having same diameter with the unit cell.

6.4. Load – Settlement Behavior of Column Group

Two series of infinite group tests having different initial undrained shear strength of soil were carried out (Group 1: $c_u = 20$ kN/m^2 and Group 2: $c_u = 30$ kN/m^2 tests) for untreated soil and three different column lengths under various foundation pressures. In all of these tests, failure is not observed up to maximum applied pressure of 150 kN/m^2.

For Group 1 tests, total settlement reduction ratio (SRR_T) increases by the decreasing column length and increasing foundation pressure. Whereas, settlement reduction ratios in upper (SRR_{UZ}) and lower zones (SRR_{LZ}) are same for both Group 1 tests with floating columns. For Group 1 tests with columns having L/H = 0.4, 0.7, 1.0 obtained total settlement reduction ratios are in the range of 0.63 – 0.74, 0.48 – 0.57 and 0.22 – 0.36, respectively.

For Group 2 tests, total settlement reduction ratio (SRR_T) increases by the increasing column length where settlement reduction ratios in upper and lower zones are same. On the contrary with Group 1 tests, settlement reduction ratios (SRR_T, SRR_{UZ} and SRR_{LZ}) obtained in Group 2 tests are being independent from the magnitude of applied foundation pressure. For Group 2 tests with columns having L/H = 0.4, 0.7, 1.0 obtained total settlement reduction ratios are 0.72, 0.55 and 0.42, respectively. For both group test series, irrespective of the column length and amount of foundation pressure, settlement reduction ratios in lower zone are close to unity, indicating no significant improvement in untreated zone. Hence, settlement of infinite group with floating stone columns can be estimated by Equation 6.1. In this equation, S_t is surface settlement of treated soil, S_{u-UZ} and S_{u-LZ} are the settlements in upper and lower zone before treatment, respectively.

$$S_t = [(SRR_{UZ}) * S_{u-UZ}] + S_{u-LZ} \qquad (6.1)$$

For all group tests, stresses measured on center and near-to-center columns are almost same. Thus, average column stresses were used in calculations of soil stresses and stress concentration factors. For Group 1 tests, stress concentration factor (n) decreases with increasing foundation pressure. Moreover, for groups with longer columns reveal to higher stress concentration factors irrespective of the foundation pressure. For Group 1 tests with columns having L/H = 0.4, 0.7, 1.0 obtained stress concentration factors are in the range of 4.5 – 7.9, 4.7 – 9.2 and 6.2 – 8.7, respectively. On the other hand, stress concentration factors obtained in Group 2 tests are being independent from the magnitude of applied foundation pressure but only increases by the increasing column length. For Group 2 tests with columns having L/H = 0.4, 0.7, 1.0 obtained stress concentration factors are 3.1, 5.3 and 6.1, respectively. In all group tests, irrespective of the length of column and the undrained shear strength of soil, stress concentration factor decreases as consolidation proceeds. Measured stress concentration factors are in the range of values, n = 2 – 8, reported by previous researchers.

6.5. Comparison of Single Columns Loaded over a Footing Having Same Diameter with the Unit Cell and Group Behavior

Stress – settlement behavior of single columns loaded over a footing having same diameter with the unit cell and group loading tests show that regardless of the column length, settlements are different under same magnitude of foundation pressure. The relationship between normalized column length (L/H), normalized foundation pressure (σ_f/c_u) and surface settlement ratio (S_G/S_{SCF}) is represented by Equation 6.2 with coefficient of determination (R^2) equal to 0.87.

$$S_G/S_{SCF} = 2.55 - 0.11\left(\sigma_f/c_u\right) - 0.76\left(L/H\right) \tag{6.2}$$

Settlement reduction ratios obtained in group loading tests in floating columns are higher than the values obtained in single columns loaded over a footing having same diameter with the unit cell tests and this difference is more pronounced as column length shortens. In other words, to represent the stress – settlement behavior of groups, unit cell concept is not valid in short columns.

Stress concentration factors (n) obtained in single columns loaded over a footing having same diameter with the unit cell and group loading are almost the same. It is found that, single columns loaded over a footing having same diameter with the unit cell can realistically represent the stress distribution between column and soil in group loading for any length of column.

6.6. Effect of Undrained Shear Strength on SRR_T and n

For all group tests, SRR_T values decrease as length of column increases regardless of the undrained shear strength of soil. Increase in SRR_T values is less pronounced at higher undrained shear strength of soil. Relationship between total settlement reduction ratio (SRR_T), undrained shear strength (c_u) and normalized column lengths (L/H) is represented by Equation 6.3 with coefficient of determination (R^2) equal to 0.95.

$$SRR_T = [0.42 - 0.25(L/H)] * (c_u)^{0.23} \qquad (6.3)$$

Stress concentration factor (n), relationship between undrained shear strength (c_u) and normalized column lengths (L/H) is represented by Equation 6.4 with coefficient of determination (R^2) equal to 0.87.

$$n = [120.0(L/H) + 74.2] * (c_u)^{-0.92} \qquad (6.4)$$

6.7. Recommendations for Future Studies

There are very few studies on stress – settlement behavior of floating stone columns in infinitely large groups. In full-scale model tests on large group of stone columns, e.g. under embankments, both the settlement and stress on soil and columns at various depths should be measured. Moreover, pore pressures and lateral stresses around the stone columns should be measured. Effect of different area replacement ratio and stone column rigidity on settlement and stress distribution is to be investigated. Also, further studies on detailed three dimensional finite element modelling of stone column groups by considering the effects of construction and time of consolidation should be performed.

REFERENCES

Aboshi, H., Ichimoto, E., Enoki, M. and Harada, K. (1979). "The Composer: A Method to Improve Characteristics of Soft Clays by Inclusions of Large Diameter Sand Columns", *Proc. Int. Conf. on Soil Reinforcement: Reinforced Earth and Other Techniques,* Vol. 1, Paris, 211 – 216.

Al-Khafaji, Z.A. and Craig, W.H. (2000). "Drainage and Reinforcement of Soft Clay Tank Foundation by Sand Columns", *Géotechnique* 50(6): 709 – 713.

Al-Shaikhly, A.A. (2000). "Effect of Stone Grain Size on the Behavior of Stone Column", *M.Sc. thesis,* University of Technology.

Ambily, A.P. and Gandhi, S.R. (2004). "Experimental and Theorotical Evaluation of Stone Column in Soft Clay", *ICGGE 2004*: 201 – 206.

Ambily, A.P. and Gandhi, S.R. (2006). "Behavior of Stone Columns Based on Experimental and FEM Analysis", *Journal of Geotechnical and Geoenvironmental Engineering*, 133(4): 405 – 415.

Atkinson, J. (2007). "Peak Strength of Overconsolidated Clays", *Geotechnique* 57(2): 127- 135.

Ayadat, T and Hanna A.M. (2005). "Encapsulated Stone Columns as a Soil Improvement Technique for Collapsible Soil", *Ground Improvement,* 9(4): 137 – 147.

Bachus, R.C. and Barksdale, R.D. (1989). "Design Methodology for Foundations on Stone Columns", *Vertical and Horizontal Deformations of Foundations and Embankments, Proceedings of Settlement'1994,* Texas, ASCE Geotechnical Special Publication No.40, pp.244-257

Bae, W-S, Shin B-W, An, B-C and Kim, J-S (2002). "Behaviors of Foundation System Improved with Stone Columns", *Proceedings of the Twelfth International Offshore and Polar Engineering Conference 2002*: 675 – 678.

Balaam, N.P. (1978). "Load-Settlement Behavior of Granular Piles", *Thesis presented to the University of Sydney in partial fulfillment of the requirements for the degree of Doctor of Philosophy.*

Balaam, N.P. and Booker, J.R. (1981). "Analysis of Rigid Rafts Supported by Granular Piles", *Proceedings of Int. Journal for Numerical an Analytical Methods in Geomechanics*, Vol.5:379-403.

Barksdale, R.D. and Bachus, R.C. (1983). "Design and Construction of Stone Columns", Report No. FHWA/RD-83/026, National Technical Information Service, Virginia, USA.

Baumann, V. and Bauer, G.E.A (1974). "The Performance of Foundations on Various Soils Stabilized by the Vibro-Compaction Method", *Canadian Geotechnical Journal*, (11): 509-530.

Bowles, E.J. (1997). "Foundation Analysis and Design", *Mc Graw-Hill Publishing Company*.

Brauns, J. (1978). "Initial Bearing Capacity of Stone Columns and Sand Piles", *Symposium on Soil Reinforcing and Stabilizing Techniques,* Syndney, 477 – 496.

Chandler, R.J. and Martins, J.P. (1982). "An Experimental Study of Skin Friction around Piles in Clay", *Geotechnique* 32(2): 119-132.

Craig, W.H. and Al-Khafaji, Z.A. (1997). "Reduction of Soft Clay Settlement by Compacted Sand Columns", *Proceeding of the Third International Conference on Ground Improvement Geosystems, London*: 219 – 224.

Datye, K.R. (1982). "Settlement and Bearing Capacity of Foundation System with Stone Columns", *Symposium on Recent Developments in Ground Improvement Techniques,* Bangkok: 85 – 103.

Elkasabgy, M.A. (2005). "Performance of Stone Columns Reinforced Grounds", *M.Sc. Thesis, Zagazig University, Faculty of Engineering at Shobra, Cairo.*

Elshazly, H.A., Hafez, D.H. and Mossaad, M.E. (2006). "Back Calculating Vibro-Installation Stresses in Stone Columns Reinforced Grounds", *Ground Improvement*, Vol.10, No.2, pp.47-53

Elshazly, H., Elkasabgy, M. and Elleboudy, A. (2008). "Effect of Inter-column Spacing on Soil Stresses due to Vibro-installed Stone Columns: interesting findings", *Geotechnical and Geological Engineering*, Vol.26, pp.225-236

Georgiannou, V. N., Burland, J. B. and Hight, D.W. (1990). "The Undrained Behaviour of Clayey Sands in Triaxial Compression and Extension", *Géotechnique* 40(3): 431-449.

Gniel, J. and Bouazza, A. (2009). "Improvement of Soft Soils Using Geogrid Encased Stone Columns", *Geotextiles and Geomembranes* (27): 167 – 175.

Gniel, J. and Bouazza, A. (2010). "Construction of Geogrid Encased Stone Columns: A New Proposal Based on Laboratory Testing", *Geotextiles and Geomembranes* (28): 108 – 118.

Goughnour, R.R. (1983). "Settlement of Vertically Loaded Stone Columns in Soft Ground", *Proceedings of 8th ECSMFE*, Helsinki, Vol.1, pp.23-25.

Goughnour, R. R. and Bayuk, A. A. (1979). "A Field Study of Long Term Settlements of Loads Supported by Stone Columns in Soft Ground", *Proceedings of Int. Conf. on In-situ Soil and Rock Reinforcement,* Paris.

Greenwood, D.A., (1970). "Mechanical Improvement of Soils below Ground Surface", *Proceedings of the Conf. on Ground Engineering*, London, ICE.

Greenwood, D.A., (1991). "Load Tests on Stone Columns", *Deep Foundation Improvements: design, construction and testing*, ASTM STP 1089, Philadelphia, pp.148-171

Han, J. and Ye, S-L. (2001). "Simplified Method for Consolidation Rate of Stone Column Reinforced Foundation", *Journal of Geotechnical and Geoenvironmental Engineering* 127(7): 597 – 603.

Hattab, M. and Fleureau, J-M. (2010). "Experimental Study of Kaolin Particle Orientation Mechanism", *Geotechnique* 60(5): 323-331.

Hong et. al. (2010). "Compression Behavior of Reconstituted Soils at High Initial Water Contents", *Geotechnique* 60(9): 691-700.

Hughes, J.M. and Withers, N.J. (1974). "Reinforcing of Soft Cohesive Soils with Stone Columns", *Ground Engineering,* 7: 42 – 49.

Ishikura, R., Ochiai, H. and Matsui, H. (2009). "Estimation of Settlement of In-Situ Improved Ground Using Shallow Stabilization and Floating-Type Columns", *Proceedings of the 17th International Conference on Soil Mechanics and Geotechnical Engineering,* 2394 – 2398.

Karim, H.K., Mahmood, M.M. and Renka, R.G. (2009). "Soft Clay Soil Improvement Using Stone Columns and Dynamic Compaction Techniques", *Engineering and Technology Journal,* 27(14): 2546 – 2565.

Kirsch, K. (2004). "Experimentelle und Numerische Untersuchungen zum Tragverhalten von Rüttelstopfsaulengruppen.", Dissertation, *Technische Universitat Carolo-Wilhelmina zu Braunschweig*.

Kirsch, F. and Borchert, K.-M. (2006). "Probebelastungen zum Nachweis der Baugrundverbesserungswirkung", *Beitrag zum 21. Christian Veder Kolloquium*, Graz April 2006.

Kirsch, K. and Kirsch, F. (2010). "Ground Improvement by Deep Vibratory Methods", *Taylor and Francis Group, Spon Press,* New York, USA.

Madhav, M.R. (1982). "Recent Developments in the Use and Analysis of Granular Piles", *Symposium on Recent Developments in Ground Improvement Techniques,* Bangkok: 117 – 129.

Madhav, M.R. and Miura, N. (1994). "One Dimensional Consolidation of Lightly Over Consolidated Clays", *Ind. Geotech. J.*, Vol. 24 (1), pp.34-49.

Madhav, M.R. and Rao, K. U. (1996). "Analysis of Granular Pile – Effect of Nonhomogeneity: Depth Dependent Modulus", *Symp. On Adv. In Geotech. Engrg.,* Kanpur, pp. 59 – 66.

Malarvizhi, S.N. and Ilamparuthi, K. (2004). "Load versus Settlement of Clay Bed Stabilized with Stone and Reinforced Stone Column", *3rd Asian Reg. Conf. on Geosynt.*: 322-329.

McKelvey, D., Sivakumar, V., Bell, A. and Graham, J. (2004). "Modeling Vibrated Stone Columns in Soft Clay", *Proceedings of the Instution of Civil Engineers – Geotechnical Engineering,* 157(GE3): 137 – 149.

Mitchell, J.K. and Huber, T.R. (1982). "Stone Column Foundations for a Wastewater Treatment Plant – A Case History", *Symposium on Recent Developments in Ground Improvement Techniques,* Bangkok: 573 – 587.

Mitchell, J.K. and Huber, T.R. (1985). "Performance of a Stone Column Foundation", *Journal of Geotechnical and Geoenvironmental Engineering* 111(2): 205 – 223.

Mitra, S. and Chattopadhyay, B.C. (1999). "Stone Columns and Design Limitations", *Proc. Indian Geotech. Conf.,* Calcutta, India, 201 – 205.

Mochtar, I.B. and Edil, T.B. (1988). "Shaft Resistance of Model Pile in Clay", *Journal of Geotechnical Engineering*: 114(11).

Murugesan, S. and Rajagopal, K. (2006). "Geosynthetic-Encased Stone Columns: Numerical Evaluation", *Geotextiles and Geomembranes,* 24 (2006): 349 – 358.

Murugesan, S. and Rajagopal, K. (2007). "Model Tests on Geosynthetic-Encased Stone Columns", *Geosynthetics International,* 14 (6): 346 – 354.

Murugesan, S. and Rajagopal, K. (2008). "Shear Load Tests on Stone Columns with and without Geosynthetic Encasement", *Geotechnical Testing Journal,* 32(1): 1 – 10.

Murugesan, S. and Rajagopal, K. (2010). "Studies on the Behavior of Single and Group of Geosynthetic Encased Stone Columns", *Journal of Geotechnical and Geoenvironmental Engineering*, 136(1): 139 – 139.

Navaneethan, T. (2003). "Pre-Yield Characteristics and Earth Pressure Coefficient of Overconsolidated Clays", *PhD thesis*.

Nayak, N.V. (1982). "Recent Innovations in Ground Improvement by Stone Columns", *Symposium on Recent Developments in Ground Improvement Techniques,* Bangkok: 17 – 29.

Özkeskin, A. (2004). "Settlement Reduction and Stress Concentration Factors in Rammed Aggregate Piers Determined from Full Scale Load Tests", *Thesis presented to the Middle East Technical University in partial fulfillment of the requirements for the degree of Doctor of Philosophy,* Middle East Technical University, Ankara/TURKEY, 211 pages.

Pham, H.T.V. and White, D.J. (2007). "Support Mechanisms of Rammed Aggregate Piers. II: Numerical Analyses", *Journal of Geotechnical and Geoenvironmental Engineering,* Vol. 133 (12): 1512 – 1521.

Pitt, J.M., White, D.J., Gaul, A. and Hoevelkamp, K. (2003). "Highway Applications for Rammed Aggregate Piers in Iowa soils", *Iowa DOT Project TR-443, CTRE Project 00-60*, USA.

Poulos, H.G. and Davis, E.H. (1970). "Elastic Solutions for Soil and Rock Mechanics", *Wiley,* 332 pages.

Priebe, H. (1976). "Estimating Settlements in a Gravel Column Consolidated Soil", *Die Bautechnik* (53): 160-162.

Priebe, H. (1995). "The Design of Vibro Replacement", *Journal of Ground Engineering,* 28(10).

Randolph, M.F. and Wroth, P. (1978). "Analysis of Deformation of Vertically Loaded Piles", *Journal of Geotechnical Engineering,* ASCE, Vol. 104 (GT12), pp.: 1465 – 1488.

Shahu, J.T., Madhav, M.R. and Hayashi, S. (2000). "Technical Note: Analysis of Soft Ground-Granular Pile-Granular May System", *Computers and Geotechnics* 27: 45 – 62.

Shahu, J.T. and Reddy, Y.R. (2011). "Clayey Soil Reinforced with Stone Column Group: Model Tests and Analyses", *Journal of Geotechnical and Geoenvironmental Engineering* 137(12): 1265 – 1274.

Sivakumar, V., Navaneethan, T., Hughes, D. and Gallagher, G. (2009). "An Assessment of the Earth Pressure Coefficient in Overconsolidated Clays", *Geotechnique* 59(10): 825-838.

Som, M.N. and Das, S.C. (2003). "Theory and Practice of Foundation Design", *PHI Learning Pvt. Ltd.,* 392 pages.

Sorensen, K.K., Baudet, B.A. and Simpson, B. (2010). "Influence of Strain Rate and Acceleration on the Behaviour of Reconstituted Clays at Small Strains", *Geotechnique* 60(10): 751-763.

Sünnetçioğlu, M.E. (2012). "A Laboratory Model Study on Settlement of Stone Columns in Soft Clay", *Thesis presented to the Middle East Technical University*

in partial fulfillment of the requirements for the degree of Master of Science, Middle East Technical University, Ankara/TURKEY, 177 pages.

Şengör, M.Y. (2002). "Model Pile Tests for Determining the Axial Capacity of Piles in Clay and Sand-Clay Mixtures", *Thesis presented to the Middle East Technical University in partial fulfillment of the requirements for the degree of Master of Science,* Middle East Technical University, Ankara/TURKEY.

Tekin, M. (2005). "Model Study on Settlement Behavior of Granular Columns under Compression Loading", *Thesis presented to the Middle East Technical University in partial fulfillment of the requirements for the degree of Doctor of Philosophy,* Middle East Technical University, Ankara/TURKEY, 223 pages.

TS 5744 (1988). "In Situ Measurement Methods of the Properties of Foundation Soils in Civil Engineering" *Türk Standartları Enstitüsü*, Ankara/TURKEY, 34 pages.

Van Impe, W.F., Madhav, M.R. and Vandercruyssen, J.P. (1997). "Considerations in Stone Column Design", *Proceeding of the Third International Conference on Ground Improvement Geosystems, London*: 190 – 196.

Vautrain, J. (1977). "Mur en Terre Armee Sur Colonnes Ballastees", *Proceedings of Int. Symposium on Soft Clay*, Bangkok

Vesic, A.S. (1972). "Expansion of Cavities in Infinite Soil Mass", *Jour. of the Soil Mechanics and Foundations div.,* ASCE (98): 265 – 290.

Watts, K.S., Johnson, D., Wood, L.A. and Saadi, A. (2000). "An In-situ-mental Trial of Vibro Ground Treatment Supporting Strip Foundations in a Variable Fill", *Geotechnique,* Vol.50, No.6, pp.699–708.

Weber, T.M., Plötze, M., Laue, J., Perchke, G. and Springman, S.M. (2010). "Smear Zone Identification and Soil Properties around Stone Columns Constructed In-Flight in Centrifuge Model Tests", *Géotechnique* 60(3): 197 – 206.

Wood, D.M., Hu, W. and Nash, D.F.T. (2000). "Group Effects in Stone Column Foundations: Model Tests", *Geotechnique* 50(6): 689 -698.

Wu, C.S. and Shen, C.Y. (1997). "Improvement of Soft Soil by Geosynthetic-Encapsulated Granular Column", *Proceeding of the Third International Conference on Ground Improvement Geosystems, London*: 211 – 218.

Zahmatkesh, A. and Choobbasti, A.J. (2010). "Settlement Evaluation of Soft Clay Reinforced by Stone Columns Considering the Effect of Soil Compaction", *IJRRAS* 3(2): 159 – 166.

APPENDIX A

PREVIOUS MODEL TESTS ON STONE COLUMNS

A.1. Physical and Material Strength Properties

In practice, area replacement ratio is in between 10-35% where length of stone columns is commonly in between L=3-15 m. McKelvey et al. (2004) stated that column diameter, column length, column spacing, area replacement ratio, size and flexibility of the footing, strength of the in-situ soil, strength of the column material and method of column installation are the parameters affecting the stress-strain relation of the stone column treated soils.

A.1.1. Boundary Conditions

Ambily and Gandhi (2006) stated that the lateral dimension of the area of test soil should be such that the minimum free distance between the periphery of the column and the side of the test area should not coincide with the failure wedges. Bowles (1997) emphasized that the failure zone extends over a radial distance of about 1.5 times the diameter of stone column and over a depth approximately equal to 2 times the diameter of column from the periphery of the pile.

Gniel and Bouazza (2010) observed during consolidation under vertical stress of 50 kPa, vertical strain was about 35% in clay. Thus, the initial thickness of clay bed so the height of tank should be calculated based on the consolidation characteristics of clay.

Shahu and Reddy (2011) mentioned that dimensions of tank should be selected by considering the stress distribution. A stress distribution with a slope of 2V:1H can be assumed from the $2/3L$ depth from the loading surface. Moreover at a depth of twice of the width of foundation from depth equal to $2/3L$, increase in stress is approximately 11% of the applied stress.

A.1.2. Stone Column

According to Mitra and Chattopadhyay (1999) minimum ratio for length of column to diameter of column, L/D, should be 4.5 to develop the full limiting axial stress on column (Ambily and Gandhi, 2006).

Gniel and Bouazza (2009) mentioned that $L/D = 6$ is within the range generally accepted for stone columns. Shahu and Reddy (2011) stated that a typical stone column has a diameter between $0.6 – 1.0$ m, length between $5 – 20$ m, thus in model tests L/D ratio should be in between 5 and 20 to represent the real scale. In their model tests, they used $D = 13 – 25$ mm, $L = 100 – 150$ mm, so $L/D = 8 – 12$ which are appropriate when compared with original scales. Hughes and Withers (1974) used model columns having 150 mm long and range in diameter of $12.5 – 38$ mm.

Practically spacing between stone columns is in the range of $1.2 – 3.0$ m for a triangular pattern (Craig and Al-Khafaji, 1997). Van Impe et al. (1997) stated that practically spacing between stone columns is in the range of 2-3 times of diameter of column.

In real case, diameter of stone columns is in the range of $0.6 – 2.0$ m where diameters less than 1.0 m have usually been used in projects constructed on land and larger diameters have usually been used in off-shore areas (McKelvey et al., 2004). Wood et al. (2000) mentioned that average particle size of stone column material (D_s) in range between 25 and 50 mm. According to Wood et al. (2000)

ratio of D/D_s should be in range of $12 - 40$. Similarly, Shahu and Reddy (2011) used sand for stone columns instead of aggregate having $D_s = 0.425 - 1$ mm for $D = 13 - 25$ mm, thus $D/D_s = 13 - 59$. Stones used for stone columns have particle range in between $D_s = 2 - 10$ mm for $D = 100$ mm diameter stone column (Ambily and Gandhi, 2004 and 2006). Murugesan and Rajagopal (2007) used stone particles which are angular granite chips having diameter $2 - 10$ mm which corresponds to $D/D_s = 10 - 50$ in their tests.

The particle size distribution of clay and stones are given in the Figure A.1 by Murugesan and Rajagopal (2007). Nayak (1982) noted that for good compaction granular fill should be well-graded. Weber et al. (2010) used quartz sand with particle size in between $0.5 - 1.0$ mm with average particle size (D_{50}) about 0.75 mm for 12 mm diameter of model stone columns. Karim et al. (2009) prepared 30 mm diameter of stone columns from crushed stone having particle sizes in between $2.0 - 8.0$ mm. This range was chosen based on the recommendations of Al-Shaikhly (2000) who mentioned the optimum particle size of material of stone columns should be in the range of $0.11 - 0.17$ of diameter of stone column (Karim et. al., 2009). Nayak (1982) suggested that particle size of stone column material should be in the range of 1/6 to 1/7 diameter of the column. Hughes and Withers (1974) proposed 2-3 cm diameter of gravel for stone columns having 0.5 m diameter. Priebe (1995) proposed the range of application of stone columns as shown in Figure A.2 Barksdale and Bachus (1983) proposed different alternatives for suitable grade distribution of material used in stone columns (Table A.1).
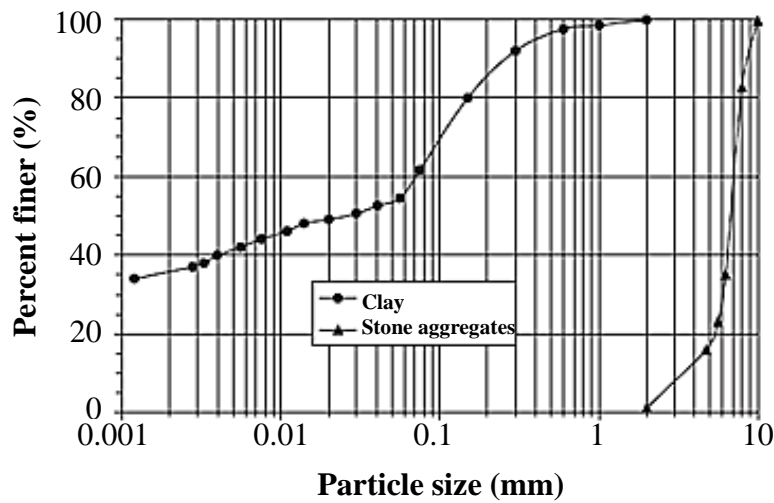
Figure A.1. Particle size distribution of stone aggregate and clay soil

(Murugesan and Rajagopal, 2007)
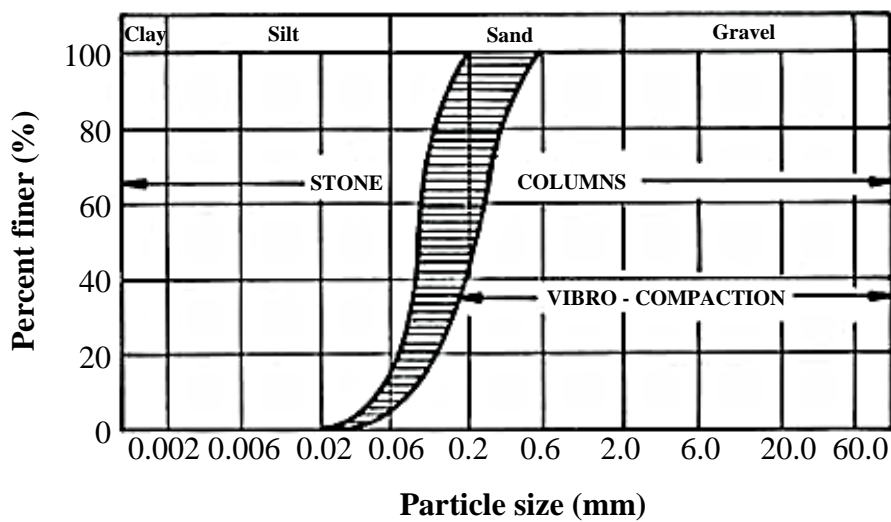
Figure A.2. Application ranges of vibro-compaction and vibro-replacement

(Priebe, 1995)

Zahmetkesh and Choobbasti (2010) stated that friction angle of stone aggregates should be larger than 40 degrees. Murugesan and Rajagopal (2007) used material with the peak angle of internal friction obtained from direct shear test of 41.5

degrees. Wood et al. (2000) stated that the ultimate critical state angle of sand is about 30 degrees.

Nayak (1982) stated that degree of compaction of aggregates in stone columns depends on several factors such as: consistency of soft soil; size, gradation, shape and quality of granular fill; depth of filling; size of borehole; weight of hammer. Shahu and Reddy (2011) stated that 50% of relative density was used for stone columns. They tried 80% of relative density in some tests, but they stated that it is difficult to ensure uniform stone column diameter after compaction at this level of relative density.

Wu and Shen (1997) stated that relative density of stone column significantly affects the stiffness of it. Moreover, they mentioned that smaller diameter of stone columns leads to steeper axial stress-axial strain curves.

Shahu and Reddy (2011) used poorly graded sand (SP) to perform stone columns with loosest unit weight of 12.93 kN/m^3 and densest unit weight of 15.75 kN/m^3.

Al-Khafaji and Craig (2000) mentioned that stone columns are generally preferred due to high angularity and stiffness of them. But for economic reasons and problems in procuring high amount of stones, sand is used in many cases.

Baumann and Bauer (1974) proposed possible values of modular ratio (E_s/E_c) as 1/8 for sandy silt, 1/16 for clayey silt and 1/25 for silty soft clay.

Table A.1. A range of gradations used in vibro-replacement applications (Barksdale and Bachus, 1983)

Sieve size (in)	Alternate 2 Percent Passing	Alternate 3 Percent Passing	Alternate 4 Percent Passing	Alternate 5 Percent Passing
4	-	-	100	-
3.5	-	-	90 – 100	-
3.0	90 – 100	-	-	-
2.5	-	-	25 – 100	100
2.0	40 – 90	100	-	65 – 100
1.5	-	-	0 – 60	-
1.0	-	2	-	20 – 100
0.75	0 – 10	-	0 – 10	10 – 55
0.50	0 – 5	-	0 – 5	0 – 5

A.1.3. Soft Soil

Kirsch and Kirsch (2010) and Zahmetkesh and Choobbasti (2010) stated that clays having undrained shear strength in between 10-30 kPa and 30-50 kPa can be improved by stone columns using vibro-replacement dry technique and vibro-replacement wet technique, respectively.

Shahu and Reddy (2011) stated that initial vertical effective stress can be evaluated as initial overburden stress which is the summation of weight of loading plate and weight of soil over that depth.

Bowles (1997) stated that soil improved by stone columns has lateral earth pressure coefficient at rest, K_0, varies from 2 to 6. Mitchell and Huber (1985) stated that K_0 through the length of stone columns can be assumed as 1.0 in order to consider the increase in lateral stress due to vibro-compaction installation.

A.1.3.1. Kaolinite Clay

In model tests performed in laboratory to ease reliable observations of the behavior of stone columns researchers need to use soils with homogeneous and isotropic characteristics. Many researchers used kaolinite clay as a soft soil. The properties of kaolinite clay obtained by previous researchers are summarized as in the followings:

- Georgiannou et. al. (1990) stated that a specimen of normally consolidated kaolin would not show any dilation.
- Chandler and Martins (1982) stated that this type of clay has a relatively high coefficient of consolidation so that at most a month, specimen can be consolidated in large triaxial cell.
- Atkinson, J. (2007) stated that linear Mohr-Coulomb failure criterion is not realistic if the level of applied effective stress in tests is different than the one in-situ. Mostly in soils having overconsolidation ratio greater than 4, the peak strength envelope strictly becomes non-linear. Thus, non-linear failure criteria should be used such as power equation $q = A'p'^b$ where q is shear strength of soil, A' is similar to a friction coefficient and b is coefficient related with the degree of curvature of failure envelope. For example, for kaolinite clay with maximum stress of 300 kPa, A' and b values are observed as 1.8 and 0.69 respectively. Critical state parameters of kaolinite clay are reported as $c = 0$ and $\phi_{cs} = 25.5°$.
- Şengör (2002) stated that kaolinite is chemically less interactive with porewater than the other minerals. This makes kaolinite mineral to have relatively stable structure which does not possess shrinkage and swelling characteristics.
- Sorensen et. al. (2010) stated that kaolinite is a good preference since it does not show developing time-dependent bonding and cementation when it meets with water.

- Hong et. al. (2010) stated that compression index, C_c, increases by the increase of water content and liquid limit.

Parameters of kaolinite clay from different references are summarized in Table A.2. In this table, LL is liquid limit, PL is plastic limit, PI is plasticity index, G_s is specific gravity, ϕ'_p is peak drained friction angle, ϕ'_r is residual drained friction angle, c_v is coefficient of vertical consolidation, c_h is coefficient of horizontal consolidation, k_s is hydraulic conductivity, C_c is compression index and C_r is recompression index.

Table A.2. Parameters of kaolinite clay obtained by different researchers

	Sivakumar et. al. (2009)	Chandler and Martins (1982)	Atkinson (2007)	Hattab and Fleureau (2010)	Mochtar and Edil (1988)	Şengör (2002)			Sorensen et. al. (2010)	Griel and Bouazza (2009)	Wood et al (2000)
Clay content (%)	80	-	-	95	96	100	50	30	-	-	60
Silt content (%)	20	-	-	5	4	0	0	0	-	-	-
Sand content (%)	0	-	-	0	0	0	50	70	-	-	-
LL (%)	70	69	-	40	58	45	25	18	65	62	63
PL (%)	34	38	-	20	33	29	17	14	35	29	36
PI (%)	36	31	-	20	25	16	8	4	30	33	27
G_s	2.65	2.61	-	2.65	2.62	-	-	-	2.68	2.64	-
ϕ'_p	-	23	-	-	-	-	-	-	-	-	23
ϕ'_r	-	11.5	-	-	-	-	-	-	-	-	-
ϕ_{cs}	23	-	25.5	-	15.5	-	-	-	-	-	-
c_v (m^2/year)	5.0	15.8	-	-	-	-	-	-	-	-	-
c_h (m^2/sec)	-	-	-	-	-	-	-	-	-	-	-
k_s (m/sec)	-	-	-	-	-	-	-	-	$10^{-10} - 10^{-9}$	-	-
C_c	-	-	-	-	-	-	-	-	-	0.80	-
C_r	-	-	-	-	-	-	-	-	-	0.09	-

A.2. Loading

Ambily and Gandhi (2006) stated that stone columns generally subjected to stresses about 100-150 kPa where maximum stress at stone column is generally about to be 750 - 800 kPa. Thus, capacity of pressure cells and loading apparatus should be selected on the basis of the statement.

Shahu and Reddy (2011) proposed that tests must be conducted in fully drained condition with load-controlled loading instead of deformation-controlled loading. This was ensured also by McKelvey et al. (2004) asserting that displacement controlled loading is different from the actual foundation loading in field where the load is applied in stages during the construction. Stress-strain response of soil is different in between stress and strain controlled tests and difference is more pronounced at low strains. McKelvey et al. (2004) stated that Navaneethan (2003) showed that for low permeable soils during consolidated drained tests are taken out, even for a very low strain rate significant amount of excess pore pressures are left in the soil body in the case of strain-controlled loading.

A.3. Procedures of Tests

Previous model tests on stone columns were prepared and performed in similar manner: preparation of slurry, preparation of bedding soil, preparation of stone columns, loading and instrumentation. In the following sections each step of test procedure is briefly explained based on the model tests done previously.

A.3.1. Preparation of Slurry

- Soil was crushed with a hammer to small size (Karim et al., 2009)
- Clay sample is air-dried for 24 hours (Ambily and Gandhi, 2006; Karim et al., 2009)

- Pulverize it by crushing machine (Ambily and Gandhi, 2006; Karim et al., 2009)

- Then soil is divided into groups each with 25 kg weight. (Karim et al., 2009)

- Sieve it

- Mix with water by kneading to have water content equal to $1.5LL$ (Bae et al., 2002; Malarvizhi and Ilamparuthi, 2004; McKelvey et al., 2004; Ambily and Gandhi, 2004 and 2006, Murugesan and Rajagopal, 2008 and 2010) or $2LL$ (Gniel and Bouazza, 2009) or $LI = 0.1$ where LI is liquidity index of soil (Ambily and Gandhi, 2004)

- After mixing with water keep it with 48 hours in order to achieve uniform consistency (Malarvizhi and Ilamparuthi, 2004; Ambily and Gandhi, 2004 and 2006)

- After 48 hours check the water content if there are any losses of water add water (Malarvizhi and Ilamparuthi, 2004; Ambily and Gandhi, 2004 and 2006)

A.3.2. Preparation of Bedding Soil

Note that; researchers written in *italic* used Kaolin clay in their tests.

- Tank with various dimensions have been used to model soil body stone columns within it. Model tests were carried out in tanks having 300 mm diameter composed of clay bed with depth of 300 mm (*Wood et al., 2000*). Murugesan and Rajagopal (2008) used a tank with 750 mm depth. On the other hand, rigid steel container with 4 mm thickness, 600 mm diameter and 500 mm height is used for tests (Karim et al., 2009). Murugesan and Rajagopal (2010) prepared clay bed in a large tank having plan dimensions of 1.2 m x 1.2 m with height of 0.85 m.

- Apply a thin coat of grease or wrap a polyethene sheet on inner side of the tank to minimize the friction (Ambily and Gandhi, 2004 and 2006; Murugesan and Rajagopal, 2008; *Shahu and Reddy, 2011*). Moreover, Murugesan and Rajagopal (2008) covered one of the longer sides of the tank with a material made of 12 mm thick Perspex sheet to ease visualization of the deformation paths.

- To allow 2-way drainage during consolidation, 75 mm thick sand layers sandwiched between geotextiles are placed at the bottom of the tank and at the top of the clay bed (Murugesan and Rajagopal, 2008 and 2010).

- Care was taken to avoid the entrapped air by tapping the clay layers gently with a wooden plank (Malarvizhi and Ilamparuthi, 2004).

- Prepare the soft clay bed in layers approximately 5 cm thick for totally 45 cm thick clay layer. Sign the all 5 cm increments and weigh the clay that you are putting in to the tank in order to satisfy a unique/constant density of clay soil uniformly (Ambily and Gandhi, 2004 and 2006; Karim et al., 2009).

- Provide a uniform compaction also with tamper until getting uniform density at each layer (Ambily and Gandhi, 2004 and 2006). Malarvizhi and Ilamparuthi (2004) noted that care was taken to avoid the entrapped air by tapping the clay layers gently with a wooden plank.

- Slurry is filled into tank and initially allowed to consolidate under load equal to designated undrained shear strength (Bae et al., 2002) or 10 kPa up to settlement rate of 1 mm/day (Ambily and Gandhi, 2006; Murugesan and Rajagopal, 2008) or 53 kPa (Gniel and Bouazza, 2009) or 30, 60 and 90 kPa 's for different tests *(Shahu and Reddy, 2011)* or 120 kPa *(Wood et al., 2000)* or 140 kPa (McKelvey et al., 2004) or up to 200 kPa (Craig and Al-Khafaji, 1997). Also Hughes and Withers (1974) stated that after the preparation of clay bed formed by Kaolin clay; it was one-dimensionally consolidated, then kept under a constant stress.

- Settlement is measured by means of mechanical dial gauges having accuracy of 0.01 mm (Murugesan and Rajagopal, 2010). Consolidation takes about 8 – 10 days (McKelvey et al., 2004; Murugesan and Rajagopal, 2010) or 20-25 days *(Shahu and Reddy, 2011).*

- After the completion of the consolidation, clay bed is unloaded and allowed to swell under 30 kPa *(Wood et al., 2000).*

- After consolidation undisturbed samples are taken for water content (Craig and Al-Khafaji, 1997; Karim et al., 2009; Murugesan and Rajagopal, 2008 and 2010), vane shear strength (Craig and Al-Khafaji, 1997; *Wood et al., 2000*; Ayadat and Hanna, 2005; Ambily and Gandhi, 2006, Gniel and Bouazza, 2009; Murugesan and Rajagopal, 2008 and 2010; Karim et al., 2009; *Shahu and Reddy, 2011*), degree of saturation (Murugesan and Rajagopal, 2010) and in-situ void ratio (Murugesan and Rajagopal, 2010) determination. Water contents from different locations vary with ± 1% is accepted (Murugesan and Rajagopal, 2008 and 2010).

- After consolidation clay bed is trimmed to height of clay bed to be tested (ex.: 600 mm in the study of Murugesan and Rajagopal, 2010).

A.3.3. Preparation of Stone Columns

Model columns are constructed after the completion of consolidation. The construction of stone columns can be either replacement method (replacing the volume of soft soil with stone column) or displacement method with lateral compaction of soft soil with a compacted column of aggregates. Former method is selected in most of the model tests on stone columns.

Wood et al. (2000) mentioned that displacement technique causes large disturbance and heave highly depending on the installation technique, leading to inconsistencies in repeatable tests the technique is eliminated.

Previous researchers prepare stone columns either of following techniques: Alternative 1 (Hughes and Withers, 1974; Craig and Al-Khafaji, 1997; Wood et al., 2000; McKelvey et al., 2004; Ambily and Gandhi, 2004 and 2006, Murugesan and Rajagopal, 2008 and 2010, Karim et al., 2009; Shahu and Reddy, 2011) or Alternative 2 (Malarvizhi and Ilamparuthi, 2004).

Alternative 1

Stone columns are constructed by a replacement method.

- Shahu and Reddy (2011) proposed that after the completion of consolidation, remove load (unloading) and then prepare stone column by introducing a thin-walled aluminum casing at the middle of the clay bed which has already signed by a centralizer

- A greased, thin (to minimize the disturbance of clay) open-ended steel pipes having internal diameter same with the stone columns are pushed in to clay bed. Shahu and Reddy (2011) marked locations of columns and pushed casing pipes manually into the soil up to required depth.

- The clay in the pipe is scooped out by helical auger of diameter just smaller than the internal diameter of pipe Hughes and Withers, 1974; Craig and Al-Khafaji, 1997; Wood et al., 2000; Ambily and Gandhi, 2004 and 2006, Murugesan and Rajagopal, 2008 and 2010, Karim et al., 2009).

Similarly Shahu and Reddy (2011) stated that the soil in the casing is extracted by auger having 10 mm diameter. Maximum 5 cm of soil is removed at a time to prevent the possible suction effects.

McKelvey et al. (2004) used a special drilling rig that consists of 25 mm diameter helical auger is used to drill the holes of stone columns. Auger was rotated at constant rate of 19 rev/min by using an electric motor. Auger is penetrated at 25 mm increments.

- The quantity of stone aggregate required to form stone columns is calculated and premeasured. Before charging, stones were moistened to prevent any water absorption from clay.
- After removing all the clay in the pipe, stones are carefully charged into the hole with a measured weight in order to have desired unique and uniform unit weight. Stone charging is gradually that at most 5 cm is charged at a time. The pipe was then raised in stages ensuring a minimum of 5 mm (Ambily and Gandhi, 2004 and 2006) - 15 mm (Murugesan and Rajagopal, 2008 and 2010) penetration below the top level of the placed gravel.

Shahu and Reddy (2011) stated that holes are filled with sand and compacted to required relative density. Similarly Wood et al. (2000) used sand instead of stone aggregate to achieve uniform relative density.

McKelvey et al. (2004) also used mass of sand which was poured into those drilled holes. They pointed out that denser columns leads to stiffer stone columns and enhanced interaction between stone column and surrounding soft soil. The relative density of the stone columns is provided by vibration during replacement. On the contrary with this type of improvement, some researchers stated vibration has adversely effects like ground disturbances in the surrounding soil.

- To achieve a uniform density, compaction was given with a 2 kg circular steel tamper with 10 blows of 100 mm drop to each layer. This light compaction effort was adopted to ensure that there is no significant lateral bulging of the column creating disturbance to the surrounding soft clay (Ambily and Gandhi, 2004 and 2006). Similar procedure was also followed by Murugesan and Rajagopal (2008 and 2010): immediately after lifting the casing pipe, the stone aggregate was compacted with a tamping rod (10 mm diameter) with 25 blow numbers falling freely from

height of 250 mm. This method of compaction gives dry density of 1.6 g/cm^3.

Alternative 2:

- Place a PVC pipe at the middle of the tank before placing the clay bed.
- Around this pipe clay bed is formed lever by level.
- Stones are carefully charged in tube 10 cm levels. While charging stones through the PVC, stones are compacted and PVC pipe is withdrawn simultaneously. Each layer is compacted using 12 mm diameter rod (for 30 mm diameter of stone columns) to achieve density of 15 kN/m^3.
- Before starting the loading, just after the preparation of bed entire area is loaded by a seating pressure of 5 kPa for 24 hours in order to obtain uniform bed and to ensure the contact between clay and stone columns.

A.3.4. Loading and Instrumentation

- Shahu and Reddy (2011) stated that loading plate on the group of stone columns has some holes to permit drainage also from top (2-way drainage). Footing load was applied in 10 – 14 equal fully drained and load controlled loading increments of 15 kPa each with letting appropriate time to complete consolidation where rate of settlement < 1mm/day (Shahu and Reddy (2011). This loading stage is completed about 20 – 25 days. Settlement was measured by 2 dual type dial gauge having sensitivity of 0.01 mm which is located in diametrically opposite directions. Miniature pressure cells having capacity of 200 kPa and 500 kPa, diameter of 34 mm and thickness of 5 mm were placed at the top of the model foundation to measure the pressures. The dial gauges and the pressure cells are connected to a nine-channel portable data acquisition system in order to record the measured data.

- At each step of loading in study of Gniel and Bouazza (2009), loading is kept constant unless settlement rate is smaller than 1 mm/day at which the dissipation of pore water is almost completed.

- Mitchell and Huber (1985) stated that: in field load tests loading is applied up to a minimum settlement rate of 0.25 mm/hr.

- Wood et al. (2000) determined rate of settlement controlled loading as 0.061 mm/min which is sufficiently small to perform drained loading. Most of the tests are ended at a settlement equal to 10 % of the diameter of tank. Miniature stress cells having 100 mm diameter is placed carefully to the loading plate on the top of the tank. Measurements obtained from stress cells the stress distribution between clay and stone columns are evaluated.

- McKelvey et al. (2004) applied strain-controlled loading by rate of 0.38 mm/hr. The vertical pressures at different locations beneath the footing are measured by miniature pressure gauges having 600 kPa of capacity.

- Murugesan and Rajagopal (2008) applied loading with a constant rate of 1.20 mm/minute. The settlement of the loading plate and the heave of clay at the front of the stone columns in large steel tank case are measured by means of mechanical dial gauges.

- Craig and Al-Khafaji (1997) installed pore water pressure transducers inside the treated area under the model tank center and at 2/3 of the tank radius and various depths. Moreover, LVDT's are placed on the edge of tank at various depths and over the loading plate at center and at 2/3 of the tank radius. Tank is loaded by 40 kPa, 80 kPa, 120 kPa, 160 kPa and one instance 185 kPa.

- Karim et al. (2009) used circular steel plate with diameter of 110 mm and thickness of 10 mm as loading plate. Settlements have been recorded by dial gauges at each load.

- Hughes and Withers (1974) applied stress-controlled loads to top of the column only and displacements in soil and column were measured by

radiography technique. Moreover, by the help of load cell installed on the edge of tank corresponding at a mid-depth of bulging measures the increase in radial stress. The entire test-setup was illustrated in the Figure A.3.

- Ambily and Gandhi (2006) applied loading with a constant strain rate of 1.2 mm/min. Pressures transmitted to stone columns and clay soils are measured by pressure cells (accuracy: 0.1 kPa).
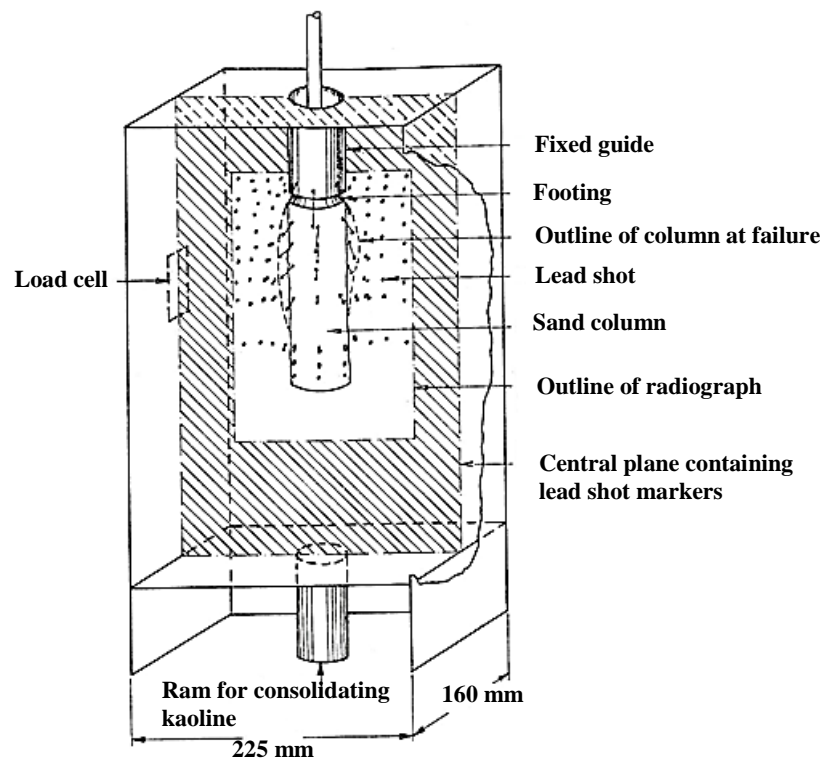
Figure A.3. Consolidometer for testing single stone column (Hughes and Withers, 1974)

APPENDIX B

CATALOGUE INFORMATION OF STRESS TRANSDUCERS

BEC-A/BED-A

● Pressure Measurement
● 200 kPa to 1 MPa

Small-Sized Soil Pressure Transducers
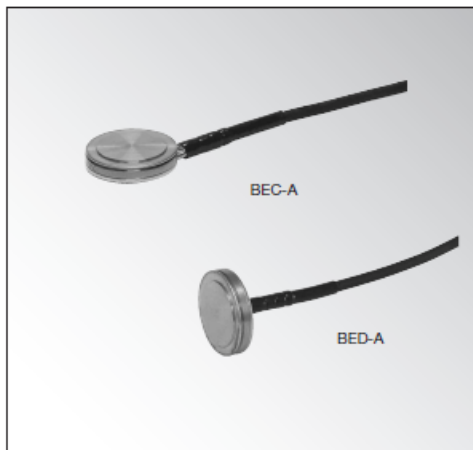
BEC-A

BED-A

A pressure-sensing surface 23mm in diameter.
Suitable for measurement fo soil pressure distribution in short-term or model experiment

● Suitable for short-term experiments

The BEC-A and BED-A series are small-sized soil pressure transducers having an outer diameter of 30 mm and a pressure-sensing surface diameter of 27 mm. They are used for measurement of soil pressure distribution in short-term or model experiments.

Specifications

Performance

Rated Capacity :	See table below
Nonlinearity :	Within±2% RO
Hysteresis :	Within±1% RO
Rated Output :	0.25 mV/V (500μm/m) or more

Environmental Characteristics

Safe Temperature Range :	-10 to 60°C
Temperature Effect on Zero Balance :	Within±0.4% RO/°C
Temperature Effect on Output :	Within±0.4%/°C

Electrical Characteristics

Recommended Excitation Voltage :	2 to 4V AC or DC
Input Resistance :	120Ω±1.7%
Output Resistance :	120Ω±1.7%
Cable : 4-conductor (0.08 mm²) chloroprene shielded cable, 4 mm diameter by 3 m long, bared at the tip (Shield is not connected to the chassis)	

Mechanical Properties

Safe Overload Rating :	120%
Weight :	Approx. 120 g

Model	Rated Capacity	Use
BEC-A-200KP	200kPa	Underground soil pressure measurement
BEC-A-500KP	500kPa	
BEC-A-1MP	1MPa	
BED-A-200KP	200kPa	Wall surface soil pressure measurement
BED-A-500KP	500kPa	
BED-A-1MP	1MPa	

APPENDIX C

CALIBRATION CHARTS OF TRANSDUCERS

$$y = (3*10^{-6})x^3 - (0.0031)x^2 + (2.2448)x$$
$$R^2 = 0.9996$$
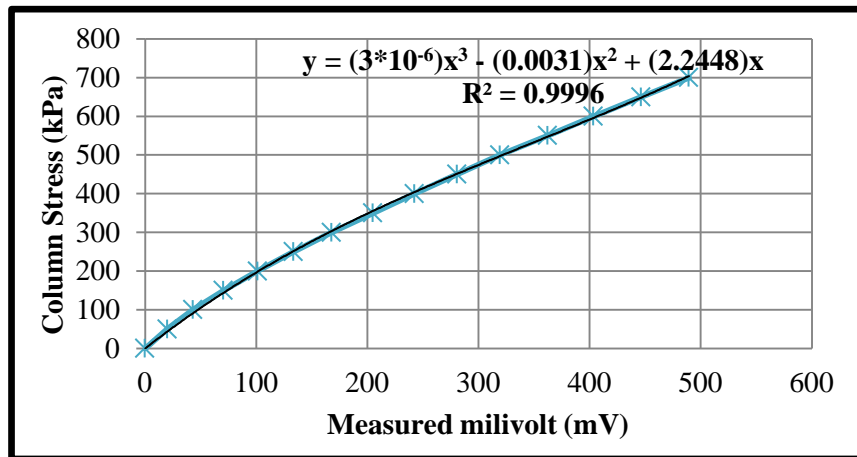
Figure C1. Calibration graph for pressure transducer#1

$$y = -10^{-4}x^2 + 1.0938x$$
$$R^2 = 1$$
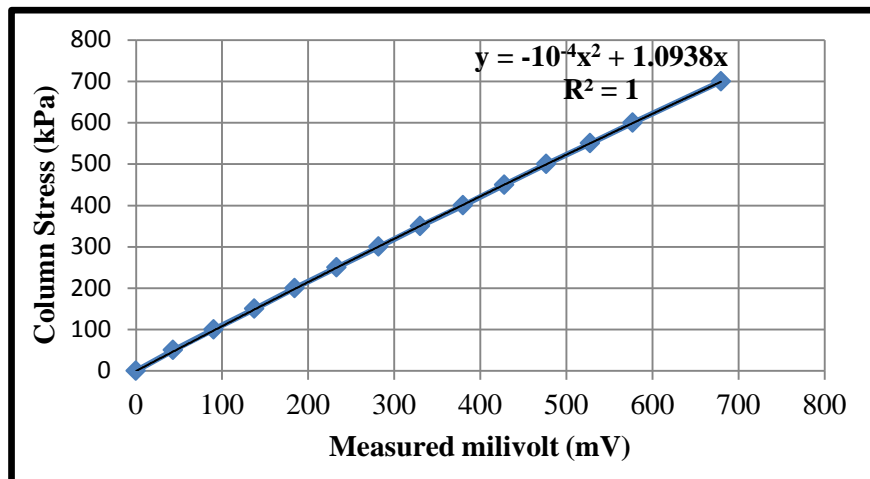
Figure C2. Calibration graph for pressure transducer#2

CURRICULUM VITAE

PERSONAL INFORMATION

E-mail	: zcekinmez@gmail.com
Nationality	: Republic of Turkey
Location of Birth	: İstanbul / Turkey
Date of Birth	: 15/07/1986
Marital Status	: Single

EDUCATION

2010 – 2014   **Doctor of Philosophy (PhD):**
Middle East Technical University, Ankara / Turkey
Faculty of Engineering, Department of Civil Engineering,
Division of Geotechnical Engineering (CGPA: 3.93/4.00)

2007 – 2010   **Master of Science (MSc):**
Middle East Technical University, Ankara / Turkey
Faculty of Engineering, Department of Civil Engineering,
Division of Geotechnical Engineering (CGPA: 3.86/4.00)

2003 – 2007   **Bachelor of Science (BS):**
Middle East Technical University, Ankara / Turkey
Faculty of Engineering, Department of Civil Engineering,
Division of Geotechnical Engineering (CGPA: 3.29/4.00 with
Rank: 9 over 278)

2000 – 2003   **High School:**
TED Ankara College Private High School, Ankara / Turkey

JOB EXPERIENCES

2007 - present   **Middle East Technical University, Ankara / Turkey**
Teaching and Research Assistant in Division of
Geotechnical Engineering

BOOK

- Erol, O. and Çekinmez, Z. (2014). Book entitled: "Geoteknik Mühendisliğinde Saha Deneyleri" *Yüksel Proje Yayınları*, Ankara, 278 pages.

PUBLICATIONS

- Çekinmez, Z. (2014). "Experimental Study on Stress Concentration Factors in Single and Groups of End Bearing and Floating Stone Columns", *Thesis presented to the Middle East Technical University in partial fulfillment of the requirements for the degree of Doctor of Philosophy,* Middle East Technical University, Ankara/TURKEY, 222 pages.
- Erol, O. and Çekinmez, Z. (2013). "Assessment of a Pile Load Test: A Case History" *7. Prof. İsmet Ordemir'i Anma Sempozyumu,* Middle East Technical University, Ankara, Turkey.
- Erol, O., Çevik, A. and Çekinmez, Z. (2012). "Settlement Reduction and Stress Concentration Factors in Rammed Aggregate Piers Determined from Full-Scale Group Load Tests" *ISSMGE – TC 211 International Syposium on Ground Improvement IS – GI Brussels*, Brussels, Belgium.
- Çekinmez, Z. (2010). "Effect of Foundation Rigidity on Contact Stress Distribution in Soils with Variable Strength/Deformation Properties" *Master of Sicence Thesis,* YÖK Thesis No: 294972*, Middle East Technical University, Ankara, Turkey.
- Erol, O., Çevik, A. and Çekinmez, Z. (2008). "Behaviour of Instrumented Test Pile" *Zemin Mekaniği ve Temel Mühendisliği 12. Ulusal Kongresi,* Selçuk University, Konya, Turkey.

PARTICIPATED DESIGNS & CONSULTANCY PROJECTS

2013 - 2014   **Masalli – Astara Motorway Project, Baku / Azerbaijan**
          Geotechnical assessment of fills and bridge approach embankments
- Short/long term static/earthquake slope stability, two and three dimensional settlement analyses of fills and bridge approach embankments between KM: 0+000 – 45+000
- Assessments on settlement – time relation
- Design of ground improvement techniques (settlement reducing piles, preloading with vertical drains)

2013   **Ankara Metro (AKM – GAR line) Project, Ankara / Turkey**
          Assessment of deformations on composite structure: two TBM tunnels intersected by NATM tunnel and quick getaway shaft

	• Three dimensional finite element analysis
2013	**Kayseri North Railway Project, Kayseri / Turkey**
	• Short/long term static/earthquake slope stability analyses of fills between KM: 17+580 – 19+400
2013	**Mahall Ankara Residence, Hotel and Office Complex Project, Ankara / Turkey**
	Geotechnical assessment on foundation systems
	• Three dimensional settlement analyses
2012	**Sludge Digestion and Drying Units of Çiğli Wastewater Treatment Facility, İzmir/Turkey**
	Geotechnical assessment on foundation systems of Drier Buildings and Digestive Tanks
	• Three dimensional settlement analyses for the influence of interaction between Digestive Tanks
	• Assessment of pile load tests, hydrotests
	• Bearing capacity, two dimensional settlement and liquefaction potential analyses
	• Design of ground improvement techniques (raft foundations with disconnected settlement reducing piles, preloading with stone columns/jet grout columns)
2012	**Gebze – Orhangazi – İzmir Motorway Project, İzmit – Bursa – İzmir / Turkey**
	Geotechnical assessment on fills, bridge approach embankments and foundation system of substructures (culverts and underpasses)
	• Short/long term static/earthquake slope stability, two dimensional settlement and liquefaction potential analyses of fills and bridge approach embankments between KM: 10+400 – 13+200 and KM: 40+075 – 42+450
	• Analyses on settlement – time relation, negative skin friction piles
	• Design of ground improvement techniques (pile foundations, preloading with stone columns/vertical drains)
2012	**Kargı Dam and HEPP Project, Ankara / Turkey**
	Slope stability analyses
2012	**Artvin Dam and HEPP Project, Artvin / Turkey**
	Upstream and downstream cofferdams
	• Assessment of mixtures for slurry trench cut-off walls
	• Flow (seepage) analyses through two dimensional finite element program
2012	**Doğuş Automotive Showroom Building Project, Ankara / Turkey**
	Geotechnical assessment of deep excavation
	• Assessment of anchored pile wall
	• Assessment of inclinometer measurements

	• Deformation analyses of deep excavation
2011	**Al-Khairat 10x125 MW 9E Gas Turbines Power Plant Project, Kerbela / Iraq**

2011 **Al-Khairat 10x125 MW 9E Gas Turbines Power Plant Project, Kerbela / Iraq**
Geotechnical assessment on foundation systems of Gas Storage Tanks, Turbines and Office Buildings
- Bearing capacity, two dimensional settlement and liquefaction potential analyses
- Analyses on settlement – time relation
- Design of ground improvement techniques (raft foundations with disconnected settlement reducing piles, preloading with vertical drains)

2011 **Alexandretta Hilton Hotel Project, Hatay / Turkey**
Geotechnical assessment of foundation systems of Hotel and Shopping Mall Buildings

2010 **Bulvar Samsun Shopping Mall Project, Samsun / Turkey**
Geotechnical assessment of braced excavation
- Design of anchored pile wall and deformation finite element analysis of braced excavation

2010 **The Underground Line II from "Daszynskiego Roundabout Station" to the "Wilenski Railway Station" in Warsaw, Warsaw / Poland**
Design of C09, C10, C11, C12, C13, C14 and C15 Underground Stations
- Design of braced systems of 7 different stations
- Design of construction sequence of top-down systems
- Assessment of deformations and structural actions through two and three dimensional finite element analyses
- Design of pile foundations and barrette piles based on EUROCODE 7
- Design of ground improvement by jet grout soilcrete body

2009 **Marmara Forum Shopping Center Project, İstanbul / Turkey**
Design of braced systems for additional foundation excavation
- Design of two-layered braced systems
- Deformation analyses through finite element program
- Assessment of inclinometer measurements

2009 **Qatif and Jizan Bulk Plant Project, Jizan / Saudi Arabia**
Geotechnical assessment on foundation systems of Diesel Tanks
- Bearing capacity and two dimensional settlement analyses
- Design of ground improvement techniques (stone columns)

2009 **Park Gorkogo Complex Project, Kiew / Ukraine**
Geotechnical assessment of braced excavation
- Design of construction sequence of top-down systems
- Two dimensional finite element analyses

2009	**Venus Towers Project, Beirut / Lebanon**

Geotechnical assessment of braced excavation

- Design of anchored pile walls and top-down systems
- Two dimensional finite element analyses for the assessment of deformations and actions on the structural elements

2009	**Girls School in King Saud University Project, Riyadh / Saudi Arabia**

Geotechnical assessment of braced excavation

- Design of anchored pile walls and top-down systems
- Two dimensional finite element analyses for the assessment of deformations and actions on the structural elements

MAIN TOPICS of EXPERIENCE

- Assessment of bearing capacity and settlement of shallow and pile foundations, slope stability analysis
- Design of negative skin friction piles, raft foundations with disconnected settlement reducing piles, settlement reducing piles, barrette piles, laterally loaded piles.
- Assessment of liquefaction potential
- Design of ground improvement techniques: stone columns, jet grout columns, preloading and vertical drains
- Design of deep excavations, retaining structures braced by struts and anchors, cantilever and gravity retaining walls, top-down construction technique
- Assessment of road embankment fills, substructures of motorways and embankment dams
- Assessment and procedures of site investigation tests including Standard Penetration Test, Cone Penetration Test, Pressuremeter Test, Field Vane Test, Dilatometer Test, Dynamic Cone Penetration Test
- Assessment and procedures of conventional laboratory tests on soil mechanics
- Design of special model tests in laboratory
- Assessment of pile load tests, plate load tests, anchor tests, inclinometer measurements
- Preparing Geotechnical Report on all of the issues listed above.

LANGUAGE

- English (*advanced*)

COMPUTER SKILLS

- Microsoft Office Programs: Word, Excel and PowerPoint
- AUTO-CAD
- Plaxis 2D
- Plaxis 3D
- SLIDE

MEMBERSHIPS

- Union of Chambers of Turkish Engineers and Architects – Chamber of Civil Engineers, Member ID No.: 73015
- American Society of Civil Engineers, Student Member, Member ID No: 9093125
- TED Ankara College Alumni Association